ACADEMY OF SCIENCES USSR

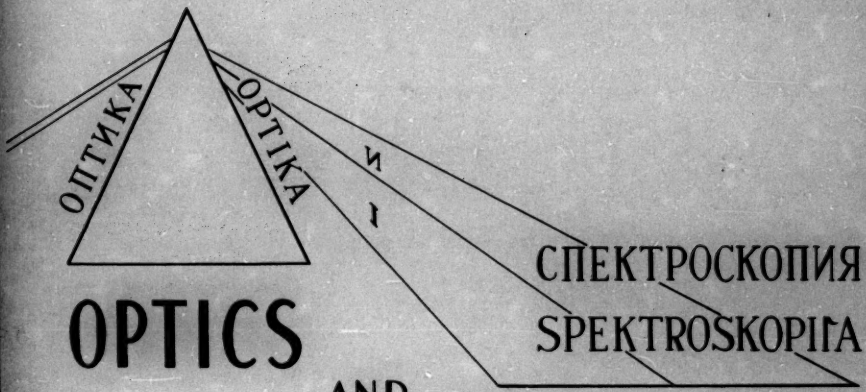

OPTICS AND SPECTROSCOPY

СПЕКТРОСКОПИЯ SPEKTROSKOPIYA

AUGUST 1959 - VOL. VII - NO. 2

Translated on the Initiative of
THE OPTICAL SOCIETY OF AMERICA, INC.
With a Grant-in-Aid from
THE NATIONAL SCIENCE FOUNDATION
by MORRIS D. FRIEDMAN, INC.

RUSSIAN EDITORIAL STAFF

Editor: S. E. FRISH

Assistant Editor: P. P. FEOFILOV

Corresponding Secretary: L. S. SAZONOV

Associate Editors:

M. M. GUREVICH M. A. EL'IASHEVICH A. A. LEBEDEV V. P. LINNIK
S. L. MANDEL'SHTAM I. V. OBREIMOV V. K. PROKOF'EV
N. N. SOBOLEV A. N. TERENIN A. I. TUDOROVSKII

Translation Editorial Staff

MORRIS D. FRIEDMAN

DR. JAMES R. ARONSON, *Arthur D. Little, Inc.*
FRED W. BEHNKE, *Perkin-Elmer Corp.*
DR. RICHARD DALVEN, *Raytheon Company, Research Division,*
DR. SUMNER P. DAVIS, *University of California*
CYRUS FELDMAN, *Oak Ridge National Laboratory*
DR. CARL GARLAND, *Massachusetts Institute of Technology*
DR. D. W. MAYO, *Massachusetts Institute of Technology*
DR. CONRAD J. RAUCH, *Massachusetts Institute of Technology — Lincoln Laboratory*
DR. JOHN S. WAUGH, *Massachusetts Institute of Technology*

Published monthly by the Optical Society of America, Inc. Executive office: 1155 Sixteenth Street, N.W., Washington, D.C. Subscriptions for one year to members of the Society: Associates $13.00; Regular members and Fellows $17.00. Subscriptions for non-members of the Society: One year U. S. and Possessions, $25.00; Foreign $28.00. Back numbers: $3.00 per copy. Subscriptions, changes of address and undeliverable copies should be referred to the Executive offices in Washington, D.C. The office of publication is 2500 South State Street, Ann Arbor, Michigan. Second class postage paid at Ann Arbor, Michigan.

Printed in the U.S.A. by Edwards Brothers, Inc., Ann Arbor, Michigan.

TOM VII, Vyp. 2 OPTIKA I SPEKTROSKOPIIA Avgust, 1959
VOL. VII, No. 2 OPTICS AND SPECTROSCOPY August, 1959

Isotope Shift in the Uranium Spectrum

L. A. KOROSTYLEVA AND G. A. STRIGANOVA

A Fabry-Perot interferometer was used to study the isotope shift in the uranium spectrum. The shift was measured for 46 lines in the visible region of the spectrum. New data were obtained on isotope shift in terms and on preliminary classification of uranium spectral lines.

A series of articles [1-5] has been written on the study of isotope shift in the uranium spectrum. However, because of the extreme complexity of the uranium spectrum, there is a great interest in conducting supplementary research using a spectral instrument of a higher resolving power than that used in previous research. To this end, we studied isotope shift in the uranium spectrum with a Fabry-Perot interferometer crossed with an ISP-51 three-prism glass spectrograph (camera f=780 mm).

Isotope shift in the uranium spectrum was studied in the region 4000-6000 Å. An external arrangement of the interferometer was used. A discharge tube with a hollow aluminum cathode served as the light source.

An enriched uranium sample, 30% U^{235}, 70% U^{238}, was used to obtain the isotope structure. A mixed oxide of uranium U_3O_8 weighing about 10 mg was put in a tube and reduced to metal in a hydrogen discharge at a current of 0.3 amp. The uranium spectrum was excited in an argon atmosphere at a pressure of about 1.5 mm Hg and a current of 0.1 amp. Three spectra were photographed with interferometer spacers of 2, 6 and 10 mm.

Isotope shift was measured on uranium lines with doublet isotope structure. Conditions of our experiment did not permit observation of the hyperfine structure of the components of the U^{235} isotope in these lines. Calculation of the shift was carried out by the parallelogram array method [6].

The results of measurement are given in Table 1, where column 1 gives the wavelength, column 2 the intensity, column 3 the isotope shift, and column 4 the classification for certain lines referred to in [7, 8] and our data on the determination of the lines for an ionized atom and the electron configuration of low terms. In Table 1, it may be seen that 40 lines have a negative shift and 6 lines a positive shift. This corresponds well with data from other research, where negative shift was also found for the overwhelming majority of lines.

In agreement with reference [5], we may consider that the uranium line at 4144.697 Å, which shows a large isotope shift, is emitted by an ionized atom. The low term of this line belongs to the electron configuration $5f^37s^2$. The five lines with positive shift obviously can be related to transitions to lower levels belonging to electron configuration $5f^46d$ and $5f^36d^2$. In the case of these configurations, the d-electrons do not have a significant effect on the isotope shift of the term. Therefore, the line shift is caused primarily by the shift in upper terms, which leads to a positive shift. Line 4067.756Å shows a positive shift even though it belongs to a transition to a lower level of configuration $5f^36d7s$. A negative shift is characteristic for such lines [5]. This fact, that a positive shift was found for line 4067.756Å, is explained either by perturbation of the upper term, which results in an abnormally large shift, or else the line referred to is incorrectly classified in reference [8].

Table 1

λ (in Å)	Intensity according to Harrison: Arc	Intensity according to Harrison: Spark	Shift $\Delta(U^{238}-U^{235})$ (in cm^{-1})	Shift $\Delta(U^{238}-U^{235})$ (in Å)	Line Classification according to References [7, 8]; Atomic state and electron configuration according to our data
4039.781	15	2	−0.27	−0.044	—
4067.756	12	20	+0.198	+0.033	II, $5f^36d7s^4L^\circ_{5/2}$ − 308$_{5/2}$
4077.786	15	6	−0.204	−0.034	—
4082.948	8	—	−0.130	−0.022	—
4095.748	18	25	−0.267	−0.045	—
4099.930	5	5	−0.295	−0.050	—
4101.905	18	1	−0.265	−0.045	—
4127.331	8	1	−0.171	−0.029	—
4144.697	10	5	−1.34	−0.238	II, f^3s^2
4155.411	12	18	−0.137	−0.024	—
4160.950	12	1	−0.128	−0.022	—
4163.225	6	6	+0.079	+0.014	II, f^3d^2 or f^4d
4165.678	8	8	−0.228	−0.040	—
4166 630	6	2	−0.208	−0.035	—
4169.050	20	2	−0.087	−0.015	—
4192.905	10	1	−0.292	−0.051	—
4229.268	6	1	−0.151	−0.027	—
4240.587	10	10	−0.157	−0.028	—
4267.934	15	4	+0.246	+0.045	II, f^3d^2 or f^4d
4269.613	20	30	−0.132	−0.024	II, $5f^36d^4L^\circ_{7/2}$ − 251$_{9/2}$
4279.331	10	—	+0.117	+0.021	II, f^3d^2 or f^4d
4309.697	12	3	−0.187	−0.035	—
4322.397	8	3	−0.247	−0.046	—
4328.742	20	1	−0.263	−0.049	I, $5f^36d7s^3K^\circ_7$ − 237$_8$
4349.388	3	5	−0.155	−0.029	—
4453.218	10	1	+0.131	+0.026	II, f^3d^2 or f^4d
4458.703	10	3	−0.191	−0.038	—
4465.133	20	25	−0.146	−0.029	—
4469.328	12	1	−0.179	−0.036	I, $5f^36d7s^3L^\circ_7$ − 223$_7$
4476.477	8	6	−0.330	−0.066	—
4559.649	15	—	−0.219	−0.045	—
4572.243	6	8	−0.195	−0.041	—
4601.794	4	4	−0.202	−0.043	—
4722.726	40	50	−0.259	−0.058	II, $5f^36d7s^4L^\circ_{7/2}$ − 229$_{9/2}$
4808.874	8	—	−0.182	−0.042	—
4810.889	6	—	−0.357	−0.083	I, $5f^36d7s^3A^\circ_4$ − 245$_5$
4885.126	18	—	−0.277	−0.066	I, $5f^36d7s^3L^\circ_6$ − 204$_7$
4928.447	20	1	−0.483	−0.117	I, $5f^36d7s^3K^\circ_7$ − 245$_7$
4942.640	6	6	−0.440	−0.107	II, $5f^36d7s^4L^\circ_{7/2}$ − 220$_{7/2}$
5011.423	8	—	−0.373	−0.094	I, $5f^36d7s^3K^\circ_6$ − 205$_6$
5088.301	10	—	−0.237	−0.071	I, $5f^36d7s^3L^\circ_6$ − 196$_5$
5205.179	10	6	−0.145	−0.039	—
5308.544	25	3	−0.166	−0.048	I, $5f^36d7s^3A^\circ_4$ − 226$_3$
5329.223	10	1	−0.417	−0.118	I, $5f^36d7s^3L^\circ_5$ − 187$_6$
5510.435	10	—	+0.129	+0.039	II, f^3d^2 or f^4d
5971.525	50	—	−0.151	−0.054	I, $5f^36d7s^3K^\circ_6$ − 173$_6$

Table 2

Upper Terms	Shift $\Delta(U^{238}-U^{235})$ (in cm^{-1})	Initial Terms
173_6	0.33	295_6
187_6	0.06	287_5
196_4	0.25	287_5
204_7	0.20	287_5
205_4	0.11	295_6
223_7	0.30	287_5
237_6	0.22	295_6
245_7	0.08	297_7
$220_{13/2}$	0.02	$6M^o{}_{13/2}$
$229_{11/2}$	0.20	$6M^o{}_{13/2}$
$251_{13/2}$	0.33	$6M^o{}_{13/2}$

Proceeding from the data obtained on isotope line shift, we succeeded, in certain cases, in establishing the shift in terms. For arc lines, the highest known upper terms of uranium, 287_5, 295_6, 295_7, 301_6 [5], were taken as initial terms. For spark lines, the terms belonging to electron configurations $5f^46d$ and $5f^36d^2$ were taken as initial terms. Table 2 gives the isotope shift for eight terms of the neutral atom and three terms of the ionized atom. As seen in Table 2, the shift in terms was positive in all cases, i. e., the level of the lighter isotope is lower than the level of the heavier isotope, which agrees with the theory of volume effect.

Thus, as a result of the work done, we succeeded in obtaining new data on isotope shift in the uranium spectrum which supplements the results obtained earlier on isotope shift in terms for neutral and ionized uranium atoms. Moreover, six spectral lines were established as belonging to U II, and the most likely electron configuration for low terms was predicted.

September 15, 1958

REFERENCES

1. O. E. ANDERSON AND H. E. WHITE: Phys. Rev., 71, 911, (1947)
2. L. E. BURKHART, G. STUKENBROEKER, AND S. ADAMS: Phys. Rev., 75, 83 (1949)
3. J. R. McNALLY: JOSA, 39, 271 (1949)
4. D. D. SMITH, G. L. STUKENBROEKER, AND J. R. McNALLY: Phys. Rev., 84, 383, (1951)
5. A. R. STRIGANOV, L. A. KOROSTYLEVA: ZETF, 29, No. 4 (10), 393, (1955)(see Sov.Phys.JETP)
6. S. TOLANSKY: High Resolution Spectroscopy, Methuen and Co., Ltd., London, 1947.
7. C. O. KIESS, C. HUMPHREYS, AND D. D. LAUN: J. Res. Nat. Bur. Stand., 37, 57, (1946)
8. J. C. van den BOSCH: Physica, 15, 503, (1949)

TOM VII, Vyp. 2 OPTIKA I SPEKTROSKOPIIA Avgust, 1959
VOL. VII, No. 2 OPTICS AND SPECTROSCOPY August, 1959

Influences on the Intensities of Spectral Lines in Flame Spectra

N. S. TSKHAI, S. L. MANDEL'SHTAM

Abstract: The causes of changes, observed in the practice of spectral analysis, in the intensities of spectral lines in the flame spectra of elements with changes in the form of compounds in which the elements are introduced to the flame, and with the introduction of additional compounds, have been investigated. The concentrations of Na and Sr atoms in the region of the flame and the temperature of the flame were measured; it was established that the observed changes of line intensities were caused by the joint action of the change in concentration of the atoms of the elements in the flame region as a consequence of the change of entrance speed of the solution into the flame, and of the change in the state of excitation of the atoms as a consequence of a change in the flame temperature.

INTRODUCTION

In many cases when using flames as a source of excitation for spectral analysis, changes are observed in the intensities of spectral lines of the element being analysed with changes in the form of the compound in which the element is introduced into the flame, and also with the introduction into the flame of additional compounds; the changes in line intensities reach as high as ten percent [1-7]. These influences hamper the execution of spectral analyses when flames are used, and independently are also physically interesting.

Although flames have been used for the excitation of spectra for a long time, the causes of the above mentioned influences have been studied insufficiently, consequently there is no single point of view on the nature of these phenomena. Pointed out as possible causes of such influences are incomplete dissociation of the molecules introduced into the flame region and the formation of new molecules [8-11], changes in the degree of ionization of the free metallic atoms [7, 12, 13], changes in the entry speed of the solution into the flame as a consequence of changes in the physical properties (viscosity, surface tension etc.) [14, 15], and finally, changes of the state of excitation of the atoms as a consequence of changes in the number of collisions of the second kind.

In all of the work, however, conclusions about the mechanisms of the influences were made only on the basis of studies of the intensities of the spectral lines. It is obvious that for elucidation of the nature of these phenomena it is necessary to study separately the changes in the concentration of free atoms of the elements and their state of excitation. Only after this is done is it possible to elucidate the causes of the corresponding changes. The execution of such an investigation was the object of the present work. Most attention was given to the measurement of the absolute concentration of the atoms of the element in the flame region with changes in the form of the compound and the addition of compounds of other elements.

DESCRIPTION OF THE METHOD

For measurement of the concentration of atoms we chose the method of anomalous dispersion. The virtues of this method for our problem are its precision and the independence of the results of the measurements of the form of intensities of the spectral lines, but somewhat of a defect is its comparatively low sensitivity.

A schematic of the experimental setup is presented in figure 1a. Its basis is the interferometer of D. C. Rozhdestvenskii. In order to make it possible to measure the concentration of atoms at different distances from the axis of the flame 1, the interference field was localized at the center of the flame parallel to its axis. By the use of three plane mirrors 2, 3, 4 and a lens 5, the flame and the interference field were projected onto the spectrograph slit 6, perpendicular to it. The ISP-51 three-prism spectrograph was used with F = 800 mm camera and collimator lenses. Exposures with 0.03 mm slit widths were made in 0.1 seconds.

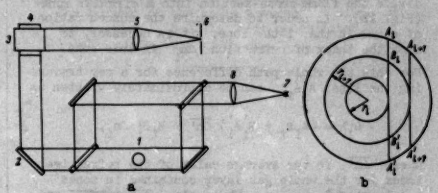

Figure 1. Schematic of the experimental setup (a) and a lateral cross-section of the flame (b).
1) Flame; 2,3,4) Plane mirrors which rotate the image of the flame by 90°; 5) Lens; 6) Spectrograph slit; 7) Source of continuous spectrum; 8) Lens.

Solutions were introduced into the flame with an atomizer of the usual construction; the diameter of the vertical and horizontal capillaries were 0.3 and 0.5 mm, respectively; the construction of the atomizer ensured that only small and homogenous droplets of the solution hit the flame.

The burner was made of pyrex glass. Acetylene was fed from the cylinders through narrow capillaries 0.3 mm in diameter. With an air pressure of 25 cm of Hg and an acetylene pressure of 40 cm of water the flame burned very stably with a sharply marked internal pale blue cone about 10 mm high. The diameter of the flame was different when different elements were introduced into it and for Na, K and Mg was 11 mm, for Li 9 mm, and for Sr, Ca, and Ba 7 mm in diameter.

Measurements of the atom concentrations were made at a height of 15 mm above the pale blue cone. The experimental method concluded with a measurement of the displacement of the interference fringe close to an absorption line of the element being studied. If δ is the displacement of the k-th fringe, expressed as the fraction of the distance between two neighboring fringes, that is $\delta = \frac{\Delta j_k}{j_{k+1} - j_k}$,

then the change of the refractive index of the flame, which is the cause of this displacement is determined from the relation $\Delta n = \frac{\delta\lambda}{d}$, where d is the thickness of the layer. The quantity Δn is directly connected with the determined concentration of atoms by Sellmeier's formula

$$\Delta n = \sum_{j=1}^{P} \frac{e^2\lambda^2\lambda_j^2 f_j}{2\pi mc^2(\lambda^2 - \lambda_j^2)} N.$$

The displacement of the interference fringes was measured on a traveling microscope with a double micrometer screw, which moves the carriage in two mutually perpendicular directions. The precision of the measurement of δ was, on the average, equal to ±5% (averaged over 5 photographs), which also gave an error in the measurements of the atom concentration of ±5%.

Along with the cross-sectional average of the concentration of atoms N obtained by this method in a series of experiments, the distribution of the cross-sectional concentration was measured. Let us divide the flame cross-section into m circular zones (Fig. 1b). In order to determine the concentration of atoms in the i-th zone, it is necessary to find the index of refraction Δn_i in this zone.

For this the whole path difference for a ray traversing the line A_iA_i' can be approximately written as

$$\delta_i\lambda = (A_iB_i + B_i'A_i')\,\overline{\Delta n'} + B_iB_i'\,\Delta n_i,$$

where $\overline{\Delta n'}$ is the average value of the refractive index for the whole gas layer contained in zones i + 1, i + 2, ..., m. Obviously, $\overline{\Delta n'} \approx \overline{\Delta n_{i+1}}$ and may be determined from the displacement of the interference fringes on the edge of the (i + 1)-th zone.

$$\delta_{i+1}\lambda = A_{i+1}A_{i+1}'\,\overline{\Delta n_{i+1}}.$$

Expressing the linear segments A_iB_i, $A_i'B_i'$ etc. in terms of the radii of the zones, we obtain the following formula:

$$\frac{\delta_i\lambda}{2} = \left[(r_m^2 - r_i^2)^{\frac{1}{2}} - (r_{i+1}^2 - r_i^2)^{\frac{1}{2}}\right]\overline{\Delta n_{i+1}} + (r_{i+2}^2 - r_i^2)^{\frac{1}{2}}\,\Delta n_i,$$

$$\overline{\Delta n_{i+1}} = \frac{\delta_{i+1}\lambda}{2(r_m^2 - r_{i+1}^2)^{\frac{1}{2}}}.$$

Thus, the measurements reduce to a determination of the displacement of the interference fringe δ_i at different distances r_i from the center of the flame.

Concurrently, with the measurement of the atom concentration the line intensities of the corresponding elements were also measured: these measurements were done by a photographic method in the usual manner.

Measurements of the temperatures of the flames were made by the method of self reversal of lines also in the usual manner.

RESULTS OF THE MEASUREMENTS

Investigations of the Influence of the Form of the Compounds

The average atom concentrations of sodium and strontium were measured by sections. Sodium was introduced into the flame in three compounds: NaCl, Na_2CO_3, and Na_2SO_4 and the strontium was introduced in two compounds: $SrCl_2$ and $Sr(NO_3)2$. The heats of formation corresponding to the compounds of each element differ very strongly.

The displacement of the center of the interference fringe was measured at a distance of 1.3 and 2.6 Å from the sodium λ = 5890 Å line at a distance of 0.52 Å from the strontium λ = 4607 Å line.

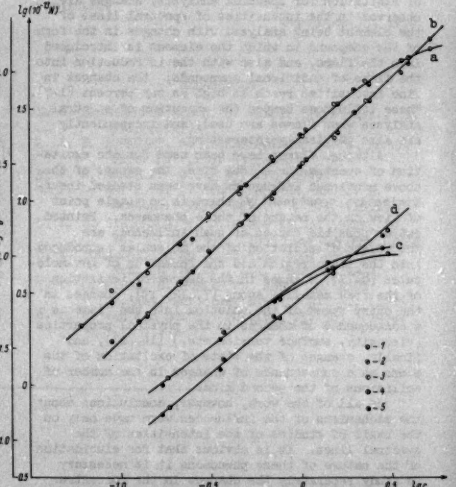

Figure 2. The dependence of the concentration of sodium atoms (a, b) and strontium atoms (c, d) in the flame on the concentration of the element in solution without (a, c) and with consideration (b, d) of the entry speed v of the solution into the flame.

The tangent of the angle between the slope of the linear portion and the abscissa: a-0.85, b-0.96, c-0.73, d-0.82. 1-NaCl, 2-Na_2CO_3, 3-Na_2SO_4, 4-$SrCl_2$, 5-$Sr(NO3)_2$. c is in moles/liter and v in cm^3/minute.

The results of the measurements are presented in figure 2a and b, where the ordinate is the value of the logarithm of the absolute concentration of atoms in the flame, and the abscissa is the logarithm of the concentration of the element in solution, in moles per liter of solution. An analysis of the graph shows that for sodium, all three compounds give points which lie on a single curve. For strontium, in the region of high concentration a very slight difference of the atom

concentration in the flame is observed for both compounds. For Na and Sr the curves have a linear form right up to a concentration region close to saturation of the element in the solution. The slope of the linear portions of the curves is significantly smaller than unity: consequently the atom concentration in the flame is not proportional to the concentration of the element in solution. This, obviously, may have been caused either by a decrease in the speed of the solution entering into the flame with an increase in the concentration of the element, or by a decrease in the degree of dissociation of molecules containing the given element in the flame region. In order to check the first assumption, the amount of solution issuing from the atomizer in a definite time was determined by weighing. It was established that the speed of entry of the solution decreases with an increase in the concentration of the element. The results of these measurements are shown in figure 2b and d and also in figure 2a and c, but plotted on the ordinate are the values of the concentration of atoms in the flame, divided by the entrance speed of the corresponding solution into the flame. The curves are linear for all concentrations: the slope increases, but the tangent is still smaller than unity; the points for $SrCl_2$ and $Sr(NO3)_2$ practically coincide.

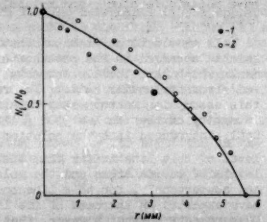

Figure 3. Distribution of the concentration of sodium atoms across sections of the flame.

N_o is the atom concentration at the center of the flame. 1–NaCl (c_{Na} = 5.4 moles/liter); 2–Na_2SO_4 (c_{Na} = 2.3 moles/liter).

The results of the measurements of the distribution of the concentration of sodium atoms by sections of the flames are presented in figure 3 for NaCl and Na_2SO_4; they are related to the saturated concentration of sodium in solution at room temperature. As is obvious from figure 3, both compounds have the same distribution of atoms by sections.

In figure 4a is given the change of intensity of the Na λ=5890 Å line as a function of the sodium concentration in the solution for all three compounds; in figure 4b the line intensity is expressed as a function of the concentration of atoms in the flame. The latter curve shows that tangent is smaller than 0.5, which is to be expected. This was caused by strong self-reversal of the lines. However, all of the points, corresponding to the different compounds, are sufficiently well confined to one curve; that is, the intensity of the sodium line does not depend on the chemical compound.

In figure 5 the dependence of the flame temperature on the sodium concentration in the solution for three compounds is presented. The temperature was measured from a line of lithium, which was put into each of the solutions in a small amount. Figure 5 shows that the temperature of the flame increases in some measure as the concentration of sodium in the solution increases; the change in temperature does not depend on the form of the compound.

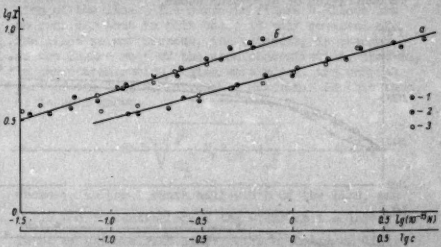

Figure 4. The dependence of the intensity of the sodium λ = 5890 Å line on the sodium concentration in the solution (a) and in the flame (b).

The tangent of the angle between the slope and the abscissa: a–0.26; b–0.31; c–in moles/liter.
1–NaCl; 2–Na_2CO_3; 3–Na_2SO_4.

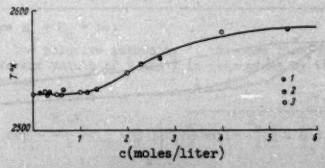

Figure 5. The dependence of the flame temperature on the concentration of sodium in solution.
1–NaCl; 2–Na_2CO_3; 3–Na_2SO_4.

AN INVESTIGATION OF THE INFLUENCE OF ADDITIONAL COMPOUNDS

Measurements were made of the average over the sections of the sodium atom concentration with solutions containing the influencing compounds $MgCl_2$, $CaCl_2$, $SrCl_2$, $BaCl_2$, and of the average strontium atom concentration with solutions containing the compounds NaCl and $CaCl_2$. Measurements were made at a concentration of 0.67 moles/liter for Na and at a concentration of 0.61 moles/liter for Sr. The displacements of the central interference field were measured at a distance of 1.3 Å from the Na λ=5890 Å line and at a distance of 0.52 Å from the Sr λ=4607 Å line.

The results of the measurements are presented in figures 6a and 7a. The concentration of the influencing element is indicated on the abscissa axis, and on the ordinate axis is the concentration of Na and Sr atoms in the flame, where taken as the unit are the corresponding concentrations in the absence of the influencing element, measured under the same conditions.

Figure 6a shows that $CaCl_2$, $SrCl_2$, and $BaCl_2$ have a strong influence on the concentration of Na atoms, while the influence of $MgCl_2$ shows up only at considerably larger concentrations. NaCl, as well as $CaCl_2$, has an influence on the concentration of strontium atoms.

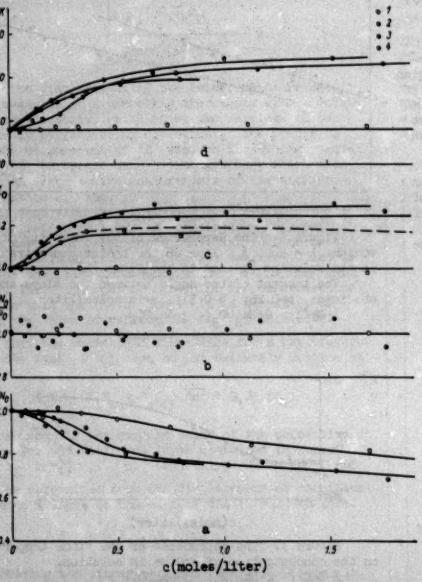

Figure 6. The dependence of the sodium atom concentration in the flame without (a) and with (b) consideration of the entry speed of the solution into the flame, and also the relative intensities of the sodium $\lambda = 5890$ Å line (b) and the temperature of the flame (d) on the concentration of the influencing element in the solution. N_0 and I_0 correspond to the atom concentrations and line intensities of sodium in the absence of the influencing element. The dashed curve shows the intensity of the sodium $\lambda = 3302$ Å line with the presence in solution of the influencing compound $CaCl_2$.

$c_{Na} = 0.67$ moles/liter

1–NaCl+$MgCl_2$, 2–NaCl+$CaCl_2$, 3–NaCl+$SrCl_2$, 4–NaCl+$BaCl_2$.

As in the case of the investigation of the influence of the form of the compound, the speed of entrance into the flame in the presence of additional compounds was measured. It was shown, that the speed of entrance changes in the presence of additional compounds and changes in its concentration. In figures 6b and 7b are shown the results of the same measurements as are given in figures 6a and 7a, but on the ordinate axis are values of the atom concentration of the element being studied, divided by the speed of entry into the flame of the corresponding solution. For Na it was found that the atom concentration in the flame was not affected by the presence of additional elements in the solution, while with Sr no influence from the NaCl and an influence in the reverse direction from the $CaCl_2$ were observed.

Further investigations were made on the intensity of the sodium and strontium lines with the presence of the compounds in solution. In figure 6 are given the curves of the changes of relative intensity of the Na $\lambda = 5890$ Å line (in relation to the line intensity without the additional compound in solution) as a function of the molar concentration of the in ncing compound. These curves show an increase of the line intensity for Na with increasing concentration of the influencing element. Thus, with an increase in the concentration of the additional compound there is also a change in the condition of excitation of the Na atoms. This change may have been caused by an increase in the temperature of the flame. In principle, an increase in the intensity of the Na line could also have been caused by an increase in the number of exciting collisions because of resonance impacts of the influencing atoms and molecules, which have metastable atomic and molecular levels close to the Na $3^2P_{3/2}$ level.

It should be pointed out that the largest gain is observed in the presence of those elements which have the closest metastable levels and strong molecular bands. In order to check this assumption measurements were made of the intensity of the Na $\lambda = 3302$ Å line with $CaCl_2$ introduced into the solution. The upper level of this line is far from the metastable levels of the Ca atoms and the molecular levels and consequently, for this line one could not have expected an increase of its intensity. Measurements showed, however, that this line became stronger together with the strengthening of the $\lambda = 5890$ Å line (compare Fig. 6c dashed line). Thus, the cause of the strengthening of the intensity of the Na line, obviously, is the increase in temperature of the flame with the introduction of additional compounds. For clarification of this question measurements were made of the temperature of the flame.

The results of temperature measurements by means of the Li line, which was introduced into all solutions in small quantities, are presented in figure 6d and corroborate this assumption. An analysis of figure 6d shows that all the additional compounds, except $MgCl_2$, noticeably raise the temperature of the flame as there the concentration increases.

The results of the measurements of the intensity of the Sr $\lambda = 4607$ Å line are presented in figure 7c. Figure 7c shows that the change in line intensity occurs in a manner parallel to the change in the concentration of strontium atoms in the region of the flame (Fig. 7a). The results of measurements of the flame temperature by means of the Li line with the introduction of the influencing compound are presented in figure 7d. They show that the flame temperature

does not change in practice; only with very large concentrations the influencing compound is some increase in temperature observed, exceeding the limits of error of the measurements.

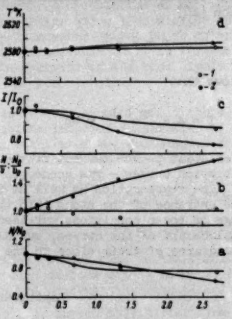

Figure 7. The dependence of the concentration of strontium atoms in the flame without (a) and with (b) consideration of the entry speed v of the solution into the flame, and also the relative intensity of the strontium $\lambda = 4607$ Å line (c) and the flame temperature (d) on the concentration of the influencing element in the solution.

N_0 and I_0 are the corresponding atom concentration and line intensity for strontium in the absence of the influencing element.

$c_{Sr} = 0.61$ moles/liter

1-$SrCl_2$+NaCl; 2-$SrCl_2$+$CaCl_2$.

Investigation of the distribution of Na atoms by sections of the flame in the presence of the influencing compound showed that the character of the distribution of sodium atoms is not changed with the introduction of the influencing compound, even though the absolute concentration of atoms decreases by approximately 30%.

DISCUSSION OF THE RESULTS

The results which have been presented show that the change in line intensities because of influences which were scrutinized in the present work takes place principally as a result of the joint action of two factors — a change in the concentration of atoms because of the change in entrance speed of the solution and a change in the conditions of excitation because of a change in the flame temperature. This conclusion is well corroborated by calculations presented below.

We have assumed for simplicity that the atoms were distributed uniformly over all sections of the flame and that self-reversal is absent. Then the line intensity, radiated by the l-th layer, equals

$$I = I_0 \int (1 - \exp[-K_\nu l]) d\nu$$

where I_0 can be expressed with sufficient precision by Wien's formula

$$I_0 = \frac{h\nu^3}{c^2} \exp\left[-\frac{h\nu}{kT}\right],$$

and $A_\nu = \int (1-\exp[-k_\nu l])\, d\nu$ is the complete absorption of the line. The curve in figure 4 allows one to consider that in this case, if self reversal of the lines is not present, the intensity is changed as the square root of the atom concentration, that is, in the concentration region we studied, the central part of the line would reach a maximum. In this case, as is well known

$$A_\nu = \sqrt{\frac{e^2}{mc^2} N_n f_{nm} \gamma_L \frac{c^2}{\nu^2}},$$

where γ_L is the Lorentz half-width of the line, and N_n is the concentration of the atoms in the lower level of the analyzed line. With a Boltzmann distribution of atoms in the excited levels

$$N_n = N \frac{g_n}{g} \exp\left[-\frac{E_n}{kT}\right]$$

and, consequently,

$$I = h\nu \exp\left[-\frac{E_m - E_n}{kT}\right] \sqrt{\frac{e^2}{mc^2} N \frac{g_n}{g} \exp\left[-\frac{E_n}{kT}\right] f_{nm} \gamma_L l},$$

where $E_m - E_n = h\nu$.

The relative intensity of the same line with different values of N and T is determined by the relation

$$\frac{I}{I_0} = \exp\left[-\frac{E_m - E_n}{k}\left(\frac{1}{T} - \frac{1}{T_0}\right)\right] \sqrt{\frac{N}{N_0} \exp\left[-\frac{E_n}{k}\left(\frac{1}{T} - \frac{1}{T_0}\right)\right]}$$

(the value of γ_L essentially does not change for the values of N and T that are of interest to us). If the line is a resonance line, that is $E_n = 0$, then

$$\frac{I}{I_0} = \sqrt{\frac{N}{N_0}} \exp\left[-\frac{E_m}{k}\left(\frac{1}{T} - \frac{1}{T_0}\right)\right]$$

In figure 8 are presented values calculated by this formula and experimental values of the line intensity for sodium as a function of the concentration of the influencing compound.

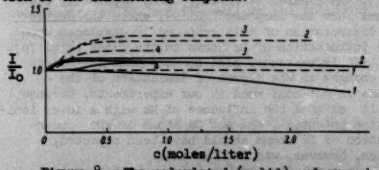

Figure 8. The calculated (solid) and experimental (dashed) curves of the dependence of the relative intensities of the sodium $\lambda = 5890$ Å line on the concentration of the influencing element in the solution. $c_{Na} = 0.67$/moles/liter. 1) NaCl+$MgCl_2$, 2) NaCl+$CaCl_2$, 3) NaCl+$SrCl_2$, 4) NaCl+$BaCl_2$.

Figure 8 shows that in spite of the approximate character of the calculation, the experimental and calculated curves agree quite well as to the nature of their changes. This circumstance, that the experimental values of the intensity changes are larger than calculated, is explained, obviously, by the presence of significant self-reversal of the sodium lines at a concentration of 0.67 moles/liter, whose effect is increased to some extent by a decrease of the concentration of the influencing compound, since here the concentration of Na atoms in the flame region is increased (Fig. 6a).

The results which have been described indicate that attempts to connect the changes of line intensity only with changes in the concentration of atoms, as is done in some work, are incorrect and lead to the opposite conclusion. It is necessary to examine the changes in atom concentration, as well as the changes in flame temperature, because depending on which of these factors predominates, one may observe a strengthening, a weakening, or finally, a constancy of the intensity of the spectral line with changes in the form of the molecular compound and with the introduction of additional compounds. Depending on the relation of the concentration of the determined and influencing elements one may observe a strengthening or weakening of the line which actually was also observed by Schuhknecht [15] for example.

The causes of the changes, observed in our experiments, of the speed of entry of the solution into the flame and the temperature of the flame have still not been clarified at present, obviously, they are connected with changes in the physico-chemical properties of the solution (viscosity, surface tension, etc.) and with changes in the burning rate of the flame.

It should further be pointed out that the results of our measurements — the independence of the concentration of Na and Sr atoms (taking into account the change in entry speed of the solution) from the form of the introduced compound — confirm the point of view expressed earlier [10], that the compounds of alkaline and alkaline earth elements introduced into the flame dissociate completely, where the atoms of these elements may partially enter the flame region as new compounds. In relation to sodium, this latter, obviously, does not take place, as follows from the closeness to 1 of the tangent to the curve $N = f(c)$ (Fig. 2b) and the independence of the atom concentration from the influencing compound (taking into account their entry speed, Fig. 6b). This conclusion is in accord with the results of James and Sugden [11]. As regards strontium, then, apparently its atoms form the compound SrO [9], where the degree of dissociation of this compound is displaced upon the introduction of Ca atoms in the flame (Fig. 7b).

It is necessary also to note that the effect of changes in the degree of ionization of the atoms is not confirmed in our experiments, because if it existed the influence of Na with a lower ionization potential, and not Ca atoms on the concentration of Sr atoms should have been expected, which, however, was not the case.

In conclusion let us point out that, as follows from our experiments, the concentration of the atoms of the element in the flame N may be connected with the concentration of the element in the solution by the relation

$$N = a_1 c^{b_1}.$$

On the other hand, the line intensity was connected with the concentration of atoms in the flame by the relation [16]

$$I = a_2 N^{b_2}$$

Hence it follows that

$$I = a_2 a_1^{b_2} c^{b_1 b_2} = a c^{b}$$

that is, the constant b — the tangent of the spectral analysis calibration curves — was connected with the conditions of line reabsorption as well as with conditions of the entrance of the atoms into the flame. Thus — a change of these conditions may lead not only to a displacement of the curves, but also to changes in the degree of their slope to the abscissa axis.

September 9, 1958

REFERENCES

1. T. F. BOROVIK-ROMANOVA: DAN USSR, 21, 334, (1938)
2. L. I. GRINGAU, G. M. LERMAN: ZL, 7, 314 (1938)
3. H. PUTZMANN: Spectrochim. Acta, 1, 408 (1940)
4. D. N. IVANOV: ZL, 10, 401 (1941)
5. R. J. BRUMBOUGH, W. E. FANUS: Anal. Chem., 26, 463 (1954)
6. T. J. CHOW, T. G. THOMPSON: Anal. Chem., 27, 18, (1955)
7. C. T. J. ALKEMADE: Spectrochim. Acta, 17, (1957)
8. V. G. ALEKSEEVA, S. L. MANDEL'SHTAM: ZTF, 17, 765, (1947)
9. A. LAGERQVIST, L. HULDT: Ark. Mat. Astron. Fys., 8, (5), 427, (1954)
10. T. HOLLANDER, A. J. BORGERS, C. T. J. ALKEMADE: Appl. Sci., Res., B 5, 409, (1956)
11. C. G. JAMES, T. M. SUGDEN: Proc. Roy. Soc., A 227, 312, (1955)
12. C. T. J. ALKEMADE: Thesis, Utrecht (1954)
13. L. HULDT: Ark. Mat. Astron. Fys., B 31, (1), 4 (1944)
14. T. D. PARKS, H. O. JOHNSON, L. LYKKEN: Anal. Chem., 20, 822, (1948)
15. W. SCHUHKNECHT: OPTIK, 10, 268, (1953)
16. S. L. MANDEL'SHTAM: IAN USSR, FS, 4, 150 (1940)

TOM VII, Vyp. 2 OPTIKA I SPEKTROSKOPIIA Avgust, 1959
VOL. VII, No. 2 OPTICS AND SPECTROSCOPY August, 1959

Theory of Infra-Red Spectra Intensities of Sulfur Dioxide, Ammonia and Phosphine Molecules, IV

L. M. SVERDLOV

Abstract: A calculation of the intensities of infra-red bands and the electro-optical parameters of ammonia, phosphine and sulfur dioxide is made. It is shown that there is no discrepancy between the values of the dipole moments of the bonds determined by infra-red spectra and those calculated from the static dipole moments of the molecules. It is further shown for polyatomic molecules that a proportionality is absent between the behavior of the bond dipole moments and the derivatives of dipole moments with respect to the change in the bond length.

1. As is well known [1, 2], the determination of the absolute integral intensities of infra-red absorption spectra of molecules opens the way to a calculation of their electro-optical parameters — the bond dipole moments $\mu^{(i)}$ and the derivatives of the dipole moment with respect to a change in the bond length $\frac{\partial \mu^{(i)}}{\partial q_i}$. In works devoted to this question, various authors came to the conclusion that the magnitudes of bond dipole moments, determined from infra-red spectra (the vibrational dipole moments $\mu^{(i)}_{vib.}$), appreciably differ from the magnitudes $\mu^{(i)}_{st.}$ of molecules determined by radiospectroscopy or other means. Hence, it was concluded that the parameters $\mu^{(i)}_{vib.}$ and $\mu^{(i)}_{st}$ have different physical meanings. This conclusion was most firmly reached in the survey of Horning and McKean [3], devoted to an investigation of bond dipole moments, and in the papers [4-7], in which the absolute integral intensities of infra-red bands of sulphur dioxide, ammonia and phosphine were determined.

In the opinion of the authors of the papers [3, 6, 7], the reason for the discrepancy between $\mu^{(i)}_{vib}$ and $\mu^{(i)}_{st}$ is that in the vibration process redistribution of the electronic cloud ("the theory of orbital sequence," "overlap of p- and s- orbitals") occurs and consequently there arises a change in the electro-optical parameters of the bonds. However, it is evident that such a point of view is contradictory: on the one hand, the equilibrium distribution of the electronic cloud determines the geometrical parameters of the molecules, their static dipole moments, force constants, and vibration frequencies; on the other hand, the intensities of infra-red bands of the same vibrations are determined by the properties of the electronic cloud which is redistributed in the process of vibration.

In all the works listed, the calculation of the electro-optical parameters was made in a zero approximation of the valence-optical scheme, the derivations of which, as we showed elarlier [8-10], do not have physical meaning, since for the calculation of infra-red band intensities corresponding to vibrating bonds of different symmetry types one is obliged to ascribe various values of the electro-optical parameters $\mu^{(i)}$ and $\frac{\partial \mu^{(i)}}{\partial q_i}$. The same results were obtained also in the papers [3-7]: in the case of SO_2, for example different values $\frac{\partial \mu^{(i)}}{\partial q_i}$ were obtained for the types of symmetry A_1 and B_1, while for NH_3 and PH_3 diferent values $\mu^{(i)}$ and $\frac{\partial \mu^{(i)}}{\partial q_i}$ were obtained for the symmetry types A_1 and E. This matter also causes one to doubt the correctness of the mentioned authors' derivations, for it is possible to explain the discrepancy between $\mu^{(i)}_{vib}$ and $\mu^{(i)}_{st}$ by the inapplicability of the valence-optical scheme in a zero approximation and by the necessity of using the first approximation.

It is of interest to calculate the infra-red spectral intensities and the electro-optical parameters of the molecules SO_2, NH_3, and PH_3 in a first approximation of the valence optical scheme, in order to determine the parameters characterizing the bond polarities of the specified molecules and to clarify whether there is actually a discrepancy between $\mu^{(i)}_{vib}$ and $\mu^{(i)}_{st}$.

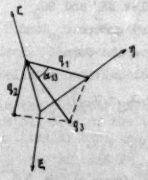

Figure 1.

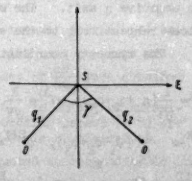

Figure 2.

2. For the calculation let us introduce normal vibrational coordinates — variations of the bond lengths and angles $q_i, \alpha_{ij} (i \neq j = 1, 2, 3)$ (see Fig. 1); $q_i (i = 1, 2)$, γ (see Fig. 2) and angular valence-optical coordinates β_{ni} —variations of the angles between bonds and axes. The valence optical coordinates of NH_3 and PH_3 satisfy the following three conditions:

$$\beta_{1\eta} - \beta_{1\zeta} = 0;\ \sqrt{3}\cos\frac{\theta}{2}\beta_{2\xi} + \lambda\beta_{2\eta} + 2\kappa\beta_{2\zeta} = 0;$$

$$-\sqrt{3}\cos\frac{\theta}{2}\beta_{3\xi} + \lambda\beta_{3\eta} + 2\kappa\beta_{3\zeta} = 0. \quad (1)$$

$$\left(\text{Here } \theta = \sphericalangle HNH,\ \lambda = \sqrt{1 - \tfrac{1}{3}\sin^2\frac{\theta}{2}},\ \kappa = \sqrt{1 - \tfrac{4}{3}\sin^2\frac{\theta}{2}}\right).$$

The 6 independent coordinates β_{nf} of NH_3 we express by the independent coordinates φ (variations of the bond angles N-H with the ζ axis) and ψ (rotations of the N-H bonds around the ζ axis).

$$(2)\quad \begin{cases} \beta_{1\xi} = \frac{2}{\sqrt{3}}\left(\sin\frac{\theta}{2}\right)\psi_1, \quad \beta_{1\eta} = \varphi_1, \quad \beta_{1\zeta} = \varphi_1; \\ \beta_{2\xi} = -\frac{1}{\sqrt{3}}\left(\operatorname{tg}\frac{\theta}{2}\right)\psi_2 - \frac{\sqrt{3}}{2}\cdot\frac{\kappa}{\cos\frac{\theta}{2}}\varphi_2, \\ \beta_{2\eta} = \frac{\sin\frac{\theta}{2}}{\lambda}\psi_2 - \frac{\kappa}{2\lambda}\varphi_2, \quad \beta_{2\zeta} = \varphi_2; \\ \beta_{3\xi} = -\frac{1}{\sqrt{3}}\operatorname{tg}\frac{\theta}{2}\psi_3 - \frac{\sqrt{3}}{2}\cdot\frac{\kappa}{\cos\frac{\theta}{2}}\varphi_3, \\ \beta_{3\eta} = -\frac{\sin\frac{\theta}{2}}{\lambda}\psi_3 - \frac{\kappa}{2\lambda}\varphi_3, \quad \beta_{3\zeta} = \varphi_3. \end{cases}$$

For SO_2

$$\beta_{1\xi} = \varphi_1, \quad \beta_{1\eta} = -\varphi_1, \quad \beta_{2\xi} = -\varphi_2, \quad \beta_{2\eta} = -\varphi_2,$$

where φ_1, φ_2 — are changes of the bond angles with the negative η axis. The molecules NH_3 and SO_2 belong respectively to the symmetry groups C_{3v} and C_{2v}. The symmetry coordinates have the form:

$$q^{A_1} = \frac{1}{\sqrt{3}}(q_1+q_2+q_3), \quad \alpha^{A_1} = \frac{1}{\sqrt{3}}(\alpha_{12}+\alpha_{13}+\alpha_{23}),$$
$$\varphi^{A_1} = \frac{1}{\sqrt{3}}(\varphi_1+\varphi_2+\varphi_3), \quad \psi^{E_{II}} = \frac{1}{\sqrt{2}}(\psi_2-\psi_3),$$
$$q^{E_{II}} = \frac{1}{\sqrt{6}}(2q_1-q_2-q_3), \quad \alpha^{E_{II}} = \frac{1}{\sqrt{6}}(2\alpha_{23}-\alpha_{12}-\alpha_{13}),$$
$$\varphi^{E_{II}} = \frac{1}{\sqrt{2}}(2\varphi_1-\varphi_2-\varphi_3).$$

In the case of NH_3

$$q^{A_1} = \frac{1}{\sqrt{2}}(q_1+q_2), \quad \gamma^{A_1}, \quad \varphi^{A_1} = \frac{1}{\sqrt{2}}(\varphi_1+\varphi_2),$$
$$q^{B_1} = \frac{1}{\sqrt{2}}(q_1-q_2), \quad \varphi^{B_1} = \frac{1}{\sqrt{2}}(\varphi_1-\varphi_2)$$

for SO_2. Expressing them in normal coordinates Q_l, we obtain $\left(S_k = \sum_l L_{kl}Q_l\right)$: for NH_3

$$q^{A_1} = \sum_{l=1}^{2} C_{ql}Q_l, \quad \alpha^{A_1} = \sum_{l=1}^{2} D_{\alpha l}Q_l, \quad \varphi^{A_1} = \sum_{l=1}^{2} E_lQ_l,$$
$$q^{E_{II}} = \sum_{l=3}^{4} C_{ql}Q_l, \quad \alpha^{E_{II}} = \sum_{l=3}^{4} D_{\alpha l}Q_l, \quad \varphi^{E_{II}} = \sum_{l=3}^{4} E_lQ_l,$$
$$\psi^{E_{II}} = \sum_{l=3}^{4} F_lQ_l;$$

for SO_2:

$$q^{A_1} = \sum_{l=1}^{2} C_lQ_l, \quad \gamma^{A_1} = \sum_{l=1}^{2} D_lQ_l, \quad \varphi^{A_1} = \sum_{l=1}^{2} E_lQ_l, \quad q^{B_1} = C_3Q_3,$$
$$\varphi^{B_1} = E_3Q_3.$$

The coefficients E_l, F_l are expressed as follows in terms of the coefficients D_l, C_{ql}, which are determined from the solution of the mechanical problem:

for NH_3

$$E_l = -\frac{1}{\sqrt{3}}\cdot\frac{\cos\frac{\theta}{2}}{\kappa}D_{\alpha l} \quad (l = 1, 2),$$

$$(3)\quad D_{\alpha l} = \frac{\sqrt{3}}{2}\cdot\frac{\kappa}{\cos\frac{\theta}{2}}E_l - \frac{\sqrt{3}}{2\cos\frac{\theta}{2}}F_l \quad (l = 3, 4);$$

$$(4)\quad 2\sqrt{3}\left(\sin\frac{\theta}{2}\right)m_HC_{ql} + \left(m_N + m_H\sin^2\frac{2\theta}{2}\right)E_l + m_NF_l = 0 \quad (l=3,4);$$

for SO_2

$$(5)\quad E_l = \frac{1}{\sqrt{2}}D_l \quad (l=1,2), \quad E_3 = \left(\frac{m_O\sin 2\theta}{m_S + 2m_O\sin^2\theta}\right)C_3.$$

We determine the relations (4) and (5) from the condition that the component of the moment of momentum be zero about the ξ-axis (for NH_3) and about the ζ-axis (for SO_2). Furthermore we obtain the following expressions for the derivatives of the dipole moment with respect to the normal coordinates $\frac{\partial p}{\partial Q_l}$ in the first approximation of the valence optical scheme:

for NH_3

$$\frac{\partial P_\zeta}{\partial q_l^{A_1}} = \sum_k \frac{\partial P_\zeta}{\partial S_k^{A_1}}L_{kl} = \left\{\left[-\kappa\sqrt{3}\left(\frac{\partial\mu_{NH}^{(1)}}{\partial q_1} + 2\frac{\partial\mu_{NH}^{(2)}}{\partial q_1}\right) - \right.\right.$$
$$\left.\left. -2\left(\sin\frac{\theta}{2}\right)\mu_{NH}\left(\frac{\partial\varphi_1}{\partial q_1} + 2\frac{\partial\varphi_2}{\partial q_1}\right)\right]C_{ql} + \left[-2\left(\sin\frac{\theta}{2}\right)\frac{\mu_{NH}}{r_{NH}} - \right.\right.$$
$$(6a)\qquad \left.\left. -2\kappa\sqrt{3}\left(\frac{\partial\mu_{NH}^{(1)}}{\partial\varphi_1} + 2\frac{\partial\mu_{NH}^{(2)}}{\partial\varphi_1}\right)\frac{1}{r_{NH}}\right]E_l\right\},$$
$$\frac{\partial P_\xi}{\partial q_l^{A_1}} = \frac{\partial P_\eta}{\partial q_l^{A_1}} = 0 \quad (l = 1,2);$$

$$\frac{\partial P_\eta}{\partial q_l^E} = \sum_k \frac{\partial P_\eta}{\partial S_k^E} L_{kl} = \left\{ \left[\sqrt{2} \left(\sin\frac{\theta}{2} \right) \left(\frac{\partial \mu_{NH}^{(1)}}{\partial q_1} - \frac{\partial \mu_{NH}^{(2)}}{\partial q_1} \right) - \right.\right.$$

$$- \kappa \sqrt{\frac{3}{2}}\, \mu_{NH} \left(\frac{\partial \varphi_1}{\partial q_1} - \frac{\partial \varphi_2}{\partial q_1} \right) \Big] C_{ql} + \left[- \kappa \sqrt{\frac{3}{2}} \cdot \frac{\mu_{NH}}{r_{NH}} + \right.$$

$$(6b) \quad + 2\sqrt{2} \left(\sin\frac{\theta}{2} \right) \left(\frac{\partial \mu_{NH}^{(1)}}{\partial q_1} - \frac{\partial \mu_{NH}^{(2)}}{\partial q_1} \right) \frac{1}{r_{NH}} \Big] E_l +$$

$$\left. + \left[- \sqrt{2} \left(\sin\frac{\theta}{2} \right) \frac{\mu_{NH}}{r_{NH}} \right] F_l \right\}; \quad \frac{\partial P_\xi}{\partial q_l^E} = \frac{\partial P_\zeta}{\partial q_l^E} = 0 \; (l = 3, 4);$$

for SO_2

$$\frac{\partial P_\eta}{\partial q_l^{A_1}} = \sqrt{2} \left\{ \left[- \left(\frac{\partial \mu_{SO}^{(1)}}{\partial q_1} + \frac{\partial \mu_{SO}^{(2)}}{\partial q_1} \right) \cos\theta + \mu_{SO} \left(\frac{\partial \varphi_1}{\partial q_1} + \frac{\partial \varphi_2}{\partial q_1} \right) \times \right.\right.$$

$$\left. \times \sin\theta \right] C_l + \left[\frac{\mu_{SO}}{r_{SO}} \sin\theta - 2 \left(\frac{\partial \mu_{SO}^{(1)}}{\partial \varphi_1} + \frac{\partial \mu_{SO}^{(2)}}{\partial \varphi_1} \right) \frac{\cos\theta}{r_{SO}} \right] E_l \Big\},$$

$$(7a) \qquad \frac{\partial P_\xi}{\partial q_l^{A_1}} = \frac{\partial P_\zeta}{\partial q_l^{A_1}} = 0 \; (l = 1, 2);$$

$$\frac{\partial P_\xi}{\partial q_3^{B_1}} = \sqrt{2} \left\{ - \left[\left(\frac{\partial \mu_{SO}^{(1)}}{\partial q_1} - \frac{\partial \mu_{SO}^{(2)}}{\partial q_1} \right) \sin\theta + \mu_{SO} \left(\frac{\partial \varphi_1}{\partial q_1} - \frac{\partial \varphi_2}{\partial q_1} \right) \cos\theta \right] C_3 - \right.$$

$$(7b) \qquad \left. - \left[\frac{\mu_{SO}}{r_{SO}} \cos\theta + 2 \left(\frac{\partial \mu_{SO}^{(1)}}{\partial \varphi_1} - \frac{\partial \mu_{SO}^{(2)}}{\partial \varphi_1} \right) \frac{\sin\theta}{r_{SO}} \right] E_3 \right\}^*,$$

$$\frac{\partial P_\eta}{\partial q_3^{B_1}} = \frac{\partial P_\zeta}{\partial q_3^{B_1}} = 0.$$

3. In order to calculate the coefficients D_l, C_l, the mechanical problem was solved. In the case of NH_3 and PH_3 we used the force constants and the mull frequencies quoted in [7]. The force constants for SO_2 were taken from [11]. Using these coefficients, and with the help of formulas (3) - (5), we computed the coefficients E_l, F_l (See Table 1).

In the calculation we used the following parameters: for NH_3 [12] $\theta = 106°47'$, $r_{NH} = 1.014$ Å; for PH_3 [13] $\theta = 93°30'$, $r_{PH} = 1.419$ Å; for SO_2 [13] $r_{SO} = 1.432$ Å, $\angle OSO = 2\theta = 119°53'$. Having substituted into formulas (6), (7), the experimental values of $\frac{\partial P}{\partial q_l}$ and coefficients C_{ql}, E_l, F_l, we obtain a system of equations, from which we calculate the derivatives of the dipole moment with respect to the symmetry coordinates $\frac{\partial P}{\partial S_k}$ of the molecules NH_3, PH_3, and SO_2.

Table 1

Coefficients C_{ql}, E_l, F_l, NH_3, PH_3 and SO_2 (in units 10^{12} $g^{-\frac{1}{2}}$)

Molecule		Type of Symmetry A_1		Type of Symmetry E	
		q_1	q_2	q_3	q_4
NH_3	q	0.7792	-0.0141	0.8065	0.0513
	φ	-0.0493	-0.8271	-0.043	0.2387
	ψ	—	—	-0.0256	-0.7643
PH_3	q	0.784	0.0075	0.7862	-0.0059
	φ	0.0415	-0.8012	-0.0142	0.3524
	ψ	—	—	-0.0364	-0.696
				Type of Symmetry B_1	
SO_2	q	0.2168	0.0052	0.2562	—
	φ	-0.0805	0.2432	0.0635	—

(For NH_3 and PH_3 the experimental data of [7] were used. In the case of SO_2 the most accurate and reliable experimental values of $\frac{\partial P}{\partial q_l}$ were obtained in the paper of Mayhood [6], in which the experimental data of the two preceding papers [4-5] are critically analyzed.) In Table 2, the values $\frac{\partial P}{\partial S_k}$ for NH_3 and PH_3 are quoted corresponding to the different sign combinations of $\frac{\partial P}{\partial q_l}$. In Table 2, for symmetry A_1 there are quoted two sets of values $\frac{\partial P}{\partial S_k^{A_1}}$, pertaining to the two sign combinations $\frac{\partial P}{\partial q_1^{A_1}}$, and $\frac{\partial P}{\partial q_2^{A_1}}$: (+ +) and (+ −). To the remaining two combinations of signs of $\frac{\partial P}{\partial q_{1,2}^{A_1}}$ (− −) and (− +) correspond the values $\frac{\partial P}{\partial S^{A_1}}$, distinguished from those quoted in Table 2 only through the sign. For symmetry vibration type E of NH_3 and PH_3, for the calculation of the three magnitudes $\frac{\partial P}{\partial S^E}\left(\frac{\partial P}{\partial q^E}, \frac{\partial P}{\partial \varphi^E} \text{ and } \frac{\partial P}{\partial \psi^E}\right)$ one must employ the two equations (6b). In the case of the third equation it is necessary to use the expression for the dipole moment of the molecules

* If $\frac{\partial \mu_{SO}^{(2)}}{\partial q_1} = \frac{\partial \varphi_1}{\partial q_1} = \frac{\partial \varphi_2}{\partial q_1} = \frac{\partial \mu_{SO}^{(1)}}{\partial \varphi_1} = \frac{\partial \mu_{SO}^{(2)}}{\partial \varphi_1} = 0$, our formulas (7a) and (7b) transform to within a normalizing factor into the corresponding formulas (21, 40) and (21, 42) of monograph [1].

NH_3 (or PH_3): $\mu_{NH_3} = 3\kappa\mu_{NH}$. We applied an analogous method earlier in the calculation of the electro-optical parameters of methyl halides [9].

Table 2

Derivatives of the Dipole Moment with Respect to the Symmetry Coordinates $\frac{\partial P}{\partial S}$ of NH_3 and PH_3 (in units D/Å).

Molecule	Derivative of the dipole moment	Signs of $\frac{\partial P}{\partial Q^{A_1}_{1,2}}$ (++)	(+−)	Derivative the dipole moment	Signs of $\frac{\partial P}{\partial Q^{E}_{3,4}}$ (++)	(+−)	(−+)	(−−)
NH_3	$\frac{\partial P}{\partial q^{A_1}}$	0.2911	0.5029	$\frac{\partial P}{\partial q^{E}}$	−0.0233	−0.2085	−0.3766	−0.5618
	$\frac{\partial P}{\partial q^{A_1}}$	−1.6794	1.6659	$\frac{\partial P}{\partial q^{E}}$	−2.9191	−6.3926	−0.8432	−6.3167
PH_3	$\frac{\partial P}{\partial q^{A_1}}$	1.1957	1.128	$\frac{\partial P}{\partial q^{E}}$	0.8204	0.7789	−0.8193	−0.8608
	$\frac{\partial P}{\partial q^{A_1}}$	−0.6288	0.6504	$\frac{\partial P}{\partial q^{E}}$	0.6748	−1.6196	0.6472	−1.6472

By this same means, we may also treat the other cases in the calculations of electro-optical parameters of dipole molecules. This is connected with the fact that for dipolar molecules rotations and some normal vibrations belong to one type of symmetry and the connection between them is expressed by the additional term in the formulas for the derivatives of the dipole moment $\frac{\partial P}{\partial Q_l}$. For the determination of this additional term we employ first the condition that the component of angular momentum be zero, and secondly the expression for the dipole moment of the molecule. For non-dipolar molecules having a center of symmetry or belonging to the symmetry groups T_d and D_{nh}, these two conditions are automatically fulfilled. Introducing μ_{NH} into (6b), it is possible to calculate $\frac{\partial P}{\partial q^E}$ and $\frac{\partial P}{\partial \varphi}_E$ according to the formulas $\frac{\partial P_\eta}{\partial S}_E = \sum_{l=3}^{4} L^{-1}_{lk} \times \left[\frac{\partial P_\eta}{\partial Q_l} + \frac{\sqrt{2}}{3\kappa}\left(\sin\frac{\vartheta}{2}\right)\frac{\mu_{NH}}{r_{NH}} F_l\right]$. In this case the quantities $\frac{\partial P}{\partial S}_E$ have different values for the various signs of $\frac{\partial P}{\partial Q_l}$. The values $\frac{\partial P}{\partial S}_E$, are quoted in Table 2 corresponding to the four different sign combinations of $\frac{\partial P}{\partial Q_l}$. Further, combining the derivatives $\frac{\partial P}{\partial S^{A_1}}$ and $\frac{\partial P}{\partial S^{E}}$ for the two types of symmetry, we find the expressions for the electro-optical parameters $\left[\frac{\partial \mu^{(1)}_{NH}}{\partial q_1}\right]$, $\left[\frac{\partial \mu^{(1)}_{NH}}{\partial q_1}\right]$, $\frac{\partial \mu^{(1)}_{NH}}{\partial \varphi_1}$, $\frac{\partial \mu^{(2)}_{NH}}{\partial \varphi_1}$.

In Tables 3 and 4, are listed the numerical values of these parameters for the 16 different sign combinations of $\frac{\partial P}{\partial Q^{A_1}_{1,2}}$ and $\frac{\partial P}{\partial Q^{E}_{3,4}}$. In an analogous manner, in the case of SO_2, we calculate the parameters $\left[\frac{\partial \mu^{(1)}_{SO}}{\partial q_1}\right]$, $\left[\frac{\partial \mu^{(2)}_{SO}}{\partial q_1}\right]$, $\left[\frac{\partial \mu_{SO}}{\partial \varphi}\right]$, by combining the the signs of $\frac{\partial P}{\partial S^{A_1}}$ and $\frac{\partial P}{\partial S^{B_1}}$ (see Table 5). In addition to this we find the values μ_{SO} in the very same way as for NH_3 with the aid of the expression for the dipole moment of the molecule SO_2: $\mu_{SO_2} = 2(\cos\tfrac{\vartheta}{2})\mu_{SO}$. Next we need to select the correct values of these parameters. Usually for the selection of the correct values of the electro-optical parameters from the various possible alternatives, one prefers the data according to the intensities of the infra-red bands of the isotope-substituted molecules. However, in our case such data are lacking. Therefore it is necessary to avail oneself of other criteria. From the results of the calculations which we quoted earlier for other molecules [8-10], it is possible to formulate the following conditions, by which it is necessary to be guided in the selection of the correct values of the electro-optical parameters. Firstly, the derivatives of the dipole moment with respect to the variation of its own bond length or with respect to the angle of contact ought to be greater than the derivatives with respect to the changes of the neighboring bond lengths and angles: $\left[\frac{\partial \mu^{(1)}_{NH}}{\partial q_1}\right] \gg \left[\frac{\partial \mu^{(2)}_{NH}}{\partial q_1}\right]$, $\left[\frac{\partial \mu^{(1)}_{NH}}{\partial \varphi_1}\right] \gg \left[\frac{\partial \mu^{(2)}_{NH}}{\partial \varphi_1}\right]$. Secondly, the derivatives of the bond dipole moments with respect to the change in the angles $\frac{\partial \mu}{\partial \varphi}$ ought to be minima. Thirdly, the derivative of the dipole moment with respect to the change in bond length $\frac{\partial \mu^{(t)}_i}{\partial q_i}$ and and dipole moment of the bond $\mu^{(t)}$ ought to have different signs. Applying these criteria to NH_3 and PH_3, we arrive at the conclusion that they are simultaneously fulfilled best for the third alternative: $-\left(\frac{\partial P}{\partial Q^{A_1}_1}\right)$, $-\left(\frac{\partial P}{\partial Q^{A_1}_2}\right)$, $+\left(\frac{\partial P}{\partial Q^{E}_3}\right)$, $-\left(\frac{\partial P}{\partial Q^{E}_4}\right)$, (both in the case of ammonia and phosphine). In the case of SO_2 the indicated criteria are best fulfilled simultaneously for the first alternative: $+\left(\frac{\partial P}{\partial Q^{A_1}_1}\right)$, $+\left(\frac{\partial P}{\partial Q^{A_1}_2}\right)$, $+\left(\frac{\partial P}{\partial Q^{B_1}_3}\right)$. In Tables 6 and 7 are presented the systems of electro-optical parameters of the molecules NH_3, PH_3 and SO_2 corresponding to these alternatives.

4. The results obtained permit one to make some general conclusions. First of all the calculation made shows that there is no discrepancy whatsoever between the values of the dipole moments determined from infra-red spectra and those from static values of the dipole moments. This is explained by the fact that, in the first place, in the calculation, we always determine $\mu^{(t)}$ in combination with some

Table 3

Electro-optical parameters of NH_3 (in units D/Å) for the various combinations of signs of $\frac{\partial P}{\partial q^{A_1}_{1,2}}$ and $\frac{\partial P}{\partial q^{E}_{3,4}}$.

Electro-Optical Parameters	Signs of $\frac{\partial P}{\partial q^{A_1}_{1,2}}$ (higher order) and of $\frac{\partial P}{\partial q^{A_1}_{3,4}}$ (lower order).							
	$\begin{matrix}(-&-)\\(-&-)\end{matrix}$	$\begin{matrix}(-&-)\\(-&+)\end{matrix}$	$\begin{matrix}(-&-)\\(+&-)\end{matrix}$	$\begin{matrix}(-&-)\\(+&+)\end{matrix}$	$\begin{matrix}(-&+)\\(-&-)\end{matrix}$	$\begin{matrix}(-&+)\\(-&+)\end{matrix}$	$\begin{matrix}(-&+)\\(+&-)\end{matrix}$	$\begin{matrix}(-&+)\\(+&+)\end{matrix}$
$\left[\frac{\partial \mu^{(1)}_{NH}}{\partial q_1}\right]^*$	0.163	0.2717	0.3705	0.4792	0.2716	0.3804	0.4791	0.5878
$\left[\frac{\partial \mu^{(2)}_{NH}}{\partial q_1}\right]^*$	0.1425	0.0881	0.0387	-0.0157	0.2511	0.1967	0.1473	0.0929
$\frac{1}{r_{NH}}\left(\frac{\partial \mu^{(1)}_{NH}}{\partial \varphi_1}\right)$	0.7828	1.8027	0.7605	1.7804	1.6405	2.6604	1.6183	2.6381
$\frac{1}{r_{NH}}\left(\frac{\partial \mu^{(2)}_{NH}}{\partial \varphi_1}\right)$	-0.2422	-0.7521	-0.231	-0.741	0.6156	0.1056	0.6267	0.1168
	$\begin{matrix}(+&+)\\(-&-)\end{matrix}$	$\begin{matrix}(+&+)\\(-&+)\end{matrix}$	$\begin{matrix}(+&+)\\(+&-)\end{matrix}$	$\begin{matrix}(+&+)\\(+&+)\end{matrix}$	$\begin{matrix}(+&-)\\(-&-)\end{matrix}$	$\begin{matrix}(+&-)\\(-&+)\end{matrix}$	$\begin{matrix}(+&-)\\(+&-)\end{matrix}$	$\begin{matrix}(+&-)\\(+&+)\end{matrix}$
$\left[\frac{\partial \mu^{(1)}_{NH}}{\partial q_1}\right]^*$	-0.1356	-0.0269	0.0719	0.1806	-0.2442	-0.1355	-0.0368	0.072
$\left[\frac{\partial \mu^{(2)}_{NH}}{\partial q_1}\right]^*$	0.1561	-0.2105	0.2599	-0.3143	-0.2647	-0.3191	-0.3685	-0.4229
$\frac{1}{r_{NH}}\left(\frac{\partial \mu^{(1)}_{NH}}{\partial \varphi_1}\right)$	1.644	2.6639	1.6217	2.6416	0.7863	1.8061	0.764	1.7839
$\frac{1}{r_{NH}}\left(\frac{\partial \mu^{(2)}_{NH}}{\partial \varphi_1}\right)$	0.619	0.1091	0.6302	0.1202	-0.2387	-0.7487	-0.2276	-0.7375

*See Table 6

Table 4

Electro-optical parameters of PH_3 (in units D/Å) for the various combinations of signs of $\frac{\partial P}{\partial q^{A_1}_{1,2}}$ and $\frac{\partial P}{\partial q^{E}_{3,4}}$.

Electro-Optical Parameters	Signs of $\frac{\partial P}{\partial q^{A_1}_{1,2}}$ (higher order) and of $\frac{\partial P}{\partial q^{E}_{3,4}}$ (lower order).							
	$\begin{matrix}(-&-)\\(-&-)\end{matrix}$	$\begin{matrix}(-&-)\\(-&+)\end{matrix}$	$\begin{matrix}(-&-)\\(+&-)\end{matrix}$	$\begin{matrix}(-&-)\\(+&+)\end{matrix}$	$\begin{matrix}(-&+)\\(-&-)\end{matrix}$	$\begin{matrix}(-&+)\\(-&+)\end{matrix}$	$\begin{matrix}(-&+)\\(+&-)\end{matrix}$	$\begin{matrix}(-&+)\\(+&+)\end{matrix}$
$\left[\frac{\partial \mu^{(1)}_{PH}}{\partial q_1}\right]^*$	-0.1056	-0.0787	0.9556	0.9825	-0.1297	-0.1028	0.9315	0.9584
$\left[\frac{\partial \mu^{(2)}_{PH}}{\partial q_1}\right]^*$	0.6908	0.6774	0.1602	0.1468	0.6668	0.6533	0.1362	0.1227
$\frac{1}{r_{PH}}\left(\frac{\partial \mu^{(1)}_{PH}}{\partial \varphi_1}\right)$	-0.3195	0.4229	-0.3106	0.4319	-0.092	0.6505	-0.0831	0.6594
$\frac{1}{r_{PH}}\left(\frac{\partial \mu^{(2)}_{PH}}{\partial \varphi_1}\right)$	0.0848	-0.2864	0.0804	-0.2909	0.3124	-0.0589	0.3079	-0.0633

*See Table 6

Table 4 (Continued)

Electro-optical parameters of PH_3 (in units D/Å) for the various combinations of signs of $\frac{\partial P}{\partial q^{A_1}_{1,2}}$ and $\frac{\partial P}{\partial q^{E}_{3,4}}$.

Electro-Optical Parameters	Signs of $\frac{\partial P}{\partial q^{A_1}_{1,2}}$ (higher order) and of $\frac{\partial P}{\partial q^{E}_{3,4}}$ (lower order).							
	(+ +) (− −)	(+ +) (− +)	(+ +) (+ −)	(+ +) (+ +)	(+ −) (− −)	(+ −) (− +)	(+ −) (+ −)	(+ −) (+ +)
$\left[\frac{\partial \mu^{(1)}_{PH}}{\partial q_1}\right]^*$	-0.9563	-0.9295	0.1049	0.1317	-0.9322	-0.9054	0.1289	0.1558
$\left[\frac{\partial \mu^{(2)}_{PH}}{\partial q_1}\right]^*$	-0.1599	-0.1731	-0.6905	-0.7039	-0.1358	-0.1492	-0.6664	-0.6798
$\frac{1}{r_{PH}}\left(\frac{\partial \mu^{(1)}_{PH}}{\partial q_1}\right)$	-0.0958	0.6466	-0.0869	0.6555	-0.3234	0.4191	-0.3144	0.428
$\frac{1}{r_{PH}}\left(\frac{\partial \mu^{(2)}_{PH}}{\partial q_1}\right)$	0.3085	-0.0627	0.3041	-0.0672	0.081	-0.2902	0.0765	-0.2947

*See Table 6.

Table 5

Electro-Optical parameters of SO_2 (in units D/Å) for the various combinations of signs of $\frac{\partial P}{\partial q^{A_1}_{1,2}}$ and $\frac{\partial P}{\partial q^{B_1}_{3}}$.

Electro-Optical Parameters	Signs of $\frac{\partial P}{\partial q^{A_1}_{1,2}}$ (higher order) and of $\frac{\partial P}{\partial q^{B_1}_{3}}$ (lower order)							
	$(+_{+}+)$	(+ +) −	(+ −) +	(+ −) −	(− −) −	(− −) +	(− +) −	(− +) +
$\left[\frac{\partial \mu^{(1)}_{SO}}{\partial q_1}\right]^*$	-5.2706	-0.0026	-3.9101	-1.3579	5.1116	-0.1565	3.7511	-1.517
$\left[\frac{\partial \mu^{(2)}_{SO}}{\partial q_1}\right]^*$	0.1565	-5.1116	1.517	-3.7511	0.0026	-5.2706	-1.3579	3.9101
$\frac{1}{r_{SO}}\left[\frac{\partial \mu^{(1)}_{SO}}{\partial q_1}\right]^*$	-0.8336	-0.8336	2.8291	2.8291	2.7489	2.7489	-0.9138	-0.9138

*See Table 7.

kind of other electro-optical parameters (and therefore it is completely natural that these combinations should differ from $\mu^{(t)}_{st}$) and, secondly, for the calculation, we always draw upon the relation connecting the dipole moment of the molecule with the dipole moment of the separate bonds in the form of a supplementary condition, and therefore the possibility of a discrepancy between $\mu^{(t)}_{vib}$ and $\mu^{(t)}_{st}$ cannot arise. In particular, in the case of dipolar molecules, for which all bonds are equivalent (for example, NH_3, SO_2,), only a knowledge of the static dipole moment of the molecule is necessary to perform the calculation of the bond dipole moment. In this case, if in the molecule there are bonds of various types (for example methyl halides) then besides the dipole moment of the molecule, it is necessary also to know the infrared band intensities.

Further, the comparison of bond dipole moments $\mu^{(t)}$ and derivatives of dipole moments with respect to the bond length $\frac{\partial \mu^{(t)}}{\partial q_i}$ of NH_3 and PH_3 shows that in constrast to the prevailing notion, a proportionality between these quantities does not occur: in the case of NH_3: $\frac{\mu_{NH}}{r_{NH}} \gg \frac{\partial \mu^{(1)}_{NH}}{\partial q_1}$, while for PH_3 $\frac{\mu_{PH}}{r_{PH}} \ll \frac{\partial \mu^{(1)}_{PH}}{\partial q_1}$.

Table 6

Electro-Optical Parameters of Ammonia and Phosphine (in Units D/Å)

Electro-Optical Parameters	NH_3	PH_3
μ_{NH} (in units D)	-1.3057	-0.3389
$\frac{\mu_{NH}}{r_{NH}}$	-1.2877	-0.2388
$\left[\frac{\partial\mu^{(1)}_{NH}}{\partial q_1} + \frac{\mu_{NH}}{\kappa\sqrt{3}\sin\frac{\theta}{2}}\left(-\cos\theta\frac{\partial\varphi_1}{\partial q_1} + \frac{\partial\varphi_2}{\partial q_1}\right)\right]$	0.3705	0.9556
$\left\{\frac{\partial\mu^{(2)}_{NH}}{\partial q_1} + \frac{\mu_{NH}}{2\kappa\sqrt{3}\sin\frac{\theta}{2}}\left[\frac{\partial\varphi_1}{\partial q_1} - \left(1-4\sin^2\frac{\theta}{2}\right)\frac{\partial\varphi_2}{\partial q_1}\right]\right\}$	0.0387	0.1602
$\frac{1}{r_{NH}}\left(\frac{\partial\mu^{(1)}_{NH}}{\partial q_1}\right)$	0.7605	-0.3106
$\frac{1}{r_{NH}}\left(\frac{\partial\mu^{(2)}_{NH}}{\partial q_1}\right)$	-0.231	0.0804

Table 7

Electro-Optical Parameters of Sulfur Dioxide (in Units D/Å)

Electro-Optical Parameters	SO_2
μ_{SO} (in units D)	1.5872
$\frac{\mu_{SO}}{r_{SO}}$	1.1084
$\left\{\frac{\partial\mu^{(1)}_{SO}}{\partial q_1} + \mu_{SO}\left[(ctg2\theta)\frac{\partial\varphi_1}{\partial q_1} - (cosec2\theta)\frac{\partial\varphi_2}{\partial q_1}\right] + a\left(\frac{\partial\mu^{(1)}_{SO}}{\partial\varphi_1} - \frac{\partial\mu^{(2)}_{SO}}{\partial\varphi_1}\right)\frac{1}{r_{SO}}\right\}^*$	-5.2706
$\left\{\frac{\partial\mu^{(2)}_{SO}}{\partial q_1} + \mu_{SO}\left[(cosec2\theta)\frac{\partial\varphi_1}{\partial q_1} + (ctg2\theta)\frac{\partial\varphi_2}{\partial q_1}\right] - a\left(\frac{\partial\mu^{(1)}_{SO}}{\partial\varphi_1} - \frac{\partial\mu^{(2)}_{SO}}{\partial\varphi_1}\right)\frac{1}{r_{SO}}\right\}^*$	0.1565
$\frac{1}{r_{SO}}\left[\frac{\partial\mu^{(1)}_{SO}}{\partial\varphi_1} + \frac{\partial\mu^{(2)}_{SO}}{\partial\varphi_1}\right]$	0.8336

*Here $a = \frac{m_o \sin 2\theta}{m_S + 2m_o\sin^2\theta}$.

Two means are available to explain this: 1) Since we compute $\frac{\partial\mu^{(i)}}{\partial q_i}$ not in exact form, but in combination with other parameters $\frac{\partial\varphi}{\partial q}$, then it is possible that the magnitude of these additional terms for NH_3 and PH_3 is different; 2) the curves giving the dependence of the bond dipole moment upon the variation of the bond length have different slopes for NH_3 and PH_3: in the case of NH_3 the curve in the equilibrium position is shallower than the curve for PH_3. Preference should be given to the second explanation, because in the first case in order that the quantities $\frac{\mu}{r}$ and $\frac{\partial\mu}{\partial q}$ should change proportionately in the transition from NH_3 to PH_3, it is necessary to equate $\frac{\partial\varphi}{\partial q}$ to some units, which is hardly possible. Thus we come to the extremely important conclusion that in distinction to ionized diatomic molecules, propotionality between the behavior of $\frac{\mu}{r}$ and $\frac{\partial\mu}{\partial q}$ is absent. Finally, let us look at the question of the sign of the dipole moments of bonds of NH_3, PH_3 and SO_2. The calculation is unable to produce the absolute sign of μ; however, from the values of the electronegativities of atoms it is possible to conclude that the negative end of the dipole $\mu_{NH}(\mu_{PH})$ is located on the nitrogen (phosphorus) atom, and the positive end is at the hydrogen atom. In the case of SO_2 the negative end of the dipole is located on the hydrogen atom and the positive end on the sulfur atom. The signs of μ in Tables 6, 7 correspond to the indicated direction of the dipole moments.

October 24, 1958

References

1. M.V.VOL'KENSHTEIN, M.A.EL'IASHEVICH, B.I.STEPANOV: Kolebaniia molekul (Vibrations of Molecules) 2, GITTL, Moscow, (1949)
2. M.V.VOL'KENSHTEIN: Stroenie i fizicheskie svoistva molekul (Structure and Physical Properties of Molecules) Akad. NAUK Press, Moscow-Leningrad, 1955
3. D.F.HORNIG, D.C.McKEAN: J. Phys. Chem., 59, 1133, (1955)
4. D.F.EGGERS, J.C.HISATSUNE, Z. van ALTEN: J. Phys. Chem., 59, 1124, (1955)
5. J. MOREILLO, J. HERRANZ: Anal. real. Soc. exper. fis. quim, A52, No. 9-10, 207, 217, Madrid, (1956)
6. J.E.MAYHOOD: Canad. J. Phys., 35, 954, (1957)
7. D.C.McKEAN, P.N.SCHATZ: J. Chem Phys., 24, 316 (1956)
8. L.M.SVERDLOV: OiS, 4, 697, (1958) (See this volume)
9. L.M.SVERDLOV: OiS, 6, 729, 1959 (See 6,477)
10. L.M.SVERDLOV: OiS, 7, 21, 1959 (See 7, 11)
11. S.R.POLO, M.K.WILSON: J. Chem. Phys., 22, 900, (1954); D. KIVELSON: J. Chem. Phys.
12. G. HERTZBERG: Vibrational and Rotational Spectra of Polyatomic Molecules. (IL, Moscow, 1949)
13. W. GORDY, W. SMITH, R. TRAMBARULO: Radio Spectroscopy (GITTL, Moscow, 1955)

TOM VII, Vyp. 2 OPTIKA I SPEKTROSKOPIIA Avgust, 1959
VOL. VII, No. 2 OPTICS AND SPECTROSCOPY August, 1959

On the Question of Force Constants of the Cyclopentane Molecule

R. S. LEBEDEV AND A. V. SECHKAREV

Abstract: By the method of variation of the force constants the dynamic coefficients of the cyclopentane molecule were determined. The results were compared with data available for molecules of similar structure. A comparison was made of calculated frequencies with experimentally determined frequencies for the spectra of cyclopentane and deuterocyclopentane.

In a previous communication one of us [1] has given a full calculation of frequencies and forms of the normal vibrations of the cyclopentane and deuterocyclopentane molecules from a mechanical model, using values for the force constants adopted from other molecules. Under this circumstance the differences between calculated and experimental values were as great as 200 cm^{-1}. The present work has as its purpose a more exact determination of the values of the force constants of the cyclopentane molecule.

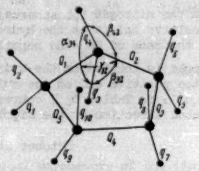

Large circles = carbon atoms
Small circles = hydrogen atoms

It was assumed in the calculations that the cyclopentane molecule possesses exact D_{5h} symmetry [1, 2]. The total number of vibrational degrees of freedom of the cyclopentane molecule are 39. By taking into account degeneracy they are reduced to 23, of which, on the strength of symmetry, vibrations of types A'_2, A''_1 and E''_2 (see table 2) are inactive both in the Raman and in the IR absorption spectra [3]. Thus we can expect only 17 lines to appear in the spectra, corresponding to the normal vibrations of the molecules. The number of independent dynamic coefficients K_{ij} in the expression of the potential energy

$$V = \frac{1}{2}\sum K_{ij}x_i x_j,$$

according to reference [4], is determined by the formula

$$N_k = \sum_S \frac{n_s(n_s+1)}{2}, \quad S = A'_1, A'_2, \ldots, E'_2,$$

and is equal to 52 in the case we are considering. If we take into account here additional relations between coefficients, connected with the motion of the molecules as a whole, and exclude from consideration non-planar vibrations of the ring*, then the total number of independent dynamic coefficients subject to determination, are shown to be equal to 43.

Table 1

Matrix Elements of the Dynamic Interactions of Cyclopentane

	q_5	β_{15}	β_{25}	q_1	α_{12}	γ_{15}	q_2	β_{11}	β_{21}
q_5	K_q	A_β	A_β	h_q	B_α	A_γ	h_q	B_β	B_β
β_{15}	A_β	K_β	l^q_β	a_β	$l_{\alpha\beta}$	l_β	b_β	l^q_β	o_β
β_{25}	A_β	l^q_β	K_β	b_β	$l_{\alpha\beta}$	$l_{\beta\gamma}$	a_β	o_β	l^q_β
q_1	h_q	a_β	b_β	K_q	a_α	b_γ	h	a_β	b_β
α_{12}	B_α	$l_{\alpha\beta}$	$l_{\alpha\beta}$	a_α	K_α	$o_{\alpha\gamma}$	a_α	$l_{\alpha\beta}$	$l_{\alpha\beta}$
γ_{15}	A_γ	$l_{\beta\gamma}$	$l_{\beta\gamma}$	b_γ	$o_{\alpha\gamma}$	K_γ	b_γ	$l_{\beta\gamma}$	$l_{\beta\gamma}$
q_2	h_q	b_β	a_β	h	a_α	b_γ	K_q	b_β	a_β
β_{11}	B_β	l^q_β	o_β	a_β	$l_{\alpha\beta}$	$l_{\beta\gamma}$	b_β	K_β	l^q_β
β_{21}	B_β	o_β	l^q_β	b_β	$l_{\alpha\beta}$	$l_{\beta\gamma}$	a_β	l^q_β	K_β
q_1	H	B_β	B_β	h_q	B_α	A_γ	h_q	A_β	A_β
β_{31}	D_β	r_β	p_β	c_β	$r_{\alpha\beta}$	$n_{\gamma\beta}$	d_β	m_β	n_β
β_{41}	D_β	P_β	r_β	d_β	$r_{\alpha\beta}$	$n_{\gamma\beta}$	c_β	n_β	m_β
q_3	-	-	-	-	-	d_γ	-	c_β	d_β
α_{34}	-	-	-	-	-	$P_{\alpha\gamma}$	-	$r_{\alpha\beta}$	$r_{\alpha\beta}$
γ_{12}	C_γ	$r_{\beta\gamma}$	$r_{\beta\gamma}$	d_γ	$P_{\alpha\gamma}$	m_γ	d_γ	$n_{\gamma\beta}$	$n_{\gamma\beta}$
q_4	-	-	-	-	-	d_γ	-	d_β	c_β
β_{32}	-	-	-	-	-	$r_{\beta\gamma}$	-	r_β	p_β
β_{42}	-	-	-	-	-	$r_{\beta\gamma}$	-	p_β	r_β
q_2	-	-	-	-	-	C_γ	-	D_β	D_β
β_{52}	-	-	-	-	-	$t_{\gamma\beta}$	-	u_β	v_β
β_{62}	-	-	-	-	-	$t_{\gamma\beta}$	-	v_β	u_β
γ_{23}	-	-	-	-	-	S_γ	-	$t_{\gamma\beta}$	$t_{\gamma\beta}$

The choice and symbols of the quasi-elastic constants of the cyclopentane molecule are clear from the figure.** In Table 1 are presented 144 matrix elements of dynamic interactions which represent 43 different quasi-elastic constants. The matrices of potential coefficients were calculated by the method of El'iashevich [4]. The listing of the matrices according to symmetry taking into account additional relationships was carried out by the method of Maiants [5]. A general form of the matrices for different

*In the calculations we did not consider vibrations connected with non-planarity of carbon atoms in the ring, which define a twice degenerate frequency of the symmetry type E''_2, forbidden in the spectrum.

** For details concerning this see the preceding communication [1].

Table 2

Type of vibration	Activity	Cyclopentane C_5H_{10} Calculated frequencies: Correlation	Calculated frequencies: ν cm^{-1}	Experimental Data: Kohlrausch and Seka [12] (Raman Spectrum)	Rosenbaum and Jacobson [13] (Raman Spectrum)	Miller and Inskeep [14] (Raman Spectrum)	Landsberg et al. [7] (Raman Spectrum)	Miller and Inskeep [14] (Infrared Spectrum)	Deuterocyclopentane C_5D_{10} Calculated frequencies: Correlation	Calculated frequencies: ν cm^{-1}	Experimental data: Miller and Inskeep [14] Raman Spectrum	Experimental data: Miller and Inskeep [14] Infrared Spectrum
A_1'	Raman Spectrum	C-H	2972	2941(12B)	2943(7B)	2906(4B)	2937(2?0) 2949(2?0)		C-D	2141	2151(8)	—
		H-C-H	1492	1480(1)	1482(1B)	1487(1)	1486(1)		D-C-D	1150	?	—
		C-C	882	886(9)	888(10)	886(9)	889(150B)		C-C	786	802(9)	—
A_2'	Forbidden	—	—	—	—	—	—	—	—	—	—	—
A_1''	Forbidden	—	—	—	—	—	—	—	—	—	—	—
A_2''	Infrared Spectrum	C-H	2943		—	—	—	2960(10)	C-D	2155	—	2220(10)
		H-C-H	955	973(½)	—	—	961(0)	964(3)	D-C-D	701		686(0)
E_2''	Forbidden	—	—	—	—	—	—	—	—	—	—	—
E_1''	Raman Spectrum	C-H	3016	2964(10)	2970(6)	2966(9B)	2969(180B)		C-D	2263	2214(6B)	
		H-C-C	1186	1216(1)	?	1207(3B)	1181(3) 1227(3)		D-C-C	937	937(5B)	
		H-C-C	1104	1102(1)	?	1104(1)	1103(0)		D-C-C	794	778(1)	
E_1'	Infrared Spectrum	C-H	2887	—	—	—	—	2890(10)	C-D	2122	—	2125(10)
		C-C	928	—	—	—	—	896(8)	C-C	777	—	738(6)
		H-C-H	1461	—	—	—	—	1456(9)	D-C-D	1104	—	1064(6)
		H-C-C	1300	—	—	—	1311(1)	1316(4)	D-C-C	1105	—	1155(3)
E_2'	Raman Spectrum	C-H	2879	2966(10)	2869(10)	2904(4B)	2870(240)	—	C-D	2110	2108(8)	—
		C-C-C	542	589(0)	?	?	628(0B)	546(3)	C-C-C	464	?	438(1)
		H-C-C	1278	1284(2)	1298(1)	1283(2B)	1263(3) 1283(3)	1264(3B)	D-C-C	1014	1064(3B)	—
		H-C-H	1411	1446(5)	1448(5B)	1453(4B)	1449(40B)	—	D-C-D	1092	1124(4B)	—
		C-C	1012	1028(4B)	1032(5)	1030(5B)	1031(45B)	1033(1)	C-C	891	937(5B)	943(1)

Note : Figures in parenthesis after values of the frequencies express the relative intensity of the spectral lines; B - broadened band.

types of symmetry ($G = 3A_1' + A_2' + A_2'' + 4E_2'' + 3E_1'' + 4E_1' + 5E_2'$) was published earlier [1].

In the determination of the force constants of the cyclopentane and deuterocyclopentane molecules some of the dynamic coefficients were set equal to zero beforehand on the strength of physical considerations. This applies to those which correspond to interaction of the most remote bonds. Determination of the values of the coefficients which differ from zero was carried out during their modification by the method of successive approximations [4]. In the variation of the coefficients values of the derivatives of the frequencies with respect to the force constants [6] were used. Correctness of the correlation of frequencies was checked by comparison of the spectra of cyclopentane and deuterocyclopentane with application of the Teller-Redlich rule. The degree of correlation between the results of the calculation and experiment is illustrated in table 2. In table 3 are presented our values for the force constants (the force constants which do not appear in this table were set equal to zero). From the data presented it is evident that many of the calculated frequencies of the cyclopentane molecule are found within the limits of scatter of the experimental values. However in separate cases the discrepancies are as large as 40-50 cm^{-1}. The fact deserves notice that lines were discovered experimentally in the spectra which should be inactive according to selection rules. This applies to the frequencies underlined in table 2. Thus, in the Raman spectrum of cyclopentane, according to the latest data [7], the existence is mentioned of lines at 961 and 1311 cm^{-1} of such little intensity that they were evidently not found in other work. According to the selection rule they ought to be active only in the infrared absorption spectrum (where they are indeed present, and have sizeable intensities). And, on the contrary, lines at 546, 1264 and 1033 cm^{-1} are found in the infrared spectrum which are permitted by the selection rules only in the Raman spectrum. The phenomenon analogous to cyclopentane also takes place in spectra of deuterocyclopentane (see Table 2). Of special interest are the results obtained in the latest work of G. S. Landsberg, P. A. Bazhulin and M. M. Sushchinskii [7]. Diffuse bands in the spectrum of cyclopentane in the 1200, 1270 and 2940 cm^{-1} regions, taken earlier as broad bands, were each resolved by these authors into two lines of equal intensity. Two of these bands belong to the deformation vibration of H-C-C in twice degenerate types of symmetry, one to the fully symmetrical stretching vibration of CH. It seems to us that the circumstances described may be explained by the assumption of significant influence of intermolecular interaction on the vibrational spectrum of the cyclopentane molecule. It is well known that intermolecular interaction can lead not only to broadening of the spectral lines, but also to their splitting into separate components [8, 9], and are also capable of strongly changing the activity of this or that vibration in the spectrum, specifically, to make forbidden lines observable. All the Raman spectra of cyclopentane we know about were studied in the liquid state, where intermolecular interaction ought to be especially strong. The high viscosity of liquid cyclopentane also advocates this supposition.

From what has been said it follows that some discrepancies between experimental data and calculation are inevitable.

Table 3

Calculated Values of the Force Constants of the Cyclopentane Molecule (in units 10^6 cm^{-2})

K_Q =	6.27	o_β =	− 0.436
H =	0.56	n_γ =	0.12
K_q =	8.05	a_α =	0.35
K_γ =	1.1	a_β =	0.35
K_β =	1.286	h =	− 0.15
K_α =	0.71	$l_{o\beta}$ =	− 0.034
A_γ =	0.43	m_β =	− 0.014
A_β =	0.43	n_β =	0.11
r_β =	− 0.26	l_β^q =	0.4
p_β =	0.26	l_β^Q =	− 0.4
u_β =	0.17	$m_{\beta\gamma}$ =	− 0.02
v_β =	− 0.17	$n_{\beta\gamma}$ =	− 0.02
		$l_{\beta\gamma}$ =	− 0.035

In this connection the comparatively small difference mentioned above between the results of our calculations and experimental data for both the spectrum of cyclopentane and deuterocyclopentane, apparently, advocates the correctness of the estimate we made, at least for the leading force constants of the molecules. Comparison of the force constants of molecules of related structure might serve as an important criterion in this respect. Using literature data for the cyclopropane [10] and cyclohexane molecules [11], we have for the important force constants of the carbon ring [in units 10^6 cm^{-2}]:

cyclopropane $K_Q = 6.1$, $H = 0.10$,

cyclopentane $K_Q = 6.27$, $H = 0.56$,

cyclohexane $K_Q = 6.62$, $H = 0.39$,

for normal paraffins $K_Q \lesssim 7.23$.

From this comparison it follows that the values obtained by calculation (both the constants K_Q and H, and the others) are found within the limits of the values expected. Moreover a definite tendency was observed toward conformity with a rule that increase of the force constants K_Q and H are a measure of the increase of the number of carbon atoms in the molecule. Further accumulation of material for the calculation of vibrational spectra of molecules will allow the carrying out of more precise estimation of the values of the force constants.

October 27, 1958

References

1. R. S. LEBEDEV: OiS, 6, 154, (1959) (See 6,p)
2. L. PAULING, L. O. BROCKWAY: JACS, 59, 1223, (1937); J. E. KILPATRICK, K. S. PITZER,
3. R. SPITZER: JACS, 69, 2483, (1947)
3. G. HERZBERG: Vibrational and rotational spectra of polyatomic molecules, Moscow, 1949
4. M. V. VOL'KENSHTEIN, M. A. EL'IASHEVICH, B. I. STEPANOV: Kolebaniia molekul (Vibrations of molecules), 1, GITTL, Moscow-Leningrad, 1949
5. L. S. MAIANTS: ZETF, 25, 393 (1953)
6. R. S. LEBEDEV: Uch. zap. Kemerovskogo ped. inst., 3, (1958) (in press)
7. G. S. LANDSBERG, P. A. BAZHULIN, M.M.SUSHCHINSKII: Ochovnie parametri spektrov kombinatsionnogo passeianiia uglevodorodov. (Fundamental Parameters of Raman spectra of hydrocarbons), Moscow, 1956
8. A. V. SECHKAREV: Assotsiatsiia molekul v molekuliarnikh kristallakh i spektri rasseianiia (Association of molecules in molecular crystals and spectra of dispersions) Leningrad, 1952
9. SH. SH. RASKIN, A. V. SECHKAREV: DAN USSR, 86, 509, (1952)
10. L. M. SVERDLOV, E. P. KRAINOV: OiS, 3, 54 (1957)
11. G. A. ALEKSANDROV; OiS, 3, 202, (1957)
12. K. W. F. KOHLRAUSCH, R. SEKA: Ber., 69, 729, (1936)
13. E. J. ROSENBAUM, H. F. JACOBSON: JACS, 63, 2841, (1941)
14. F. A. MILLER, R. G. INSKEEP: J. Chem. Phys., 18, 1519, (1950)

TOM VII, Vyp. 2 OPTIKA I SPEKTROSKOPIIA Avgust, 1959
VOL. VII, No. 2 OPTICS AND SPECTROSCOPY August, 1959

Calculation of the Characteristic Vibrations of Phosphorus Compounds
II. Characteristic Vibrations of the $(CH_3O)_3PO$ and $(CH_3O)_3PS$ Molecules

L. S. MAIANTS, E. M. POPOV AND M. I. KABACHNIK

Abstract: Frequencies and forms of fully symmetrical vibrations of several of the possible conformations of the $(CH_3O)_3PO$ and $(CH_3O)_3PS$ molecules were calculated for some approximate values of the force coefficients and the sensitivities of the frequencies to changes of these coefficients were determined. The question of how characteristic are the vibrations which correspond to the so-called stretching frequencies P=O, P=S, P-O, C-O and deformation frequency C-H was examined. On the basis of P=O and P-O frequencies a likely choice was made of the conformations present in the $(CH_3O)_3PO$ molecule.

In a previous article [1] results were presented of a calculation of the normal vibrations of the $POCl_3$, $POBr_3$, $PSBr_3$ molecules, and the question was raised of how characteristic are the vibrations of these molecules which correspond to the so-called P=O and P=S frequencies. It was shown that the symmetrical vibration ν_1 in the four calculated molecules was not fully characteristic in form for the coordinates Q which determine the change of the length of the bonds P=O and P=S.

In order to elucidate the participation of coordinates more removed from Q in the vibration ν_1, the fully symmetrical vibrations of the molecules $(CH_3O)_3PO$ and $(CH_3O)_3PS$ were calculated.

Infrared [2] and Raman [3,4] spectra of the molecules $(CH_3O)_3PO$ and $(CH_3O)_3PS$ and have been published in the literature, with interpretations of many of the bands of these spectra. Of special interest was the circumstance that a doublet band was found in the P=O stretching frequency region in IR spectra of trimethylphosphate and triethylphosphate.

Mortimer [2] investigated the IR spectra of trimethylphosphate in crystalline and liquid states at different temperatures, and also in solutions of isooctane, carbon tetrachloride, carbon disulfide, acetone and chloroform. Bands, found in the spectrum of the crystalline material at 1290 and 750 cm^{-1}, are split respectively into doublets at 1290 and 1275 cm^{-1} and 755 and 740 cm^{-1} in spectra of the liquid compound and its solutions. The relative intensities at the maxima of the corresponding absorption bands are changed significantly with temperature and solvent. From these data Mortimer concluded that there were present at least two rotational isomers of trimethylphosphate, with the bands at 1290 and 740 cm^{-1} corresponding to one conformation and those at 1275 and 755 cm^{-1} to the other.

SUBJECTS OF THE CALCULATION, NOTATIONS AND VALUES OF THE PARAMETERS

For the calculation we selected four of the possible rotational isomers of the $(CH_3O)_3PO$ and $(CH_3O)_3PS$ molecules, where the isomers are distinguished by the position of the methyl groups, and the models of which are depicted in the figure. Models I and II have C_{3v} symmetry, model III has C_3 symmetry (in this model the C-O bonds are positioned in the plane perpendicular to the third order axis) and model IV has C_s symmetry*.

In accordance with the symmetry of these models there must be 12, 15, and 26 fully symmetrical vibrations.

As generalized coordinates we selected changes in the length of the bonds P=O (P=S) $-Q$, P-O $-q'_i$ (i = 1, 2, 3), O-C $-q''_i$ (i=1, 2, 3), C-H $-q'''_i$ (i = 1, 2, ..., 9) and changes of the angles γ_i (i=1, 2, 3), δ_i (i=1,2,3), $-\alpha_i$ (i = 1, 2, 3), $-\beta_i$ (i = 1, 2,..., 9) and $-\varphi_i$ (i = 1, 2..., 9).**

The angular generalized coordinates are related by the equations:

$$\sum_{i=1}^{3} \gamma_i + \sum_{i=1}^{3} \delta_i = 0$$

and

$$\sum_{i} \beta_i + \sum_{i} \bar{\varphi}_i = 0$$

(for each CH_3 group).

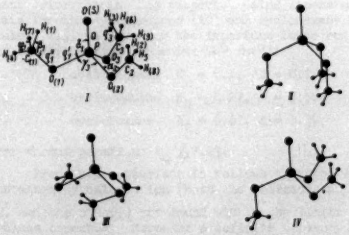

*In Model IV we calculated only the vibrations ν_1 (which correspond to the P=O and P=S frequencies) and ν_2 and ν'_2 (which correspond to the P-O frequencies).

**The angles φ_i are indicated by the numbers of the three hydrogen atoms in the corresponding CH_3 group.

Table 1

Force Coefficients (in units 10^6 cm^{-2})

Molecule	K_Q	$K_{q'}$	K_γ	K_δ	$K_{q''}$	K_α	K_β	K_φ	$h_{Qq'}$	$a_{Q\delta}$	$b_{Q\gamma}$	$a_{q'\gamma}$	$a_{q'\delta}$	$h_{q'q'}$	$h_{q\,q''}$	$a_{q'\alpha}$	$l_{\gamma\gamma}$	$l_{\delta\delta}$	$l_{\gamma\delta}$	$m_{\gamma\alpha}$	$m_{\delta\alpha}$	$a_{q'\alpha}$	$a_{q''\beta}$	$m_{\alpha\beta}$	$a_{q''\varphi}$	$l_{\beta\varphi}$
$(CH_3O)_3PO$ . . .	17.90	7.90	1.75	2.50	8.20	1.00	1.06	0.71	1.00	1.00	0.20	0.40	0.60	0.45	0.40	0.40	−0.05	−0.05	−0.05	0.05	0.05	0.40	0.53	0.12	0.35	−0.03
$(CH_3O)_3PS$ . . .	7.50	7.90	2.00	2.00	8.20	1.00	1.06	0.71	1.15	1.00	0.00	0.40	0.40	0.45	0.40	0.40	−0.05	−0.05	−0.05	0.05	0.05	0.40	0.53	0.12	0.35	−0.03

Table 2

Form of Vibrations ν_1

Molecule	Model of Rotational Isomer	Exptl. Frequencies (w. m. s.) (in cm^{-1})	Calc. Frequencies (in cm^{-1})	Q	q_1^1	q_2^1	q_3^1	γ_1	γ_2	γ_3	δ_1	δ_2	q_1''	q_2''	q_3''
$(CH_3O)_3PO$	I	1272	1276	1	−0.11	−0.11	−0.11	0.15	0.15	0.15	−0.15	−0.15	0.01	0.01	0.01
	II		1279	1	−0.10	−0.10	−0.10	0.15	0.15	0.15	−0.15	−0.15	−0.03	−0.03	−0.03
	III		1274	1	−0.11	−0.11	−0.11	0.15	0.15	0.15	−0.15	−0.15	−0.01	−0.01	−0.01
	IV		1276	1	−0.13	−0.11	−0.11	0.15	0.16	0.16	−0.15	−0.16	—	—	—
$(CH_3O)_3PS$	I	816	627	1	−0.04	−0.04	−0.04	0.19	0.19	0.19	−0.19	−0.19	0.02	0.02	0.02
	II		638	1	−0.02	−0.02	−0.02	0.29	0.29	0.29	−0.29	−0.29	0.03	0.03	0.03
	III		624	1	−0.04	−0.04	−0.04	0.15	0.15	0.15	−0.15	−0.15	0.03	0.03	0.03
	IV		624	1	−0.10	−0.10	−0.10	0.22	0.22	0.22	−0.22	−0.22	—	—	—

Table 2 (continued)

Molecule	α_1	α_2	α_3	β_1	β_2	β_3	β_4	β_5	β_6	β_7	β_8	β_9	φ_4	φ_5	φ_6	φ_7	φ_8	φ_9
$(CH_3O)_3PO$	0.16	0.16	−0.16	−0.08	−0.08	−0.08	−0.06	−0.06	−0.06	−0.06	−0.06	−0.06	0.06	0.06	0.06	0.06	0.06	0.06
	−0.17	−0.17	−0.17	0.10	0.10	0.10	0.03	0.03	0.03	0.03	0.03	0.03	−0.04	−0.04	−0.04	−0.04	−0.04	−0.04
	−0.01	−0.01	−0.01	0.03	0.03	0.03	−0.01	−0.01	−0.01	−0.01	−0.01	−0.01	0.01	0.01	0.01	0.01	0.01	0.01
	0.01	0.00	0.00	—	—	—	—	—	—	—	—	—	—	—	—	—	—	—
$(CH_3O)_3PS$	0.16	0.16	0.16	−0.04	−0.04	−0.04	0.00	0.00	0.00	0.00	0.00	0.00	0.01	0.01	0.01	0.01	0.01	0.01
	−0.42	−0.42	−0.42	−0.11	−0.11	−0.11	0.09	0.09	0.09	0.09	0.09	0.09	−0.06	−0.06	−0.06	−0.06	−0.06	−0.06
	−0.09	−0.09	−0.09	−0.07	−0.07	−0.07	0.04	0.04	0.04	0.04	0.04	0.04	−0.02	−0.02	−0.02	−0.02	−0.02	−0.02
	−0.03	−0.08	−0.08	—	—	—	—	—	—	—	—	—	—	—	—	—	—	—

Table 3

Partial Derivatives $\frac{\partial \nu_1}{\partial t}$ $(t = K_Q K_q, \ldots, l_{\beta\varphi})$

Molecule	Model of Rotational Isomer	K_Q	$K_{q'}$	K_γ	K_δ	$K_{q''}$	K_α	K_β	K_φ	$h_{Qq'}$	$a_{Q\delta}$	$b_{Q\gamma}$	$a_{q'\gamma}$	$a_{q'\delta}$	$h_{q'q'}$	$h_{q''q''}$	$a_{q'\alpha}$	$l_{\gamma\gamma}$	$l_{\delta\delta}$	$l_{\gamma\delta}$	$m_{\gamma\alpha}$	$m_{\delta\alpha}$	$a_{q''\alpha}$	$a_{q''\beta}$	$m_{\alpha\beta}$	$a_{q''\varphi}$	$l_{\beta\varphi}$
$(CH_3O)_3PO$	I	37	1	4	4	0	3	0	0	−25	−34	34	− 8	4	3	0	−4	8	8	−16	8	−8	0	0	8	0	0
	II	37	1	4	4	0	3	0	0	−23	−34	34	− 7	4	3	0	4	8	8	−16	− 8	6	0	0	−6	0	0
	III	37	1	4	4	0	0	0	0	−24	−34	34	− 7	4	3	0	0	8	8	−16	0	0	0	0	0	0	0
	IV	37	1	3	3	—	0	—	—	−26	−34	34	− 8	4	3	0	0	2	−2	0	4	−2	0	—	0	—	—
$(CH_3O)_3PS$	I	46	0	4	4	0	3	0	0	− 9	−55	55	− 4	2	0	0	−1	8	8	−16	13	−9	0	0	0	0	0
	II	45	0	10	10	0	19	2	0	−13	−76	76	− 7	3	0	0	5	20	20	−40	−42	29	−3	6	−3	0	0
	III	46	0	4	4	0	1	0	0	− 8	−52	52	− 3	2	0	0	1	8	8	−16	− 8	5	−1	0	0	0	0
	IV	49	1	7	7	—	−2	—	—	−25	−66	66	−10	5	2	0	0	5	0	0	4	−2	0	—	0	—	—

Table 4

Frequencies of ν_1 in Phosphoric and Thiophosphoric Compounds

Compound	ν_1 (in cm^{-1})	Ref.	Compound	ν_1 (in cm^{-1})	Ref.
$POCl_3$	1290	[11]	$PSCl_3$	748	[11]
$(CH_3O)_2POCl$	1286	[3]	CH_3PSCl_2	664	[12]
$(C_2H_5O)_2POCl$	1289	[3]	$C_2H_5PSCl_2$	665	[12]
$(C_3H_7O)_2POCl$	1291	[3]	$C_3H_7PSCl_2$	660	[12]
$(CH_3O)_2POH$	1258	[3]	$(CH_3O)_3PS$	616	[4]
$(C_2H_5O)_2POH$	1257	[3]	$(C_2H_5O)_3PS$	608	[12]
$(C_3H_7O)_2POH$	1254	[3]	$(C_2H_5O)_2P(S)OCH_2CH_2SC_2H_5$	607	[19]
$(C_4H_9O)_2POH$	1258	[3]	$(C_2H_5O)_2P(S)OPO(OC_2H_5)_2$	609	[12]
CH_3POCl_2	1285	[12]	$(CH_3O)_2PSH$	636	[14]
$C_2H_5POCl_2$	1285	[12]	$(C_2H_5O)_2PSH$	633	[12]
$(CH_3O)_2CH_3PO$	1243	[13]	$(CH_3O)_2PSCl$	660	[12]
$(C_2H_5O)_2CH_3PO$	1250	[13]	$(C_2H_5O)_2PSCl$	660	[12]
$(i\text{-}C_3H_7O)_2CH_3PO$	1249	[13]	$(C_3H_7O)_2PSCl$	665	[12]
$(C_4H_9O)_2CH_3PO$	1250	[14]	$(C_4H_9O)_2PSCl$	667	[12]
$(C_4H_9O)_2C_2H_5PO$	1250	[14]	$(i\text{-}C_3H_7O)_2PSCl$	656	[12]
$(C_4H_9O)_2C_4H_9PO$	1250	[15]			
$(C_2H_5O)_2C_4H_9PO$	1243	[16]	$(CH_3O)_2P(S)NHCH_3$	635	[12]
			$(C_2H_5O)_2P(S)NHCH_3$	638	[12]
$(C_2H_5O)C_2H_5P(O)SCH_3$	1215	[17]	$(C_3H_7O)_2P(S)NHCH_3$	645	[12]
$(C_2H_5O)C_2H_5P(O)SC_2H_5$	1215	[17]	$(C_4H_9O)_2P(S)NHCH_3$	645	[12]
$(C_4H_9O)C_2H_5P(O)SC_4H_9$	1215	[17]	$(i\text{-}C_3H_7O)_2P(S)NHCH_3$	637	[12]
$(C_2H_5O)_2P(O)SCH_3$	1258	[18]	$(CH_3O)CH_3PSCl$	620	[12]
$(C_2H_5O)_2P(O)SC_2H_5$	1257	[14]	$(C_2H_5O)CH_3PSCl$	625	[12]
$(C_2H_5O)_2P(O)SCH_2OCH_3$	1255	[18]	$(i\text{-}C_3H_7O)CH_3PSCl$	629	[14]
$(C_2H_5O)_2P(O)SCH_2C_6H_5$	1254	[18]			
$(C_2H_5O)_2P(O)SCOOCH_3$	1263	[18]	$(CH_3O)_2P(S)SH$	654	[14]
$(C_2H_5O)_2P(O)SCH_2CH_2SC_2H_5$	1255	[19]	$(C_2H_5O)_2P(S)SH$	654	[12]
			$(CH_3O)_2P(S)SCH_3$	655	[12]
$(CH_3O)_2POF$	1305	[15]	$(C_2H_5O)_2P(S)SC_2H_5$	655	[12]
$(C_2H_5O)_2POF$	1309	[15]	$(C_2H_5O)_2P(S)SCH_2SC_3H_7$	655	[12]
			$(C_2H_5O)_2P(S)SCH_2CH_2SC_3H_7$	656	[12]

Diagonal force coefficients are designated by K_i; non-diagonal coefficients which correspond to different bonds by h_{ij}; the corresponding bonds and adjacent angles by a_{ij}; the corresponding bonds and opposite angles by b_{ij}. The force coefficients which correspond to adjacent angles are designated by l_{ij}; while these which correspond to angles with a common bond are designated by m_{ij}. The subscripts i and j show to which coordinate a given force coefficient applies.

The matrix elements T^{-1} are calculated from the corresponding tables using the following values for bond lengths: S(P = O) - 1.58 Å, S(P = S) - 1.94 Å, S(P - O) - 1.80 Å, S(C - O) - 1.44 Å and S(C - H) - 1.09 Å. The angles γ_i, δ_i, α_i, β_i and φ_i are assumed to be tetrahedral. The length of the CH bond was chosen as the unit of bond length.

Table 5

Calculated Frequencies of the Fully Symmetrical Vibrations

Molecule	No. of Vibration	Exptl. Frequency (v. m. s.) (in cm-1)	Model of Rotational Isomer	Calc. Frequency (in cm-1)
$(CH_3O)_3PO$	ν_2	734	I	730
			II	707
		751	III	712
			IV	715
				813
	ν_3	—	I	317
			II	373
			III	350
	ν_4	1031	I	1016
			II	1028
			III	1014
	ν_5	—	I	226
			II	150
			III	159
$(CH_3O)_3PS$	ν_2	737	I	707
			II	702
			III	704
	ν_3	—	I	263
			II	336
			III	324
	ν_4	1024	I	1027
			II	1025
			III	1014
	ν_5	—	I	217
			II	138
			III	160

The mass of the hydrogen atom, $m_H = 1.008$, was chosen as the unit of mass.

The values of the force coefficients used in the calculation are presented in table 1. The force coefficients which correspond to the CH_3O group were taken from calculations of the vibrations of the methanol molecule [6]. The remaining coefficients were chosen by analogy with other molecules.

The calculation of symmetry and additional relations was by well-known methods [7, 8]. Partial derivatives of the frequencies with respect to the parameters were calculated by an improved method [9]. Calculation was done by the first approximation method of calculating characteristic frequencies [10]. In the calculation of models I, II, and III, the q'''_i coordinates were discarded, as were the q''_i, q'''_i, β_i and φ_i in the calculation of the ν_1 vibration of model IV, and the coordinates Q and q'''_i in the calculation of the ν_2 and ν'_1 vibrations in model IV.

DISCUSSION OF RESULTS

The results of the computations are presented in tables 2, 3, 5, and 6.

Table 6

$(CH_3O)_3PO$. Partial Derivatives $\frac{\partial \nu_2}{\partial t}$ $(t = K_Q, K_{q'}, \ldots, e\delta\varphi)$

No. of Vibration	Model of Rotational Isomer	K_Q	$K_{q'}$	K_7	K_δ	$K_{q''}$	K_α	K_β	K_φ	$h_{Qq'}$	$a_{Q\beta}$	$b_{Q\gamma}$	$a_{q'\delta}$	$a_{q'\gamma}$	$h_{q'q''}$	$h_{q'q'}$	$a_{q'\alpha}$	l_{77}	l_{88}	l_{76}	$m_{7\alpha}$	$m_{\delta\alpha}$	$a_{q''\alpha}$	$a_{q''\beta}$	$m_{\alpha\beta}a_{q''\varphi}$	$l_{\beta\varphi}$
ν_2	I	0	37	2	2	1	12	31	4	0	0	0	20	-40	4	74	-44	4	4	-8	17	-11	1	2	-10	-22
	II	0	35	0	0	3	8	20	3	0	0	0	2	-5	21	70	-34	0	0	0	2	-1	-10	2	-4	-12
	III	0	37	2	2	3	18	-5	-11	0	0	0	17	-34	22	74	-51	4	4	-8	18	-12	-15	4	-35	-14
	IV	-	35	3	4	1	13	40	11	-24	4	-5	24	-40	17	70	-44	5	-2	1	19	-11	-9	1	-1	-16
																									6	
																									-2	
																									-8	
																									17	
																									6	
																									-1	
																									-16	

In table 2 the results are given of a calculation of the fully symmetrical vibrations ν_1 which correspond to the P=O frequency in $(CH_3O)_3PO$ and to the P=S frequency in $(CH_3O)_3PS$. It is evident from the table that chiefly the coordinate Q is changed in the ν_1 vibration. The nearest coordinates q'_1, γ_1, δ_1 and α_1; also participate to a small extent. The remaining coordinates take essentially no part. This is true for all four models of each molecule examined. From examination of partial derivatives of the frequency ν_1 with respect to the force coefficients (see table 3) we conclude that the probable change of values of all these parameters cannot change the values of the frequency ν_1 very much. Thus, taking into account the data obtained and results of previous studies [1], we can assert that the vibration ν_1 is very characteristic in form and frequency for the coordinate Q, and the directly connected coordinates q'_1, γ_1, δ_1 and α_1. This is in agreement with experimental data on the vibrational spectra of the phosphoro-organic compounds. In table 4 are presented values of the frequencies of P=O and P=S for several types of phosphorus compounds. Deviations in the P=O and P=S frequencies in spectra of compounds with the same nearest environment of the phosphorus atom do not exceed 10 cm^{-1}. This is not true for compounds whose molecules are strongly associated, nor for those which have intramolecular hydrogen bonding.

In table 5 are presented calculated frequencies of the fully symmetrical vibrations ν_2, ν_3, ν_4 and ν_5 of models I, II, and III of the $(CH_3O)_3PO$ and $(CH_3O)_3PS$ molecules, and ν_2 and ν'_2 of model IV of the $(CH_3O)_3PO$ molecule. From analysis of the form of the vibrations * we conclude that vibrations ν_2 and ν_4 are not characteristic in form for the coordinates q'_1 and q''_1 which correspond to the P-O and O-C bonds. The values of the particular derivatives of these frequencies with respect to the parameters ** also show their large sensitivity to changes of the force coefficients which correspond to coordinates related to the organic part of the molecule. Since the vibrations ν_2 and ν_4 are not characteristic in form for the coordinates q'_1 and q''_1, they can scarcely be characteristic in frequency for these coordinates. Experiment confirms this conclusion. The frequency ν_2 in the spectra of trialkylphosphates and trialkylthiophosphates changes its value on replacement of one of the alkyl radicals by another. The frequency ν_4 is constant in the spectra of trialkylphosphates, but changes significantly in the spectra of triarylphosphates.

The calculated frequencies of the fully symmetrical deformational CH vibrations are close to found values. The forms of these vibrations [20] show that coordinates which correspond to the phosphorus part of the molecule take very little part and CH deformational vibrations are characteristic for the methyl group on the whole. This is also confirmed by the values of the partial derivatives [20].

The appearance in the spectrum of liquid trimethylphosphate of two P=O frequencies in place of one might be explained as due to a change of the potential correlations, as well as to a change of the force field of the molecule on going from one conformation to another. A calculation, carried out assuming equality of the force fields of the different conformations, shows that the ν_1 frequencies practically coincide for them, while the difference of ν_2 frequencies for conformations I and II is close to the experimental value. Calculation of the possible errors in the choice of values of the force coefficients cannot bring $\Delta\nu_1$ for the different conformations nearer to the experimental value (ca. 15 cm^{-1}). The possible changes of angles γ_1 and δ_1 also cannot change values of ν_1, as is shown in the first communication [1]. To explain the experimental values of $\Delta\nu_1$, therefore, we must assume that the force field of the different conformations are somewhat different, in particular because of the difference in the force coefficients K_Q (approximately 2%). This difference does not cause a noticeable change of values of other frequencies since they are not sensitive to a change in the coefficient K_Q. We can assume that this difference is caused by the presence of very weak intramolecular interaction between the oxygen atoms of the P=O group and the hydrogen atoms of the methyl group in one isomer, and the absence of such interaction in the other. Conditions for the realization of this interaction are most favorable in isomers I and IV, and absent in isomers II and III. Realization of such interaction in isomer II is most unlikely on account of steric difficulties.

The influence of the possible errors in the choice of values of the force coefficients (see table 6) also cannot significantly change the differences of the ν_2 frequencies for the different conformations. Since the difference of the ν_2 frequencies for the I and III conformations is close to experimental, then we can assume with high probability that the experimental frequency at 740 cm^{-1} is related to conformation III. As regards the 755 cm^{-1} frequency, that is probably related to conformation I. Such a choice of assigned conformations is due to the assumption concerning the differences in their K_Q coefficients. Thus, conformation I ought to correspond to the lower value of the K_Q coefficient, and, consequently, to the lower value of the ν_1 frequency.

November 24, 1958

---

* The values of the forms of the vibrations and of the particular derivatives of the frequencies for the different parameters are not presented in the articles (see [20]).

** (See [20])

References

1. L. S. MAIANTS, E. M. POPOV, M. I. KABACHNIK: OiS (In press)
2. F. S. MORTIMER: Spectrochim. Acta, 9, 270, (1957)
3. M. BAUDLER: Zs. Electrochem., 59, 173, (1955)
4. A. SIMON, G. SCHULZE: Naturwissensch., 25, 669, (1937), Zs. anorg.allg.Chem., 242, 313, (1939)
5. M. A. EL'IASHEVICH., ZFKH, 15, 847, (1941)
6. B. I. STEPANOV: ZFKh, 19, 497, (1945)
7. L. S. MAIANTS: ZETF, 25, 393, (1953)
8. L. S. MAIANTS: DAN USSR, 89, 423, (1953)
9. L. S. MAIANTS: OiS, 5, 379, (1958)
10. L. S. MAIANTS: Tr. FIAN USSR, 5, 63, (1950)
11. R. C. GORE: Discuss.Farad. Soc., 9, 138, (1950)
12. E. M. POPOV, T. A. MASTRIUKOVA, H. P. RODIONOVA, M. I. KABACHNIK: ZOKh (In press)
13. C.I. MEYRICK, H. W. THOMPSON: J.Chem.Soc., 225 (1950)
14. R. A. MCIVOR, G. A. GRANT, C. E. HUBLEY: Can. J. Chem., 34, 1611, (1956)
15. L. W. DAASCH, D. C. SMITH: Anal.Chem., 23, 853 (1951)
16. L. I. BELLAMY, L. BEECHER: J.Chem., Soc., 475, (1952)
17. M. I. KABACHNIK, N. I. KUROCHKIN, T. A. MASTRIUKOVA, E. M. POPOV, N. P. RODIONOVA: DAN SSSR, 104, 861, (1955)
18. M. I. KABACHNIK, T. A. MASTRIUKOVA, N. P. RODIONOVA, E. M. POPOV: ZOKH, 26, 120, (1956)
19. A. HENGLEIN, G. SCHRADER, R. MUHLMAN: Zs.anal. Chem., 141, 276, (1954)
20. E. M. POPOV: Kand.Diss. INEOS AN SSSR, Moscow, 1959.

TOM VII, Vyp. 2 OPTIKA I SPEKTROSKOPIIA Avgust, 1959
VOL. VII, No. 2 OPTICS AND SPECTROSCOPY August, 1959

Spectroscopic Investigation of the Influence of the Mutual Orientation of Cyclopropane and Phenyl rings upon Their Conjugation

V. T. ALEKSANIAN, KH. E. STERIN, M. IU. LUKINA, I. L. SAFONOVA, B. A. KAZANSKII

Abstract: The Raman spectra of stereoisomers of 1, 2-dphenyl-cyclopropane and 1-phenyl-2-cyclopropyl-cyclopropane were studied. The observed sharp increase of intensity of the lines ~1200 and ~1600 cm^{-1} as compared with alkylbenzenes, is evidence for a significant conjugation of the three membered and the phenyl rings. The effect of the conjugation is very weakly marked in the spectra of the lower boiling stereoisomers. This can be explained by steric hindrances which disturb the most favorable arrangement for conjugation of phenyl rings relative to the threemembered ring. Such steric hindrances are possible only with cis-isomers. The latter circumstance served as a basis for assignment of the isomers of both hydrocarbons to the cis- and trans-forms.

INTRODUCTION

It is known that compounds whose molecules contain a three-membered carbon ring, even if they are in the saturated form (e. g., cyclopropane and its homologues), are similar to the olefins in a number of chemical and physical properties [1, 2]. A current theory explains this peculiarity of compounds of the cyclopropane series by the closeness of the state of hybridized valencies of the carbon atoms of the cyclopropane ring to sp^2, with the result that of the two valencies of the carbon taking part in the formation of the C-C bond, the hybridized state of one is close to sp^2, while the other has a p-character, i.e., it resembles the one which takes part in the formation of the π-bond in ethylene [2, 3].

In view of the analogy between the cyclopropane compounds and the unsaturated systems, it was natural to assume that the cyclopropane ring possesses the ability to form a conjugated double bond. Kizhner [4] was the first to make this assumption when he pointed out the anomalous value for the molecular refraction of 1, 1-dimethyl-2-isobutenylcyclopropane and 1, 2-diphenylcyclopropane. Later Robinson [5] noticed the bathochromic shift of the longwave absorption band in the ultraviolet spectra of the compounds which have a cyclopropane ring in series with a double bond and attributed this to conjugation. Later similar data about the behavior of a longwave band in absorption spectra of compounds of the type under discussion were often found in the literature (see e. g. [2, 6, 7]).

It should be mentioned that the opinion about the presence of conjugation because of the bathochromic shift of the longwave band in the ultraviolet absorption and the increase of its intensity cannot be acknowledged as correct, since the conjugation influences chiefly the position and the intensity of the bands of the so-called transitions N - V [8,9]* and the longwave band in the absorption spectra is not always, but only in a few cases, a transition of that type. Thus, the longwave band of methylcyclopropylketone is displaced to the shortwave side [10] as compared with the bands of aliphatic and alicyclic ketones, although a short time ago we succeeded in showing that in methylcyclopropylketone a conjugation takes place between the group C=O and the threemembered ring.

In the given case the apparent discrepancy can be explained by the fact that the band of the ketones in question is caused by a transition of another type, namely N - Q [11].**

Therefore, for a corrct idea of the presence of conjugation according to the ultraviolet absorption bands, the latter should be reliably interpreted which, in may cases, presents a difficult task.

A much safer and more sensitive criterion for the presence of conjugation is the increase in intensity of some lines of the Raman spectra.*** Thus, the intensity of the lines of stretching vibrations of C=C is magnified 10-15 times [13] with conjugation of two double bonds. Such sharp effects represent the advantage of the Raman spectra, which is especially important in the study of compounds in which the conjugation is more weakly expressed. Since the intensity of lines in the Raman spectra of similar compounds of the cyclopropane series were not previously investigated, we made it our task to study spectra of some hydrocarbons of this series in which the presence was assumed of conjugation of a double bond with the threemembered ring.

Table 1

Integral intensities I_{∞} of spectral lines of cyclopropane hydrocarbons and of the corresponding model compounds

Compound	Frequency (in cm^{-1})		
	~1200	~1600	1640 - 1650
Pentene - 1	—	—	340
Ethylcyclopropane	290	—	—
Vinylcyclopropane	430	—	660
2-Methylpentene - 1	—	—	290
Isopropylcyclopropane	260	—	—
Isopropenylcyclopropane	410	—	620
Toluene	220	290	—
Isopropylbenzene	190	330	—
Phenylcyclopropane	800	1150	—

* These transitions, accompanied by excitation of an electron from a bonding orbital into an antibonding one are polarized along the bonds. Under the influence of conjugation the bands of these transitions shift toward long wavelengths and become more intense.

** These transitions, accompanied by excitation of an electron of an undivided pair to a bonding or an antibonding orbital, are polarized perpendicular to the axes of the chemical bonds and react weakly to the presence of a conjugated bond in the molecule [9].

*** It is appropriate to mention that the noted increase of intensity of the lines of the Raman spectra depends mainly on the bathochromic displacement and increase of the oscillator strength of the bands of the same transitions of the type N-V [12].

A previous study of the spectra of such systems as vinylcyclopropane, isopropenylcyclopropane and phenylcyclopropane convincingly shows the presence of conjugation of the threemembered ring with a double bond (simple and aromatic) [14]. This is shown in table 1, where integral intensities of some spectral lines of cyclopropane hydrocarbons and the corresponding model compounds are compared. The intensity of the lines of double bonds of vinyl- and isopropenylcyclopropane is approximately doubled as compared with pentene-1 and 2-methylpentene-2. The intensity of the lines ~1200 and ~1600 cm^{-1} of phenylcyclopropane is increased to still greater degree as compared with alkylbenzenes of a similar structure*. It is remarkable that in comparison with alkylcyclopropanes in vinyl- and isopropenylcyclopropane the intensity of the~1200 cm^{-1} line of the pulsation vibration of the threemembered ring is considerably increased, which also stresses its unsaturated character.

In connection with the obtained results it was of interest to study conjugation in such molecules in which, thanks to steric factors, there should predominate one of the mutual orientations of the threemembered ring with the double bond. This would allow one to explain the character of the orientation of the π- electron cloud in the threemembered ring.

In the present work results are given of an investigation of the Raman spectra of the stereoisomers of 1,2-diphenylcyclopropane and 1-phenyl-2-cyclopropenylcyclopropane, especially synthesized for this purpose.

THE METHOD OF THE EXPERIMENT AND THE RESULTS OF THE MEASUREMENT

The hydrocarbons were synthesized according to the method of Kizhner [4] and Smith and Rogier [16]. The separation into stereoisomers was carried out by a vacuum distillation through a column of 100 theoretical plates.

The Raman spectra were obtained with the ISP-51 spectograph with a F 270 mm. camera. The measurements of the frequencies and line intensities were carried out according to the method which was described previously [17]. The uncertainty of the measured frequencies was ± 1 cm^{-1} in the overwhelming majority of cases and that of the intensity ± 10%. The integral intensities were determined by means of direct microphotometry of the line contours at intervals of 1-1.2 cm^{-1}. As a standard we used the line at 802 cm^{-1} in the spectrum of cyclohexane whose molar integral intensity was taken equal to 500.

In the spectra of the mixtures of stereoisomers of 1,2-diphenylcyclopropane known from literature [15, 18] are given frequencies and visual intensities. Our measurements agree relatively well with the data in reference [18] but considerably less well with those of [15]. Judging by our data, compounds studied in the papers [15, 18] were predominantly in the trans - form. The spectra of the stereoisomers of 1-phenyl-2-cyclopropylcyclopropane were studied first.

* Later measurements of intensity of the lines of phenylcyclopropane [15] gave results which were close to ours.

Cis-1,2-diphenylcyclopropane

B.P. 131.6-131.7° (4.8 mm Hg); F.P. 36.7°; n_D^{20} =1.5887; d_4^{20} =1.0290; found: C-92.70%, H-7.24%; calculated: C-92.74%, H-7.26%; purity: 99.8%.

$\Delta\nu$ (cm^{-1}): 238(80, w),** 268(5,w), 351(12, w), 372(5, w, b), 404(8, w), 449 (15, w), 471 (5, w, b), 491 (3), 517 (10), 583 (4), 619 (120,sh), 702 (8), 722 (70), 737 (76), 759(41), 778 (15), 830 (66, w), 880 (88, w, d), 915 (48), 928(60), 989 (5, b), 1001 (600, sh), 1029 (165, sh), 1040 (20), 1068 (40,w) 1078 (35, w), 1100(15), 1124(7), 1157(82,sh), 1183(40), 1200(72, sh), 1235(82), 1261(5), 1280(10), 1300(40, w), 1330(20, w), 1361(62), 1380(110), 1440(41), 1460(56), 1499(34), 1521(5), 1578(41), 1603(440, sh), 2982(70), 3006(150), 3027(40, b), 3060(330), 3157(15), 3181(10, 3202(10).

Trans-1, 2-diphenylcyclopropane

B.P. 144.1 – 144.2° (5.2 mm Hg); F. P. + 15.3°; n_D^{20} = 1.5997; d_4^{20} = 1.0346; found: C-92.70%, H-7.19%; purity 99.8%

$\Delta\nu$(cm^{-1}): 234(20,w), 258(25,w), 297(5), 348(15,w), 363(8, w, b), 379(5,w,b), 408(25,w), 422(25,w), 467(3), 490(5), 517(8), 538(4), 585(10), 596(5), 621(125,sh), 658(2,), 701(6), 720(5), 735(125), 750(20, sh), 763(50), 778(66), 840(430, v. w. d.), 884(10), 908(62,w), 940(90, w. d.), 989(250), 1003(520, sh), 1032(170, sh), 1040(12,b), 1073(95,) 1156(96, sh), 1184(50), 1211(35), 1247(330), 1284(40, w), 1296 (35, w. b), 1311(30, w, b), 1328(40, w), 1397 (310, sh), 1438(110, sh), 1464(140,sh), 1500(120, sh), 1582(15), 1604(650), 1628(15), 2930(20,w), 2984(20, w), 3003(120), 3032(80,b), 3056(320), 3066(320), 3113(10), 3122(20).

Cis - 1-phenyl-2-cyclopropylcyclopropane

B.P. 1002 – 100.5° (11 mm Hg); n_D^{20} = 1.5330, d_4^{20}= 0.9574; found: C – 91.16%, H – 8.93%; calculated C – 9109%, H – 8.91%.

$\Delta\nu$(cm-1): 168(20, w), 192(30, w), 214(5, b), 263 (15, w), 287(20), 315 (2), 341(2), 354(8, w), 369(10, w), 388(5), 404(5), 456(8, w), 478(4, w, b), 515(2, w), 528(0), 540(0), 589(2), 607(10), 621(58, sh), 643(2), 701(1), 731(70, w), 750(1), 769(25), 795(5), 814(31), 832(32, w), 875(35), 891 (33), 900(30), 913(20), 931(50), 960(7), 973(30), 989(8), 1002(360, sh), 1029(56, 1037(10), 1061(15), 1098(8, w), 1133(11), 1156(30), 1181(10, b), 1194(84, sh), 1203(15,b), 1233(60), 1270(4), 1295(12), 1309(10), 1330(5), 1349(3), 1370(41, w), 1389(9), 1413(12, 1427(8), 1442(13), 1460(43), 1498(15), 1520(3), 1579(8), 1603(150), 2817(20), 2844(20), 3001(390), 3063(280), 3119(10), 3159(20), 3201(10).

Trans - 1-phenyl-2-cyclopropylcyclopropane

B. P. 111.3 – 111.5° (13.8 mm Hg.); n_D^{20} = 1.5371; d_4^{20} = 0.9585; found: C – 90.95%, H – 8.95%.

$\Delta\nu$(cm^{-1}): 212(18, w), 248(10, w), 284(8, w), 300(8, w), 365(5), 374(5), 410(10), 428(6), 490(7,w), 528(2,w), 573(5,w), 620(64 sh), 696(3), 711(10),

** Designations: w-wide, b-background, sh-sharp, d-double, v.w.-very wide.

721(15, w), 735(10), 752(60), 765(47), 790(3), 807(15), 818(15), 835(5), 857(60), 874(100), 891(40), 907(80), 922(44), 943(58,sh), 957(43,sh), 984(5,b), 1002(400,sh), 1032(85,w), 1043(15,b), 1074(21), 1101(10,w), 1122(15,w), 1156(42), 1180(52), 1191(25), 1211(76), 1230(140), 1274(10), 1290(25,w), 1322(8), 1333(5), 1364(19), 1402(78,sh), 1422(12), 1441(30), 1463(94), 1498(34), 1576(8,w), 1604(250), 3001(400,w), 3035(50), 3063(280,w), 3116(10), 3160(20), 3203(30).

DISCUSSION

As is well known, the determination of the configuration of stereoisomers is ordinarily carried out on the basis of the so-called rule of Auwers-Skit which states that isomers with lower constants (boiling point, specific gravity and index of refraction) have the trans configuration. However, investigations of recent years show a series of exceptions, so that the determination of configuration on the basis of this rule is unreliable [19].

It is well known that the difference in configurations of stereoisomers shows in their vibrational spectra. In our case, we also observed this difference; moreover, on the basis of a study of intensities in the spectra of stereoisomers, we succeeded in assigning them to cis- and trans- forms.

Let us first look at the question of the conformation of phenylcyclopropane. If the present theory about the structure of the cyclopropane ring is correct, then the axis of the π-electron cloud, taking part in the conjugation with unsaturated systems, has to lie in the ring plane and pass through the carbon atom perpendicular to the plane of the CH_2-group [2]*. Thus it is apparent that from the two possible limiting conformations A and B (fig. 1), the second (B), in which the planes of the three-membered and the phenyl rings are perpendicular to each other and the axes of the π-electron clouds of both rings are parallel, is more favorable since then the conjugation is at its maximum. The most favorable conformation probably is somewhat different from B, since the repulsion of the hydrogen atoms in B is greater than in A (the minimum $r_{H\ldots H}$ in A equals about 3.0 Å, in B - 1, 75 Å.) **

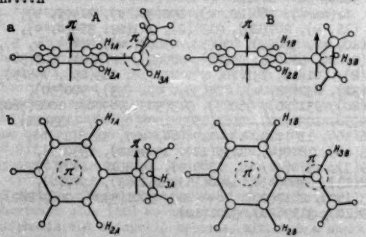

Figure 1. Limiting conformations of phenylcyclopropane. a) side view; b) top view.

By analogy to phenylcyclopropane each of the phenyl rings in the molecules of 1,2-diphenylcyclopropane can have two limiting positions relative to the threemembered ring: A and B, and therefore for each stereoisomer there are conceivable three limiting conformations: AA, BB and AB. Elementary calculations show that the conformations AA and BB of the cis-isomer are very unfavorable because of the presence of closely lying hydrogen atoms, belonging to different phenyl rings: for AA the minimum $r_{H\ldots H}$ equals 1.0 Å, for BB - 0.1 Å. This is much smaller than twice the value of the van der Waals radius of hydrogen (2.4 Å), and naturally such a conformation is unfavorable. More favorable is the conformation AB, where the minimum value for $r_{H\ldots H}$ is 1.75 Å. As far as the trans isomer is concerned, the phenyl rings do not interfere with each other (the distance between the two hydrogen atoms of different phenyl rings is over 3 Å), and from this point of view, all conformations AA, AB and BB are, in principle, possible (the minimum $r_{H\ldots H}$ is 1.75 Å).

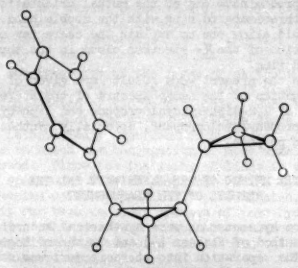

Figure 2. The most favorable conformation of cis-1-phenyl-2-cyclopropylcyclopropane.

Although the most favorable conformation of the cis-isomer is probably different from AB and both phenyl rings take positions intermediate between A and B, the steric conditions of the conjugation in the cis-isomer are undoubtedly less favorable compared with those in the trans-isomer.

With the stereoisomers of 1-phenyl-2-cyclopropylcyclopropane where the substituents are not alike, the number of possible limiting conformations is larger by far and the differences between them are not so sharp. In order to find the most favorable conformation here, one must not restrict oneself to an examination of only the limiting cases, but it is necessary to solve the problem in a general form which requires a calculation of a concrete dependence of the repulsion energy of the hydrogen atoms on the separation. Therefore, we have limited ourselves to examining the possible conformations on models. It was found that in the most favorable conformation of the cis-isomer the phenyl ring has a position which is very close to A, while the second cyclopropane ring is turned to the side and almost parallel to the first one (Fig. 2). The conformation in which the phenyl ring is located more favorably for conjugation (B), proves to be less favorable sterically. For the trans-isomer, also in this case, any conformations, are possible.

* The theories of Walsh [2], Coulson and Moffit [3] predict the identical qualitative picture of the distribution of the electron cloud in the cyclopropane molecule.

** The separation in conformation B between the Atom H_{1B} of the phenyl ring and the hydrogen atom on the substituted carbon atom of the cyclopropane ring (H_{3B} in Fig. 1). The remaining $r_{H\ldots H}$ is greater than 3 Å.

Thus, a discussion of possible conformations of stereoisomers of the investigated compounds has shown that in cis-isomers of both hydrocarbons it is necessary to expect weaker conjugation, which should appear in the Raman spectra.

Our experimental data have confirmed to a considerable degree the considerations just discussed.

Table 2

Integral intensities of spectral lines of cyclopropane hydrocarbons and of the corresponding model compounds.

Compound	~1200 cm^{-1}		~1600 cm^{-1}	
	I_∞	I_∞ calc. for 1 phenyl ring	I_∞	I_∞ calc. for 1 phenyl ring
Toluene	220	220	290	290
Isopropylbenzene	190	190	330	330
Phenylcyclopropane (lines 1221 and 1605 cm^{-1})	800	800	1150	1150
1,2-Diphenylcyclopropane (lines 1235 and 1603 cm^{-1}, the lower boiling isomer)	500	250	2200	1100
1,2-Diphenylcyclopropane (lines 1227 and 1604 cm^{-1}, the higher boiling isomer). . . .	2000	1000	4100	2050
1-Phenyl-2-cyclopropylcyclopropane (lines 1233 and 1603 cm^{-1}, the lower boiling isomer)	340	340	600	600
1-Phenyl-2-cyclopropylcyclopropane (lines 1230 and 1604 cm^{-1}, the higher boiling isomer)	600	600	1100	1100

Table 2, in which are given the integral intensities of some lines of the spectra of the investigated and model compounds, shows the following:

1. In the transition from alkylbenzenes to stereoisomers of 1, 2-diphenylcyclopropane the intensity of the lines ~1200 * and ~ 1600 cm^{-1} increases sharply. The frequency ~1600 cm^{-1} is generally ascribed to the asymmetric stretching vibration C=C on the phenyl rings, analogous to the vibration ν_{16} in benzene [20]; it is used more often than any other in the investigation of conjugated systems including phenyl rings. The interpretation of the lines 1220-1235 cm^{-1} is not so simple. In this region the spectra of monoalkyl substituted benzene derivatives have the lines ~ 1155, ~1180, and ~1200 cm^{-1} [21], of which the last is the most intense. In the observed spectra in this region four and even five lines (the second pair of stereoisomers) are found which are related also to the presence of threemembered rings, whose pulsation vibration line is usually situated at about ~1190-1200 cm^{-1} [14]. Thus, the lines 1220-1235 cm-1 in the studied spectra can be attributed either to the pulsation vibration of the threemembered ring, or to a vibration analogous to that which determines the appearance of the ~1200 cm-1 line in the spectra of monoalkylbenzenes. The second assignment seems to be more probable although it is not definitely proved. First, because the shift toward frequencies (from 1190-1200 to 1220-1235 cm-1) of the pulsation vibration line of the threemembered ring is not observed in other known conjugated cases (vinylcyclopropane, isopropenylcyclopropane). Secondly, the intensity of the line ~1190-1200 cm-1 in the spectra of vinyl- and isopropenylcyclopropane is magnified 1.5 - 1.7 times because of conjugation instead of 4-6 times for the line 1220-1235 cm-1 in the spectra of stereisomers of 1, 2-diphenylcyclopropane. Thirdly, the analogous, very intense line in the same region (1200 cm^{-1}) is present in the spectrum of 2-methyl-1-phenylpropene-1 which we studied, where there is the usual conjugation of the phenyl ring with the double bond, while there is no threemembered ring** In this case the lines in the region 1190-1200 cm-1, observed in all studied spectra, can be attributed to the pulsation vibration of the threemembered rings.

2. The integral intensity of the lines ~1200 and ~1600 cm^{-1} in the spectra of the lower boiling isomers is considerably lower than in the higher boiling ones. This is evidence that the conjugation of the lower boiling isomer is weaker. Therefore, in accordance with the stated considerations we attribute the cis-configuration to the lower boiling isomers and the trans-configuration to the higher boiling isomers. Hence, the stereoisomers studied by us represent another example of violation of the Auwers-Skit rule.

We mention also some other peculiarities of the studied spectra. The trans-1, 2-diphenylcyclopropane shows a very intense and broad line at 820 cm-1 (I_o = 430, I_m = 3900). There is no similar line either in the spectra of alkyl- or alkenyl benzenes, or in alkyl- or alkenylcyclopropanes. We find an interpretation for it difficult.

In the region ~1500 cm^{-1} (including phenylcyclopropane) a rather strong line is observed whose intensity is the greater the stronger the conjugation. A similar line, as a rule, is present in the Raman spectra of compounds in which the phenyl ring is conjugated with a double bond or with other unsaturated systems. On the other hand, in the spectra of alkylbenzenes this line either is absent or very weak ($I_o \approx 1$-3). This line can be attributed to asymmetric vibrations of C=C of the phenyl ring, analogous to ν_{13} in benzene [20], manifest in the infrared spectra of benzene and its alkylhomologues as a very intense band. In the Raman spectra these vibrations (prohibited in the benzene spectrum), although formally allowed, have apparently a very low intensity [21].

A series of lines, including some characteristic of monosubstituted benzene derivatives (such as ~620, ~1000, ~1030 and ~1585 cm-1), do not show any

* In the spectra of phenylcyclopropane of the stereoisomers of 1, 2-diphenylcyclopropane and 1-phenyl-2-cyclopropylcyclopropane the frequency of this line is shifted to 1220-1235 cm^{-1}.

**The spectrum of 2-methyl-1-phenylpropene-1 will be published in another paper.

substantial intensification *.

Thus, when conjugation occurs apparently only some lines increase in intensity, mainly the lines of the phenyl ring determined by asymmetric stretching vibrations of the C=C bond.

September 23, 1958

References

1. E. VOGEL: Fortschr.Chem.Forsch., 3,430, (1955)
2. A.D.WALSH: Trans.Farad.Soc., 45, 179, (1949)
3. C.A.COULSON, W.E.MOFFIT: Phil.Mag., 40, 1, (1949)
4. N.M.KIZHNER: ZhRFKhO, 47, 1102, (1915)
5. R.ROBINSON: J.Chem.Soc., 109, 1042 (1916)
6. G.W.PEROLD: J.S.African Chem.Ins., 6,(1-2),22(1953)
7. W.W.ROBERTSON, J.F.MUSIK, F.A.MATSEN: JACS, 72, 5260, (1950)
8. R.S.MULLIKEN, C. RIEKE: Rep.Progr.Phys., 8, 231, (1942)
9. M.V.VOL'KENSTEIN, M.A.EL'IASHEVICH, B.I.STEPANOV: Kolebaniia molekul. (Vibrations of Molecules), 2, GITTL, M-L., 1949
10. R.P.MARIELLA, R.R. RAUBE: JACS., 74, 518, (1952)
11. R.A.FORD, F.PARRY: Spectrochim.Acta, 12, 78 (1958)
12. M.V.VOL'KENSHTEIN: Vestn. LGU, (5), (1948)
13. P. P. SHORYGIN: IAN, USSR, SF, 12, 576 (1948)
14. V.T.ALEKSANIAN, KH. E.STERIN, M.IU. LUKINA, L.G.SAL'NIKOVA, I. L. SAFONOVA: Mat. X Vsesoiuznovo soveshch. po spektroskopii. (Proceedings of the X All Union Conf. on Spectr.) L'vov Univ., 64, 1957
15. R. IA. LEVINA, IU.S.SHABAROV, K.S.SHANAZAROV, E. G. TRESHCHOVA: Vestn.MGU, (5), 145 (1957)
16. L.I.SMITH, E. R. ROGIER: JACS., 73, 3840 (1951)
17. V.T.ALEKSANIAN, KH. E. STERIN: OIS, 3, 562 (1957)
18. R.LESPIEAU, M. BOURGEL, R.L.WAKEMAN: C.R., 193, 1802 (1931)
19. B. A. KAZANSKII, A.L.LIBERMAN, N.I.TIUN'KINA, I. M. KUZNETSOVA: DAN USSR, 122, 1025, (1958)
20. G. HERZBERG: Infrared and Raman Spectra of Polyatomic Molecules Van Nostrand, 1951 (IL., 1949)
21. G.S.LANDSBERG, B.A.KAZANSKII, V.T.ALEKSANIAN, T.F.BULANOVA, A.L.LIBERMAN, E.A.MIKHAILOVA, A.F.PLATE, KH.E.STERIN, S.A.UKHOLIN: IAN USSR FS, 18, 704, (1954) (See CTT Bulletin)

*A small increase (appr. 1.5 times) is observed in practice only for the 1000 cm^{-1} line in the spectrum of cis-1, 2-diphenylcyclopropane.

TOM VII, Vyp. 2 OPTIKA I SPEKTROSKOPIIA Avgust, 1959
VOL. VII, No. 2 OPTICS AND SPECTROSCOPY August, 1959

On the Study of Hydrogen Bonding Equilibria in Solutions by Infrared Absorption Spectra. Case of Unseparated Bands

M. O. BULANIN, G. S. DENISOV, AND D. N. SHCHEPKIN

Abstract: We consider the question of determining the equilibrium constant K and the integrated absorption coefficients ϵ_k for molecules in a complex in the case that the absorption bands of monomeric and associated species are superimposed. It is shown that treatment of the experimental data by the method worked out by Lord and coworkers leads to significant errors. A more rigorous means is proposed for determining K and ϵ_k, based on use of the method of least squares.

The quantitative characteristics of the hydrogen bond, chief among which is its energy, play an essential role in construction of a theory not only of the hydrogen bond itself but of a theory of liquids and solutions. Recently there has been a considerable increase in interest in these questions and in the chemistry of polymers, albumins, amino acids and other biological acids, whose properties or biological functions largely depend on the nature of the hydrogen bonds existing in such materials.

One of the most promising methods for experimental determination of hydrogen-bond energy is infrared absorption spectroscopy. This method permits highly accurate measurement of the concentration of free and bonded molecules and determination of the equilibrium constant for the formation of a hydrogen bond. It is possible to determine the energy of this reaction from the temperature dependence of the equilibrium constant.

However, such a task is simple only when there are well-separated bands in the spectrum of the system which correspond to the monomeric and associated molecules, so that within a certain range of concentration their integrated intensities (which are much less dependent on the parameters of the spectrograph than the intensities at maximum) can be measured independently. The majority of the work on determination of the equilibrium constant and hydrogen-bond energy has been carried out just for this simplest case (for example, [1-5]). But many systems do not satisfy this condition, i. e., the bands of the monomeric and associated molecules over a wide range of concentrations cannot be separated with sufficient accuracy. The need arises for working out methods of determining the equilibrium constant in cases where the experimentally registered quantity is the integrated intensity of the total band, dependent on absorption of both monomeric and associated molecules at the same time.

The present work is devoted to an analysis of a method, proposed for this purpose, for working out a scheme for solution of the problem on the basis of the general theory of data processing and for using this scheme in certain particular cases. The investigation was carried out for binary systems with a single equilibrium of the type $A + B \rightleftarrows AB$ (the association of molecules of the solute with the molecules of the solvent).

Let C_0^A and C_0^B be the initial concentrations of components A and B in the mixture, V_A and V_B their molar volumes, C_k the concentration of the complex, and C_M^A and C_M^B the concentrations of monomeric molecules. Then, by definition, the equilibrium constant K equals

$$K = \frac{C_k}{C_M^A \cdot C_M^B} = \frac{C_k}{(C_0^A - C_k)(C_0^B - C_k)}. \quad (1)$$

In the future we will assume that work is being carried out in a region where component A absorbs while the absorption of component B is zero or has already been taken into consideration. Let ϵ_M and ϵ_k be the integral absorption coefficients of monomeric and associated molecules of component A; ϵ_M can be measured by taking the spectra of pure liquid. Assuming that Beer's law is satisfied, the integrated intensity of the entire absorption band

$$I = \frac{1}{d}\int \left(\ln \frac{T_0}{T}\right) d\nu = \epsilon_M C_M^A + \epsilon_k C_k \quad (2)$$

depends on two unknown parameters, the equilibrium constant K and the absorption coefficient for the molecules in the complex ϵ_k.

A method for determining K and ϵ_k from the experimentally known dependence $I = I(C_0)$ was proposed in the work of Lord, Nolin and Stidham [6]. This method is essentially as follows: if the dependence of the function $I/C_0^A + C_0^B$ on m is considered (where m is the mole fraction of one of the components of the solution), then the tangents of the angle of incidence to the curve at the points $m = 0$ and $m = 1$ will equal respectively

$$\tan \alpha_1 = \epsilon_M + \frac{(\epsilon_k - \epsilon_M) K}{K + V_B}; \quad (3)$$

$$\tan \alpha_2 = \epsilon_M + \frac{(\epsilon_M - \epsilon_k) K}{K + V_A}.$$

If we neglect V_A and V_B in comparison with K, then

$$\tan \alpha_1 = \epsilon_k^{(1)}; \quad \tan \alpha_2 = 2\epsilon_M - \epsilon_k^{(2)}. \quad (4)$$

Where $\tan \alpha_1$, $\tan \alpha_2$ and ϵ_M are known, the absorption coefficient ϵ_k is defined as the mean of these values, obtained by solving equation (4). Using the coefficients thus obtained, we calculate the concentration of associated molecules

$$C_k = \frac{I - \epsilon_M C_0^A}{\epsilon_k - \epsilon_M}$$

and the value of K is obtained for several values of m in the interval $0.3 < m < 0.7$, where the error of calculation is minimal. The error in K is estimated from the deviation of the values obtained from the arithmetic mean.

Using the method described by the authors of Ref. [6], ϵ_k of the band, ν(CD) and K were obtained for the system diethyl ether-chloroform-d and ϵ_k for mixtures of chloroform-d with acetone, p-dioxane, ethyl acetate, and certain other substances. Later Josien, Leicknam and Fuson [7], using this same method for treating experimental data, determined K and ϵ_k for mixtures of chloroform-d with diethyl ether and butyl iodide.

From Eq. (3) it is obvious that neglecting V_A and V_B in comparison to K leads to a value of ϵ_k which is smaller than the true value, and the more so the smaller K is. Calculation of K using the value of ϵ_k obtained by this means leads to values of K very much larger than the true values (see Appendix). The dependence of $\frac{K'}{V}$ on $\frac{K}{V}$ (K' is the equilibrium constant calculated by Lord's method; K is the true equilibrium constant) set up under the hypothesis $V_A = V_B = V$ for $C_0^A = \frac{1}{2V}$ is shown in figure 1. Obviously it is impossible to obtain $\frac{K'}{V} < 4$ using Lord's method. At the same time, it follows from figure 2, which shows the dependence of $\frac{K'}{K}$ on $\frac{K}{V}$, that as K increases, the ratio $\frac{K'}{K}$ very slowly approaches unity.

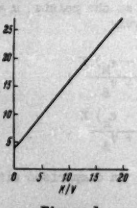

Figure 1

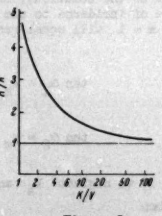

Figure 2

Further, the agreement or closeness of the values for $\epsilon_k^{(1)}$ and $\epsilon_k^{(2)}$ may be caused either by closeness of the values of V_A and V_B, or by insufficient accuracy in measuring $\tan\alpha_1$ and $\tan\alpha_2$. It is all the more incorrect to evaluate the error in ϵ_k according to the deviation of these values from the arithmetic mean.

Thus it is clear that Lord's method gives a significant systematic error in the determination of K and ϵ_k for systems for which it is known a priori that the equilibrium constant of the reaction of hydrogen-bond formation is rather large, and that this method is inapplicable to systems with small K. Some improvement in the method can be achieved if we solve the system of (3) for the two unknowns K and ϵ_k and use the value obtained for ϵ_k to calculate K in the range $0.3 < m < 0.7$. However, when $V_A \simeq V_B$, the error in determining $\tan\alpha_1$ and $\tan\alpha_2$ greatly affects the value of ϵ_k, so that this method is also unsatisfactory.

The rigorous method of determining K and ϵ_k from the experimentally obtained concentration dependence of the integrated intensity must come down to a search for values of these parameters such that Eq. (2) will best describe the experimental curve. The most accurate method of solving this kind of problem is the method of least squares (see for example [8]). According to this method, the values of the parameters ϵ_k and K are selected so as to minimize the sum of the squares of the deviation of the function $I = I(C_0)$ from the experimental curve. The function $I(C_0)$ can be written

$$I(C_0) = \epsilon_M C_0^A + (\epsilon_k - \epsilon_M) C_k.$$

Substituting C_k from the law of mass action (1), we obtain

$$I(C_0) = \epsilon_M C_0^A + (\epsilon_k - \epsilon_M) X$$

$$X \left\{ \frac{C_0^A + C_0^B + \frac{1}{K}}{2} - \sqrt{\left(\frac{C_0^A + C_0^B + \frac{1}{K}}{2} \right)^2 - C_0^A C_0^B} \right\}. \quad (5)$$

The function $I(C_0)$ depends nonlinearly on the parameters ϵ_k and K; therefore in treating experimental data we use its expansion in a Taylor series in the neighborhood of a certain point ϵ_k^0, K^0 in powers of $\Delta\epsilon_k$ and ΔK and restrict the expansion to the first powers. We then find the correction for $\Delta\epsilon_k'$ and $\Delta K'$ by the method of least squares.

The latter are determined as roots of the system of normal equations

$$\begin{cases} \sum_{i=1}^{n} \alpha_i^2 \Delta\epsilon_k' + \sum_{i=1}^{n} \alpha_i\beta_i \Delta K' = \sum_{i=1}^{n} \alpha_i\gamma_i \\ \sum_{i=1}^{n} \alpha_i\beta_i \Delta\epsilon_k' + \sum_{i=1}^{n} \beta_i^2 \Delta K' = \sum_{i=1}^{n} \beta_i\gamma_i, \end{cases} \quad (6)$$

where

$$\alpha_i = \left[\frac{\partial}{\partial \epsilon_k} I(C_o^i, K, \epsilon_k)\right]_{K^o, \epsilon_k^o};$$

$$\beta_i = \left[\frac{\partial}{\partial K} I(C_o^i, K, \epsilon_k)\right]_{K^o, \epsilon_k^o};$$

$$\gamma_i = I_i - I(C_o^i, K^o, \epsilon_k^o);$$

I_i is the experimental value of the intensity at the initial concentration C_o^i; n is the number of points on the experimental curve. The mean square deviations $\delta\epsilon_k$ and δ_K are

$$(7)\quad \begin{cases} \delta\epsilon_k = \sqrt{\dfrac{\sum \beta_i^2}{\sum \alpha_i^2 \sum \beta_i^2 - \left(\sum \alpha_i \beta_i\right)^2}} \cdot \sqrt{\dfrac{\sum \gamma_i^2}{n-2}} \\ \delta_K = \sqrt{\dfrac{\sum \alpha_i^2}{\sum \alpha_i^2 \sum \beta_i^2 - \left(\sum \alpha_i \beta_i\right)^2}} \cdot \sqrt{\dfrac{\sum \gamma_i^2}{n-2}}. \end{cases}$$

The best values of ϵ_k and K are obtained by successive approximations, the number of which depends on our success in choosing ϵ_k^o and K^o.

Values of Absorption Coefficients ϵ_k (in liters/mole · cm²) and the Equilibrium Constant K (in liters/mole)

System	Parameter	Values Obtained by the Authors of Refs. [6] & [7]	Improved Values According to Curves in Figs. 1 & 4	Values According to Method of Least Squares
$(C_2H_5)_2O$+$CDCl_3$*	ϵ_k	2360	3000	—
	K	0.80 ± 0.15	0.33	—
$(C_2H_5)_2O$+$CDCl_3$**	ϵ_k	2610 ± 100	3200	3170 ± 230
	K	0.9 ± 0.4	0.4	0.33 ± 0.09
n-C_4H_9I+$CDCl_3$**	ϵ_k	445 ± 35	580	575 ± 45
	K	0.6 ± 0.4	0.18	0.19 ± 0.02

* According to the data of Lord, Nolin and Stidham [6].
** According to the data of Josien, Leicknam and Fuson [7].

We have carried out similar calculations using experimental data on the intensity of the infrared absorption band ν(CD) of chloroform-d at various concentrations, mixed with $(C_2H_5)_2O$ and n-C_4H_9I, obtained in Ref.[7]. In the treatment, the values of I_i were all considered to be equally accurate. The values obtained by the authors of Ref. [7] were taken for K^o and ϵ_k^o. The results obtained are given in the table. Three iterations were sufficient for both systems. In processing the data for the $CDCl_3$ + C_4H_9I system, three points, corresponding to concentrations of $CDCl_3$ 11.80; 9.60 and 2.99 moles/liter were excluded as not satisfying Shoven's [9] criteria. The dependence $I(C_o) - \epsilon_M C_o$ on the mole fraction m for the three approximations [in the system $CDCl_3$ + $(C_2H_5)_2O$] are shown in figure 3.

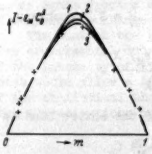

Figure 3

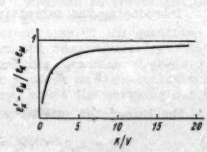

Figure 4

In order to lessen the labor of calculation, the following method may be used for choosing the parameters ϵ_k^o and K^o for the zero approximation. It may be shown that

$$\lim_{C_o \to 0} \frac{I}{C_o} = \epsilon_M + \frac{(\epsilon_k - \epsilon_M) K}{K + V_B} = \tan \alpha_1 = \epsilon_k^{(1)}.$$

We will consider that the value of $\epsilon_k^{(1)}$ determined by extrapolation of the experimental curve $\frac{I}{C_o} = f(C_o)$ to zero is more accurate than the value $\tan \alpha_1$. Using this value of $\epsilon_k^{(1)}$ to calculate K', according to the graph in figure 1, we find an improved value for K^o, and according to the graph in figure 4 [see Eq. (1) of the Appendix], an improved value for ϵ_k^o, which values are then used as initial ones in further processing by means of least squares. These values for K^o and ϵ_k^o are also given in the table. Thus, using the scheme here described to treat experimental data, sufficiently accurate values may be obtained for the equilibrium constant K and the absorption coefficient of the complex ϵ_k. These may be made even more accurate, if necessary, by increasing the number of measurements. This scheme may be developed for any equilibrium whose type is known beforehand.

The authors thank Professor V. M. Chulanovskii for his constant attention and discussion of the results of this work.

APPENDIX

The dependence of $\frac{K'}{V}$ on $\frac{K}{V}$ is sought under the following assumptions: 1) the molar volumes of

the components of the mixture are equal: $V_A = V_B = V$; 2) the initial concentrations are equal $C_0^A = C_0^B = \frac{1}{2V}$. If ϵ_k and ϵ_k' are the true and the approximate values (calculated by Lord's method) of the absorption coefficient of the molecules in the complex, and K is the true value of the equilibrium constant, then

$$\tan \alpha_1 = \epsilon_M + \frac{\epsilon_k - \epsilon_M}{1 + \frac{V}{K}} = \epsilon_k'.$$

Introducing the definition $\frac{K}{V} = X$, we obtain

$$\epsilon_k' - \epsilon_M = \frac{(\epsilon_k - \epsilon_M) X}{1 + X} . \tag{1}$$

The integrated intensity of the entire band is

$$I = \epsilon_M C_0 + (\epsilon_k - \epsilon_M) C_k. \tag{2}$$

C_k', the concentration of the complex determined with the aid of an approximate value of the absorption coefficient ϵ_k' from (1) and (2), is

$$C_k' = \frac{I - \epsilon_M C_0}{\epsilon_k - \epsilon_M} \cdot \frac{1 + X}{X} = C_k \frac{1 + X}{X} . \tag{3}$$

The approximate value of K' from the law of mass action under the assumptions made is given by the relation

$$K' = \frac{C_k'}{\left(\frac{1}{2V} - C_k'\right)^2} \quad \text{or} \quad \frac{K'}{V} = \frac{VC_k'}{\left(\frac{1}{2} - C_k'V\right)^2} \tag{4}$$

Using the true value of K, we find

$$C_k = \frac{1}{2}\left(\frac{1}{V} + \frac{1}{K}\right) - \sqrt{\frac{1}{4}\left(\frac{1}{V} + \frac{1}{K}\right)^2 - \frac{1}{4V^2}}$$

or, transforming to X,

$$C_k V = \frac{1}{X}\left(\frac{1 + X}{2} - \sqrt{\left(\frac{1 + X}{2}\right)^2 - \frac{1}{4} X^2}\right) \tag{5}$$

From (3) and (5) we determine

$$C_k' V = \frac{1 + X}{X^2}\left[\frac{1 + X}{2} - \sqrt{\left(\frac{1 + X}{2}\right)^2 - \frac{1}{4} X^2}\right]. \tag{6}$$

Substituting (6) in (4), we obtain $\frac{K'}{V}$ as a function of $\frac{K}{V}$. It is easy to see that

$$\lim_{X \to 0} C_k' V = \frac{1}{4} \text{ and } \lim_{X \to 0} \frac{K'}{V} = 4.$$

November 28, 1958

References

1. H. KEMPTER, R. MECKE: Zs.phys. Chem., B46, 229 (1940)
2. N. COGGESHALL, E. SAIER: J.Am.Chem.Soc., 73, 5414 (1951)
3. G. M. BARROW, E. A. YERGER: J.Am.Chem.Soc., 76, 5247 (1954)
4. S. MIZUSHIMA, M. TSUBOI, T. SHIMANOUCHI, Y. TSUDA: Spectrochim. Acta, 7, (2),100 (1955)
5. A. ENS, F.E. MURRAY: Can. J. Chem., 35, 170, (1957).
6. R. C. LORD, B. NOLIN, H. D. STIDHAM: J.Am.Chem.Soc., 77, 1365, (1955)
7. M. L. JOSIEN, J. P. LEICKNAM, N. FUSON: Bull. Soc. Chim. France, 188, (1958)
8. A. N. KRYLOV: Lecture on Approximate Calculations, 1950.
9. A. S. CHEBOTAREV: Method of Least Squares with the Fundamentals of the Theory of Probabilities. 1958.

TOM VII, Vyp. 2 OPTIKA I SPEKTROSKOPIIA Avgust, 1959
VOL. VII, No. 2 OPTICS AND SPECTROSCOPY August, 1959

Investigation of the Temperature Dependence of the Intensity of Infrared Absorption Bands of Gases

V. N. SMIRNOV AND P. A. BAZHULIN

Abstract: Quantitative measurements of the intensity of infrared absorption bands of a series of substances in the gaseous phase were carried out at various temperatures. It was found that most of the bands show an increase in intensity with a rise in temperature. The effect of the gas pressure on the intensity of the infrared absorption was investigated. A discussion of the results obtained is given.

INTRODUCTION

In a previous communication [1] it was pointed out that a study of the temperature dependence of the intensity of molecular vibrational spectra shows a divergence of the experimental results from the statistical theory. The experimental data often show a markedly negative effect (decreasing intensity with increasing temperature), whereas the theory predicts a positive effect (increasing intensity). These results were obtained for both Raman and infrared absorption spectra of substances mainly in the liquid phase. The question arises as to whether the observed anomalies are to be considered as peculiarities of the condensed state with its characteristic types of intermolecular interaction, or whether it is necessary to seek the origin of the discrepancy in the internal dynamics of the molecule.

An immediate answer to this question might be given by measurements in the gas phase, where molecular interactions are reduced to a minimum and where it is possible to study the simplest diatomic molecules. In fact it is precisely for gases that the statistical formulae have been derived. However, because of the experimental complications involved in measuring the temperature dependence of the intensity of spectral lines of gases, such investigations have been practically nonexistent up to the present.

There are only a few investigations pertaining to the subject* which merit mention [2-4]. Schmidt [2], who studied CO_2 in the region of 2.7μ observed that the absorption of the band increased with a rise in temperature. Bahr [3] confirmed this result for CO_2, but in a study of CO, N_2O and ether she came to the conclusion that the temperature effect in these cases was merely a broadening of the band without any increase in absorption. Finally, Taylor and his coworkers [4], investigating the rotation-vibrational spectrum of CO_2 and H_2O at +200 and +500° C, found that an increase in temperature gave a marked increase in absorption, especially in the region of low frequencies. No quantitative data are reported in the papers mentioned, and at best the qualitative conclusions which are given concerning the observed changes do not always seem convincing. In connection with the question of the temperature dependence of absorption one must also mention papers which deal with the investigation of the emissive power of gases at various temperature [5-7]. The reported decrease in the degree of "blackness" of the gases CO_2 and H_2O and, consequently, the decrease of their absorptive power with temperature is apparently explained simply as a nonobservance of the Stefan-Boltzmann law for emission from gases. As far as Raman spectra are concerned no investigation of temperature changes in gases exists.

The lack at the present time of any quantitative experimental data on the temperature dependence of the intensity of vibrational spectra of gases, which would allow a direct check on the conclusions of the statistical theory, makes the carrying out of such investigations most urgent.

*If one does not include investigations concerned with the study of the effect of temperature on rotational isomerism in gases.

EXPERIMENTAL

Although gas cells for temperature measurements have been described in the literature [8-14], they have various deficiencies and could not be used for our purpose. We have therefore developed a special cell, the design of which is shown in figure 1.

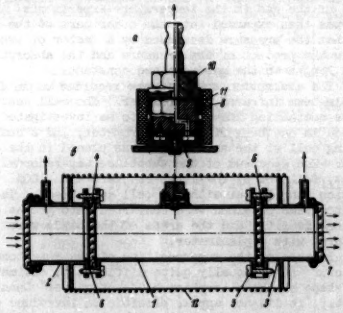

Figure 1. Gas cell for absorption measurements at various temperature: (a) valve, (b) cell.

The gas to be investigated is contained in the brass cylinder 1, (10.75 cm long), with well polished end plates. Two evacuated end cylinders, 2 and 3, serve to equalize the temperature of the windows 4 and the body of the cell 1; they would also prevent condensation of water vapor on the windows if the tube were used at low temperatures. The windows 4, made of rocksalt suitably polished, are pressed by the screws 5 against thin layers of silicone grease 6, giving a good vacuum seal and withstanding temperatures up to +350° C. It should be mentioned that the use of silicone grease [13], which is thermally and chemically stable, seems to furnish a highly successful solution of the problem of sealing windows [8, 9, 15-17] in gas cells for temperature investigations. The outer windows 7,

cooled by running water, were sealed with picein wax. The filling of the cell with the gas to be investigated at a given pressure was carried out with special vacuum equipment. After the cell was filled, the nut 8, carrying the teflon gasket 9, was tightened and the upper part of the valve 10 along with the rubber sealing ring 11 was taken away. The tube was heated by the electric heater 12, wound on an outer jacket; cooling would also be possible by circulating the vapor of liquid nitrogen. The arrangement used provided satisfactory uniformity in the heating or cooling of the whole cell including the valve and the windows. The temperature was measured by thermocouples attached to the edges of the windows 4. The temperature difference between the windows and the center of the cell did not exceed 100 C. It was verified that the sealing of the cell was not disturbed by the heating. The cell gave completely stable performance and no breaking of the windows occurred.

During the measurements at different temperatures the number of molecules in the cell remained constant but the pressure of the gas changed proportionally with the absolute temperature. To ascertain the effect of changes in pressure a special cell [18] was used; this consisted of two nearly identical compartments connected by a capillary with a stopcock. Initially the gas was entirely in one compartment at a pressure equal to the maximum pressure of the gas in the temperature experiments. The gas was then expanded into the other part of the cell, so that the pressure decreased by a factor of two while the product of the pressure and the absorption path length in the gas remained constant.

The absorption spectra were recorded on an IKS-2 double beam infrared spectrometer. The cell described above containing the substance to be investigated was placed in one beam of the spectrometer, and a compensating cell of the same length was placed in the other beam. The spectrum of the substance was recorded first, followed by the lines for zero and 100% transmission (the latter with the cell evacuated). The spectrograms obtained were converted into graphs of optical density, and the areas of the bands were measured with a planimeter.

Because of the superposition of the rotational structure it is usually quite difficult to estimate the shape of the absorption bands of gases. Consequently, it did not appear possible to introduce corrections for intensity lost in the the wings of the band. To minimize the effect of this on the integrated intensity, a region of integration was always used which extended to the regions where the absorption did not exceed 1 - 1.5% of the value at the maximum of the band. This condition was easily satisfied since the bands studied were well separated. With the boundaries of the region of integration, defined as above, the area lost in the wings of a band of dispersion would be form 6-7%. It should also be noted that bands observed in gases do not as a rule have intense wings, but correspond more closely to a Gaussian distribution. Thus the correction in question can be neglected without introducing any large error in the results. This method of measuring the intensity excludes almost completely any effect of temperature broadening of the bands on the measured relative changes in intensity [19].

Because of the complicated rotational structure of absorption bands of gases it is not possible to calculate accurate corrections for the finite width of the spectrometer slit using given shapes for the band profile and for the instrumental line form. An integrated absorption coefficient, K_m, which is free from the effect of the finite width of the spectrometer slit, is usually determined for bands of gases by an extrapolation procedure [20, 21]. However, because of the complications involved in changing the length of the cell or the pressure of the gas, it was impractical to use the extrapolation method in investigating the temperature dependence of the intensity. Moreover, the determination of the relative change in K_m by the change in the slope of the tangent at the origin would entail a greater error than the scaling method used in the present investigation. Finally, if, as is usual, the curves to be extrapolated are obtained from measurements at various gas pressures, some indefiniteness of the results for temperature changes could occur as a consequence of the existence of departures from the Lambert-Beer law.

The effect of finite slit-width is determined in the most general case by the ratio of the width of the instrumental line shape and the width of the band under study. Thus, absorption bands observed in gases are subject to somewhat less instrumental distortion* than the much narrower absorption bands of liquids and solutions. Moreover, the effect of the correction under discussion, which is in itself relatively small (cf. Fig. 2), can be reduced to a minimum by the choice of appropriate optimal conditions of measurement. This question has been given special study [22], and it has been shown that the magnitude of the slit correction for K_m is dependent only slightly on the shape of the true profile of the band and to a greater extent on the value of the observed optical density D_0^{obs} at the maximum of the band. Figure 2 shows the calculated [22] variation of the ratio of the true and observed values of K_m for three values of D_0^{obs}; the solid curve refers to a true profile of dispersion shape and the dashed curve to one of Gaussian shape. From this it is seen that for $D_0^{obs} < 0.8$ the magnitude of the correction does not exceed 5 - 6% even for the case of wide slits. The lower limit of the optimal region for D_0^{obs}, where the errors in measurement begin to increase rapidly, was taken to be 0.4. The correction for the observed relative change in intensity depends only on the temperature broadening of the bands and consequently is even less important. An estimation was made which showed that the neglect of any correction for spectral impurity did not introduce any appreciable error in the experimental results in the determination of the temperature dependence of the intensity.

A calculation, using the formulae of Planck and Kirchhoff, of the effect of self-emission of the substances investigated for the temperatures reached in the experiments (~ + 300° C) showed a decrease in intensity at higher temperatures. However, these changes in the case of a light source at a temperature of 1500° C (Globar) do not exceed 1.5 - 2% and lie within the limits of the error of the measurements.

A significant effect of the self-emission of substances and of the background of heat radiation [23]

---

* This is true for bands with unresolved rotational structure. For almost all the substances considered in the present investigation, the rotational structure of the bands is not resolved; the exceptions are HCl and methane.

on the measured temperature dependence of the absorption coefficient is present only for sources with relatively low brightness.

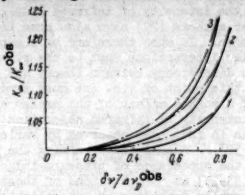

Figure 2. Correction to K_m for the width of the spectrometer slit, as a function of the ratio of the width of the instrument line width, $\delta\nu$, and the observed band width, $\Delta\nu_D^{obs}$. The solid curve refers to a true profile of dispersion form and the dotted curve to one of Gaussian form. Curve 1 - $D_0^{obs} = 0.4$; 2 - $D_0^{obs} = 1.0$; 3 - $D_0^{obs} = 1.6$.

In order to estimate the reproducibility of the experimental results, three to four tracings of the spectrum were made for each temperature; in every case a tracing was made before the cell was heated and also after it had cooled down. The latter was an important precaution since it permitted a check of the constancy of the seal of the tube and also of the absence of any irreversible chemical change of the substance while the measurements were being made. In order to prevent possible condensation in working with the vapors of liquids, the measurements were carried out at pressures well removed from saturation.

The total random error in the integrated absorption coefficient is determined mainly by errors in the limits of the recorded area of the band and in the measurement of the pressure of the gas. For the vapors of organic liquids, which were the principal objects of study, the error in the observed value of K_m was on the average 15 - 20%. The sources of error in the recorded area of the band include some instability in the working of the detector-amplifier unit and the motors of the apparatus (~ 2%), inaccuracy in the measurement of the temperature of the gas (~ 0 - 2%), and planimeter error (~ 0.5 - 1%). The error in the measurement of the cell length was 0.5%. The error in the measurement of the gas pressure amounted to a few percent at moderate pressures and rose to 50% or higher when it was necessary to work at low gas pressures of the order of 2 - 4 mm Hg. However, the aim of the investigation was to obtain, not absolute values of the integrated absorption coefficient, but its change with temperature. The relative changes of K_m in their dependence on the temperature were of course determined with much greater accuracy, (on the average, of the order of 5%). This error remained more or less constant for all the bands investigated.

RESULTS AND DISCUSSION

Substances which showed in the liquid state [1] a more or less marked discrepancy with theory were chosen for study. Of these, the most suitable for the measurements seemed to be acetone, methyl iodide, chloroform and cyclopentane, which have relatively low boiling points. A number of other molecules of simple structure were also studied.

The results of the measurements for fundamental vibrations of the substances studied are given in Table 1. The integrated absorption coefficient K_m are expressed in units with the dimensions, cm^2 sec^{-1} per mole, using the relation

$$(1) \qquad K_m = K'_m \cdot \frac{cRT}{p} \cdot \frac{cm^2}{\text{mole} \times \text{sec}},$$

where K'_m is the measured integrated absorption coefficient in cm^{-2}, p the gas pressure, c the velocity of light, R the gas constant, and T the absolute temperature. Values of K_m are given in the table for two extreme temperatures, although measurements were always made also at several intermediate points in this range. The values of K_m obtained by us for the vapors of the substances investigated show satisfactory agreement within the limits of the experimental error with data available in the literature [24-26]. The measurement of absolute intensities of infrared absorption bands was not the aim of the present investigation.

Table 1

Temperature dependence of the intensity of the infrared absorption bands of some substances in the gas phase

Substance	Vibration form	ν_Q (cm^{-1})	$\delta\nu$ (cm^{-1})	$\Delta\nu_D^{obs}$ cm^{-1} (at 25°C)	$K_m \cdot 10^{-15}$ (cm^2 sec^{-1} per mole)		$\frac{(K_m)_{275°C}}{(K_m)_{25°C}}$	
					+25°C	+275°C	Observed*	Theoretical
$(CH_3)_2CO$	ν(CC)	1223	14	45	175	170	0.97	1.04
	$\delta(CH_3)$	1373	15	43	160	150	0.94	1.03
	ν(CO)	1745	17	53	245	270	1.10	1.01
CH_3J	δ(HCH)	1258	11	43	45.5	55.5	1.22	1.04
	ν(CH)	2964	12	48	32.5	38.5	1.19	1.00
$CHCl_3$	ν(CCl)	767	8	19	470	500	1.07	1.13
	δ(HCCl)	1225	8	16	105	105	1.00	1.04
	ν(CH)	2970	12	180	11.0	15.5	1.40	1.00
C_5H_{10}	ν(CC)	894	10	52	12.5	12.5	1.00	1.09
	δ(HCH)	1463	15	45	32	33	1.03	1.02
C_2Cl_4	ν(CCl)	788	6	23	200	235	1.18	1.12
	—	918	8	21	390	445	1.14	1.09
CCl_4	ν(CCl)	780	9	15	620	770	1.24	1.12
CS_2	ν(CS)	1527	10	37	255	450	1.75	1.02
CH_4	δ(HCH)	1305	15	120	-	-	1.45	1.03
	ν(CH)	3033	12	-	-	-	1.57	1.00
NO	-	1883	9	120	-	-	1.29	1.01
CO	-	2144	10	120	-	-	1.18**	1.00
HCl	-	2887	11	-	-	-	1.33	1.00

*The observed changes of the intensity are given, uncorrected for the effect of pressure.

**A linear extrapolation was used from +225°C to 275°C, since above +225°C an irreversible change in the spectrum sets in, which is probably related to the chemical instability of the CO moelcule.

Experimental difficulties associated with absolute measurements of the quantity K_m are particularly great in the case of light molecules, such as HCl, CO, etc., which were studied with the secondary purpose of ascertaining the part played by anharmonicity (see below). On these grounds data on the absolute intensities of these molecules are not included in Table 1.

The intensity of each band at room temperature was taken as the unit for expressing the relative changes in K_m. The theoretical temperature dependence of the intensity of a fundamental frequency is given by the well-known formula of Placzek:

$$f(T) = \frac{1}{1 - \exp[-h\nu/kT]} . \qquad (2)$$

The experimental results show that for the majority of the bands there is an increase of the intensity with temperature; the increase, however, often exceeds considerably the corresponding change of intensity predicted by the statistical theory. The fact that in gases the deviation from theory is observed to be in the opposite direction from that observed in liquids, definitely indicates different origins of the anomalies in the two cases. However, it is probably necessary to seek the cause of the discrepancy with theory for both gases and liquids, not in intramolecular factors, but in the intermolecular interactions.

One is lead to this conclusion by the results of the investigation of the temperature dependence of the intensity for the simplest diatomic gases. In these cases certainly the observed temperature dependence of the intensity is not complicated by the effect of the intramolecular interaction of the normal vibrations, which can be accompanied by transfers of energy from some degrees of freedom to others. Also, for diatomic molecules it is possible to estimate directly the part played by the anharmonicity of the vibrations.

A simple calculation leads to the temperature dependence of the root-mean-square value of the coordinate in the form,

$$\sqrt{(q^2)} = \alpha \cdot \sqrt{\frac{1 + \exp[-h\nu/kT]}{1 - \exp[-h\nu/kT]}} \qquad (3)$$

where α is the zero-point amplitude of the vibration. This calculation shows that the increase in temperature attained in our experiment does not render invalid the series expansion of the potential energy or of the dipole moment about the equilibrium configuration of the molecule. It also shows that it is impossible to accept as well-founded the attempt of Venkateswarlu [27] to explain the anomalous temperature dependence of the intensity in terms of the inapplicability of the series expansion in question at high temperatures. Moreover, a calculation of the mechanical and electrical anharmonicities, neglected in the derivation [28] of the expression for the temperature factor (Eqn. 2), does not explain the observed variation of the intensity. An estimation made by us of the role of the anharmonicity in the case of the diatomic molecules NO, CO and HCl gives a negligibly small correction, not exceeding 1%; this acts nevertheless in the direction of an increase in intensity with rising temperature.

Thus it is clear that the anharmonicity effect cannot be responsible for the observed temperature behavior of the intensity of infrared absorption bands. Other authors [29] have also come to this same conclusion. It must therefore be accepted that molecular interactions must be the principal cause of the discrepancy between theory and experiment. From this point of view one must expect the existence of a marked effect of the pressure of the gas on the intensity of infrared absorption; such an effect has in fact been observed by various authors [30-32]. In some cases raising the pressure even causes the appearance of pressure-induced absorption [33-35] at the positions of those bands which are normally forbidden by the selection rules.

Table 2

Effect of pressure on the intensity of infrared absorption bands

Substance	ν_0 (cm-1)	Pressure p_0 (mm Hg)	$\frac{(K)_{2p_0}}{(K)_{p_0}}$
$(CH_3)_2CO$	1223	10.0	1.01
	1745	8.0	1.01
CH_3I	1258	40	1.06
	2964	40	1.05
$CHCl_3$ . . .	1225	7.0	1.00
C_2Cl_4 . . .	918	2.5	1.02
CS_2	1527	6.0	1.12
CH_4	1305	135	1.19
	3033	135	1.18
NO	1883	280	1.13
CO	2144	200	1.29
HCl	2887	250	1.37

The pressure effect was also considered in our investigation. For this purpose the cell described above was employed; the gas pressures used corresponded to the pressures involved in the temperature measurements. The results of the measurements are given in Table 2, from which it is seen that with rising pressure the intensities of the majority of the bands increase; to a certain degree the increase parallels the corresponding increase with temperature. However, in order to compare directly the results given in Tables 1 and 2 for the effects of temperature and pressure on the intensity, it is necessary to take into account the fact that, in reality, the pressure of the gas changed by a factor of 1.85, rather than 2, on heating. It is not difficult to see that a temperature change affects the intensity more strongly than a change in pressure. To illustrate this point figure 3 gives a comparison of the observed temperature and pressure effects on an infrared absorption band of CS_2. It must be noted that the spectrograms, reproduced in figure 3, (a) and (b), refer to different cell lengths and for this reason they cannot be used for a direct comparison of the intensities.

The theoretical description of the mechanism of the effect of molecular interactions on the intensity of spectral lines is at present still unsatisfactory in many respects. For the time being any discussion must therefore be limited to qualitative considerations. In the case of liquids the

intermolecular forces have in general an interaction potential of the Van der Waals type. When the temperature of a liquid is lowered the molecules come closer together and the energy of this type of interaction, which is inversely proportional to the sixth power of the intermolecular distance, increases considerably. When this happens it appears that the transition probabilities in the molecule, that is, the intensities of the spectral lines, must increase. For gases the situation is different in so far as molecular interactions are present here only during molecular collisions. The number of collisions, which determines in gases the effectiveness of the external perturbations, increases with a rise in temperature; accordingly one should expect also an increase in the transition probabilities in the molecule. The experiments show however that the pressure, on which the number of molecular collisions also depends, has much less effect than the temperature on the absorption intensity.

Brown [36] also tried to explain the temperature behavior of the intensity as an effect of molecular collisions, and came to a conclusion opposite to ours. Guided by the fact that, according to the kinetic theory, the collision width of a spectral line is proportional to $\sqrt{T}$, where T is the absolute temperature, Brown obtained a dependence of the integrated absorption coefficient on temperature in the form: $K_m \sim \frac{1}{\sqrt{T}}$. This conclusion cannot be considered valid, inasmuch as it is derived from the arbitrary assumption that the quantity, $K_0 \Delta\nu^2$ in the Lorentz distribution, where K_0 is the absorption coefficient at the maximum of the band, does not depend on the temperature.

Experiment shows that in both gases and liquids characteristics of the vibrations themselves play a positive part in the observed temperature dependence of the intensity. In this connection the following might be noted: for a given molecule in the gas phase

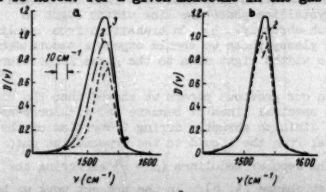

Figure 3. The 1527 cm^{-1} band of carbon disulphide: (a) the effect of change in temperature; curve 1– +25° C, 2– +150° C, 3– +275° C; (b) effect of change in pressure; curve 1– 6 mm Hg, 2– 12mm Hg.

an increase in temperature causes the greatest increase in intensity for those vibrations which in the liquid show the greatest decrease in intensity. This is indicative of the unequal sensitivity of the various vibrations and bonds of molecules to external perturbations. These conclusions require of course further experimental confirmation.

October 31, 1958

References

1. P. A. BAZHULIN, V. N. SMIRNOV: OiS, 6, 745 (1959)
2. H. SCHMIDT: Ann. der Phys., 42, 415 (1913)
3. E. BAHR: Ann. der Phys., 38, 206 (1912)
4. J. H. TAYLOR, W. S. BENEDICT, J. STRONG: J.Chem. Phys., 20, 1884 (1952)
5. A. SCHACK: Naturwiss., 15, 91 (1927)
6. C. TINGWALDT: Phys. Zs., 35, 715 (1934); 39, 1 (1938)
7. H. C. HOTTEL: Trans.Amer.Inst.Chem.Engrs., 31, 517 (1935)
8. L. G. SMITH: Rev. Sci. Instr., 13, 63, (1942)
9. G. L. SIMARD, J. STEGER: Rev. Sci.Instr., 17, 156 (1946)
10. F. A. MILLER, S. D. KOCH: J.Amer.Chem.Soc., 70, 1890 (1948)
11. H. J. BERNSTEIN: J.Chem.Phys., 18, 897 (1950)
12. H. S. GUTOWSKY, C. J. HOFFMAN: J.Amer.Chem. Soc., 72, 5751 (1950)
13. J. T. NEU: JOSA., 43, 520 (1953)
14. R. B. HOLDEN, W. I. TAYLOR, H. L. JOHNSTON: JOSA, 40, 757, (1950)
15. R. C. LORD, R. MCDONALD: Rev. Sci.Inst., 23, 442 (1952)
16. R. FRANK, R. STOW: Rev. Sci. Inst., 25, 514, (1954)
17. V. ROBERTS: J. Sci. Instr., 31, 251, (1954)
18. K. ANGSTROM: Ann. der Phys., 6, 163 (1901)
19. F. ROESSLER: Asta phys.austriaca, 5, 477, (1952)
20. D. G. BOURGIN: Phys.Rev., 32, 237, (1928)
21. E. B. WILSON, A. J. WELLS: J.Chem.Phys., 14, 578 (1946)
22. V. N. SMIRNOV: Vestnik, Moscow Univ., (1), (1959)
23. B. I. STEPANOV, IA.S. KHVASHCHEVSKAIA: DAN USSR, 116, 588, (1957)
24. D. H. WHIFFEN: Trans.Farad.Soc., 49, 878, (1953)
25. A. D. DICKSON, I. M. MILLS, B. CRAWFORD: J. Chem.Phys., 27, 445, (1957)
26. S. A. FRANCIS: J. Chem.Phys., 19, 942 (1951)
27. K. VENKATESWARLU: Nature, 159, 96, (1947); Curr.Sci., 16, 15 (1947)
28. M. V. VOL'KENSHTEIN, M. A. EL'IASHEVICH, B.I.STEPANOV: Kolebaniia molekul (Vibrations of Molecules), Vol. II, GITTL, Moscow, 1949;
29. IA. S. BOBOVICH, V. M. PIVOVAROV: OiS, 3, 227 (1957)
30. G. BECKER: Zs. f. Phys., 34, 255, (1926)
31. H. W. KUSSMAN: Zs. f. Phys., 48, 831, (1928)
32. J. STRONG, K. WATANABE: Phys. Rev., 57, 1049 (1940)
33. M. F. CRAWFORD, H. L. WELSH, J. L. LOCKE, J.C.F. MacDONALD: Phys.Rev., 80, 469, (1950)
34. S. MINOMURA: Rev. phys. chem. Japan, 24, 49 (1954)
35. R. COULON, L. GALATRY, J. ROBIN, B. VODAR: Disc. Faraday Soc. No. 22, 22 (1956)
36. T. L. BROWN: J.Chem.Phys., 24, 1281, (1956)

TOM VII, Vyp. 2. OPTIKA I SPEKTROSKOPIIA Avgust, 1959
VOL. VII, No. 2. OPTICS AND SPECTROSCOPY August, 1959

The Influence of Intermolecular Interaction on Line Width in the Raman Spectra of Liquids

A. V. RAKOV

Abstract: A change of the widths of lines in the Raman spectra of 2-methylpentane and 2-methylhexane with temperature has been observed on transition from the liquid to the glassy state. It has been shown that this transition is not accompanied by any abrupt change in line width. Reorientation times of the molecules in the liquid have been calculated from the magnitude of the temperature broadening of the lines. A connection has been shown between the widths of Raman lines and the molecular nature of viscosity.

At present there is a number of papers in which it is shown that the width of lines in the Raman spectra of liquids is a sensitive parameter, characteristic of intermolecular interactions [1-4]. Therefore the investigation of Raman line widths relative to their dependence on temperature, state of aggregation, and viscosity is of great interest.

As is well known, molecules of a liquid execute chaotic motions accompanied by changes of their orientations. Sobel'man has shown that such rotational Brownian motion of the molecules in a liquid might lead to a significant broadening of the Raman lines having a degree of depolarization $\rho \approx \frac{6}{7}$ [5]. Actually, a change of orientation of the molecule leads to a change of the directions of the induced moments of all the vibrations in which the derivative of the polarizability tensor α'_{ik} has an anisotropic part. This means that the projections of the induced moment of the i'th vibration in laboratory coordinates, in which the observation is performed, will be random functions of time.

From the theory of stationary random processes it is well known that the values of any random function $f(t)$ at the times t and $t + \tau$ are connected by a correlation function

$$\varphi(\tau) = \overline{f(t)f(t+\tau)}, \tag{1}$$

which has a maximum at $\tau = 0$, decreases monotonically with increasing τ, and has a half life τ_0. The value of τ_0 is the time in which, on the average, the correlation function of the random process halved. Then expansion of the function $f(t)$ into a frequency spectrum gives a line contour with half-width $\Delta\omega = \frac{1}{\tau_0}$ [6,7]. Consequently, when the projections of the induced moment of the i'th vibration (the tensor α'_{ik} having an anisotropic part) is a random function of time, the Raman lines with depolarization $\rho \approx \frac{6}{7}$ (in contradistinction to those with small ρ) should be additionally broadened by an amount

$$\Delta\omega = \frac{1}{\tau_0}. \tag{2}$$

Since in the present case the correlation function characterizes the random process of reorientation of the molecules of the liquid, we will use τ_0 below to mean the average time of such reorientation.*

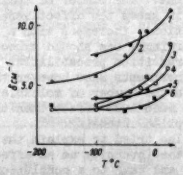

Figure 1. Temperature dependence of the width of spectral lines of 2-methylpentane and 2-methylhexane.

1) 2-methylhexane, ($\Delta\nu$ = 1304 cm^{-1}, ρ = 0.74); 2) 2-methylpentane, ($\Delta\nu$ = 1440 cm-1, ρ = 0.85); 3) 2-methylhexane, ($\Delta\nu$ = 1144 cm-1, ρ = 0.6); 4) 2-methylpentane, ($\Delta\nu$ = 1147 cm-1, ρ = 0.6); 5) 2-methylhexane, ($\Delta\nu$ = 894 cm-1, ρ = 0.4); 6) 2-methylpentane, ($\Delta\nu$ = 815 cm-1, ρ = 0.2).

If these assumptions are correct, then it is possible to reveal experimentally the following relationships: 1) The widths of depolarized lines ($\rho \approx \frac{6}{7}$) will have stronger temperature dependence than the widths of lines with small values of ρ; 2) On transition of a substance from the liquid to the crystalline phase the line widths ought to diminish abruptly. 3) On transition from the liquid to the glassy phase we should expect a smooth decrease in line widths right down to the glass temperature T_g.

In our previous papers we showed that the widths of the spectral lines of benzene and dichlorobenzene indeed diminish abruptly during transition of the material from the liquid to the crystalline phase, with the depolarized lines ($\rho \approx \frac{6}{7}$) suffering the greatest change [3, 8]. In the present work we have carried out an investigation of the temperature dependence of Raman line widths for substances which become glasses at low temperature: 2-methylpentane (T_g = -155° C) and 2-methylhexane (T_g = -118° C)**. The investigation was carried out over a wide temperature range. The results of the measurements are presented in figure 1. As can be seen from the graph, the line widths decrease smoothly with lowering of the temperature, and are practically independent of temperature in the glassy region. Just as for the substances

*Strictly speaking, there may be a different τ_{0i} for each vibration i. However, for molecules which have no specially preferred axes of rotation (i.e., whose moments of inertia about the various axes do not differ greatly from one another), these times will be nearly the same, and we can define an average time of reorientation of the molecule as the average of all the τ_{0i}.

**The vitrification of the materials studied has also been observed by other authors. (See Ref. [9]).

that crystallize, the strongly depolarized lines ($\rho \approx \frac{6}{7}$) undergo the greatest change. At high temperatures, the widths of the depolarized lines are greater than those of the polarized lines. The same regularities have been found by other authors, [1, 2, 4].

Study of the temperature dependence of Raman line widths permits us to estimate the average reorientation time for a molecule in a liquid, τ_o. To do this, it is necessary to pick out, from the whole width of the lines with some degree of depolarization, that part of the broadening which is caused by the rotary motion of molecules of the liquid. If it is assumed that the width of lines for a substance in the solid phase is produced by other agencies than the chaotic rotatory motion of molecules, then the width of lines with a degree of depolarization $\rho \approx \frac{6}{7}$ caused by the reorientation of molecules in the liquid at a given temperature might be written

$$\Delta\omega(T) \approx \delta(T) - \Delta^{o}, \tag{3}$$

where $\delta(T)$ is the width of the line in the liquid at temperature T and Δ^{o} is the width of the same line for the material in the solid phase.

Table 1

Material	Line investigated $\Delta\nu$ cm-1	Degree of depolarization ρ	$\tau_o \cdot 10^{12}$ sec. at 20°C
Benzene	607	0.88	5.0
	1586	0.81	
Toluene[4]	623	0.73	6.0
	1606	0.70	
p-Xylene[2]	318	0.94	12.0
	645	0.89	
	1616	0.72	
Cyclopentane [4]	1031	0.82	4.5
	1449	0.72	
Isopentane [1]	954	0.7	3.4
	909	0.5	
2-Methylpentane	1039	0.4	3.5
	1147	0.6	
2-Methylhexane	1144	0.6	7.5
	1304	0.74	

In table 1, estimates are presented of the average reorientation time τ_o of a molecule in the liquid for various substances at 20° C. The data of other authors are also presented in the table.

In the present work we also investigated the spectrum of ethyl alcohol. The results of the measurements are presented in figure 2. As is evident from the graph, the nature of the temperature dependence of the line widths is the same as for nonpolar molecules, which do not give rise to complexes. The time τ_o for the ethyl alcohol molecule at 20° is 5×10^{-12} sec.

The average reorientation time of a molecule in the liquid, obtained from the broadening of Raman lines, is in good order-of-magnitude agreement with the relaxation times given by Fabelinskii [10] and Vuks and Litvinov [11] for fluctuations of anisotropy measured in works on Rayleigh scattering. This is connected with the fact that the random reorientation of molecules of a liquid presumably influences the fluctuation of anisotropy. We can therefore expect that the rotatory Brownian motion of the molecules will be reflected in the structure of the wing of the Rayleigh line, with an average reorientation time τ_o.

Determination of the average time τ_o from the Raman spectrum, where the object of investigation is the molecule itself, is of great interest also for the study of viscosity of liquids. As is well known, the viscosity is connected with the relaxation time of a macroscopic Brownian particle of liquid having the form of a small sphere by the relation

$$\tau = \frac{4\pi a^3 \eta}{3kT}, \tag{4}$$

where a is the radius of the particle, η is the coefficient of viscosity, k is Boltzmann's constant and T is the absolute temperature.

In many physical problems formula (4) is applied to molecular processes. However, the validity of applying (4) to a single molecule is not established theoretically. Much interest attends verification of the correctness of (4) when applied to a single molecule, as can be done by studying the dependence of average reorientation time τ_o on viscosity. [We can neglect temperature variations in equation (4), since viscosity changes very rapidly with temperature].

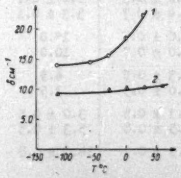

Figure 2

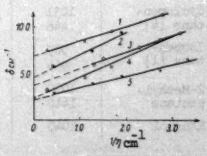

Figure 3

Figure 2: Temperature dependence of the width of lines of the spectrum of ethanol: 1) $\Delta\nu = 1040$ cm^{-1}, $\rho = 0.52$; 2) $\Delta\nu = 880$ cm^{-1}, $\rho = 0.22$.

Figure 3: Dependence of the width of lines of the spectra of benzene, 2-methylpentane and 2-methylhexane on the value $1/\eta$: — 1) 2-methylhexane, ($\Delta\nu = 1304$ cm^{-1}, $\rho = 0.76$); 2) 2-methylpentane, ($\Delta\nu = 1440$ cm^{-1}, $\rho = 0.85$); 3) benzene, ($\Delta\nu = 607$ cm^{-1}, $\rho = 0.88$); 4) 2-methylhexane, ($\Delta\nu = 1144$ cm^{-1}, $\rho = 0.6$); 5) 2-methylpentane, ($\Delta\nu = 1147$ cm^{-1}, $\rho = 0.6$).

In figure 3 the dependence of the widths of depolarized lines ($\rho \approx \frac{6}{7}$) in the Raman spectra of of various materials on $1/\eta$ is presented. Data on the dependence of viscosity on temperature has been culled from the literature [12, 13]. It is clear from the graph that the widths of the depolarized lines in the spectra of the materials studied are linear functions of $1/\eta$ within experimental error. These results agree well with the work of other authors [1, 2, 4]. Analysis of the curves shows

that, for all the compounds investigated, the widths of the lines begin to change approximately when the viscosity is several tenths of a poise, and to increase with a further decrease in viscosity. Since the viscosities of liquids close to their boiling points are in the neighborhood of a few thousandths of a poise, experimental verification of the validity of applying (4) is limited to the region 0.1 - 0.001 poise. Experiment shows that in this interval the viscosity of homogeneous, nonpolar liquids is a linear function of the average reorientation time τ_o of a molecule in the liquid*.

The different slopes of the straight lines (Fig. 3) for different spectral lines of one and the same material can be explained by the fact that the change in direction of the induced moment for each vibration is caused by reorientation of the molecule relative to some axis of rotation. Then to each different vibration will correspond a different effective radius of the molecule, which can lead to a difference in the slope of the line $\delta = f(1/\eta)$.

It is interesting to note that extrapolation of these straight lines to the value $1/\eta = 0$ (Fig. 3) gives linewidths which are the same as those in the solid, within experimental error.

Table 2

Material	Line investigated $\Delta\nu$ cm^{-1}	Width of lines (in cm^{-1})	
		By extrapolation from graphs(fig 3)	Direct measurement of materials in the solid phase
p-Xylene[2]	318	9.0 ± 0.3	9.0 ± 0.7
	1616	2.4 ± 0.7	3.3 ± 0.1
Cyclopentane [4]	1031	13.0 ± 0.7	14.0
	1448	9.0 ± 0.7	10.0
Isopentane [1]	909	4.3 ± 0.5	4.5
	954	3.0 ± 0.5	3.5
2-Methylpentane	1039	2.3 ± 0.5	3.0 ± 0.5
	1440	4.5 ± 0.8	5.3 ± 0.5
Ethanol	1040	13.5 ± 0.3	14.0 ± 0.8

Moreover, the assumption that line broadening in the spectra of solid substances arises from causes other than reorientation of molecules does not contradict the experiment. (In Table 2, data of other authors have been used.)

We must note that in [many] investigations of viscosity the notion of a potential barrier is used, leading to a formula deduced by Frenkel', Eyring and others [15, 16]:

$$\eta = A \exp\left(\frac{U}{RT}\right), \tag{5}$$

where A is a constant, T is the absolute temperature, R is the gas constant and U is a potential barrier which the molecule must surmount in going from one equilibrium state to another.

*Analogous data with respect to the linear dependence of τ_o on viscosities of liquids has been obtained by Bloembergen et al by the method of nuclear magnetic resonance (see ref. [14]).

Table 3

Material	U Kcal/mole From viscosity data	U_1 Kcal/mole From data on the width of lines
Ethanol	3.6 ± 0.3	3.8 ± 0.5
Isopentane	1.8 ± 0.3	1.6 ± 0.5
Cyclopentane	1.6 ± 0.3	1.4 ± 0.5
Benzene	2.4 ± 0.3	2.4 ± 0.5
p-Xylene	2.2 ± 0.3	2.2 ± 0.5

For the probability of reorientation of a molecule in the liquid an equation analogous to (5) must be written:

$$W = B \exp\left(-\frac{U_1}{RT}\right),$$

where B is a constant and U_1 is the potential barrier which the molecule must overcome in reorientation. Since W is inversely proportional to the average time of reorientation of a molecule, τ_o, then by taking equation (2) for the line broadening caused by rotational motion of the molecule into account, we have the following expression:

$$\Delta\omega = B \exp\left(-\frac{U_1}{RT}\right). \tag{6}$$

Our experimental data allow us to compare the potential barriers appearing in equations (5) and (6). Table 3 presents a comparison of these values at room temperature.

As can be seen from the table, the potential barriers calculated from viscosity data and from the broadening of Raman lines are the same within experimental error. We must note that this experimental material does not contradict Frenkel's assumption concerning the nature of viscous flow in liquids.

Thus the results of this work on the widths of Raman lines reveal a new possibility for investigating the molecular nature of viscosity.

In conclusion, I express my deep gratitude to Prof. P. A. Bazhulin, under whose direction this work was carried out, and also to I. I. Sobel'man and A. I. Osipov for their constant interest and valuable counsel in discussions of the work while it was in progress.

November 18, 1958

References

1. G.V.MIKHAILOV: Materialy X Soveshch.po spektroskopii, 1, L'vov. Univ, 1957.
2. N.I.REZAEV: Materialy X Soveshch. po spektroskopii, 1, L'vov. Univ, 1957.
3. A.B.RAKOV: Materialy X Soveshch. po spektroskopii, 1, L'vov. Univ, 1957.
4. A. I. SOKOLOVSKAIA, P. A. BAZHULIN: Sb.posviashchennyi pamiati akad. G.S. Landsberg (Memorial to academician G.S.L.) (In Press)
5. I.I.SOBEL'MAN: IAN USSR FS, 17, 554, (1953)
6. L.LANDAU, E. LIFSHITS: Statisticheskaia fizica (Statistical physics) OTTI, 1951

7. V.V.SOLODOVNIKOV: VVedenie v statisticheskuiu dinamiku sistem avtomaticheskovo upravleniia. (Introduction to statistical dynamics of automatic control systems), Moscow-Leningrad, 1952.
8. P.A.BAZHULIN, A.V.RAKOV: DAN USSR, 105, 54, (1955)
9. J.H.BRAUN, M.M.HICKS-BURNS AND W.B.MASON FAULCONER: JACS, 59, 2355, (1937). G. CALINGAERT, R.E.MARKER, G. EDGAR: JACS, 51, 1483, (1929)
10. I. L. FABELINSKII: OIS, 2, 510, (1957)
11. M. F. VUKS, V.L.LITVINOV: DAN USSR, 105, 696, (1955)
12. Spravochnik Khimika (Chemical handbook), 1, Goskhimizdat, 1951
13. Spravochnik T.E.: (Handbook T.E.) 10, 1930
14. N.BLOEMBERGEN, E.M.PURCELL, R.V.POUND: Phys.Rev. 73, 679 (1948)
15. IA. I. FRENKEL': Kineticheskaia teoriia zhidkostei. (Kinetic theory of liquids). Akad. NAUK Press, Moscow, 1945. (English version extant)
16. G. EYRING: Theory of absolute reaction rates (IL Moscow, 1948)

TOM VII, Vyp. 2 OPTIKA I SPEKTROSKOPIIA Avgust, 1959
VOL. VII, No. 2 OPTICS AND SPECTROSCOPY August, 1959

Optical Activity and Intermolecular Interaction

V. M. ASLANIAN AND M. V. VOL'KENSHTEIN

Abstract: A theory is proposed on the influence of intermolecular interaction on optical activity which applies to solutions of active substances in polar and nonpolar solvents. The theory is based upon consideration of inductive effects. Agreement of theory and experiment is discussed.

INTRODUCTION

Optical activity — natural rotatory power — represents an optical property of molecules which is most sensitive to internal and intermolecular interaction. It is well known that optical activity of one and the same substance in various solutions can differ by a hundred percent, and even in the sign of the rotation, (see for example [1]). In view of the fact that optical activity as a rule is measured in the condensed phase — in a pure liquid or a liquid solution — the definition of the true molecular constant characteristic of optical activity requires that direct account be taken of intermolecular interaction.

The theory of the influence of intermolecular interaction on optical activity was developed by Beckmann and Cohen [2], who applied the method proposed by Darwin [3] for calculating the optical constants of a substance. In Reference [2] variation of optical activity is related to the deformation of the molecule by the electrostatic field surrounding its dipole. That is, we consider the small displacement of the atoms from a state of equilibrium caused by this field. Beckmann and Cohen obtain the expression

$$\Omega = \Omega_0 + \Omega' \frac{2\mu}{d^3} \frac{\epsilon - 1}{\epsilon + 2}, \tag{1}$$

where Ω is the observed molecular rotation

$$\Omega = \frac{[M]}{n^2 + 2},$$

Ω_0 its value in vacuum, i.e. the true molecular constant, Ω' a certain coefficient, μ the dipole moment of the molecule being considered d the minimum distance between centers of neighboring molecules and ϵ the dielectric constant of the medium. Beckmann and Cohen's formula agrees with experiment: the dependence of Ω on the molecular polarization of the medium, characterized by $\frac{\epsilon - 1}{\epsilon + 2}$, appears to be linear. Equation (1) has been successfully made use of in a few studies (see e.g. [4]) to define the molecular constant Ω_0. Beckmann and Cohen's theory however is a formal one, which does not take into account the real electronic mechanism by which the surrounding molecules act upon the one under consideration. On the other hand, taking into account the intermolecular field in the fluid in the manner of Debye, as made by these authors, is also insufficient.

The aim of the present work is to examine the influence of intermolecular interaction on optical activity, on the basis of models which take direct account of the polarizability of the molecules and their composite parts. As a first approximation such a treatment may employ classical theory, which is apparently sufficient for investigation of dilute solutions. It is necessary however to take account of quantum mechanical effects for the treatment of pure fluids and concentrated solutions, because in such cases resonant interaction plays a substantial role.

We shall start from a theory of optical activity based on the valence optical scheme, according to which the characteristic polarizability tensors incorporate the separate couplings and groups of atoms in the molecule. Optical activity is manifested as the result of inductive interaction between anisotropically polarized and asymmetrically situated groups. A quantum mechanical variation of this theory was proposed by Kirkwood [5]; subsequently it was shown by one of us that the same result could be obtained by classical means [1, 6]; moreover the next approximation is obtained without difficulty which takes into account pairwise and more complex group interactions [7]. The indicated theory allows estimation of the optical activity of molecules directly from their structure. With this substantial foundation, it is applied to the investigation of intermolecular interactions which are effective at larger distances than intramolecular ones.

In addition, we shall take into account variations of the anisotropic polarizability of component parts of active molecules under the influence of inductive interaction with neighboring molecules.

Further, we investigate changes of these polarizabilities caused by the electrostatic field of surrounding molecules, which is expressed in terms of the macroscopic constants of the medium in accordance with the contemporary theory of the electrical properties of liquids.

GYRATION CHANGES DUE TO INTERACTIONS WITH ISOTROPIC MOLECULES

Molecular rotatory power [M] is expressed by means of a molecular constant: the gyration g [1]:

$$[M] = [\vartheta] \frac{M}{100} = \frac{4\pi^2}{3} \frac{N_A}{100} \frac{n^2 + 2}{n\lambda_0} g, \tag{2}$$

where $[\vartheta]$ is the specific rotation, M the molecular weight, N_A Avogadro's number and λ_0 the wave length in vacuum. In accordance with the first approximation of the theory of polarizability [1, 5, 6]

$$g_0 = \frac{\pi}{3\lambda} \sum_{k,l}{}' \frac{1}{R_{kl}^3} (\alpha_{k1} - \alpha_{k2})(\alpha_{l1} - \alpha_{l2})(\vec{R}_{kl}, [\vec{i}\vec{1}, \vec{k}\vec{1}]) \times$$

$$\times \left\{ \frac{3}{R_{kl}^2} (\vec{R}_{kl}, \vec{k}\vec{1})(\vec{R}_{kl}, \vec{i}\vec{1}) - (\vec{k}\vec{1}, \vec{i}\vec{1}) \right\},$$

where R_{kl} is the distance between interacting ellipsoids of polarizability k and l. These ellipsoids are considered to be axially symmetric with longitudinal and transverse values of polarizability equal respectively to α_1 and α_2. $\vec{k}\vec{1}$ and $\vec{i}\vec{1}$ are unit

vectors along the axes of the ellipsoids. Without loss of generality we examine the model of an optically active molecule consisting of two ellipsoids of polarizability. Such a model is equivalent to that of Kuhn [1, 6]. In this case

$$(4)\quad g_o = \frac{\pi}{3\lambda}\frac{1}{R_{12}^3}(\alpha_{11}-\alpha_{12})(\alpha_{21}-\alpha_{22})\,(\vec{R}_{12}[\vec{2\imath},\vec{1\imath}])\times$$

$$\times\left\{\frac{3}{R_{12}^2}(\vec{R}_{12},\vec{1\imath})(\vec{R}_{12},\vec{2\imath}) - (\vec{1\imath},\vec{2\imath})\right\}.$$

In the presence of neighboring molecules, in addition to the direct inductive interaction inside the molecule between the ellipsoids of polarizability 1 and 2, which are taken into account in formula [4], interactions between ellipsoids 1 and 2 will take place through the mediation of the neighboring molecules. Because the intermolecular distances are larger than the intramolecular ones, it is possible to simplify the calculations by considering that neighboring molecules are isotropically-polarized; i.e. to take into account the trace of the polarizability tensor, but to neglect its anisotropy. Under the influence of the electrical field of a light wave $\vec{E}$, a dipole moment with components

$$(5)\quad p_{2\sigma} = \sum_{\tau}\alpha^{(2)}_{\sigma\tau}E_\tau,\quad \sigma,\ \tau = \xi,\ \eta,\ \zeta.$$

is induced in group 2.

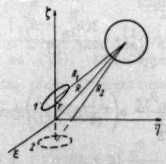

Figure 1

This dipole creates in the neighboring molecule (at a distance R_2 and assumed to possess isotropic polarizability a) a field

$$(6)\quad \vec{E}^{(2)} = \frac{3(\vec{p}_2\vec{R}_2)\vec{R}_2}{R_2^5} - \frac{\vec{p}_2}{R_2^3},$$

and an induced dipole moment with components

$$(7)\quad p_\nu = a\left\{\sum_{\varkappa,\tau}\frac{3R_{2\nu}R_{2\varkappa}}{R_2^5}\alpha^{(2)}_{\varkappa\tau}E_\tau - \sum_{\tau}\frac{1}{R_2^3}\alpha^{(2)}_{\nu\tau}E_\tau\right\},$$

which, in turn induces in ellipsoid 1 the dipole moment

$$(8)\quad p_{1\nu} = a\left\{\sum_{\rho}\sum_{\varkappa}\sum_{\sigma}\sum_{\tau}\frac{9R_{1\rho}R_{1\sigma}R_{2\sigma}R_{2\varkappa}}{R_1^5R_2^5}\alpha^{(1)}_{\nu\rho}\alpha^{(2)}_{\varkappa\tau}E_\tau - \right.$$

$$-\sum_{\rho}\sum_{\sigma}\sum_{\tau}\frac{3R_{1\rho}R_{1\sigma}}{R_1^5R_2^3}\alpha^{(1)}_{\nu\rho}\alpha^{(2)}_{\sigma\tau}E_\tau -$$

$$-\sum_{\rho}\sum_{\varkappa}\sum_{\tau}\frac{3R_{2\rho}R_{2\varkappa}}{R_1^3R_2^5}\alpha^{(1)}_{\nu\rho}\alpha^{(2)}_{\varkappa\tau}E_\tau +$$

$$\left.+\sum_{\rho}\sum_{\tau}\frac{\alpha^{(1)}_{\nu\rho}\alpha^{(2)}_{\rho\tau}E_\tau}{R_1^3R_2^3}\right\},$$

where R_1 is the distance between neighboring molecules and ellipsoid 1 (see Fig.1).

Averaging over all positions of the neighboring molecule on the surface of a sphere of radius R (Fig. 1), we obtain

$$(9)\quad \vec{P}_{1\nu} = \frac{a}{(R^2+r^2)^4}\sum_{\tau}\left\{(2R^2-r^2)\,\alpha^{(1)}_{\nu\xi}\alpha^{(2)}_{\xi\tau} + \right.$$

$$\left.+\ (2R^2-r^2)\alpha^{(1)}_{\nu\eta}\alpha^{(2)}_{\eta\tau} + 2(R^2+r^2)\alpha^{(1)}_{\nu\zeta}\alpha^{(2)}_{\zeta\tau}\right\}E_\tau.$$

Thus, we have calculated the change in the dipole moment defined by the indicated interaction. Calculating the gyration in accordance with the theory of optical activity [1, 6], we obtain, after transferring to coordinate axes fixed in the axial ellipsoids 1 and 2,

$$\Delta g = \frac{\pi}{3\lambda}a\,(\alpha_{11}-\alpha_{12})\,(\alpha_{21}-\alpha_{22})\,\frac{(\vec{R}_{12}[\vec{2\imath},\vec{1\imath}])}{(R^2+r^2)^4}\times$$

$$(10)\quad \times\left\{(2R^2-r^2)\,(\vec{1\imath},\vec{2\imath}) + \frac{3R^2}{r^2}(\vec{r},\vec{1\imath})(\vec{r},\vec{2\imath})\right\}.$$

Comparing (10) with (4), we have

$$(11)\quad \Delta g = \frac{8r^3}{(R^2+r^2)^4}\,\frac{(2R^2-r^2)(\vec{1\imath},\vec{2\imath}) + \frac{3R^2}{r^2}(\vec{r},\vec{1\imath})(\vec{r},\vec{2\imath})}{\frac{3}{r^2}(\vec{r},\vec{1\imath})(\vec{r},\vec{2\imath}) - (\vec{1\imath},\vec{2\imath})}\,ag_o$$

$$= S\,ag_o,$$

where S is a purely geometrical factor. If the given molecule is surrounded by γ symmetrically-situated neighboring molecules (γ - is a coordination number), then Δg increases on the average γ. Expressing a according to the Lorentz-Lorenz formula

$$a = \frac{3}{4\pi N_1}\frac{n^2-1}{n^2+2},$$

we finally get

$$(12)\quad g = g_o + \Delta g = g_o\left(1 + A\frac{n^2-1}{n^2+2}\right),$$

where g_o is the gyration in vacuum and

$$A = \gamma S\frac{3}{4\pi N_1},$$

in which S decreases with an increase of the intermolecular distance R approximately as $\frac{1}{R^3}$.

THE INFLUENCE OF CHANGES IN ANISOTROPIC POLARIZABILITIES

In the previous calculation no account was taken of the change of anisotropic polarizabilities $\alpha^{(1)}$ and $\alpha^{(2)}$, caused by the inductive effect. Such a change, however, exists, as has been shown by Silberstein [1, 9, 10]. Due to inductive interaction the effective anisotropy of the particle increases, while the trace of the polarizability tensor remains practically unchanged.

Let us examine the model sketched in figure 1. In taking into account the mutual induction, the effective polarizabilities of the system consisting of the ellipsoid 1 and anisotropic molecules, can be calculated as follows. The dipole moment, induced in group 1 is

$$(13)\quad p_{1\sigma} = \sum_{\tau}\sum_{\rho}\alpha^{(1)}_{\sigma\tau}\left\{E_\tau + \frac{3aR_{1\tau}R_{1\rho}}{R_1^5}E_\rho\right\} - \sum_{\tau}\alpha^{(1)}_{\sigma\tau}\frac{a}{R_1^3}E_\tau$$

and in the isotropic molecule is

$$(14)\quad p_\sigma = aE_\sigma + a\sum_{\tau}\sum_{\rho}\frac{3R_{1\sigma}R_{1\tau}}{R_1^5}\alpha^{(1)}_{\tau\rho}E_\rho - a\sum_{\tau}\frac{\alpha^{(1)}_{\sigma\tau}}{R_1^3}E_\tau.$$

The polarizabilities of the system may be calculated according to the formula

$$(15)\quad a_{\sigma\tau} = \frac{p_\sigma + p_{1\sigma}}{E_\tau} \quad \text{for} \quad E = E_\tau.$$

We get

$$a_{\xi\xi} = a^{(1)}_{\xi\xi} + a + \left(\frac{6R^2_{1\xi}}{R_1^5} - \frac{2}{R_1^3}\right)a\alpha^{(1)}_{\xi\xi} + \frac{6R_{1\xi}R_{1\eta}}{R_1^5}a\alpha^{(1)}_{\xi\eta} + \frac{6R_{1\xi}R_{1\zeta}}{R_1^5}a\alpha^{(1)}_{\xi\zeta},$$

$$a_{\eta\eta} = a^{(1)}_{\eta\eta} + a + \left(\frac{6R^2_{1\eta}}{R_1^5} - \frac{2}{R_1^3}\right)a\alpha^{(1)}_{\eta\eta} + \frac{6R_{1\xi}R_{1\eta}}{R_1^5}a\alpha^{(1)}_{\xi\eta} + \frac{6R_{1\eta}R_{1\zeta}}{R_1^5}a\alpha^{(1)}_{\eta\zeta}.$$

$$(16)\quad \begin{cases} a_{\zeta\zeta} = \alpha^{(1)}_{\zeta\zeta} + a + \left(\dfrac{6R^2_{1\zeta}}{R_1^5} - \dfrac{2}{R_1^3}\right)a\alpha^{(1)}_{\zeta\zeta} + \\ + 6a\alpha^{(1)}_{\xi\zeta}\dfrac{R_{1\xi}R_{1\zeta}}{R_1^5} + 6a\alpha^{(1)}_{\eta\zeta}\dfrac{R_{1\eta}R_{1\zeta}}{R_1^5}, \\ a_{\xi\eta} = a_{\eta\xi} = \alpha^{(1)}_{\xi\eta} + \left[\dfrac{3(R^2_{1\xi} + R^2_{1\eta})}{R_1^5} - \dfrac{2}{R_1^3}\right]a\alpha^{(1)}_{\xi\eta} \\ + \dfrac{3R_{1\xi}R_{1\eta}}{R_1^5}a\left(\alpha^{(1)}_{\xi\xi} + \alpha^{(1)}_{\eta\eta}\right) + \\ + \dfrac{3R_{1\eta}R_{1\zeta}}{R_1^5}a\alpha^{(1)}_{\xi\zeta} + \dfrac{3R_{1\xi}R_{1\zeta}}{R_1^5}a\alpha^{(1)}_{\eta\zeta}, \\ a_{\xi\zeta} = a_{\zeta\xi} = \alpha^{(1)}_{\xi\zeta} + \left[\dfrac{3(R^2_{1\xi} + R^2_{1\zeta})}{R_1^5} - \dfrac{2}{R_1^3}\right]a\alpha^{(1)}_{\xi\zeta} \\ + \dfrac{3R_{1\xi}R_{1\zeta}}{R_1^5}a\left(\alpha^{(1)}_{\xi\xi} + \alpha^{(1)}_{\zeta\zeta}\right) + \\ + \dfrac{3R_{1\eta}R_{1\zeta}}{R_1^5}a\alpha^{(1)}_{\xi\eta} + \dfrac{3R_{1\xi}R_{1\zeta}}{R_1^5}a\alpha^{(1)}_{\eta\zeta}, \\ a_{\eta\zeta} = a_{\zeta\eta} = \alpha^{(1)}_{\eta\zeta} + \left[\dfrac{3(R^2_{1\eta} + R^2_{1\zeta})}{R_1^5} - \dfrac{2}{R_1^3}\right]a\alpha^{(1)}_{\eta\zeta} + \\ + \dfrac{3R_{1\eta}R_{1\zeta}}{R_1^5}a\left(\alpha^{(1)}_{\eta\eta} + \alpha^{(1)}_{\zeta\zeta}\right) + \\ + \dfrac{3R_{1\xi}R_{1\zeta}}{R_1^5}a\alpha^{(1)}_{\xi\eta} + \dfrac{3R_{1\xi}R_{1\eta}}{R_1^5}a\alpha^{(1)}_{\xi\zeta} \end{cases}$$

and after averaging over all values of angles ϕ and φ:

$$(17)\quad \bar{a}_{\sigma\tau} = a\delta_{\sigma\tau} + \alpha^{(1)}_{\sigma\tau} + \frac{1+\rho^2}{R^3},$$

where

$$\delta_{\sigma\tau} = \begin{cases} 1 \text{ for } \sigma = \tau \\ 0 \text{ for } \sigma \neq \tau \end{cases}$$

$$\rho = \frac{r}{R}.$$

For the system formed by the second ellipsoid and an isotropic molecule, we get an analogous result. Expression (17) may be written in the following way

$$(18)\quad \bar{a}_{\sigma\tau} = a'_{\sigma\tau}\delta_{\sigma\tau} + \alpha'^{(1)}_{\sigma\tau},$$

where

(19) $$a'_{\sigma\tau} = a\left(\delta_{\sigma\tau} + \alpha^{(1)}_{\sigma\tau}\frac{1+\rho^2}{2R^3}\right),$$

(19a) $$\alpha'^{(1)}_{\sigma\tau} = \alpha^{(1)}_{\sigma\tau}\left(1 + a\frac{1+\rho^2}{2R^3}\right).$$

Equation (19a) indicates a change of effective anisotropic polarizability of group 1. Analogously, for group 2

(19b) $$\alpha'^{(2)}_{\sigma\tau} = \alpha^{(2)}_{\sigma\tau}\left(1 + a\frac{1+\rho^2}{2R^3}\right).$$

Substituting these values of $\alpha'^{(1)}$ and $\alpha'^{(2)}$ into the equation for the gyration of a molecule characterized by ellipsoids 1 and 2, and introducing the coordination number 2, we get

(20) $$g = g_0\left[1 + \frac{a\gamma}{2R^3}(1+\rho^2)\right]^2 \simeq g_0\left[1 + \frac{a\gamma}{R^3}(1+\rho^2)\right]$$

and after substituting for a according to the Lorentz-Lorenz formula

(21) $$g \cong g_0\left[1 + B\frac{n^2-1}{n^2+2}\right],$$

where

$$B = \frac{1+\rho^2}{R^3}\gamma\frac{3}{4\pi N_1}.$$

Thus, this effect also leads to a relation of the same type as (12). As an approximation, taking into account the order of magnitude of $\frac{a}{R^3}$, both effects add simply to give

(22) $$g = g_0\left[1 + (A+B)\frac{n^2-1}{n^2+2}\right].$$

In this formula, the quantity B is always positive and the sign of A, according to (11), depends on the geometry of the optically active molecule.

THE INFLUENCE OF THE INTERNAL FIELD ON OPTICAL ACTIVITY

Formula (22) is applicable to the case of non-polar molecules, lacking a permanent dipole moment, and also to the case of polar molecules in a nonpolar solvent. A polar molecule surrounded by polar molecules is affected by the fields of all neighboring dipoles. It is precisely this effect which is examined in the work of Beckmann and Cohen [2]. We allow the anistropic polarizabilities of the separate groups of an active molecule to depend on the internal field $\vec{F}$. In the first approximation we have

(23) $$\alpha_{\sigma\tau} = \alpha^0_{\sigma\tau} + \sum_\nu \beta_{\sigma\tau\nu}F_\nu,$$

where $\beta_{\sigma\tau\nu}$ are the components of a certain tensor of the third rank. Considering (without loss of generality) a field F which is homogenous and directed along the axis ζ of the model (Fig. 1), we obtain the following expression for the gyration

(24) $$g' = g_0(1 + \beta_\zeta F_\zeta),$$

where

$$\beta_\zeta = \frac{\beta_{11\zeta} - \beta_{12\zeta}}{\alpha_{11} - \alpha_{12}} + \frac{\beta_{21\zeta} - \beta_{22\zeta}}{\alpha_{21} - \alpha_{22}}.$$

Beckmann and Cohen calculate the field $\vec{F}$ according to Debye. It is well known, however, that contemporary theories of the electrical properties of liquids are better justified and agree better with experiment [11]. According to Buckingham [12] we have

(25) $$F_\zeta = \frac{2\mu}{d^3}\left\{\frac{\epsilon_\infty - 1}{\epsilon_\infty + 2} + \frac{(\epsilon - \epsilon_\infty)(2\epsilon + \epsilon_\infty)}{\epsilon\kappa(\epsilon_\infty + 2)^2}\right\},$$

where μ is the dipole moment of the molecule under consideration, d the minimum distance between centers of neighnoring molecules, ϵ the permittivity, and $\epsilon_\infty \cong n^2$. The factor κ is equal to

$$\kappa = 1 + \sum_{i=1}^{\gamma}\overline{\cos\vartheta_i},$$

where ϑ_i is the angle between the dipole of the molecule under consideration and the dipole of the i-th molecule in its most immediate vicinity. In the theory of Onsager the factor κ is equal to 1. We obtain the following expression for molecular rotation

(26) $$\Omega = \Omega_0 + \Omega_2\left[\frac{\epsilon_\infty - 1}{\epsilon_\infty + 2} + \frac{(\epsilon - \epsilon_\infty)(2\epsilon + \epsilon_\infty)}{\epsilon\kappa(\epsilon_\infty + 2)^2}\right],$$

where

$$\Omega_2 = \beta_\zeta\frac{2\mu}{d^3}\frac{4\pi}{3n\lambda_0^2}N_A g_0,$$

and, adding terms taking account of the previously examined inductive effect, we obtain

(27) $$\Omega = \Omega_0 + \Omega_1\frac{\epsilon_\infty - 1}{\epsilon_\infty + 2} + \Omega_2\frac{(\epsilon - \epsilon_\infty)(2\epsilon + \epsilon_\infty)}{\epsilon\kappa(\epsilon_\infty + 2)^2},$$

where

$$\Omega_1 = \Omega_2 + (A+B)\frac{4\pi^2}{3n\lambda_0^2}N_A g_0.$$

DISCUSSION OF RESULTS AND COMPARISON WITH EXPERIMENT

The above results differ essentially from those calculated by Beckmann and Cohen. In Eq.(1), as found by these authors, the terms corresponding to inductive effects not connected with deformations are absent; they are expressed by the term

$$\Omega_1 \frac{\epsilon_\infty - 1}{\epsilon_\infty + 2} = \Omega_1 \frac{n^2 - 1}{n^2 + 2}$$

in our Eq. (27). According to Beckmann and Cohen, Ω differs from Ω_0 only if the asymmetrical molecule itself possesses an appreciable dipole moment. As shown in the present work, in reality even though $\mu \cong 0$ the solvent will noticeably influence the optical activity. This is corroborated by experiment. Let us examine experimental data relating to the actual nonpolar rotatory substances d-pinane and d-limonene, mentioned in the work of Beckmann and Cohen.

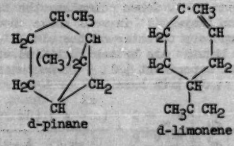

d-pinane d-limonene

Beckmann and Cohen found that Ω for pinane does not depend on $\frac{\epsilon - 1}{\epsilon + 2}$. However, if we examine the dependence of Ω on $\frac{n^2 - 1}{n^2 + 1}$, we find an approximately linear dependence with considerable scattering of the data (Fig. 2); $c = \frac{100}{M}$, and M is the molecular weight of pinane. The scatter here is not surprising, because the data refer to various solvents with and without dipoles, in which the factors A and B can differ substantially.

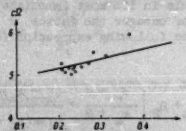

$\frac{n^2-1}{n^2+2}$

Figure 2

For d-limonene we find an excellent coincidence of theory with experiment in mixtures of benzene with nitrobenzene (Fig. 3). In this case there is no noticeable scatter of the data, which implies nearly equal values of A and B in various mixtures. In our opinion the apparent independence of Ω and $\frac{\epsilon - 1}{\epsilon + 2}$ for di-pinane is fortuitous. Considerable scatter of the data in this case makes Beckmann and Cohen's deduction concerning experimental confirmation of Eq. (1) for this substance insufficiently convincing.

The second difference between our results and those of Beckmann and Cohen consists in our application of the theory of Buckingham and Onsager to solutions of optically active dipole molecules and not the theory of Debye.

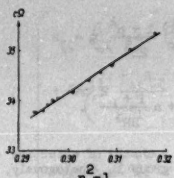

$\frac{n^2-1}{n^2+2}$

Figure 3

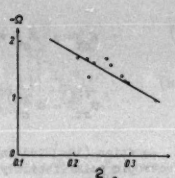

$\frac{n^2-1}{n^2+2}$

Figure 4

It is evident that this type of calculation is better justified for polar liquids. Comparison of theory with experiment for an optically active polar substance may be shown as follows.

Figure 5

$$A = -\left[\Omega - \Omega_1 \frac{n^2 - 1}{n^2 + 2}\right]; \quad B = \frac{(\epsilon - n^2)(2\epsilon + n^2)}{\epsilon(n^2 + 2)^2}.$$

1) Aromatic solvents; 2) aliphatic solvents

We construct the dependence of Ω on $\frac{n^2-1}{n^2+2}$ for nonpolar solvents. For this the third term of Eq. (27) will be small, because of the factor $\epsilon - n^2$, and the dependence of Ω on $\frac{n^2 - 1}{n^2 + 2}$ will be approximately linear. This in fact is borne out by our examination of the case of l-menthyl-methylnaphthalate (Fig. 4). We find the value of Ω_1 from this dependence and then investigate the dependence of

$$\Omega - \Omega_1 \frac{n^2 - 1}{n^2 + 2} \quad \text{on}$$

$$\frac{(\epsilon - n^2)(2\epsilon + n^2)}{\epsilon(n^2 + 2)^2}$$

According to Eq. (27) this dependence appears also to be approximately linear (Fig. 5). Considerable scatter of the data is to be expected, since the constants A, B, and d may differ substantially for various solvents (in particular for polymer solvents). The present status of the molecular theory of fluids does not permit calculation of the constants A and B, which are determined by the geometrical factors S and ρ, and by the effective coordination number γ. These values must be determined by experiment. For this complex situation the quantities A and B enter our formula

as a sum and it appears that they cannot be separately determined. However, the sum A and B may be represented by the expression

$$(28) \qquad A + B = \frac{3}{4\pi N_1} \frac{1}{R^3} f(\rho) = \varphi(\rho).$$

γ appears in $f(\rho)$ as a multiplicative factor. it is evident that

$$\frac{3}{4\pi N_1} \frac{1}{R^3} \cong \text{const } (R).$$

To investigate the temperature dependence of Ω (i.e. on specific volume), it is necessary to find the form of the function $\varphi(\rho)$, which characterizes the influence of intermolecular interaction on the gyration of the molecule. In this way, the optical activity may be used for investigating intermolecular interaction.

The theory proposed here does not apply to investigation of interactions of the hydrogen-bond type, which substantially change the electron configuration of atoms or their bonds. We submit that the problem of analyzing experimental data on the basis of the proposed theory is a very real one. It would be essential to measure optical activity in vapors and in different solvents over a wide temperature range.

February 19, 1959

References

1. M. V. VOL'KENSHTEIN: Molekuliarnaia optika, (molecular optics) XI, GTTI, 1951
2. CH.O.BECKMANN, K. COHEN: J.Chem.Phys., 4, 784, (1936)
3. CH.G.DARWIN: Trans. Camb. Phil. Soc., 23, 137, (1924)
4. N.M.BAZHENOV, M.V. VOL'KENSHTEIN; ZFKh., 28, 1299, (1954)
5. J. KIRKWOOD: J. Chem.Phys., 5, 479, (1937)
6. M. V. VOL'KENSHTEIN: DAN SSSR, 71, 447, (1950)
7. M. V. VOL'KENSHTEIN: IAN USSR, SF, 17, 574, (1953)
8. M. V. VOL'KENSHTEIN: DAN SSSR, 71, 643, (1950)
9. L. SILBERSTEIN: Phil. Mag., 33, 92, 215, 521, (1917)
10. M. V. VOL KENSHTEIN: DAN SSSR, 32, 185, (1941)
11. H. FRÖLICH: Theory of dielectrics. Oxford, 1949; G. I. SKANAVI: Fizika Dielektrikov, (Physics of Dielectrics), GTTI, 1949.
12. A. D. BUCKINGHAM: Proc. Roy. Soc., A238, 1213, 235, (1956)

TOM VII, Vyp. 2 OPTIKA I SPEKTROSKOPIIA Avgust, 1959
VOL. VII, No. 2 OPTICS AND SPECTROSCOPY August, 1959

Spectroscopy of Certain Simple Aromatic Hydrocarbons in Frozen Crystalline Solutions

T. N. BOLOTNIKOVA

Abstract: The influence of the solvent on the character of the spectrum of frozen solutions of aromatic hydrocarbons — naphthalene, anthracene, naphthacene — in paraffin hydrocarbons was investigated.

It is shown that the spectra of frozen solutions are quite sharp (band width 10-15 cm-1) for the case in which the linear size of the fluorescent molecule is close to the size of the solvent molecule. In this case, the assumption is made that, on freezing, the fluorescent molecule substitutes for one molecule of the solvent without substantial deformation of the crystal lattice, which would explain the sharpness of the spectrum of such a solution.

INTRODUCTION

In recent times more and more methods have been developed for the investigation of spectra of complex compounds in mixed crystals. When the molecules under investigation are introduced into a crystal lattice of another substance and the study is carried out at a sufficiently low temperature, a condition is achieved in which, first of all, the interaction between the emitting molecule and surrounding medium is at a minimum, and secondly, the amount of vibrational energy of each molecule is small. With a fortunate selection of the crystalline structure into which the molecule is introduced, it is possible to obtain very sharp spectra of quite complex compounds [1-7].

Shpolskii, Il'ina and Klimova [8,9] made wide use of such a method of mixed crystals for the study of luminescence spectra of condensed aromatic hydrocarbons — coronene, pyrene and benzpyrene. It was found that the fluorescence spectra of these compounds in frozen solutions of n-paraffins (from hexane to decane) have an exceptionally sharp line-like character. The spectra were studied at liquid nitrogen temperature. The following regularities were found: 1) the spectra of coronene, pyrene and benzpyrene which are continuous for crystals of these compounds and diffuse for frozen glassy solutions (in paraffin oil, ethyl alcohol, the mixed solvent EPA) become resolved in frozen crystalline solutions into very sharp narrow lines; 2) to each diffuse band corresponds a doublet or a more complex multiplet with a constant frequency difference in such a way that the whole spectrum is represented by several sharp spectra displaced relative to each other; 3) the number of components in each group depends mainly on the solvent and the molecule of the fluorescent substance; 4) the use of n-paraffins with large molecules, e.g. $C_{15}H_{32}$ and $C_{16}H_{34}$ as solvents, leads again to diffuse spectra.

The splitting of diffuse bands into groups of sharp lines was the most characteristic part of the phenomenon. The cause for the splitting remained unclear in spite of many experiments; in addition, an analysis of the spectra was made difficult by the absence of independent data on vibrational frequencies of the investigated molecules in the normal state. Thus, the interpretation of obtained spectra remained unexplained. Under such circumstances it seemed worthwhile to study under the same conditions the spectra of simpler aromatic hydrocarbons which have been previously studied and analyzed in great detail under the most varied conditions: in the vapor, in solutions, in the crystalline state and in solid solutions

In this connection, we have investigated fluorescence spectra of frozen solutions of naphthalene, anthracene, 9-, 10-dichloro-anthracene, anthraquinone and naphthacene.

RESULTS

Naphthalene. The results of studies on frozen solutions of naphthalene in n-paraffins were given previously by us [10, 11]. It was shown, first, that allowing for a small displacement, the spectra of these solutions agree well with the spectra of the previously investigated frozen glassy solutions of naphthalene, and, second, that the spectrum of a solution of naphthalene in n-pentane is very sharp, similar to the spectrum of naphthalene crystals, but differing from it in some details. Comparison of the naphthalene spectrum in n-pentane with the spectrum of a crystalline solution of naphthalene in durene [4, 5] shows that in the spectrum of naphthalene in n-pentane two systems of bands are present, corresponding to optical transitions polarized along the long and short molecular axes.

Table 1

Fluorescence spectrum of the solution of naphthacene in nonane at 77.3°K

Line No.	ν (in cm-1)	$\nu_0-\nu$ (in cm-1)	Interpretation (in cm-1)	Error (in cm-1)
1	21156	0	—	—
2	20837	319	0-320	- 1
3	20694	462	0-465	- 3
4	20546	610	0-615	- 5
5	20420	736	0-735	+ 1
6	20238	918	0-918	0
7	20108	1048	0-735-320	- 7
8	19991	1164	0-1165	0
9	19782	1374	0-1380	- 6
10	19677	1473	0-1273	0
11	19463	1693	0-1380-320	- 7
12	19313	1843	0-1380-465	- 2
13	19235	1921	0-1921	0
14	19167	1989	0-1380-615	- 6
15	18921	2235	—	—
16	18810	2346	0-2×1165	+16
17	18605	2551	0-1380-1165	+ 6
18	18501	2655	—	—
19	18394	2762	0-2×1380	+ 2
20	18298	2858	0-1380-1473	+ 5
21	18077	3079	0-2×1380-320	- 1
22	17920	3236	0-2×1380-465	+11
23	17859	3297	0-1380-1920	- 3
24	17318	3838	—	—
25	17261	3895	—	—
26	17101	4055	—	—
27	16904	4252	0-2×1380-1473	+19
28	16704	4452	0-3×1380- 320	- 8
29	16461	4695	0-2×1380-1921	+14

The transition along the long axis which is resolved for the naphthalene molecule according to the selection rules is found to be weak, whereas the most intense bands are those whose appearance is connected with the influence of the second electronic state [5]. Thus the impression is created that the transition polarized along the long molecular axis is subject to some kind of additional restriction conditioned probably by the symmetry of the position of the naphthalene molecule in the crystal lattice of the solvent.

Figure 1: Fluorescence spectrum of the solution of napthacene in nonane at 77° K. The line numbers correspond to those in table 1.

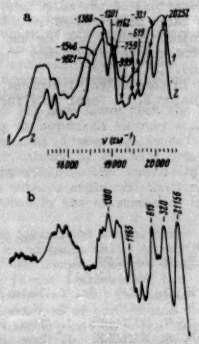

Figure 2: Microphotograms of fluorescence spectra. a-mixed crystals(1-naphthacene in anthracene, 2-naphthacene in naphthalene[7]); b-frozen solution of naphthacene in nonane.

Anthracene. The spectrum of crystalline anthracene is considerably more diffuse than that of the crystalline naphthalene taken under the same conditions [12], and it was therefore of special interest to obtain a different spectrum of anthracene. The sharpest spectrum was that in n-heptane solution, which when shifted by 385 cm^{-1} toward short wavelengths agrees well with the sharp spectrum of mixed anthracene and naphthalene crystals [6].

We gave the analysis of the spectrum of a frozen solution of anthracene in heptane and its comparison with the spectrum of anthracene in naphthalene previously [10]; the results have verified the molecular character of the spectra of frozen paraffin solutions of anthracene.

Napthacene. We have photographed spectra of frozen solutions of naphthacene in n-hexane, n-heptane, n-octane, and n-nonane. The spectrum of naphthacene in nonane was the sharpest (table 1, figure 1*). The vibrational analysis of this spectrum shows that the most intense lines are connected with the frequency of the totally symmetric vibration 1380 cm^{-1}, the frequencies 321, 462, 610, 1165, 1380, 1480 cm^{-1} are distinctly developed. A comparison of the fluorescence spectra of naphthacene in nonane and in naphthalene [7] shows the vibrational structure of both spectra to be identical (Fig. 2).

Anthraquinone and 9-, 10-dichloroanthracene. The results of the studies of spectra of these compounds are reported in reference [10]. The sharpest were the spectra of solutions in hexane and heptane.

*In the illustrations, frequency values are given in cm^{-1}.

DISCUSSION OF RESULTS

In the present paper we have studied the spectra of a series of polycyclic aromatic hydrocarbons which gave us the opportunity to investigate in more detail the influence of the solvent on the character of the spectrum of the solution.

The molecules of normal paraffin hydrocarbons are zig-zag chains with the carbon atoms located in a plane, at the vertices of the chain [13].

The hydrogen atoms of the CH_2 group are lying in planes perpendicular to the plane of the chain. The period down the chain equals 2.53 Å. The cross section of the chain, perpendicular to the axis, is approximately a circle with a radius 2.62 Å.

The molecules of the studied hydrocarbons represent linear chains of benzene rings: two for naphthalene, three for anthracene, dichloroanthracene and anthraquinone, and four for naphthacene. The addition of one benzene ring increases the length of the molecule by about 2.5 Å, the distance between the hydrogen atoms along the short axis of the molecule is about 5.3 Å, which corresponds well with transverse dimensions of the solvent molecule.

The length of the naphthalene molecule is about 7 Å, which is very close to the length of the pentane molecule. The addition of one benzene ring corresponds to the addition of two carbon atoms to the molecule of the solvent, i.e., the anthracene molecule is similar in its linear dimensions to the heptane molecule, and the naphthacene molecule to the molecule of nonane (Table 2).

Table 2

Comparative data [13] on linear dimensions of the fluorescent molecule and of the solvent molecule (in Å)

Compound	Long axis	Short axis
Naphthalene	7.2	5.5
Pentane	7.36	5.3
Anthracene	10	5.5
Heptane	10.0	5.3
Naphthacene	12.8	5.5
Nonane	12.8	5.3

The spectra of frozen solutions are sharpest in the case where the linear dimensions of the studied molecules correspond well with the dimensions of the molecules of the solvent. The good match of linear dimensions of the molecules — of the substance under study and the solvent — allows us to assume that during the formation of the frozen solution the molecule under investigation takes the place of one of the solvent molecules in the crystal

lattice of the solvent in such a way that their long molecular axes coincide.

The crystals of normal paraffin hydrocarbons are close-packed lattices with monoclinic or rhombic symmetry, two molecules per unit cell, whereby the long axis of the molecule almost coincides with the C axis of the unit cell.

The sharpness of the spectra of all investigated compounds could be explained first by the definite position of the fluorescent molecule in relation to the lattice of the solvent, second, by the small amount of interaction between aromatic molecules, by reason of their low concentration, and between them and the solvent molecules. This is confirmed by qualitative experiments which were carried out in the investigation of temperature dependence of the spectra: increase of temperature leads to a gradual diffusion of the fluorescence spectra of anthracene in heptane. The fact is that since the cross-section of the chain is approximately a circle, it causes a comparatively greater mobility of the chain in the crystal. Thermal motions for such crystals can be represented by rotational vibrations around the molecular axis [13]. At temperatures close to the melting point there can set in limited rotations in the crystal which, without doubt, cause the crystal to lose some elements of symmetry. Vibrations of this kind should stop at the temperature of liquid air.

An increase of concentration also leads to gradually diffuse spectra, while the fact that there is no spectral shift shows that, as before, we are dealing with the spectrum of the solution and not with the spectrum of the crystal.

CONCLUSIONS

As a result of a comparison of all the experimental facts we can come to the following conclusions:

1. The spectrum of aromatic hydrocarbons in frozen solutions has a sharp character if the lattice of the solvent does not undergo considerable deformation. The deformation of the lattice arises in the following cases: a) the dimensions of the fluorescent molecule are such that on substitution of molecules of the solvent it deforms the crystalline lattice; b) the comparatively easy excitation of thermal rotational vibrations leads to deformation of the lattice with increase of temperature; c) the increase of concentration of the investigated compound leads on the one hand to its crystallizing out and formation of more complicated complexes, which on the other hand, is likely to deform the lattice substantially.

2. The comparison of spectra of naphthalene, anthracene [6] and naphthacene [7] in frozen solutions with known molecular spectra of the same compounds confirms the assumption about the molecular character not only of the solutions of these compounds, but also of all the aromatic hydrocarbons which were previously studied.

3. The absence of a fine band structure in the spectra of linear aromatic hydrocarbons shows the great probability of such orientation in which the long axes of the fluorescent molecule and of the solvent molecule coincide in direction.

4. The appearance of a fine structure in the spectra of more complex aromatic hydrocarbons can be explained by comparable probabilities for different orientations of the molecules. It is also possible that large molecules of such hydrocarbons as coronine, replace not one but two molecules of the solvent and therefore show sharp spectra even in hexane.

In conclusion, I express my deep gratitude to professor E. V. Shpol'skii for supervising this work.

September 6, 1958

References

1. F. R. LIPSETT, A. J. DEKKER: Can. J. Phys., 30, 165, (1952)
2. H. C. WOLF: Zs. f. Naturforsch., 10a, 3, (1955)
3. H. C. WOLF: Zs. f. Phys., 143, 266, (1955)
4. D. S. MCCLURE: J. Chem. Phys., 22, 1687, (1954)
5. D. S. MCCLURE: J. Chem. Phys., 24, 1, (1956)
6. J. W. SIDMAN: J. Chem. Phys., 25, 115, (1956)
7. J. W. SIDMAN: J. Chem. Phys. 25, 122, (1956)
8. E. V.SHPOL'SKII, A.A. IL'INA, L.A.KLIMOVA: DAN USSR, 87, 935, (1952)
9. E. V. SHPOL'SKII, L. A. KLIMOVA: IAN USSR, SF, 20,471 (1956);(See CTT Bulletin)
10. T. N. BOLOTNIKOVA: IAN USSR, SF,23,29 (1959) (See CTT Bulletin) 9
11. T. N. BOLOTNIKOVA: OIS, (in print)
12. I. V. OBREIMOV, K. G. SHABALDAS: J. Phys. USSR, 7,168 (1943);(in English)
13. A. I. KITAIGORODSKII: Organicheskaia kristallokhimiia. (Organic Crystal Chemistry) Akad. NAUK Press, Moscow, 1955.

TOM VII, Vyp. 2 OPTIKA I SPEKTROSKOPIIA Avgust, 1959
VOL. VII, No. 2 OPTICS AND SPECTROSCOPY August, 1959

Luminescence and Vavilov-Cherenkov Radiation in Solutions Bombarded by Gamma Rays

Z. A. CHIZHIKOVA

Abstract: The gamma luminescence is investigated of solutions in which energy transfer from the solvent to the solute does not exist. In such solutions the luminescence intensity is comparable to the Vavilov-Cherenkov radiation intensity. Vavilov-Cherenkov radiation was used as a standard to determine the luminescence excitation efficiency ρ during bombardment by high-speed electrons. The average value of ρ is $3.9 \pm 0.5\%$ for the solutions investigated.

INTRODUCTION

An investigation of the radio luminescence of solutions has shown that the yield under bombardment by high-speed particles is comparatively large only in such solutions in which an effective energy transport from the solvent to the solute occurs. Among such solvents are the aromatic solvents used in liquid scintillation counters; benzene, xylene, toluene, phenyl cyclohexane etc.

Kallman and Furst [1] have shown that the radio luminescence intensity of solutions is very small in solvents of another kind ("poor" solvents) such as, for example, water, alcohols, limiting hydrocarbons, and it is comparable to the luminosity of pure solvents. These authors explained the luminescence of pure solvents by the existence of small impurities.

Belcher [2] investigated the luminescence of aqueous solutions with inorganic salts of various radioactive isotopes. He showed that the luminescence of solutions is not luminescence but depends on Vavilov-Cherenkov (V-Ch) radiation. Undoubtedly, the luminescence of pure fluids observed by Kallman and Furst also depends to a considerable degree on V-Ch radiation.

The substantial role of the luminescence of a solvent was quite explicit from the original work of Cherenkov [3] on the gamma luminescence of uranyl salts.

An investigation of the radio luminescence of solutions in "poor" solvents is of great interest for the study of the process of luminescence excitation by charged particles since the process of transfer of energy from the solvent to the solute, which complicates this phenomenon, is absent in this case.

The purpose of the present paper was to clarify the relation between luminescence and V-Ch radiation in solutions in "poor" solvents and to use V-Ch radiation as a standard to determine the luminescence yield under bombardment by high-speed electrons.

The luminescence observable under bombardment by high-speed electrons consists of: 1) V-Ch radiation which is not absorbed in the solution; 2) V-Ch radiation, absorbed in the solution and converted to luminescence of the solute; 3) luminescence of the solute excited directly by the electrons. For sufficiently small concentrations, the refractive index of the solution differs slightly from the refractive index of the pure solvent, consequently, the intensity of V-Ch radiation is practically independent of concentration. The relation between the absorbed and the unabsorbed parts of the V-Ch radiation also depends slightly on the concentration and is determined by the long wavelength absorption edges of the solution. On the other hand, the intensity of the directly excited luminescence should increase in proportion to the concentration. Consequently, a measurement of the luminescence intensity as a function of the concentration of the solution affords the possibility of finding the ratio of the luminescence intensity to the intensity of V-Ch radiation. Hence, it is expedient to use the part of the V-Ch radiation which is absorbed and converted into luminescence since the radiations to be compared have the same spectral composition and the same angular distribution in this case. The relation between the absorbed and the unabsorbed parts of the V-Ch radiation can be calculated. As is shown herein, the magnitude of the radio luminescence yield can thus be determined.

EXPERIMENTAL PART

Solutions investigated. Water, alcohol and acetone, distilled once, were selected as solvents. These fluids do not luminesce and it can be assumed, with high probability, that energy will not be transferred to the solute. The selection of substances for the solutions was rather difficult since the solutes should satisfy the following conditions: Have adequate solubility, slight concentration quenching, high yield and a luminescence spectrum within the limits of the photomultiplier response.

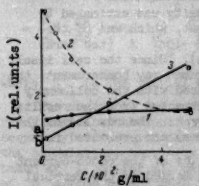

Figure 1. Luminescence intensity as a function of concentration of sodium salicylate solutions in water. 1) Luminescence intensity under gamma ray bombardment (I_γ); 2) Relative photo-luminescence yield (I_f); 3) Curve corrected for the unabsorbed part of V-Ch radiation and for concentration quenching $\frac{I_\gamma - kI_{V\text{-}Ch}}{I_f}$; a) $I_{V\text{-}Ch}$; b) $I_{V\text{-}Ch}$.

The following solutions were selected: sodium salicylate in water, quinine sulfate in water with 0.3% sulfuric acid, 3-aminophthalimide in alcohol; 2, 5-diphenyl oxazole in alcohol, 2, 5-diphenyl oxazole in

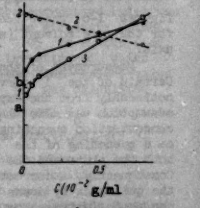

Figure 2. Luminescence intensity as a function of concentration of quinine sulfate in water with 0.3% H_2SO_4. Notation same as in figure 1.

acetone and anthracene in acetone.

Measurement of the Luminescence of Solutions Bombarded by Gamma Rays. The intensity of the luminescence of solutions bombarded by gamma rays was measured as a function of the concentration of the substance. A Co^{60} compound of 6 milli-Curie activity was used as gamma ray source. The ampoule with the compound was placed in a lead shield with a hole 10 cm long and 8 mm in diameter to collimate the beam. The beam of gamma rays was directed onto the cell with the solution which was placed at the window of an FEU-29 photomultiplier. The glass cell was 30 mm long and 25 mm in diameter. In order to accelerate and to increase the accuracy of the measurements, a special mechanical adapter was made for the rapid readjustment of the cell.

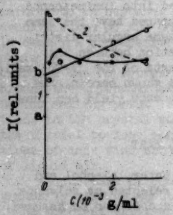

Figure 3. Luminescence intensity as a function of concentration of 3-aminophthalimide in ethyl alcohol. Same notation as in figure 1.

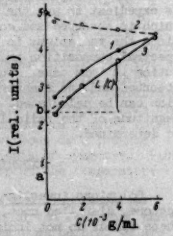

Figure 4. luminescence intensity as a function of the concentration of 2, 5 diphenyl oxazole in ethyl alcohol. Same notation as in figure 1.

The luminescence intensity was estimated by means of the FEU photocurrent, which was of the order of magnitude of 10^{-8}—10^{-7} A (the dark current was about $4 \cdot 10^{-9}$ A). Since the cell itself glowed slightly under the gamma ray bombardment, the current intensity was measured with the cell empty ($2 \cdot 10^{-9}$ A) and this was subtracted from the results of measuring the photo-current. The results of the measurements (the I_γ curves) are presented in figures 1-6 where the values of the photo-current for the pure solvent (a) is marked on the vertical axis.

Measurement of the Concentration Quenching. Certain of the I curves on figures 1-6 deviate noticeably from the expected linear dependence. The assumption was made that this is a consequence of concentration quenching. Concentration quenching, as a quenching of the II kind, should affect both the photo and the radio luminescence identically. Consequently, a correction could be introduced for the quenching by means of the results of measuring the photo luminescence. The relative yield of photo luminescence was determined by measuring the intensity of the spectrum by using a UM-2 monochromator and a photo-multiplier with frontal excitation by mercury 313 or 365 mμ lines isolated by filters. Concentrations were measured for which the absorption was complete and the relative yield of the unquenched solution was determined by extrapolation to zero concentration. The results of these measurements are given on figures 1-6 (I_γ curves).

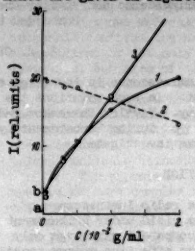

Figure 5. Luminescence of 2,5-diphenyl oxazole in acetone. Same notation as in figure 1.

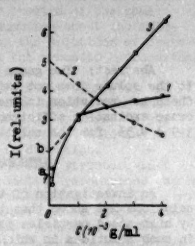

Figure 6. Luminescence intensity as a function of anthracene concentration in acetone solutions. Same notation as in figure 1.

Determination of the Long Wavelength Absorption Boundaries of Solutions and Solvents. In order to estimate the relation between the parts of the V-Ch radiation absorbed and not absorbed by the luminescing substance, it is necessary to determine the long wavelength absorption boundary of the solutions (ω_0) and the pure solvents (ω_2). The absorption spectra of the solutions and the acetone were measured on an SF-4 spectrometer with a hydrogen lamp in order to determine their absorption edge. Taken as the absorption edge of the solutions was the wavelength at which the absorption coefficient of the solution with concentrations on the order of $5 \cdot 10^{-4}$ g/cm^3 equalled 1 cm^{-1}. Taken as the absorption boundary for acetone was the beginning of strong absorption (above 10 cm^{-1}). The solvent absorption boundaries were taken from literature data [4]. The results of these measurements are presented in the table.

Luminescing material and solvent	$\lambda_0=\frac{2\pi c}{\omega_0}$ in mμ	$\lambda_2=\frac{2\pi c}{\omega_2}$ in mμ	k	C g/ml	$\frac{L(C)}{L_{V\text{-}Ch}}$	ρ in %
Sodium salicylate, Water	330	190	0.88	$1 \cdot 10^{-2}$	1	3.6
Quinine sulfate Water with 0.3% H_2SO_4	390	200	0.43	$3 \cdot 10^{-3}$	0.33	3.4
3-aminophthalimide, Ethyl alcohol	430	200	0.26	$2 \cdot 10^{-3}$	0.27	4.2
2,5-diphenyl oxazole, Ethyl alcohol	346	200	0.76	$4 \cdot 10^{-3}$	0.55	4.1
2,5-diphenyl oxazole, acetone	350	310	0.77	$1 \cdot 10^{-2}$	6.25	3.3
Anthracene, Acetone	382	310	0.49	$2 \cdot 10^{-3}$	1.14	4.7

DISCUSSION OF RESULTS

Let us assume that the intensity of V-Ch radiation in a pure solvent is $I_{V\text{-}Ch}$ and that a (1-k)-th part of this radiation is absorbed in the solution. As has already been mentioned in the introduction, the luminescence under gamma ray bombardment consists of three parts: 1) V-Ch radiation not absorbed in the solution ($kI_{V\text{-}Ch}$); 2) V-Ch radiation being absorbed in the solution and converted into luminescence of the solute ($L_{V\text{-}Ch}$); 3) luminescence of the solute excited directly by electrons [L(C)].

Calculation of the Unabsorbed Portion $kI_{V\text{-}Ch}$. Values of the luminescence intensity of pure solvents bombarded by gamma rays (marked off with an a on figures 1-6) were used to calculate this part of the luminescence. The intensity of V-Ch radiation received by the FEU is proportional, in this case, to the integral $\int f(\omega)\alpha d\omega$, where $f(\omega)$ is the spectral response of the FEU, ω the spectral distribution of the V-Ch radiation. In the case of a solution, the unabsorbed part of the V-Ch radiation is expressed by the same integral but its limits are the long wavelength boundary of the FEU response ω_1 and the long wavelength absorption edge of the solution ω_0: $\int_{\omega_1}^{\omega_0} f(\omega)\alpha d\omega$.*

The unabsorbed portion (k) of the V-Ch radiation was defined as the ratio of these two integrals which were calculated graphically. The magnitude of $kI_{V\text{-}Ch}$ was subtracted from the values of the luminescence intensity I_γ obtained in the measurements. These differences, corrected for concentration quenching, i.e., the quantity $\frac{I_\gamma - kI_{V\text{-}Ch}}{I_f}$, are shown on figures 1-6.

Calculation of the Medium Energies of V-Ch Radiation. Upon bombardment by Co^{60} gamma rays with 1.33 and 1.18 MeV energies, the absorption in the solutions investigated occurs almost exclusively because of the formation of Compton electrons. In order to compute the energy of V-Ch radiation theoretically, an average must be taken over the velocities of the Compton electrons. The intensity of V-Ch radiation per unit path length per electron with velocity $v = \beta c$ is (see [5])

$$F(\beta) = \frac{dW}{dx} = \frac{e^2}{c^2}\beta n \int_{\beta n > 1} \frac{\beta^2 n^2 - 1}{\beta^2 n^2}\,\alpha d\omega$$

*As has been mentioned earlier, the long wavelength absorption boundary ω_0 was selected so that the absorption for a solution with concentration of the order of 5×10^{-4} g/cm^3 would be about 1 cm^{-1}. Under these conditions, complete absorption of the part of the V-Ch radiation spectrum with frequency higher than ω_0 would be guaranteed, in practice. Because the long wavelength part of the absorption spectrum of solutions usually drops very steeply, the absorbed part of the V-Ch radiation increases slightly with a further increase in concentration and k can be considered independent of the concentration. In certain cases (see Fig. 2, 4, 6) this absorption would apparently not be complete at low concentrations, which is manifest in the deviations of the points below the I_γ curve.

In order to find the V-Ch radiation energy $W_{V\text{-}Ch}$ for the complete transit of one electron, it is necessary to integrate $\frac{dW}{dx}$ over the path or, more accurately, over the part of the path where the condition of V-Ch radiation $\beta n > 1$ is satisfied. Hence,

$$W_{V\text{-}Ch} = \int_0^l F(\beta)\,dx.$$

Let us transform from integration over the electron path to integration over the velocity. To do this, let us express dx in terms of $d\beta$ by using the relation

$$dx = \frac{dx}{dE}\cdot\frac{dE}{d\beta}\,d\beta,$$

where E is the particle kinetic energy. From the usual relation between the energy and the velocity we obtain

$$\frac{dE}{d\beta} = \frac{\mu\beta}{(1-\beta^2)^{3/2}},$$

where $\mu = m_0c^2$.

The quantity $\frac{dx}{dE}$ was taken from the approximate dependence between the path and the energy [6,7] which equals 0.5 cm/MeV for water, 0.63 cm/MeV for alcohol and acetone. Hence

$$W_{V\text{-}Ch} = \int_{\beta_0}^{\beta=\frac{1}{n}} F(\beta)\frac{dx}{dE}\cdot\frac{dE}{d\beta}\,d\beta =$$

$$= \frac{e^2\mu}{c^2}\cdot\frac{dx}{dE}\int\alpha d\omega\cdot\int_{\beta_0}^{\beta=\frac{1}{n}}\frac{\beta^2n^2-1}{\beta^2n^2}\cdot\frac{\beta}{(1-\beta^2)^{3/2}}\,d\beta,$$

where β_0 is the initial electron velocity.

The change in the refractive index in the transparency region of the solvent in insignificant and, consequently, dispersion can be neglected. To simplify the calculation, the value of the refractive index was taken as 1.38 for all cases. The effective values of n differ by not more than 0.05 on either side of this value for the solvents investigated, which leads to a change of not more than 10% in the value of $W_{V\text{-}Ch}$. The integral over β was calculated graphically for a number of values of β_0. The velocity distribution of the Compton electrons, $\Phi(\beta_0)$, was computed from the Klein-Nishina formula in order to average the electrons over the velocities. (The mean gamma ray energy was taken equal to 1.25 MeV.) The average V-Ch radiation energy from the Compton electron having been absorbed is

$$\overline{W}_{V\text{-}Ch} = \frac{\int\Phi(\beta_0)W_{V-Ch}(\beta_0)d\beta_0}{\int\Phi(\beta_0)d\beta_0}$$

The averaging was carried out by graphical integration with the result that the following expression is obtained for the average V-Ch radiation energy

$$W_{V\text{-}Ch} = \frac{0.21e^2\mu}{c^2} \cdot \frac{dx}{dE} \int \omega d\omega$$

Calculation of the Luminescence Intensities $L_{V\text{-}Ch}$ and $L(C)$. According to the Vavilov law, the luminescence energy yield excited by the frequency ω is

$$B_f^e = B_f^q \frac{\omega_o}{\omega},$$

where B_f^q is the maximum value of the yield equal to the quantum yield; ω_o is the corresponding frequency usually close to the long-wavelength edge of the absorption band of the material. When V-Ch radiation is absorbed in the solution each frequency is converted into luminescence with a corresponding energy yield. The luminescence intensity is defined as

$$L_{V\text{-}Ch} = \frac{0.21e^2\mu}{c^2} \cdot \frac{dx}{dE} B_f^q \omega_o \int_{\omega_o}^{\omega_2} d\omega,$$

where ω_2 is the long-wavelength absorption boundary of the solvent. It is assumed that the absorption in the solvent is much greater for a frequency greater than ω_2 than in the solute and that the solvent does not luminesce and does not transmit energy to the luminescing material. These conditions are complied with in the solvents under investigation.

Furthermore, let us consider the solute luminescence excited by electrons. Since the solvent and solute consist of atoms with similar atomic numbers, the fraction of energy absorbed in the solute can be considered proportional to the concentration by weight C g/g. Consequently, the luminescence energy under the bombardment by a single electron can be expressed as follows:

$$L(C) = \rho B_f^q C\bar{E},$$

where $\bar{E}$ is the average energy of a Compton electron and ρB_f^q is the radio luminescence energy yield.

Here as in [8], it is assumed that the energy yield of radio luminescence can be represented as the product of the photo luminescence quantum yield B_f^q and the excitation effectiveness ρ. The quantity ρ is the fraction of absorbed energy which is expended in transporting the molecule to the excited state.* The average energy $\bar{E}$ =0.6 MeV was calculated graphically from the energy distribution of the Compton electrons according to the Klein-Nishina formula.

The $L(C)$ and $L_{V\text{-}Ch}$ radiations have the same spectral composition and the same angular distribution, consequently, they can be compared directly and the quantity ρ can be determined from their ratio

$$\rho = \frac{0.21\mu e^2}{c^2} \cdot \frac{dx}{dE} \cdot \frac{\omega_o(\omega_2 - \omega_o)}{C\bar{E}} \cdot \frac{L(C)}{L_{V\text{-}Ch}}$$

The method of determining $L(C)$ and $L_{V\text{-}Ch}$ from the experimental curves is seen clearly on figure 4. The quantity $L_{V\text{-}Ch}$ is found by extrapolating the $\frac{I_\gamma - kI_{V\text{-}Ch}}{I_f}$ curve to zero concentration, the quantity $L(C)+L_{V\text{-}Ch}$ is the value of the ordinate of the same curve for any concentration. The values of ρ obtained and those necessary for the calculations are presented in the table.

CONCLUSION

The determination of the excitation effectiveness ρ by the method described has specific advantages over other methods. The luminescence under the effect of V-Ch radiation which is used as etalon has the same spectrum and the same angular distribution as does radio luminescence. Consequently, corrections for the spectral response of the FEU and the geometry of the apparatus are not necessary. This method yields the value of the excitation effectiveness directly and does not require a separate measurement of the quantum yield of photo luminescence for the calculation of ρ.

The values of ρ obtained are in agreement with the results of measuring radio luminescence [9, 10, 11].** On the other hand, significant errors are possible in theoretical calculations of the V-Ch radiation intensity because of an inaccurate determination of the absorption boundaries of the solvent (ω_2) and of the solution (ω_o). It can apparently be considered that the values of ρ for various solutions lie within the limits $3.9 \pm 0.5\%$.

It also follows from the results obtained that the radio luminescence intensity becomes comparable to the intensity of V-Ch radiation at comparatively high concentrations (on the order of 10^{-3} g/ml), consequently, the luminescence under bombardment by high-speed particles of even not very pure fluids such as the class of "poor" solvents depends on V-Ch radiation or on luminescence excited by this radiation.

The results herein also show that the excitation effectiveness of solutions of low concentrations in "poor" solvents is the same, in practice, as in good scintillator-crystals, plastics and solutions.

This does not verify the hypothesis that a low radio-luminescence yield is explained by quenching during the interaction between excited molecules [13, 10]. Actually, the density of the excited molecules of the luminescing substance in solutions in "poor" solvents is considerably less than in those cases when the substance consists entirely of luminescing molecules. Therefore, the bimolecular quenching hypothesized should have been weaker and the excitation effectiveness ρ considerably higher. The identical value of ρ for excitation by weakly ionizing particles for the solutions investigated and for the usual scintillators means that the low radio luminescence yield does not apparently depend on bimolecular quenching.

*Kept in mind is the excited state from which luminescence proceeds. The relation between radiative and non-radiative transitions determines the photo luminescence quantum yield B_f^q.

** The value of the absolute gamma luminescence yield, obtained in [12] and used to determine ρ for the case of organic crystals by the author and Galanin [8], is apparently underestimated.

M. D. Galanin supervised the present research and the author is, therefore, grateful.

September 26, 1958

References

1. H. KALLMAN, M. FURST: Phys. Rev., 79, 857, (1950); J. Chem.Phys., 23, 607, (1955)
2. E. H. BELCHER: Proc.Roy.Soc., 216A, 90, (1953)
3. P. A. CHERENKOV: Tr.FIAN USSR, 1, 41, (1936)
4. LANDOLT-BORNSTEIN: 6 Aufl. 1955, J. L. R. MORGAN
5. R. H. C. RIST: JACS, 49, 338, (1927)
5. I. M. FRANK, I. E. TAMM: DAN USSR, 14, 109, (1937)
6. E. SEGRE: Experimental nuclear physics, part 1. (IL, Moscow 1955)
7. L. V. SPENCER: Phys. Rev., 98, 1597, (1955)
8. Z. A. CHIZHIKOVA, M.D. GALANIN: ZETF, 30, 137, (1956) (See Sov.Phys.JETP)
9. M. FURST, H. KALLMAN, B. KRAMER: Phys.Rev., 89, 416, (1953)
10. G. T. WRIGHT: Proc.Phys. Soc., B68, 929, (1955)
11. E. A. ANDREESHCHEV, I. M. ROZMAN: OiS, 5, 39, (1958)
12. M. D. GALANIN, A. P. GRISHIN: ZETF, 30, 33, (1956) (See Sov.Phys., JETP)
13. I. M. ROZMAN, E. A. ANDREESHCHEV, S. F. KILIN: IAN USSR FS, 23,102, (1959), (See CIT Bulletin)

TOM VII, Vyp. 2 OPTIKA I SPEKTROSKOPIIA Avgust, 1959
VOL. VII, No. 2 OPTICS AND SPECTROSCOPY August, 1959

Luminescence of Unactivated CsI Monocrystals

Z. L. MORGENSHTERN

Abstract: The emission spectra, duration and spectral distribution of the absorption coefficient and the relative yield of "activator-less" luminescence of crystals of CsI, excited by a narrow band which lies on the edge of the natural absorption of the crystals, were investigated. Luminescence was also excited by γ-rays.

1. It has been thought for a long time that alkali-halide crystals which were unactivated and not subjected to preliminary exposure to hard radiation do not luminesce.

In the last few years, however, work has appeared which indicates that this assertion is unjustified.

Bonanomie and Rossel, Hahn and Rossel [1] investigated the luminescence of unactivated alkali iodides excited by α and γ-excitation and detected the increase of the yield of luminescence at low temperatures. Van Sciver and Hofstadter [2] have shown, that pure NaI crystals, under strong irradiation and also on photoexcitation at low temperatures, give a luminescence band in the ultraviolet region of the spectrum with λ_M approximately equal to 300 mμ. Teegarden [3] detected luminescence at low temperatures in what was apparently unactivated KI. In the work of Knopfel, Loepfe, and Stoll [4], the luminescence of unactivated CsI was investigated(in relation to the temperature), chiefly under α-excitation.

In pure crystals, grown from an aqueous solution, the authors detected luminescence, whose intensity increases with decreasing temperature (the "cold" component). In crystals activated with Tl, luminescence is displayed, whose intensity falls with decreasing temperature (the "hot" component). If the pure crystal is remelted or strongly heated in Na vapors (approximately 610° C), then, in addition to the "cold" component, the "hot" component also appears and behaves just as it does in crystals activated with Tl.

There is still no unified point of view on the nature of the luminescence of unactivated alkali halides. Van Sciver and Hofstadter, and also Teegarden, assume that the luminescence they detected is a lattice luminescence not associated with the presence of defects; Knopfel, Loepfe, and Stoll consider that the "hot" component is linked with structural defects of the vacancy type and the role of the activator Tl reduces to the fact that, forming complex bonds with the matrix, it leads to an increase of the number of these vacancies.

2. Aiming to investigate the luminescence in pure crystals, monocrystals of CsI were prepared at our request, in which we were unable to detect traces of Tl either on absorption or on emission *. In these crystals, luminescence is displayed at room temperature which is excited by a narrow band lying on the edge of the crystal's own absorption. The luminescence spectrum represents a wide band, with a maximum at around 420 mμ, with a half width of approximately 0.44 electron volts. The same luminescence is also excited by the action of γ-rays. In the presence of the activators Tl or In, this luminescence is also observed but its intensity decreases with an increase in the concentration of the activator.

In figure 1 are shown averaged graphs of blackening for an unactivated CsI crystal under photo- or γ-excitation and for crystals activated with small additions of Tl (approximately 10^{-6}) or In (less than 10^{-5}). As seen from the graphs, one and the same band of activator-less luminescence** is displayed in all crystals; in crystals containing Tl or In, in addition, longer wavelength bands of activator luminescence are observed.

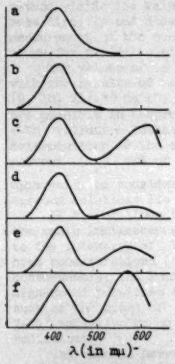

Figure 1. Emission spectra. a)- CsI, photoexcitation, λ_B = 240 mμ; b)- CsI, γ-excitation (Co^{60}); c)- CsI-Tl, photo-excitation, λ_B = 240 mμ; d)- CsI-Tl, γ-excitation (Co^{60}); e)- CsI-In, photo-excitation, λ_B = 240 mμ; f)- CsI-In, γ-excitation (Co^{60}).

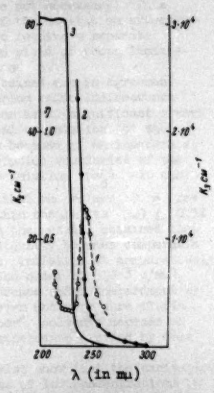

Figure 2. Spectral distribution of the absolute luminescence yield η of the CsI monocrystal; 2)- absorption coefficient K_2 of the same crystal; 3)- absorption coefficient K_3 of a crystal of thickness 1 μ.

The spectral distribution of the excitation for the activator-less luminescence represents a narrow

*I would like to express my gratitude to L. M. Shamovskii, in whose laboratory the crystals used in this investigation were prepared.

**According to the data of [4], the luminescence maximum of inactivated CsI is located at about 4600 Å. In reference [6], published after this communication was completed, an emission spectrum of an inactivated CsI crystal grown from aqueous solution is shown. It consists of a band in the ultraviolet region with two maxima at 3250 and 3500 Å.

band with a half width of 0.23 electron volts with λ_M = 240 mμ which is found on the steep downward slope in the absorption curve. On the basis of the data of absorption and excitation measurements, we calculated the dependence of the relative quantum yield on the wave length of the exciting light. The yield also has a sharp spectral dependence. The band of the yield has a half width of 0.29 electron volts, and its maximum is somewhat displaced toward the long wavelength region (λ_M = 242 mμ). We measured the absolute value of the luminescence quantum yield for the excitation maximum by a method described in [5]. In figure 2, curve 1, depicts the data for the spectral dependence of the absolute luminescence yield. The sharp drop of the yield in the region of intrinsic crystal absorption and its subsequent rise toward still shorter wave lengths seems particularly interesting. An analogous drop and the beginning of a rise were previously detected for iodides of sodium, potassium, and cesium activated with thallium [7].

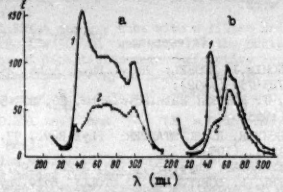

Figure 3. Spectral distribution of excitation for crystals of CsI-Tl (a) and CsI-In (b). 1)- without light filters; 2)- with a yellow light filter.

In the excitation spectrum of crystals, activated with small additions of Tl or In, along with the activator bands, a boundary band of excitation in the 240 mμ region is also clearly seen (Fig. 3, curves 1). In the excitation spectrum of activator luminescence (measured through a yellow light filter) its intensity at this boundary band falls strongly (curves 2). Thus, from these experiments, just as from investigations of the emission spectra, one can conclude, that in CsI crystals with small concentrations of the activator (Tl or In), on excitation in the boundary band, (λ_B = 240 mμ) both kinds of luminescence, activator-less and activator luminescence are simultaneously observed. The transmission of energy from the centers of activator-less luminescence to the activator centers is apparently insignificant, and the luminescence of the activator is chiefly evoked by absorption of the activator itself, which also is in this region (in CsI-Tl there is an absorption band, located at 241 mμ [8], and in CsI-In at 234 mμ [9]). For large activator concentrations, as is well known, excitation in this region leads to luminescence of the activator only.

4. The luminescence of unactivated crystals is distinguished from the luminescence of activated crystals by its duration. With the aid of the method of single time oscillography, worked out in our laboratory by I. K. Plisvin' [10], the temperature dependence of the time to damp for inactivated CsI and CsI activated with thallium (CsI-Tl) was measured by L. Bubnov for excitation by the boundary band (λ_B = 240 mμ). As a source of excitation, a short-time spark with a luminescence duration no greater than 3×10^{-8} sec. was used, the light from which passed through a quartz monochromator. The results of the measurements are shown in figure 4. It follows from these data, that the short wavelength emission band in the activated crystal, being excited by the boundary band, has the same duration as the luminescence of the unactivated crystal (curve 1; at room temperature $\tau = 0.55 \times 10^{-6}$ sec.). Both luminescences have identical spectral compositions and, consequently, one and the same nature. The luminescence of the activator in this same crystal has a different value of τ, a different temperature dependence for τ (curve 2) and a different spectral composition* .

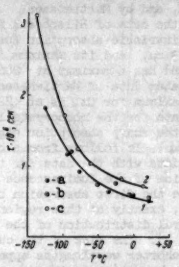

Figure 4. Temperature dependence of τ. 1— λ_B = 240 mμ; τ(20° C) = 0.55 x 10^{-6} sec.; a— CsI; b— CsI-Tl (blue light filter). 2— λ_B = 300 mμ; τ(20° C) = 0.7 x 10^{-6} sec; c—CsI-Tl (yellow light filter).

5. One can conclude from the data presented, that in the unactivated crystals of CsI there is luminescence with a characteristic emission spectrum, excitation spectrum, and duration. It arises on both photo- and γ-excitation. One can consider it established that this luminescence is not associated with impurities.

To elucidate the nature of this luminescence it seemed essential to compare the spectral distribution of its yield with the data pertaining to the spectral distribution of absorption. The available literature data of Hilsch and Pohl [11], Schneider and O'Bryan [12] and Martienssen [13] pertain to fine sublimed layers. We made an attempt to obtain fine monocrystalline layers by fusing the crystal between quartz plates. We succeeded in obtaining layers around 1 μ in thickness. The interference patterns from which one could determine the thickness

* When the CsI-Tl crystal was excited in the absorption band of the activator (λ = 300 mμ) and measured through a blue light filter at temperature below -50° C another short-time component was detected. At -60° C, $\tau = 1.8 \times 10^{-7}$ sec. for this component.

of the layers, were defined. The spectral distribution of the absorption coefficient for such a crystal is shown on figure 2, curve 3. The sharp absorption edge is at 229-230 mμ, and the value of the absorption coefficient in the region of intrinsic absorption is approximately 3×10^4 cm^{-1}. These measurements were carried out with the aid of a powerful hydrogen lamp,* a vacuum monochromator with a fluorite prism, and an FEU-19 photomultiplier with an amplifier. Supplementary measurements were conducted on individual lines (Zn - arc 2137 Å and Hg 1850 Å). These measurements gave that same result, i.e., the value of the absorption coefficient in the region of intrinsic absorption was of the order of $3 - 5 \times 10^4$ cm^{-1}. The behavior of the curve we obtained for the absorption coefficient in the region of intrinsic absorption does not have as clear a structure as for the sublimed layers. This, apparently, is explained by the fact that our layers had a thickness which was an order of magnitude greater than that measured by Hilsch and Pohl, and by Martienssen.

According to the data of Hilsch and Pohl [11], the first band of intrinsic absorption for CsI is in the region 214-223 mμ, and its maximum is at 219 mμ. The second band has a maximum at 206 mμ. According to the later data of Martienssen [13], the first absorption maximum for CsI is at 225 mμ. It follows from our data for the monocrystalline layer that in each case the sharp absorption edge in CsI is at around 230 mμ. It follows from a comparison of the absorption data with the data for the spectral distribution of the luminescence yield, that at room temperature the first absorption band of the host is not active, exactly at this region there is a gap in the spectral distribution of the luminescence yield (Fig. 2). The rise of the curve of the quantum yield for shorter wavelengths apparently indicates that the absorption in the second intrinsic absorption band is active.

With what can one associate the presence of a maximum of excitation at the intrinsic absorption edge, i. e., the presence of a band of "edge" excitation of the crystal ? Analogous to the explanation of the excitation spectrum of the blue luminescence of ZnS [14], one can assume that there is an absorption band due to some sort of structural defects of the lattice in our crystals at the intrinsic absorption edge. This band was not successfully measured in the absorption spectrum since it is masked by a strong increase in the absorption of the host. The absorption of light in it leads to activator-less luminescence. If there is an activator in the crystal, absorbing in this same region, there then arises a competition between the absorption by the structural centers and by the activator. If the concentration of the activator is large, mainly the activator absorbs and then emits.

One can, however, explain the edge band of excitation without the hypothesis of the existence of structural absorption centers. In fact, it follows from our experiments that the second absorption of the host is active, but the first is not. They overlap strongly which, generally speaking is a common phenomenon in solids. If the second band is substantially wider than the first and the overlapping of the bands is such that the long wavelength tail of the second band passes through the first, we obtain a superposition of the inactive and the active absorptions on the intrinsic edge absorption of the crystal. The luminescence yield in the edge excitation band will depend on the ratio of the inactive and active absorption coefficients and on their relative efficiency. Evidently, its maximum will be found where the difference between the active and inactive absorption will be greatest. The region of the gap will be found where the inactive absorption exceeds the active absorption.

Starting from these considerations, one can obtain for the luminescence yield a curve which has the same spectral behavior as that we obtained experimentally. However, the available experimental data is insufficient for the preference of one point of view over another, and further parallel investigations of the luminescence and absorption yields at low temperatures are required.

I would like to express my gratitude to M. N. Alentsev and M. D. Galanin for discussion of the results and advice, and to N. V. Kostina for aid in the work.

October 18, 1958

References

1. J. BONANOMIE, J. ROSSEL: Helv. Phys. Acta, 25, 725-752 (1952); B. HAHN, J. ROSSEL: Helv.Phys.Acta, 26, 803-810, (1953)
2. W. VAN SCIVER, R. HOFSTADTER: Phys.Rev., 97, 1181, (1955)
3. K. J. TEEGARDEN: Phys.Rev., 105, 1222, (1957)
4. H. KNOPFEL, E. LOEFFE AND P. STOLL: Helv.Phys. Acta, 29, 241-243 (1956); 30, 521-552, (1957); Zs. f. Naturforsch., 12a, 348, (1957)
5. H. ENZ, J. ROSSEL: Helv.Phys.Acta, 31, 25, (1958)
6. Z. L. MORGENSHTERN: ZETF, 29, 903-904, (1955) (See Sov.Phys. JETP)
7. Z. L. MORGENSHTERN: DAN USSR, 105, 250-252, (1955)
8. M. FORRO: Zs. f. Phys., 58, 613, (1929)
9. A. A. DUNINA, Z. L. MORGENSHTERN, L. M. SHAMOVSKII: OiS, 4, 105, (1958)
10. I. K. PLIAVIN': Dissertation, FIAN [Physical Institute of the Academy of Sciences], Moscow (1958)
11. R. HILSCH, R. W. POHL: Zs. f. Phys., 59, 812, (1930)
12. E. G. SCHNEIDER, H. M. O'BRYAN: Phys.Rev., 51, 293, (1937)
13. W. MARTIENSSEN: J.Phys.Chem. Solids, 2, 257, (1957)
14. M. N. ALENTSEV: OiS, 1, 240, (1956); Z. A. TRAPEZNIKOVA: Materialy V soveshchaniia po liuminestsentsii [Materials of the Fifth Conference on Luminescence], page 37, Tartu, (1957).

* I would like to thank I. A. Prager, who supplied an experimental model of a powerful hydrogen lamp.

TOM VII, Vyp. 2 OPTIKA I SPEKTROSKOPIIA Avgust, 1959
VOL. VII, No. 2 OPTICS AND SPECTROSCOPY August, 1959

Comparative Study of the Storage of Light Sums and the Temperature Quenching of ZnS-Ag Phosphor Excited by β-rays and Light*

V. L. LEVSHIN AND V. N. REBANE

Abstract: This article describes a comparative study of the curves of thermoluminescence and temperature quenching of a ZnS-Ag luminophor excited by light of $\lambda = 365$ mμ and β-particles from P^{32}, Tl^{204}, and S^{35}. It is shown that the nature of filling the localization levels and, to a considerable extent, the shape of the temperature quenching curves when ZnS-Ag phosphor is excited by β-particles, is connected with low excitation densities.

In recent years, due to wide use of scintillation counters and light substances of constant quantum efficiency, there has been a great increase in interest in luminescence phenomena originating from high energy of fast-particle excitation of such practically and technically important crystallophosphors as Zn-sulphide luminophors.

This article will study the thermoluminescence and temperature quenching curves of ZnS-Ag phosphor ($1 \cdot 10^{-4}$ g/g) -$MgCl_2$ ($1 \cdot 10^{-2}$ g/g)** under photoexcitation and excitation by β-particles. The phosphor was tempered at 800° in a crucible with an air inlet.

A PRK-4 mercury tube with a filter transmitting the line $\lambda = 365$ mμ was used for the photoexcitation. Sources of β-particles were radioactive isotopes of P-32 (maximum energy of β-particles $E_\beta = 1.7$ MeV, mean energy $\bar{E}_\beta = 0.7$ MeV), Tl^{204} ($E_\beta = 0.783$ MeV, $\bar{E}_\beta = 0.261$ MeV) and S^{35} ($E_\beta = 0.167$ MeV, $\bar{E}_\beta = 0.055$ MeV).

The excitation was carried out in a Dewar vessel with a holder for the phosphor sample on the wall of the internal flask. Inside the Dewar the β-particle source was $d = 4$ cm distant from the phosphor. The Dewar was evacuated by a fore-vacuum pump. The holder for the phosphor was made of cuprite and could be cooled by liquid nitrogen or heated to 300° by an oven. The phosphor was precipitated from alcohol directly onto the surface of the holder. The thickness l of the phosphor layer was 0.25 mm. The temperature of the phosphor was measured by a thermocouple.

The phosphor was excited at the temperature of liquid nitrogen, then excitation was removed and the phosphor was kept in darkness for one minute. After this, the phosphor was warmed at a rate of 15 degrees/min. The intensity of the phosphor luminescence was registered by an FEU-19 photomultiplier and an M-91 microammeter with scale division of 10^{-2} μA.

In these conditions, under excitation by light, two peaks appear on th thermoluminescence curve (Fig. 1, a) at -(150-165°) (the position of the peaks varies somewhat as a result of changing the ratio of their intensity) and at -(75-80°).

Under excitation by β-particles from P-32, Tl^{204} and S35 (Fig. 1, b, c, d), the same sort of system of localized levels is seen; however, they are filled quite differently. Under photoexcitation the shallow levels were filled more completely than the deeper ones, but under β-excitation the picture is reversed.

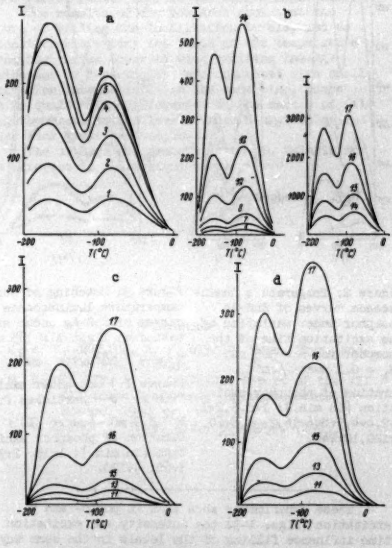

Figure 1. Temperature Luminescence Curves of ZnS-Ag under Excitation by:
a) light $\lambda = 365$ mμ ($E = 30 \frac{\mu \text{ watts}}{\text{cm}^2}$);
b) β-particles from P^{32} (43 mCu, $E_\beta = 1.7$ MeV, $\bar{E}_\beta = 0.7$ MeV);
c) β-particles from Tl^{204} ($E_\beta = 0.783$ MeV, $\bar{E}_\beta = 0.261$ MeV);
d) β-particles from S^{35} ($E_\beta = 0.167$ MeV, $\bar{E}_\beta = 0.055$ MeV).

Duration of phosphor excitation (in sec.): 1) 1, 2) 3, 3) 10, 4) 30, 5) 45, 6) 60, 7) 120, 8) 240, 9) 270, 10) 480, 11) 900, 12) 960, 13) 1800, 14) 1920 15) 3600, 16) 7200, 17) 14,400. (Microammeter readings are shown on the ordinate axis.)

*Reported by M. D. Galanin at the VII All-Union Conference on Luminescence, July 1, 1958, in Moscow.

**The phosphor was prepared by V. I. Shchaenko to whom the authors are grateful.

It is known [1] that the intensity and excitation time greatly influence the filling of localized levels; therefore, we studied the influence of the intensity and excitation time on filling the localized levels in the phosphor under consideration. In photoexcitation the intensity was varied by screens, while in β-excitation the natural decay of P^{32} (half-life 14.3 days) was used. In order to obtain the necessary excitation intensity, the β-particle source was held for a fixed number of days.

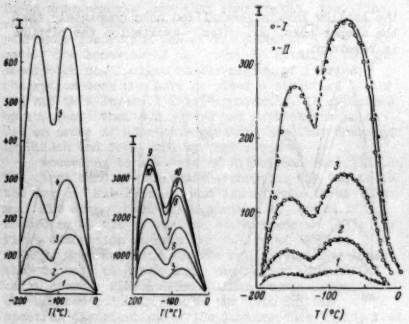

Figure 2: Temperature luminescence curves of ZnS-Ag phosphor under variation of the excitation time of the phosphor for $\lambda = 365$ mμ, ($E_\lambda = 0.1$ μwatt/cm^2). Duration of phosphor excitation (in min.): 1÷0.5, 2÷1, 3÷2, 4÷4, 5÷8, 6÷16, 7÷30, 8÷60, 9÷120, 10÷240.

Figure 3: Matching of the temperature luminescence curves of ZnS-Ag under excitation by light $\lambda = 365$ mμ, $E_\lambda = 3 \times 10^3$ μwatt cm^2 (curve I) and under excitation by β - particles from P^{32} 5.7 mCu (curve II). Duration of phosphor excitation (in min.): 1÷15, 2÷30, 3÷60, 4÷120.

These experiments show that in photo- and β-excitation (Figs. 1-3) the intensity and excitation time influence filling of the levels in the same way: with low intensity or small excitation time, the deep levels are more completely filled, and with high intensity or excitation time the shallow levels are more completely filled. In particular, the intensity and excitation time may be selected so that both groups of levels will be equally filled (Fig. 2, curve 5). Incomplete filling of the shallow levels under β-excitation could be caused by marked local initial heating in the region through which the β-particles move. However, such initial heating in ionic crystals of great thermal conductivity is not very likely. The absence of this influence is seen particularly in the fact that filling the levels depends materially on the density of β-radiation (Fig. 1, b, c, d and Fig. 3); moreover, the temperature within the region ought to have been the same, both for low densities of β-excitation and for high. (The excitation density which we used was in all cases negligible, and overlapping of the excitation regions could hardly have played any kind of appreciable role). In order to insure the appearance of low temperature peaks on the curve of temperature luminescence under photo-excitation, the intensity of photo-excitation was decreased 10^4 times as compared to the maximum intensity used earlier. Under these excitation conditions, the time dependence for filling the localization levels under photo-excitation was the same as when exciting the same sample with 5.7 mCu P^{32} (Fig. 3).

In this experiment the curves of temperature luminescence under photo- and β-excitation were recorded for equal excitation times. The curves obtained under excitation by β-particles and light $\lambda = 365$ mμ agreed very well, both in form and in the absolute value of the ordinates.

It was most interesting to compare the excitation densities of a phosphor under photo-excitation ($\lambda = 365$ mμ) and excitation by β-particles (of mean energy $\bar{E}_\beta = 0.7$ MeV). We evaluated the excitation density taking into account absorption of light and β-particles only on the surface layer. Evaluation of the excitation density of the surface layer of a phosphor under excitation by light of wavelength $\lambda = 365$ mμ and P^{32} β-particles of mean energy $\bar{E}_\beta = 0.7$ MeV was carried out in the following manner. In the case of maximum density of photo-excitation the excitation intensity (measured in absolute units by a thermocolumn calibrated according to energy by a Hefner lamp) was $E_{\lambda max} = 30$ μwatt cm^{-2}. When the curves of temperature luminescence excited by light and P^{32} β-particles coincided, the intensity of photo-excitation was $E_\lambda = 10^{-4} E_{\lambda max} = 3 \cdot 10^{-3}$ μW/cm^2 = $= 2 \cdot 10^{10}$ eV/cm^2·sec. According to the data of Galanin and Raevskii [2], the absorption coefficient for ZnS-Ag ($1 \cdot 10^{-4}$ g/g) at $\lambda = 365$ mμ equals $k = 500$ cm^{-1}. Hence it follows that the density of the energy absorbed in the surface layer of phosphor per second under photo-excitation is $\varepsilon_\lambda = k \cdot E_\lambda = 1 \cdot 10^{13}$ eV/cm^3·sec.

In β-excitation the density (σ) of electron current across the surface of phosphor was calculated according to the formula

$$\sigma = \frac{\sigma_1}{4\pi d^2},$$

where σ_1 is the number of electrons emitted by the β-particle source per second, and d is the distance from the source to the phosphor ($d = 4$ cm). The strength of the source (5.7 mCu) which we used gives the value $\sigma_1 = 2.1 \cdot 10^8$ electrons/sec. Thus $\sigma = \approx 1 \cdot 10^6$ electrons/cm^2 · sec.

The density of the energy absorbed in the surface layer of the phosphor equals $\varepsilon_\beta = \sigma \left(\frac{dE}{dl}\right)_0$, where $\left(\frac{dE}{dl}\right)_0$ is the energy loss by β-particles, which have the mean energy for P^{32}, $\bar{E}_\beta = 0.7$ MeV, per unit path length at the beginning of the run in ZnS. (We disregard the diffuseness of the energies of the β-particles with $E = 0.5$ MeV in aluminum [3] on the assumption that there is little change in the form of this curve when applied to a β-particle with energy $\bar{E}_\beta = 0.7$ MeV in ZnS-Ag phosphor. After introducing correction factors to account for the difference of the 0.5 MeV from the $\bar{E}_\beta = 0.7$ MeV of

the particles which we used, and the difference of the lengths of the maximum runs of β-particles in Al and ZnS, it was found, approximately

$$\left(\frac{dE}{dl}\right)_0 \approx 16 \frac{\text{MeV}}{\text{cm} \cdot \text{electron}}.$$

Substituting this value in the formula for E_β gives the following density of β-particle energy absorbed in the surface layer of phosphor per second, which is very close to the value ϵ_λ:

$$E_\beta = 1.6 \cdot 10^{13} \text{ eV/cm}^3 \cdot \text{sec}.$$

We recall that the adduced values E_λ and E_β are in the nature of highly approximate estimates. They show that in the case of matching curves of temperature luminescence, the effective density of β-particle excitation is, according to order of magnitude, the same as under photo-excitation, i.e., an approximately equal amount of energy is used to produce one electron-hole pair in both β-particle excitation and in photon excitation.

In addition to the temperature luminescence curves, the same apparatus was used to measure the curves of temperature quenching under photo- and β-excitation (Fig. 4). These curves were recorded under continuous excitation. As before, light of $\lambda = 365$ mμ was used in photo-excitation, and a P^{32} preparation with an activity of 30 mCu was used in β-excitation. In the case of photo-excitation the curves of temperature quenching were recorded for excitation intensities from 3 to 0.003 μwatt/cm^2. As in reference [2], we observed that temperature quenching begins earlier at low excitation intensities

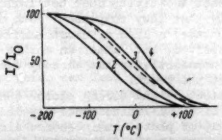

Figure 4. Temperature quenching curves of ZnS-Ag luminophor under excitation by light λ = = 365 mμ (solid lines) and P^{32} mCu β-particles (broken line). Intensity of incident light (in μwatt/cm^2): 1) 0.003, 2) 0.03, 3) 0.3, 4) 3.

The temperature quenching curve recorded when exciting the same ZnS-Ag phosphor sample by β-particles (the dotted line on Fig. 4) almost matches the quenching curve for photo-excitation at an excitation intensity of 0.3 μwatt/cm^2. However, we did not succeed in completely matching the curves by means of selection of photo-excitation intensity.

A certain difference in the appearance of the temperature quenching curves and the thermoluminescence curves with regard to their dependence on the nature of the excitation is entirely natural, since the temperature quenching is observed in excited phosphors. Experiments with thermoluminescence curves relate only to the stored light sums.

The results of our research show that the nature of filling the localization levels, and to a considerable extent the shape of the temperature quenching curves observed when exciting ZnS-Ag luminophor by β-particles, are connected with small excitation intensities. At the same time, there are no qualitative differences in the nature of filling the localization levels under β-excitation and under weak photo excitation.

The authors are grateful to M. D. Galanin for his interest in the present work.

September 2, 1958

References

1. G. F. J. GARLICK, A. F. GIBSON: Proc. Phys. Soc., B60, 574, (1948)
2. M. D. GALANIN, A. V. RAEVSKII: Report of the VII All-Union Conference on Luminescence, Moscow, 1958
3. L. V. SPENCER: Phys. Rev., 98, 1597, (1955)

TOM VII, Vyp. 2 OPTIKA I SPEKTROSKOPIIA Avgust, 1959
VOL. VII, No. 2 OPTICS AND SPECTROSCOPY August, 1959

On the Simultaneous Effect of Photo and Electroexcitation on Electroluminophors

L. N. VINOKUROV AND M. V. FOK

In previous papers [1, 2] we have principally studied the effect of applying photo- and electro-excitation successively to an electro-luminophor. It was shown that the light sum stored in an electro-luminophor influences the brightness of its electro-luminescence: it can be both increased and decreased, independently of whether the light sum is produced by means of electro- or photo- excitation. In view of this, it is of interest to study the simultaneous effect of photo- and electro- excitation on electro-luminophors.

It appears that photo- and electro- excitation are nonadditive: in some cases the brightness of luminescence for combined excitation is larger than the sum of the brightnesses of the two kinds of luminescence (positive nonadditivity), but in others it is less (negative nonadditivity). By changing the excitation condition, it is possible to pass from positive nonadditivity to negative, and vice versa. For some definite relation between the photo- and electro- excitation we can get exact additivity. The logarithms of the brightness of the photo- luminescence and of the corresponding electro-luminescence are shown on the coordinate axes. Each point of the coordinate plane will then correspond to some combination of the conditions of the over-all excitation. With the symbols + and −, signifying positive and negative nonadditivity, the coordinate plane is then divided into regions of positive and negative nonadditivity, and the boundary between them will correspond to exact additivity.

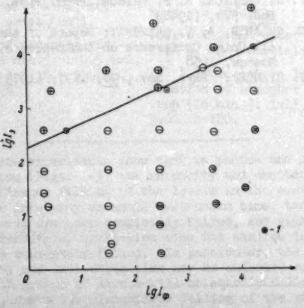

Figure 1. Nonadditivity of photo- and electro-excitation of Phosphor No. 1. (Nonlinear, nonstorage). Symbol 1 denotes exact additivity.

Figures 1 and 2 present the data for two electroluminophors ZnS-Cu, Al. The largest degree of nonadditivity we found was ≈ 10%. Phosphor No. 1 at room temperature stores a small light sum under electro- excitation. The brightness of its photo-luminescence depends nonlinearly on the intensity E of light excitation: it is proportional to $E^{3/2}$ which indicates a strong extrinsic saturation. Phosphor No. 2, on the other hand, stores considerable light sum under electro- excitation, and the brightness of its photo- luminescence is almost exactly proportional to the intensity of the light excitation, so that the extrinsic saturation of the phosphor is small.* As we see from the figures, the lines of exact additivity for these phosphors are completely different. Thus, it is impossible to separate phosphors according to the sign of their nonadditivity because the latter depends on the condition of excitation; moreover the behavior of the lines of exact additivity are closely related to the intrinsic properties of the phosphor, in particular to its mechanism of storing the light sum under electroexcitation and to the presence of extrinsic saturation.

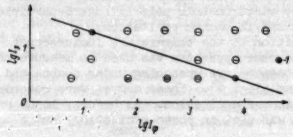

Figure 2. Nonadditivity of photo- and electro-excitation of phosphor No. 2. (linear, storage). The symbol 1 designates exact additivity.

It should be noted that processes leading to this or some other type of nonadditivity apparently coexist, and exact additivity does not indicate their absence but only that they compensate each other. In the opposite case, a line of exact additivity would not be observed, but rather an entire region where positive nonadditivity has already ceased and negative has not yet begun.

For weak electro- and strong photo- excitation the brightness of total luminescence appears even smaller than that of photo- luminescence alone (the corresponding points in the figures are denoted by two minus signs). That is, the electric field can decrease the brightness of photo- luminescence. This may come about, for example, because the extrinsic saturation may be strengthened due to acceleration of free electrons and holes by the electric field. Indeed, an increase in the electron energy decreases the probability of their localization and recombination, but according to Sui Sui-Yun [3], the probability of recombination decreases faster than the probability of localization. In reference [4] we showed that the brightness of luminescence under conditions of extrinsic saturation can be expressed in terms of the intensity of excitation and parameters characteristic of the phosphor as follows:

$$I_\phi = \frac{\alpha_\phi L}{L + Q} + \frac{\alpha_\phi}{v_1 (L + Q)^{3/2}} \frac{^{3/2} QL}{}, \quad (1)$$

* This phosphor and similar ones were considered in references [1] and [2].

where α_ϕ is the number of acts of ionization of centers of luminescence per unit volume per unit time, proportional to the intensity of light excitation, $L = \frac{\beta w_1}{\delta_1}$, $Q = \frac{\beta_1 w}{\delta_1}$, β and β_1 are proportional to the recombination probabilities of free electrons and free holes, respectively; δ_1 and δ to their probabilities of localization, and w_1 and w to their probabilities of dissociation. The subscript 1 signifies that the corresponding process does not take place at the luminescence centers but at the electron capture levels. All probabilities are normalized to unit time.

As shown in reference [3], the ratio $\frac{\beta}{\delta_1}$, at room temperature is 1 - 2 orders of magnitude for high energy electrons than for thermal electrons. If we suppose that for holes the corresponding ratio $\frac{\beta_1}{\delta}$ decreases in the same way, then the intensity of photo- luminescence under the action of an electric field is expressed by the formula

$$I = \frac{\alpha_\phi L}{L+Q} + \frac{\alpha_\phi^{3/2} QL\sqrt{M}}{w_1 (L+Q)^{3/2}}, \tag{2}$$

where all quantities retain their previous significance, and $\frac{1}{M}$ indicates by how much the ratios $\frac{\beta}{\delta_1}$, and $\frac{\beta_1}{\delta}$ are changed under the influence of the electric field, ($M < 1$). It is evident that if the second term of Eq. (1) plays an appreciable role, then the brightness of photo- luminescence must decrease with the connection of an electric field. However, Eq. (2) does not take into account the fact that the electric field itself creates some excitation which can lead to positive nonadditivity under conditions of extrinsic saturation. To account for this, it is necessary to replace α_ϕ by $\alpha_\phi + \alpha_e$, in Eq. (2) where α_e is the number of ionization acts of luminescent centers per unit volume per unit time caused by the electric field. In the calculations discussed, we consider that this does not depend on α_ϕ.

$$I_{\phi+e} = \frac{(\alpha_\phi + \alpha_e) L}{L+Q} + \frac{(\alpha_\phi + \alpha_e)^{3/2} QL\sqrt{M}}{w_1 (L+Q)^{3/2}} \tag{3}$$

now must not be compared with Eq. (1) but with the expression

$$I_\phi + I_e = \frac{\alpha_\phi L}{L+Q} + \frac{\alpha_\phi^{3/2} QL}{w_1 (L+Q)^{3/2}} + \frac{\alpha_e L}{L+Q} + \frac{\alpha_e^{3/2} QL\sqrt{M}}{w_1 (L+Q)^{3/2}}, \tag{4}$$

which also takes into account the intensity of electro- luminescence.

The condition for exact additivity, i. e., $I_{\phi+e} = I_\phi + I_e$ is compliance with the equality

$$\left(1 + \frac{\alpha_e}{\alpha_\phi}\right)^{3/2} = \frac{1}{\sqrt{M}} + \left(\frac{\alpha_e}{\alpha_\phi}\right)^{3/2}. \tag{5}$$

The solution of this equation is of the form

$$\frac{\alpha_e}{\alpha_\phi} = \text{const}.$$

This does not mean that $\frac{I_e}{I_\phi} = \text{const}.$, because I_ϕ and I_e depend on α_ϕ and α_e according to a complex law. The constant ratio $\frac{\alpha_e}{\alpha_\phi}$ for exact additivity only indicates the simultaneous growth of I_e and I_ϕ. with additivity preserved, as is represented in figure 1. Thus nonadditivity of photo- and electro- excitation of phosphor No. 1 is precisely explained by the causes considered.

There still exists a whole series of processes capable of producing nonadditivity. They are related inasmuch as α_e depends on α_ϕ, or more correctly, on the light sum stored in the phosphor. The nature of this dependence, and also of experiments proving its existence, are examined in references [1,2,5]. To present quantitative calculations here is yet difficult. It is possible that the nonadditivity of photo- and electro- excitation in phosphor No. 2 may be explained basically by these latter reasons, and likewise why the lines of exact additivity behave differently for it.

October 13, 1958

References

1. E. E. BUKKE, L. A. VINOKUROV, M. V. FOK: OiS, 5, 172, (1958)
2. E. E. BUKKE, L. A. VINOKUROV, M. V. FOK: Inzh.-Fiz. Zh., 1, 113, (1958)
3. SUI SUI-YUN: DAN USSR, 106, 818, (1956)
4. L. A. VINOKUROV, M. V. FOK: OiS, 1, 248, (1956)
5. V. V. ANTONOV-ROMANOVSKII: OiS, 6, 229, (1959)

(See 6 pp)

TOM VII, Vyp. 2 OPTIKA I SPEKTROSKOPIIA Avgust, 1959
VOL. VII, No. 2 OPTICS AND SPECTROSCOPY August, 1959

Infrared Absorption of Thin Films of Tin Dioxide

V. K. MILOSLAVSKII

Abstract: The optical and electrical properties of thin films of tin dioxide have been investigated. Transmission and absorption in the 1-18μ range were measured, as well as the temperature dependence of these quantities between -150° and +200° C. The effects of various impurities were studied.

A method has recently been developed for preparing highly conductive transparent films of tin dioxide on glass surfaces [1, 2]. Similar films are used in various technical applications. Their electrical and optical properties, however, have been studied very little. What draws attention to this material is its rare combination of high transmittance over the entire visible and near infrared with high electrical conductivity (specific conductivity $\sigma = 10^2 - 10^3$ ohm^{-1} cm^{-1}), and high density of conduction electrons (density $N = 10^{19} - 10^{20}$ cm^{-3}). This paper is devoted to a study of the optical and electrical properties of thin films of tin dioxide.

Thin films of SnO_2 were obtained by pyrolytic decomposition of vapors of tin chlorides ($SnCl_2$, $SnCl_4$) on the surface of glass heated to a high temperature (500 - 600°). By dissolving the chlorides in different media, we obtained films of different conductivities. The films prepared by spraying anhydrous $SnCl_2$ and $SnCl_4$ or alcohol solutions of these compounds possessed the highest conductivities; films prepared from 50% aqueous solutions of $SnCl_4$ (σ = 10-50 ohm^{-1} cm^{-1}) had lower conductivity. Thickness of the films was controlled by observing interference patterns. Transparent films were obtained having 5-7 interference orders, with low resistivity ($R \sim 100$ ohm/cm^2). Transparent films of greater thickness could not be obtained successfully because scattering increased with increasing film thickness. The index of refraction of the films was determined by the interferometric method [3]. The observed index of refraction was $n = 1.98 \pm 0.02$ for $\lambda = 5900$ Å, which is close to $n = 1.999$ found on a natural monocrystal of tin dioxide. The high conductivity of the films is caused by a high concentration of impurity introduced in the chosen method of preparation, and also by the low energy of ionization of the impurity centers. For this reason an additional absorption caused by impurities should be observed in the infrared region of the spectrum.

Absorption was studied in films deposited on thin plane-parallel plates of rock salt cut from a monocrystal. At the same time that the sample was being made from rock salt, a film for measuring electrical conductivity was deposited on glass. It was established that the conducting properties of the films do not depend on the nature of the substrate. Measurement of transmission was made using an IKS-2 infrared recording spectrophotometer in the 1-18μ wavelength range.

In the long wavelength region a correction was applied for light scattered within the instrument.

Two absorption bands were observed on all the films obtained by the above described method (see Fig. 1)† a narrow band with a maximum at 16.4μ and a wide band whose maximum is somewhat indeterminate (8.5-9μ). Both absorption bands increase with increasing conductivity of the samples. It is seen from figure 1 that in the films with low conductivity, the narrow, long wavelength band is more intense. With increasing conductivity, the absorption at the maximum of the short-wave length band becomes comparable to the long-wave length absorption. Widening and overlapping of absorption bands is also observed on films of high conductivity. Samples of SnO_2 obtained by oxidizing thin films of tin deposited by vaporization in vacuum, have a considerably lower conductivity ($\sigma \approx 1$ ohm^{-1} cm^{-1}) and are transparent throughout the measurable range of the spectrum. The appearance of new absorption bands of the samples of SnO_2 obtained from the pyrolitic decomposition of chlorides is related, apparently, to introduction of a large number of impurity atoms at the time of preparation of the film. This very impurity is what changes the electrical properties.

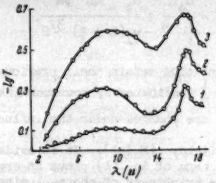

Figure 1. Conductivity (in ohm^{-1} cm^{-1}): 1 - 15, 2 - $1.2 \cdot 10^2$, 3 - $6 \cdot 10^2$. Film thickness (in μ): 1 - 0.35, 2 - 0.35, 3 - 0.3.

In order to determine the nature of impurity bands, the temperature dependence of absorption in the infrared region and electrical conductivity were measured. Measurements at low temperatures (-150°C) were made using a simple cryostat intended for use with liquid air. The samples were mounted on a copper pin of the inner cylinder having a rectangular cutout for passage of the beam. The space between the inner and outer cylinders was pumped down to 10^{-4} mm. The outer windows of the cryostat were fitted with panes of rock salt. The temperature of the outer windows was brought up to room temperature by using an electric heater, which prevented the condensation of moisture. The temperature of the sample was measured with a thermocouple. For measurements at 200° C, the sample was placed in a cylindrical oven with windows for passage of the beam.

Measurement of transmission was made on films having sufficient electrical conductivity (σ approximately 50-100 ohm^{-1} cm-1) and absorption. Figure 2 shows -lg T as a function of photon energy hν, at various temperatures, for one of the samples. A considerable increase is observed in the coefficient of absorption of the two bands as the temperature decreases. The long wave-length band increases faster than the short wave-length one. A decrease in the half-width of the absorption bands from 0.03 to 0.15 eV is noticed as the temperature is

decreased from +217 to -141°, while the maximum of absorption shifts by 0.005 eV toward short wavelengths. A similar temperature dependence of absorption bands was observed in alkali-halide crystals containing an excess of alkaline metal [4]. These absorption bands must therefore be attributed to electron transitions from the ground state of the impurity center to higher energy levels. The long wave-length band, with its maximum at 0.075 eV at room temperature, corresponds, apparently, to a transition of an impurity atom to an excited energy state, while the short-wave length broad band corresponds to a transition to a conduction band. This fact is indicated by the asymmetrical shape of the absorption band: a slow drop in absorption in the high energy range and a sharper drop in the long wavelength range. Asymmetrical bands of similar shape were observed for p-type silicon containing elements of group III, [5], and for cadmium oxide with an excess of cadmium [6]. The increase of these bands as the temperature decreases is caused by an increase in the degree of occupancy by electrons in the ground state. An increase of absorption in the long wave length band may also be related to its temperature narrowing.

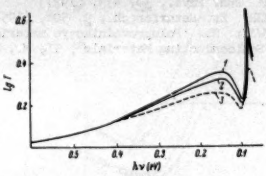

Figure 2. Temperature (in °C.) 1 (-141), 2 - +17, 3 - +217.

In order to measure the temperature dependence of electrical conductivity, contacts made of a liquid alloy of indium and gallium were deposited on the samples made on glass, to which platinum electrodes were clamped. The measurements were made from -150 to +300°. Above +350° C, the resistance of the films changes (increases) irreversibly which limits the range of temperature measurements. The measurements show that the temperature dependence of samples with σ of the order of 10-100 ohm^{-1} cm^{-1} does not follow the usual exponential law. Two ranges of temperatures can be distinguished below +150°, the resistance varies little over a wide range, having a small negative temperature coefficient. Above +150°, the resistance drops sharply with increasing temperature, following an exponential law. Since the semiconductor has a wide forbidden band (approximately 3.5 eV according to optical measurements in ultraviolet range of the spectrum), all of the conductance in the temperature range under investigation can be attributed to impurities. Such a temperature dependence points up the presence of a narrow impurity band, which appears as a result of overlapping of wave functions of neighboring impurity atoms. The widening of absorption bands (Fig. 1, curve 3) as the concentration of impurity is increased also speaks for the formation of impurity bands. By measuring temperature dependence above +150°, one can determine the location of impurity band with respect to the lower limit of the principal conduction band of a semiconductor. It is seen from the curve of $\ln(\sigma T^{\frac{3}{4}})$ vs. $1/T$ (Fig.3) that above +150°, the experimental points form a straight line. The calculated energy of ionization (0.12 eV) is close to the optical value (0.15 eV), which was found from the maximum of the shortwave band corresponding to a transition to a continuous spectrum.

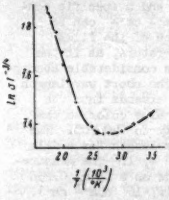

Figure 3

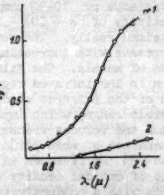

Figure 4. Conductivity (in ohm^{-1} cm^{-1}): 1- $17 \cdot 10^3$, 2- $6 \cdot 10^2$. Film thickness (in μ): 1- 0.25, 2- 0.3.

The nature of the impurity centers in thin films of tin dioxide is still not clear. The assumption that impurity centers arise as a result of chemical interaction between the heated glass substrate and the vapors of stannic chloride [7], does not bear up under examination since the conductivity of the films is the same for different substrate (glass, quartz, mica, rock salt). It is more natural to think that as a result of preparation of the film a certain excess of tin atoms is formed, which excess is also responsible for the conductivity of SnO_2 [8]. Films of tin dioxide can be prepared by oxidizing thin films of tin at +400-600°. These have a lower conductivity ($\sigma < 1$ ohm^{-1} cm^{-1}) than pyrolytically obtained films. The concentration of electrons is also lower by two orders of magnitude ($N < 10^{18}$ cm^{-3}) [9]. Baking oxidized films in vacuum (10^{-4} mm) increases their conductivity ($\sigma \approx 30$ ohm^{-1} cm^{-1}), however, the values typical for films prepared pyrolytically are not reached. Thus, one can assume that for the cited method of preparation, an additional impurity is introduced [10], which considerably increases the conductivity of the films and the carrier concentration. Additional impurity of chloride ions can occur if the pyrolysis of stannic chloride vapors is not complete. In the film being formed, some oxygen ions can be replaced by chloride ions, which have a charge greater by one. This leads to the formation of donor levels, lying close to the conduction band, i. e., to electronic conduction. At impurity concentration greater than 10^{19} cm^{-3}, donor levels apparently blend into the impurity band. The irreversible decrease of the resistance of the films during baking at temperatures above +350° may be caused by the removal of excess Cl and subsequent oxidation of the film.

The electrical conductivity of SnO_2 films can be increased considerably by introducing antimony ions into the crystal lattice [11]. Antimony ions, by replacing tin ions, form additional impurity levels in the forbidden band of the semiconductor. Since the charge of an antimony ion is greater by one than the charge of a tin ion, the position of the antimony level, just as in the case of chloride ions

replacing oxygen, must be close to the conduction band. Films of SnO_2 containing Sb are obtained by spraying $SnCl_4$ containing a small amount (several %) of $SbCl_3$. Increasing the concentration of $SbCl_3$ increases both the electrical conductivity and the absorption of the films obtained. Films with a resistance of 10-30 ohm cm^{-2} and a specific conductivity of $\sigma \approx 10^3 - 10^4$ ohm^{-1} cm^{-1} can be obtained easily. The resistance of the films increases with increasing temperature, as in the case of metals. The films have considerable absorption in the infrared region. The short wavelength end of the infrared absorption extends into the visible range, which imparts a blue color to the films and reduces transmissivity to 50-70%. The dependence of absorption on wavelength for a film with 1% Sb is shown in figure 4, 1. The measurement of optical density was made on a film 0.25μ thick with a conductivity of $1.7 \cdot 10^3$ ohm^{-1} cm^{-1}. The absorption observed was apparently due to free electrons. This is indicated by the quantity -lg T and the monotonic rise of absorption with increasing wavelength. The absorption of a tin dioxide sample without antimony having the highest conductivity ($\sigma = 6.10^2$ ohm^{-1} cm^{-1}, t = 0.3 μ, curve 2 in Fig.4) is an order of magnitude smaller in the same range of wavelengths.

In conclusion the author expresses his gratitude to K. D. Sinel'nikov for suggesting the topic, I. N. Shkliarevskii and N. A. Vlasenko for discussing the work, and D. Smelov for helping to carry out the experiment.

November 11, 1958

References

1. V. A. RIABOV, O. V. VOROB'EVA, A. S. EGOROVA: Steklo. Inform. Biull. VNIIS, 1, 1957.
2. A. IA. KUZNETSOV, A. V. KRUGLOVA, B.F.KYRZHANOVSKII: ZL, (8), (1956)
3. I. N. SHKLIAREVSKII, V.K.MILOSLAVSKII: ZTF, 24, 1387, (1954)
4. N. MOTT, R. GURNEY: Electronic processes in ionic crystals, Clarendon Press, Oxford, 1940, (IL, Moscow, 1950)
5. E. BURSTEIN, E. E. BELL, J. W. DAVISSON, M. LAX: J. Phys. Chem., 57, 849, (1953)
6. V. K. MILOSLAVSKII: OIS, 3, 251, (1957)
7. R. GOMER: Rev.Sci.Instru., 24, 993, (1953)
8. B. P. KRYZHANOVSKII: ZTF, 28, 1489, (1958) (See Sov. Phys Tech Phys)
9. G. BAUER: Ann. Phys., 30, 433, (1937)
10. A. FISHER: Zs. Naturforsch., 9, 508, (1954)
11. E. FAIRWAY: Sb. 'Poluprovodnikovye materialy'. "Semiconducting Materials", IL, M., 1954.

TOM VII, Vyp. 2 OPTIKA I SPEKTROSKOPIIA Avgust, 1959
VOL. VII, No. 2 OPTICS AND SPECTROSCOPY August, 1959

BRIEF REPORTS

On the Role of the Angle of Light Incidence in Observation of the Ultraviolet Minimum of Silver Reflectance

G. P. SKORNIAKOV AND I. I. SASOVSKAIA

One of the singular features of metals is the dependence of their optical parameters on the angle of incidence. This is stated by Ketelaar's [1] formulas, and is confirmed by experiment [2].

In the light of these features it is of interest to trace the angular dependence of silver reflectance in the region of the ultraviolet minimum, where reflection attains a value characteristic of dielectrics. Here, we may expect a change in the amount of reflection in the region of the minimum, but it is difficult to predetermine the tendency of the points of the minimum to shift on the wavelength scale.

The experimental results are given below. The figure shows the curves described by the reflectance coefficient R in the region from 3000 Å to 3400 Å with various angles of light incidence on a massive sample of silver.

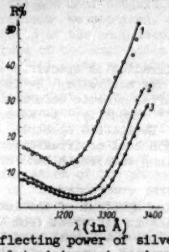

Reflecting power of silver in the region of the ultraviolet minimum at various angles of light incidence.

1- 65°, 2- 45°, 3- 25°. Positions of the minima correspond to 3200, 3217, and 3225 Å

The experimental results show that as the angle of incidence increases, there is a progressive shift toward shorter wavelengths in the region of the reflectance minimum, and at the same time the amount of reflection increases.

In an attempt to explain the observed phenomena, we must consider the available data on the optical properties of silver in the region of the reflectance minimum. Existing experiments indicate that the region of the minimum shifts toward shorter wavelengths when the silver contains impurities [3], when it is cooled [4], and when it is polished*. On the other hand, the point of the minimum moves toward the longer wavelengths upon heating [6] and upon relaxation of the surface.

These facts are adequately explained from the viewpoint of perturbations which are set up in the lattice of the metal and which produce changes in the energy spectrum of the electrons.

In addition to the above, we must take into consideration the characteristics of the surface layer of the metal, and its difference from the deep layers in structure and chemical composition. Firstly, a significant part of the optically active layer involved in reflection is deformed as a result of preliminary treatment of the surface, and secondly, part of its thickness consists of passivating films and adsorbed vapors and gases. The existence of chemical nonuniformity and structural disparity between the surface and the bulk metal below it, is undoubtedly a disturbing factor as regards the lattice of the bulk metal.

Bearing these ideas in mind, and considering that the light wave penetrates the field less deeply as the angle of incidence increases, it is possible to explain the experimental results described above.

The shift of the region of reflectance minimum toward shorter wavelengths when the angle of incidence is increased is apparently due to the fact that layers with various degrees of deformation of the crystal lattice are involved in reflection. Inasmuch as deformation of the lattice increases near the surface, it is natural that the greatest shift of the point of reflectance minimum is observed for large angles of incidence, when the path of the light wave in the surface layer of the metal is increased.

In conclusion the authors thank A. V. Sokolov for discussion of the work.

November 26, 1958

*The latter statement concerning the influence of polishing on the position of the reflectance minimum for silver is based on the results of many of our observations carried out both on silver and on its alloys, but it contradicts Ref. [5], in which a shift of the reflectance minimum toward the shorter wavelengths was observed after annealing a mechanically polished surface.

References

1. K. SHEFER: Theoretical Physics, 3, No. 2, GONTI NKTP, 1938
2. W. KÖNIG: Hand. d. Phys., 20, 209 (1928)
3. M. M. NOSKOV, G. P. SKORNIAKOV: IAN USSR FS, 14, (6), 754 (1950)
4. G. P. SKORNIAKOV, I. I. SASOVSKAIA: T. P. CHUKINA: Fiz. Sb. L'vovsk. Univ., 4, 505 (1958)
5. H. MARGENAU: Phys. Rev., 33, 1035 (1929)
6. G. GRAZ: Zs. Metalkunde, 45, (9), 538 (1954)

TOM VII, Vyp. 2 OPTIKA I SPEKTROSKOPIIA Avgust, 1959
VOL. VII, No. 2 OPTICS AND SPECTROSCOPY August, 1959

Centers of Luminescence in Alkali-Halide Phosphors With Large Concentrations of the Activator and Microdefects of the Host Lattice

T. ABDUSADYKOV

Centers of luminescence of alkali-halide phosphors with small concentrations of the activating ions Tl^+, In^+, Pb^{++}, and Sn^{++} have been investigated in a number of works. It has been shown that the spectra of activator absorption and irradiation correspond to an electron transition in the ions of the activator, interacting with the neighboring ions of the host substance [1-4].

A complication of the spectra of irradiation of phosphors, activated by thallium and lead during an increase in the concentration of the activator and mechanical breaking up of the crystals, which has been observed by the investigators [2, 5-10], has led to the hypothesis of the existence in alkali-halide phosphors of centers of luminescence of several types differing from each other in the character of the immediate surroundings of the ions of the activator.

Not only individual ions of the activator in regular sites of the crystalline lattice (Seitz-model), but also complexes of ions of the activator, and also complexes of ions of the activator and of point microdefects (cation and anion vacancies) and, possibly, linear (dislocations) microdefects of the host lattice, can serve as centers of luminescence, exactly as activator trapping centers do [11-13], in alkali-halide crystals.

It is evident that the number of such complex centers must increase with an increase in the concentration of activator, or with the introduction of bivalent Ca^{++} and Sr^{++} impurity ions (and, consequently, of an equivalent quantity of cation vacancies) or with plastic deformation of the crystal, leading to a "multiplication" of the dislocations and the generation of a large number of point microdefects.

The correctness of this hypothesis was verified experimentally on 17 phosphors on the basis of halide salts NaCl, KCl, NaBr, KBr, and NH_4Br, activated by the mercury-like ions In^+, Tl^+, Sn^{++}, and Pb^{++}.

The samples for investigation were prepared by the method of heating monocrystalline bases of the phosphors grown by the Chropolous method in vapors of the activating metals in evacuated glass ampoules at high temperature. Each phosphor was prepared with three different concentrations of activator of the host material, containing and not containing Ca^{++} or Sr^{++} impurity ions. In addition, samples were studied, which were plastically deformed 10 - 60%, via compression of the crystals under a hydraulic press. For all the samples, the spectra of absorption, excitation, and irradiation were investigated by the photoelectric method. All the necessary corrections have been introduced into the spectra presented below.

In figure 1, the data for the phosphor KBr-Tl are presented as an illustration of the effects being observed. As the figure shows, when the concentration of activator is increased, the intensity of the long wavelength band of the irradiation is considerably intensified. In phosphors, containing bivalent Ca^{++} or Sr^{++} impurity ions its intensity grows still more. Plastic deformation also leads to the redistribution of the intensity in favor of the long wavelength irradiation band.

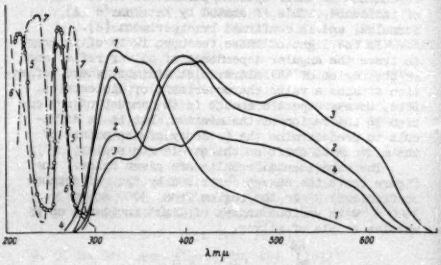

Figure 1. Irradiation spectra: 1- for a small concentration of the activator; 2- for a large concentration; 3- after plastic deformation; 4- phosphor containing a Sr^{++} impurity; 5- absorption spectrum of the phosphor. Excitation spectra: 6- for the KBr-Tl short wavelength band of irradiation with a λ_m=320 mμ; 7- for the long wavelength band of irradiation with λ_m=520 mμ.

The excitation spectrum of the long wavelength band of irradiation is different from the excitation spectrum of the short wavelength band, which dominates in phosphors with a small activator concentration and microdefects of the host lattice. If one takes account of the influence of the partial reabsorption of light in the phosphor, then one can draw the conclusion that the ultraviolet band and the visible band of irradiation have completely different excitation spectra. Analogous results have been obtained by us for NaCl-In (Fig. 2) and a whole series of other phosphors.

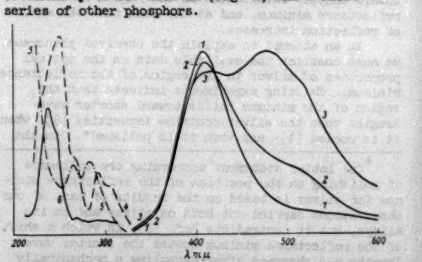

Figure 2. Irradiation spectra. 1- for a low concentration of the activator; 2- after 14% plastic deformation: 3- after 46% plastic deformation. Excitation spectra: 4- for the short wavelength irradiation band; 5- for the long wavelength irradiation band; 6- absorption spectrum of the NaCl-In phosphor.

It appears that in the phosphors we studied with a large concentration of activator and microdefects of the crystalline lattice, there exist at least two types of centers of luminescence*.

In the table are presented the positions of the excitation and irradiation bands of centers of the first type, characteristic for phosphors with a low concentration of activator and microdefects of the host lattice, and centers of the second type, arising in phosphors with a high concentration of microdefects.

It should be noted that the appearance of new centers strongly depends on the relation of the ionic radii of the activator and the cations of the host lattice of the phosphors. Second centers readily arise in all the thallium phosphors (NaCl-Tl, KCl-Tl, NaBr-Tl, KBr-Tl and NH_4Br-Tl) and in all phosphors with mercury-like activating ions on a base of sodium halide salts (NaCl-In, NaCl-Tl, NaCl-Pb, NaBr-In and NaBr-Tl), where the ionic radius of the activating ions is greater than the ionic radius of the cations of the host substance of the phosphors. In KCl and KBr with indium, tin, and lead, second centers are not manifest within the limits of the concentrations we attained, of the activator and of microdefects of the host lattice.

The structure of the excitation spectra (see Fig. 1 and Fig. 2) of centers of the first and second types are identical in general aspects, which is associated with the fact, that irradiation of the second centers corresponds to electron transitions in the ions of the activator. The fact that the centers of the second type are formed not only for a rise in the concentration of activator, but also for plastic deformation of the phosphors with low concentrations of the activator, permits one to advance the preliminary hypothesis, that centers of luminescence of the second type are complexes of ions of the activator and microdefects of the host lattice.

Maxima of the Excitation and Irradiation Bands of Centers of Luminescence of the First and Second Types (in mμ)

Phosphors	Centers of the first type			Centers of the second type		
	$\lambda^{exc.}_m$	$\lambda^{exc.}_m$	$\lambda^{irrad.}_m$	$\lambda^{exc.}_m$	$\lambda^{exc.}_m$	$\lambda^{irrad.}_m$
NaCl-Tl	199	255	291	235	267	~365
KCl-Tl	195	247	305	235	275	~380; ~485
NaBr-Tl	216	268	294;314	242	273	~430; ~490
KBr-Tl	210	261	317;364	238	275	~400; ~520
NH_4Br-Tl	224	258	395	242	282	~510
NaCl-In	239	294	410	265	284	~470
NaBr-In	252;259	302	420	259	320	~490
NaCl-Pb	193	273	320	245	290	~450

*As became known to us after the bulk of the experiments had been carried out, Butler [14] also came to a similar conclusion on the basis of investigations of thallium phosphors.

It should be noted that for ions of an activator with a radius greater than the radius of the cation of the host material (it is precisely such ions which yield, according to our data, centers of the second type), the formation of complex centers from an ion of the activator and microdefects of the host lattice, starting from the principle of compensation of volume [15], is energetically advantageous.

In work [16] the polarized luminescence of centers of the second type in KCl-Tl and NaCl-Ag was investigated. It was noted that complex centers in these phosphors are oriented in the cation-anion direction (for example, Tl → an anion vacancy). Analogous investigations need to be conducted with centers of luminescence of the second type in other phosphors also.

It has been made clear by our preliminary experiments with KCl-Tl and NaCl-In that the "topography" of the luminescence of crystal phosphors with centers of luminescence of the first and second types, observed under the MUF-2M ultraviolet microscope is different.

A more detailed exposition of the results obtained will be given in work [17].

The present work was carried out under the direction of F. D. Klement and Ch. B. Lushchik, to whom the author expresses his profound gratitude. The author also is sincerely grateful to L.A. Teiss for aid in conducting a portion of the experiments.

December 1, 1958

References

1. F. SEITZ: J. Chem Phys., 6, 150-162, (1938)
2. F. D. KLEMENT: Dissertation, Leningrad University, (1942)
3. F. E. WILLIAMS: J. Chem. Phys., 19, 457-466, (1951)
4. N. E. LUSHCHIK, CH. B. LUSHCHIK: Tr. IFA AN ESSR, No 6, 5-62, (1957)
5. O. V. FIALKOVSKAIA: Candidate's Dissertation, Leningrad University, 1944
6. P. PRINGSHEIM: Rev. Mod. Phys., 14, 132-138, (1942); J. of Phys., USSR, 10, 495-498, (1946) [in English]
7. J. H. SCHULMAN, R. J. GINTHER, C. C. KLICK: JOSA, 40, 854-862, (1950)
8. K. V. SHALIMOVA: Doctoral Dissertation, FIAN USSR (1952)
9. N. I. IVANOVA: Candidate's Dissertation, Leningrad University, 1952
10. F. D. KLEMENT, R. I. GINDINA: Tr. IFA AN ESSR No 4, 3-25, (1956) [in Russian]
11. J. H. SCHULMAN, R. J. GINTHER, C. C. KLICK, R. SL ALGER, R. A. LEVY: J. Appl.Phys., 22, 1479-1487, (1951)
12. M. K. KATS: DAN USSR, 85, 539-542, (1952)
13. CH. B. LUSHCHIK: Tr. IFA AN ESSR, No 3, 3-230,(1955)
14. K. H. BUTLER: J. Electrochemic.Soc., 103, No.9, 508-512, (1956)
15. F. A. KROGER, et al: Tr.Electrochem.Soc., 93, 156-171, (1948); Physica, 14, 488-488, (1948); 16, 297-316, (1950)
16. L. I. TARASOVA, P. P. FEOFILOV: OiS, 4, 696-697, (1958)
17. T. ABDUSADYKOV: Tr. IFA AN ESSR, No 10, (1959) [in press]

TOM VII, Vyp. 2 OPTIKA I SPEKTROSCOPIIA Avgust, 1959
VOL. VII, No. 2 OPTICS AND SPECTROSCOPY August, 1959

A Comparison of the Energy Levels of a Three-Dimensional and One-Dimensional Metallic Model of the Benzene Molecule

L. A. BOROVINSKII AND L. M. FEDOROVA

In the work of Ruedenberg and Scherr [1] a comparison was given of a three-dimensional and a one-dimensional metallic model of molecules composed of a straight conjugated chain of atoms. It was shown that for a rectangular potential well it is possible to separate the variables corresponding to longitudinal and transverse motion of the π-electrons with respect to the chain of conjugated bonds, i. e., the wave function is represented as a product of wave functions each of which depends only on one co-ordinate. It turns out to be possible to separate the total energy of a π-electron into longitudinal and transverse energies, corresponding to longitudinal and transverse motion. Thus the true absorption band corresponds to transitions between levels of the longitudinal motion, since the intervals between these levels are considerably smaller than the intervals between the levels for transverse motion. The energies of the π-electrons, calculated according to the one-dimensional model, correspond to the energy of longitudinal motion in the three-dimensional model.

The conclusions of reference [1] cannot be applied directly to cyclic molecules. For those forms of the potential well which it is natural to choose for the cyclic model, it is, strictly speaking, impossible to separate out the energy of longitudinal motion from the total energy of the π-electron. The separation of energies is possible only approximately under certain assumptions.

In the present paper a comparision is given of the three-dimensional and one-dimensional models of the benzene molecule; also the assumptions are given under which it is possible to separate the energy of longitudinal motion from the total energy of the π-electron, as well as the conditions for passing from the three-dimensional to the one-dimensional model. Furthermore, the error in the calculation of the energy levels associated with these assumptions is estimated.

As a model of the benzene molecule we take a three-dimensional potential well having the form of a right cylinder of height H and having a base in the form of an annulus bounded by circles of radius R_1 and R_2. We put

$$R = \frac{R_1 + R_2}{2} = \frac{6a}{2\pi},$$

where a is the length of the C-C bond. We write

$$l = R_2 - R_1.$$

We take the potential inside the potential well to be zero, and the potential outside the well to be infinite. As the unit of energy we take the quantitity

$$E_c = \frac{\hbar^2}{2mR^2} = 2.17 \text{ eV}$$

Then in cylindrical co-ordinates the Schrödinger equation has the form:

$$(1) \qquad \frac{1}{\rho}\frac{\partial}{\partial\rho}\left(\rho\frac{\partial\Psi}{\partial\rho}\right) + \frac{1}{\rho^2}\frac{\partial^2\Psi}{\partial\varphi^2} + \frac{\partial^2\Psi}{\partial z^2} = -\frac{E}{R^2}\Psi.$$

The functions Ψ must be single-valued and equal to zero at the boundaries of the potential well. For the potential well chosen equation (1) may be easily solved by separation of variables. We put

$$(2) \qquad \Psi(\rho, \varphi, z) = F(\rho, \varphi)\, Z(z).$$

The functions $F(\rho, \varphi)$ and $Z(z)$ satisfy the equations

$$(3) \qquad \frac{1}{\rho}\frac{\partial}{\partial\rho}\left(\rho\frac{\partial F}{\partial\rho}\right) + \frac{1}{\rho^2}\frac{\partial^2 F}{\partial\varphi^2} = -\frac{W}{R^2}F,$$

$$(4) \qquad \frac{\partial^2 Z}{\partial z^2} = -\frac{E^{(z)}}{R^2}Z(z),$$

with

$$W + E^{(z)} = E.$$

Solving equation (4) and using the boundary conditions, we find the following eigenvalues $E^{(z)}$:

$$(5) \qquad E^{(z)} = \frac{\pi^2\hbar^2}{H^2}\nu^2.$$

Equation (3) may be solved by separating the variables ρ and φ. If we assume $l \ll R$, then within the boundaries of the well ρ varies only between narrow limits, and we may replace the term

$$\frac{1}{\rho^2}\frac{\partial^2 F}{\partial\varphi^2} \text{ in equation (3) by } \frac{1}{R^2}\frac{\partial^2 F}{\partial\varphi^2}.$$

With this substitution, the energy W separates into terms corresponding to radial and azimuthal motion of the electron

$$(6) \qquad W = E^{(\rho)} + E^{(\varphi)}.$$

Putting

$$F(\rho, \varphi) = \Phi(\varphi)\, Q(\rho),$$

and after making the indicated substitution and separating variables we find the following equations for the determination of $\Phi(\varphi)$ and $Q(\rho)$:

$$(7) \qquad \frac{d^2\Phi}{d\varphi^2} + E^{(\varphi)}\Phi = 0,$$

$$(8) \qquad \frac{1}{\rho}\frac{d}{d\rho}\left(\rho\frac{dQ}{d\rho}\right) + \frac{E^{(\rho)}}{R^2}Q = 0.$$

Equation (7) corresponds to the Schrödinger equation in the one-dimensional model. From this equation and the requirement of periodicity on the function Φ we find the eigenvalues $E_k^{(\varphi)}$ and the eigenfunctions Φ_k:

(9) $$E_k^{(\varphi)} = k^2; \quad (k = 0, \pm 1, \pm 2\ldots),$$

(10) $$\Phi_k(\varphi) = A_{1k} \cos k\varphi + A_{2k} \sin k\varphi.$$

The solutions of equation (8) have the form:

(11) $$Q(\rho) = B_1 I_o\left(\frac{\rho}{R}\sqrt{E^{(\rho)}}\right) + B_2 Y_o\left(\frac{\rho}{R}\sqrt{E^{(\rho)}}\right),$$

where I_o and Y_o are the Bessel and Neumann Functions of zero order.

The boundary conditions

(12) $$Q(\rho)\big|_{\rho = R \pm \frac{l}{2}} = 0$$

give a system of equations for B_1 and B_2. The conditions that there be a non-trivial solution of this system have the form

(13) $$I_o\left[\sqrt{E^{(\rho)}}\left(1 - \frac{l}{2R}\right)\right] \cdot Y_o\left[\sqrt{E^{(\rho)}}\left(1 + \frac{l}{2R}\right)\right] - I_o\left[\sqrt{E^{(\rho)}}\left(1 + \frac{l}{2R}\right)\right] \cdot Y_o\left[\sqrt{E^{(\rho)}}\left(1 - \frac{l}{2R}\right)\right] = 0.$$

From equations (13) we find the eigenvalues $E_n^{(\rho)}$ $(n = 1, 2, \ldots)$. For $l \ll R$, these values may be determined approximately from the formula

(14) $$E_n^{(\rho)} = \frac{\pi^2 R^2}{l^2} n^2.$$

According to (6) we have

(15) $$W_{n,k} = E_n^{(\rho)} + k^2.$$

The total energy of the electron is equal to

(16) $$E_{n,k,\nu} = \frac{\pi^2 R^2}{l^2} \nu^2 + E_n^{(\rho)} + k^2.$$

The magnitude of $E_n^{(\rho)}$ may be estimated roughly from formula (14). Since we assume that

$$\frac{\pi^2 R^2}{l^2} \gg 1$$

and

$$\frac{\pi^2 R^2}{l^2} \gg 1,$$

it follows that the low-lying levels of the π-electrons correspond to the values of the quantum numbers:* $\nu = 2$, $n = 1$, $k = 0$, ± 1, $\pm 2\ldots$ Thus the first two terms in the right member of (16) play the role of an additive constant.

If we do not make the indicated substitution in equation (3) but solve it in the form in which it is given, we arrive by an analogous method at the following equations for the determination of W:

(17) $$I_k\left[\sqrt{W}\left(1 - \frac{l}{2R}\right)\right] \cdot Y_k\left[\sqrt{W}\left(1 + \frac{l}{2R}\right)\right] - I_k\left[\sqrt{W}\left(1 + \frac{l}{2R}\right)\right] \cdot Y_k\left[\sqrt{W}\left(1 - \frac{l}{2R}\right)\right] = 0$$

$$(k = 0, 1, 2\ldots)$$

For $k = 0$, equation (17) corresponds to equation (13). The values of $W_{n,k}$ obtained by solving equation (17) may not be split up into terms corresponding to radial and azimuthal motions of the electron. Equations (17) were solved for values of l equal to 0.5R, R, 1.5R, 2R. In the last case, the ring bounded by the circles of radius R_1 and R_2 goes over into a circle of radius 2R, and the values of $W_{n,k}$ may be found from the equation

(18) $$I_k(2\sqrt{W}) = 0.$$

A reasonable order of magnitude estimate of l is R.

We are interested only in the first root of equation (17), corresponding to $n = 1$. The remaining roots of the equation give higher energy levels for the electron and are not of interest in explaining optical absorption. This corresponds to the so-called "principle of longitudinal excitation". In the table we give the values of W calculated for the indicated values of l from formula (15) (in the left part of each column) and from equation (17) (in the right half of each column).

Eigenvalues of the Energy of the π-Electron, W (in conditional units).

k \ l	0.5R		1 R		1.5 R		2 R	
0	39.25	39.25	9.61	9.61	4.06	4.06	1.45	1.45
±1	40.25	40.31	10.61	10.74	5.06	5.35	2.45	3.67
±2	43.25	43.32	13.61	13.89	8.06	8.52	5.45	6.59

The results of the calculations show that the energy levels calculated from equation (17) differ very little from the levels calculated from formulae (13) and (15). The corrections to the frequencies of the four fundamental transitions in benzene — from the occupied levels $k = \pm 1$ to the lowest empty levels $k = \pm 2$ — are no more than 5 - 6 %. (In the approximation considered the frequencies of these four transitions coincided). One may thus consider that deformation of the trajectory in which the π-electron moves has but little effect on the energy of the electron. This conclusion may be applied, clearly, not only to benzene but also to other cyclic molecules. Thus one may consider the one-dimensional model to describe the behaviour of the π-electron in cyclic molecules just as well as the models consisting

*The value $\nu = 1$ corresponds to wave functions which are symmetric with respect to the plane of the molecule. Since the plane of the molecule is the principal plane of the π-electron it is necessary to take $\nu = 2$.

of linear chains of conjugate bonds. However, the application of the one dimensional model to molecules containing branching chains of conjugate bonds leads in certain cases to contradictions and to clearly incorrect results. These limitations and the reasons for them have been considered in previous papers [2 - 4].

December 31, 1958

References

1. K. RUEDENBERG, C. W. SCHERR: J.Chem.Phys., 21, 1565, (1953)
2. L. A. BOROVINSKII: OIS, 4, 526, (1958)
3. L. A. BOROVINSKII: IAN, SSSR, SF, 22, 1019, (1958) (See CTT Bulletin)
4. L. A. BOROVINSKII: OIS, 6, p173 (1959)

TOM VII, Vyp. 2 OPTIKA I SPEKTROSKOPIIA Avgust, 1959
VOL. VII, No. 2 OPTICS AND SPECTROSCOPY August, 1959

The Use of Selective Radiation of Gas in Infrared Gas Analyzers

A. O. SALL' AND S. B. STANEVICH

The radiation source in infrared gas analyzers is usually a chrome-nickel spiral heated to a temperature of 700 - 800° C. The selectivity of these gas analyzers is ensured by the use of a selective optical-acoustic receiver [1]. However, in place of a radiation source with a continuous spectrum in the infrared region, one can use the selective radiation of a heated gas.

In Fig. 1a is presented the diagram of an optical-acoustic gas analyzer with selective sources of radiation, consisting of heated cylindrical chambers 1, equipped with a radiation-transparent window. The inner surface of the chamber is chromium-plated and polished. The chamber is filled with a gas, whose concentration is determined in the mixture being analyzed. The operating principle of the apparatus is as follows. The beams of radiation are interrupted in the same phase by the chopper 2 with a frequency of 6 cycles. The right beam passes through the gaseous mixture being analyzed, 3, where absorption of the radiation proceeds in conformity with the concentration of the component to be determined in the gaseous mixture being analyzed. The difference of the alternating pressures in the right and left radiation receiving cylinders, 5, is converted by the condenser microphone, 6, into an alternating voltage, which is magnified by the amplifier, 7, and fed to the recorder, 8. The basic constituent errors of the gas analyzer are determined in a first approximation according to the magnitude of the ratio F of the signal which arises when carbon dioxide is introduced into the working chamber to the signal which arises from the total flux [2]. In figure 2 are presented curves of the dependence of this ratio F on the concentration C of carbon dioxide in the mixture being analyzed. The curves were obtained by filling the selective sources with carbon dioxide (curve a) and a mixture of 8.4% CO_2 in nitrogen (curve b). The gas in the sources was heated to 860 C while the temperature of the surrounding medium was 20° C.

The use of selective sources in optical-acoustical gas analyzers permits one to improve their selectivity further. An increase of selectivity can be expected by the use of a selective source in infrared gas analyzers with nonselective receivers of radiation.

In figure 1b is presented a variant of a single beam gas analyzer which uses the radiation of the gaseous mixture being analyzed, in the heated chamber,

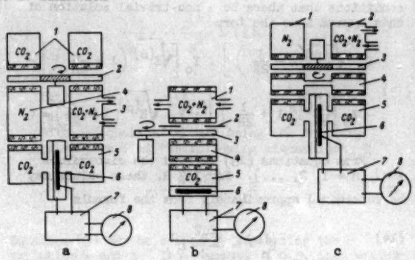

Figure 1

1. (The heating of the chamber is accomplished by a coil of nichrome wire.) To diminish the radiation of the working chamber in the direction of the radiation receiver, its rear wall is prepared from a material which is transparent to the radiation. The filter chamber, 4, filled with those components of the mixture which are not to be determined, serves to filter out their radiation. Between the working and filter chambers is fixed a diaphragm, 2, which is used so that the radiation of the side walls of the working chamber will not reach the receiver.

The diaphragm and the chopper, 3, have a temperature which is practically equal to the temperature of the radiation receiver. The radiation of the heated gaseous mixture being analyzed, interrupted by the chopper, gets into the radiation receiving cylinder, 5, of the optical-acoustical radiation receiver. The signal, developed by the microphone, 6, is intensified in the amplifier, 7, and is fed to the recorder, 8.

The radiation of the window and walls of the working chamber gets into the radiation receiver, as a consequence of which a signal arises even when the working chamber is filled with nitrogen or with another gas which does not absorb radiation. In order to eliminate this signal, two heated radiating chambers were used -- a comparison chamber, 1, and a working chamber, 2, (see figure 1, c). The mixture being analyzed passes through the working chamber. The comparison chamber is filled with nitrogen or with air and heated to the temperature of the working chamber. The internal surfaces of the chamber are chromium plated and polished. The

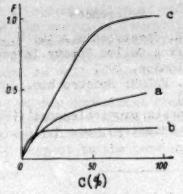

Figure 2

beams of radiation from the working and comparison chambers are interrupted by the chopper 3, and get into the radiation receiving cylinder of the receiver 5, via the filter chamber 4. Then the signal from the microphone 6, amplified in 7, gets into the recording apparatus 8. In figure 2 (curve c) is presented the curve of the signal as a function of the concentration of carbon dioxide in the mixture being analyzed. The temperature of the heated chambers is 94° C; the temperature of the surroundings, 20° C.

January 24, 1959

References

1. M. L. VEINGEROV: ZL, (4) 426 (1947)
2. A. O. SALL': Priborostroenie, (6), 14 (1956); ZTF, 29, 330 (1959)(See Sov. Phys Tech Phys)

TOM VII, Vyp. 2 OPTIKA I SPEKTROSCOPIIA Avgust, 1959
VOL. VII, No. 2 OPTICS AND SPECTROSCOPY August, 1959

Photoelectric Recording of Raman Spectra Excited by the 5875 Å Line of a Helium Lamp

V. M. PIVOVAROV, L. A. KIR'IANOVA, IA. S. BOBOVICH AND G. N. TARKHOV

For the excitation of Raman spectra of strongly colored compounds we have constructed a version of the spiral helium lamp with a cold cathode, which operates under the conditions of a glow discharge [1 - 3]. The total length of the spiral is 2 m, and the helium pressure is 2 mm Hg. The lamp is supplied from high voltage AC, and runs on a current of 0.2 amp with a voltage drop of 3000 V. The spectra are obtained with a grating monochromator of high light power, using an FEU-27 photomultiplier as the radiation detector [4].

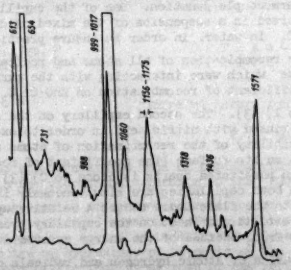

Figure 1. Recorder tracings of the spectrum of iodobenzene for different amplification coefficients.

Since it is roughly sensitive to 7000 Å (with a maximum sensitivity around 5000 Å), this detector, unlike the FEU-17 tube, for example, is suitable for recording Raman spectra excited by He 5875 up to vibrational frequency shifts of the order of ~1600 cm^{-1}. Attempts to use even very good specimens of photomultipliers with cesium oxide photocathodes (FEU-22) as radiation detectors were unsuccessful. Amplification and recording of the electrical signals were carried out using the corresponding units of the DFS-12 spectrometer.

To illustrate the results which can be obtained with this equipment, recordings of spectra of several substances are presented. Figure 1 shows two spectra of iodobenzene obtained with different amplifications; these indicate the sensitivity of the arrangement in the region of vibrational frequencies up to ~1600 cm^{-1}. The reproducibility of the results and the resolution attained in the Raman spectra are illustrated in figure 2 by the 1004 and 1030 cm^{-1} lines of toluene and the 999 and 1017 cm^{-1} lines of iodobenzene.

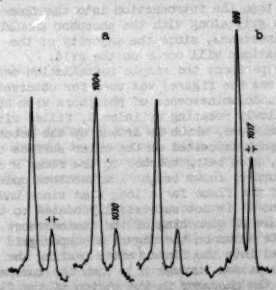

Figure 2. Successive recorder traces of the (a) 1004 and 1030 cm^{-1} lines of toluene; (b) the 999 and 1070 cm^{-1} lines of iodobenzene.

As can be seen from the figure the first doublet is completely resolved at moderate noise levels, and the second is approximately 80% resolved. We might mention that the resolving power obtained by

us is apparently not exceeded by the best arrangements described in the literature, even though these use the blue line of the mercury arc for exciting the Raman spectrum.

We have thus demonstrated the possibility of the photoelectric recording of Raman spectra excited by the 5875 Å line; the method is particularly suited for quantitative investigations of strongly colored substances.

January 24, 1959

References

1. H. STAMMREICH: Spectrochim. Acta, 8, 41, (1956)
2. M. DELHAYE: Proc. Colloq. Spectr. Internat., VI. 485, London, 1957
3. N. S. HAM, A. WALSH: Spectrochim. Acta, 12, 88, (1958)
4. Radioelektronnaia promishlennost' (Radio-electronic Industry), No. 3, 52, (1958)

TOM VII, Vyp. 2 OPTIKA I SPEKTROSKOPIIA Avgust, 1959
VOL. VII, No. 2 OPTICS AND SPECTROSCOPY August, 1959

On the Question of the Physico-Chemical Nature of Candoluminescence

A. N. GORBAN' AND V. A. SOKOLOV

In work [1], demonstrating the existence of a true luminescence under the action of flames, called candoluminescence, the hypothesis was advanced, that one of the basic causes of such a luminescence is the absorption by the phosphor of energy liberated as a result of the recombination of atoms and radicals of the flames into molecules on the surface of the phosphor. In the given article experimental facts are set forth, which demonstrate that such a mechanism of luminescence of phosphors actually takes place under conditions of flames. This has successfully been demonstrated graphically with the aid of the following simple experiment.

It is well known, that the recombination of atoms and radicals proceeds well on metallic surfaces, and also on the surfaces of oxides of certain metals of the Second and Third groups of the periodic system; among the metals, Pt, V, Cu [2] possess a particularly good activity in this respect. If the candoluminescence of the phosphor is occasioned to a significant extent by recombination of atoms and radicals of the flame on its surface then the introduction into the flame of a metallic grid along with the phosphor should diminish its luminescence, since the majority of the recombinations will occur on the grid.

In our experiment the simple installation described in [1] (see the figure) was used for observation of the candoluminescence of phosphors with the aid of the slowly rotating cylinder 1, filled with a cooling mixture, which is driven by the motor 4. The phosphor deposited on the outer surface of the cylinder, upon being touched by the flame 2 of a bunsen burner, shows bright luminescence under the action of the flame for a long time since under such conditions it is not successfully heated to the temperature of quenching of the luminescence. If now, as is shown on the figure a copper grid 3 is introduced into the flame (after heating the grid the flame passes through it), then the luminescence of the phosphor in the region of the flame, directly over the grid is sharply weakened. Upon removal of the grid the bright luminescence of the phosphor is immediately restored to the previous strength. This experiment is a direct demonstration of the coparticipation of the recombination processes mentioned above in candoluminescence.

In this connection it was interesting to establish experimentally the quantity of atomic hydrogen and radicals in the flame of the illuminating gas, which we used for exciting the phosphors, and also to determine directly the coefficients of recombination of the atoms and radicals on certain phosphors we investigated under the conditions of our flame, as had also been done with the aid of the method of thermoelectric probes [3].

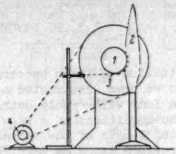

For this we introduced into the flame two thin-walled quartz capillaries (with an outer diameter less than 1 mm), within which was placed a differential thermocouple junction. One of the capillaries was immersed in a suspension of the mixed oxide $ZnO \cdot Cr_2O_3$ in water. In order to ensure practically complete recombination of all atoms and radicals of the flame which were interacting with the surface (the coefficient of recombination on $ZnO \cdot Cr_2O_3$ is equal to 1) [3]. The second capillary on the other hand is rinsed with nitric acid in order to exclude the possibility of the recombination of atoms and radicals on its surface (the coefficient of recombination on passivated quartz is close to 0) [3].

When both capillaries are simultaneously introduced into the flame there occurs a relative spontaneous evolution of heat on the capillary treated with $ZnO \cdot Cr_2O_3$ because of the energy evolved during recombination of atomic hydrogen and radicals of the flame on its surface.

An equation has been obtained by Kondrat'eva and Kondrat'ev [3] which links the magnitude of the self-heating ΔT with the relative concentration of hydrogen atoms

$$\Delta T = 1000 \frac{P_H}{P}$$

where P_H is the partical pressure of atomic hydrogen, while P is the total pressure of the gas.

The energy of recombination of radicals is close to the value of the energy of recombination of atomic hydrogen. Consequently the formula presented above is applicable both to the case of recombination of hydrogen atoms as well as to the case of recombination of radicals.

As a result of the experiment described above under the conditions of an illuminating gas flame, a self-heating was obtained of the capillary with $ZnO \cdot Cr_2O_3$ with respect to the pure quartz of $\Delta T = 75^\circ$, whence

$$\frac{P_H}{P} = \frac{\Delta T}{1000} = \frac{75}{1000} = 0.075$$

or 7.5% of the quantity of fuel mixture, which in relation to the quantity of gas in a stoichiometric mixture (the theoretically necessary quantity of air is approximately equal to 2.0 m^3/m^3 of gas) amounts to

$$\frac{P_H}{P_{gas}} = 22.5\%$$

Thus, in our flame a sufficient quantity of hydrogen atoms and radicals was contained to evoke luminescence of the phosphor introduced into the flame as a result of recombination.

The coefficients of recombination were determined for the phosphor ZnS·CdS-Cu, on which we observed true candoluminescence in flames, and also on the natural phosphor CaO (lime), capable, as we have established, of also showing true luminescence in the case of excitation by flames [4].

To determine the coefficients of recombination of the phosphors a linear dependence was used between the relative self-heating ΔT and the magnitude of the coefficient of recombination ϵ. A calibrated graph was compiled on the basis of the data on the recombination coefficients for $ZnO \cdot Cr_2O_3$ ($\epsilon = 1$) and quartz ($\epsilon = 0$) [5].

In the case of the phosphor ZnS·CdS-Cu, the self-heating ΔT of the capillary treated with this substance was 25-30°, which gives 0.33-0.4 for the coefficient of recombination.

For lime the recombination coefficient proved to be high and equal to approximately 1, since the self-heating of a capillary treated with lime was the same, as that treated with $ZnO \cdot Cr_2O_3$ ($\Delta T \approx 75^\circ$).

The samples of the phosphor ZnS·CdS-Cu and lime we investigated gave a bright luminescence under the action of the flame. Thus, the phosphors which candoluminesce well possess high recombination coefficients.

We consider that the facts set forth indicate that the physico-chemical processes, associated with recombination on the surface of the phosphor of atoms and radicals of the flame into molecules have decisive significance during candoluminescence in flames.

January 26, 1959

References

1. V. A. SOKOLOV: OiS, 4, 409-411 (1958)
2. K. F. BONHOEFFER : Zs. phys. Chem., 113, 199-219 (1924)
3. E. I. KONDRAT'EVA, V. N. KONDRAT'EV: ZFKh, 20, 1239-1247 (1946).
4. A. N. GORBAN', V. A. SOKOLOV: OiS, 5, 713, (1958)
5. A. B. NALBANDIAN, S. M. SHUBINA: ZFKh, 20, 1249-1258 (1946)

TOM VII, Vyp. 2 OPTIKA I SPEKTROSKOPIIA Avgust, 1959
VOL. VII, No. 2 OPTICS AND SPECTROSCOPY August, 1959

Infrared Absorption Spectrum of Hydrargillite $Al(OH)_3$

V. A. KOLESOVA AND IA. I. RYSKIN

The appearance of a band of bending vibration $\delta(OH)$ in the vibrational spectrum in the 700-2000 cm^{-1} range can be considered as evidence of the considerable portion of covalency of the A-O bond in the AOH system. According to literature data, in the spectra of hydroxides of elements of the first two groups of the four upper rows of the periodic system of elements, the band $\delta(OH)$ is not observed in the indicated range of frequencies. For the hydroxides of the elements of the third and fourth groups there are experimental data, which permit one to assume the existence of a dependence between the position of the $\delta(OH)$ band and the character of the A-O bond. Thus, the $\delta(OH)$ was identified [1] as equal to 1197 cm^{-1} for crystalline boric acid $B(OH)_3$. For boehmite AlOOH two bands were detected in the 950-1100 cm^{-1} region, which were ascribed to $\delta(OH)$ vibrations [2]. In work [3] the dependence between the frequencies of the bending vibrations $\delta(OH)$ and the stretching vibrations $\nu(OH)$ in the infrared spectra of hydroxides of various elements is discussed. The following frequencies are assigned to the bending vibrations in the $Al(OH)_3$ spectrum: 1060, 1020, 969, 916, 798, and 747 cm^{-1}. The interpretation of the 798 and 747 cm^{-1} bands evokes doubt since stretching vibrations of Al-O can be located [4] in this region.

We have conducted an investigation of the infrared absorption spectra of synthetic and natural (Arkalyk, Kazakhstan) hydrargillite $Al(OH)_3$ and its deuteroanalog $Al(OD)_3$ in the 420-3700 cm^{-1} frequency range. The $Al(OD)_3$ was obtained by the reaction of sodium aluminate $NaAlO_2$ with heavy water D_2O at a temperature of 80° C. The identification of the product was done by X-ray means (on the basis of a powder-gram) and by the infrared absorption spectrum. The spectra were recorded on

IKS-11 apparatus with an LiF prism (3700-2000 cm^{-1} region) a VIKS-M3 with a NaCl prism (2000-7000 cm^{-1}) and an ISP-14b with a KBr prism (700-420 cm^{-1}). The samples were prepared in the form of disks, compressed from a mixture of the substance being investigated with a specially dried potassium bromide (the concentration of the substance in the mixture amounted to 0.15%), and also in the form of a suspension in "fluoroble" and paraffin oil.

The spectra obtained are presented on the figure.

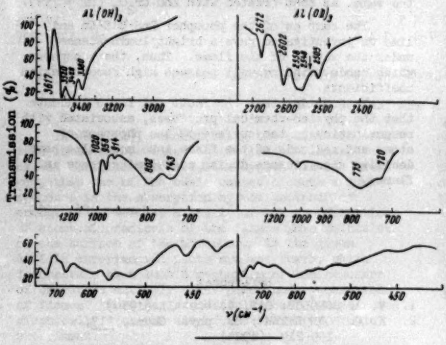

In the stretching vibration range of the hydroxyl group ν(OH) in the spectrum of $Al(OH)_3$ there are observed four maxima: 3617, 3520, 3428, and 3380 cm^{-1}.* In the spectrum of $Al(OD)_3$ the following maxima correspond to them: 2672, 2602, 2558, 2548, and 2505 cm-1; the two components 2558 and 2548 cm^{-1} correspond to the wide band 3428. The ratio of the frequencies ν(OH)/ν(OD) of the corresponding bands is identical within the limits of error and amounts to 1.35 (±0.002).

In the lattice of hydrargillite [6] there are six different spacings between the neighboring oxygen atoms: 3.10, 2.98, 2.94, 2.82, 2.80, and 2.75Å. It is well known that there exists a monotonic dependence between the values of the O-O spacing in the O-H...O system and the frequency of the stretching vibrations ν(OH) [7]. Consequently, the presence of a number of ν(OH) bands in the spectrum of hydrargillite appears quite natural: lower ν(OH) frequencies correspond to the smaller distances between the oxygen atoms of the hydroxyl groups. Under these conditions, of course, one can not always compare a single definite band in the spectrum to every O-O distance.

A detailed discussion of the ν(OH) bands in the spectrum of hydrargillite should be set forth before obtaining more complete experimental data. Apparently, in the spectrum of the monocrystal of hydrargillite there should appear supplementary maxima. The presence of inflection points (noted on the figure by arrows) on the slopes of certain bands argues in favor of this.

*In work [5] besides these maxima, there is also presented the frequency 3360 cm-1, which is not observed in our samples.

The 1020, 958, and 916 cm^{-1} bands** observed in the spectrum of $Al(OH)_3$ disappear in the spectrum of $Al(OD)_3$, which permits one to ascribe them to vibrations of the hydroxyl groups;* and specifically to bending vibrations δ(OH).

One can assume, that the 1020 cm^{-1} band is evoked by δ(OH) vibrations of the hydroxyl groups, associated under the influence of the hydrogen bond, while the 958 and 916 cm^{-1} bands are evoked by δ(OH) vibrations of weakly interacting hydroxyl groups. Actually, the application of a not very strong hydrogen bond should raise the frequency of the bending vibrations δ(OH). The increase in the frequency δ(OH) observable in our case was of an order of magnitude such as one would expect for a moderate hydrogen bond. Let us note that the δ(OH) 958 cm^{-1} band has a halfwidth of 42 cm^{-1}, while the corresponding band of the weakly interacting hydroxyl groups (1020 cm-1) is considerably narrower (12 cm^{-1}). Apparently, the hydrogen bond in the given case increases the anharmonicity of the δ(OH) vibration. However, in spite of the influence of the hydrogen bond, the absolute value of the halfwidth of the δ(OH) band of the linked hydroxyl groups is not large (42 cm^{-1}). The halfwidth of the stretching vibrations bands of associated hydroxyl groups (less than 70 cm^{-1}) is similarly small for the given object, although the frequencies of certain of these bands ν(OH) are lowered considerably by the hydrogen bond (up to 3380 cm-1).

Taking the isotopic coefficient equal to 1.35, the δ(OD) bands in the spectrum of $Al(OD)_3$ should be sought in the 700-750 cm^{-1} region. Thus, they fall in the range where two strong wide bands with maxima of 802 and 743 cm^{-1} are located in the spectrum of $Al(OH)_3$. The form of the spectrum of $Al(OD)_3$ in the range being discussed is different from the spectrum of $Al(OH)_3$: besides the two equally intense bands 802 and 743 cm^{-1} in the spectrum of $Al(OD)_3$ there is observed a wide 775 band and a point of inflection approximately equal to 720 cm^{-1}.**

We assume that the wide and intense 802 cm-1 band in the spectrum of $Al(OH)_3$ is evoked by vibrations of the ν(Al-OH) type; in the spectrum of $Al(OD)_3$ there corresponds to it a 775 cm^{-1} band similar to it in form. The lowering of the frequency by 27 cm-1, i.e., by 2.5%, corresponds in order of magnitude to that expected when the mass of OH is replaced by that of OD.

The small width of the 720 cm-1 band suggests that it is a δ(OD) band. If this is the case, then the ratio of frequencies δ(OH)/δ(OD) will be equal to 1.4. It ensues from what has been said, that

**The 1060 cm^{-1} band [3] was not observed by us.

*The presence of a weak 1020 cm^{-1} band in the spectrum of $Al(OD)_3$ indicates the presence in its structure of a small quantity of OH groups. This is also indicated by the spectrum of $Al(OD)_3$ in the region of stretching vibrations of the hydroxyl groups.

**In the spectrum of $Al(OD)_3$, obtained on an ISP-14b apparatus (region 700-420 cm-1), two bands, 780 and a narrower 726 cm-1 band, are clearly differentiated.

the second wide 743 cm^{-1} band in the $Al(OH)_3$ spectrum disappears upon deuterization, and we conjecturally ascribe it to the γ(OH) vibration. We did not detect a γ(OD) band, but in the region, where one should expect its appearance, many wide bands were located which could mask it.

The presence in the spectrum of hydrargillite of 1020 cm^{-1} bands of bending vibrations of the hydroxyl group and of the sharp bands 958 and 914 cm^{-1}, placed in correspondence with the δ(OH) vibrations of the weakly bound hydroxyl groups, proves that the Al-O bond in hydrargillite has rather a clearly expressed covalent character. This confirms the previously expressed hypothesis [4], according to which absorption in the 700-800 cm^{-1} range corresponds to vibrations of the Al-O bond of a partially covalent character.

February 3, 1959

References

1. D. BETHELL, N. SHEPPARD: Trans.Farad.Soc., 51, 9-15 (1955)
2. O. GLEMSER, E. HARTERT: Naturwiss., 40, 552-553 (1953)
3. E. HARTERT, O. GLEMSER: Zs.Elektrochim., 60, 746-751, (1956)
4. V.A.KOLESOVA: OiS, 6, p 20 (1959)
5. L. D. FREDERICKSON, JR.: Anal. Chem., 26, 1883-1885, (1954)
6. A. F. WELLS: Structural Inorganic Chemistry, Oxford, 1945, 1950, (IL, M. 1948)
7. R. E. RUNDLE, M. PARASOL: J.Chem.Phys., 20, 1487-1488, (1952)

TOM VII, Vyp. 2 — OPTIKA I SPEKTROSKOPIIA — Avgust, 1959
VOL. VII, No. 2 — OPTICS AND SPECTROSCOPY — August, 1959

Investigation and Interpretation of Bands in the Absorption Spectra of Crystals Colored by Chromium Ions

I. I. ANTIPOVA-KARATAEVA

Absorption spectra of crystals colored with the Cr^{3+} ion (one of the elements with an incomplete 3d-shell) have been investigated. These include chromium potassium alum $KCr(SO_4)_2 \cdot 12H_2O$ and synthetic ruby. Solutions of chromium potassium alum have also been studied. The measurements were carried out on an SF-4 spectrophotometer in the spectral range 200 - 1200 mμ. The measurements show that in the absorption spectra of solutions of chromium potassium alum in water, there are two broad bands with maxima ν_1 = 17,400 cm^{-1} and ν_2 = 24,300 cm^{-1} (Figure 1) independent of the concentration of the solution. In the spectra of the crystals which were investigated one observes three bands with frequencies at the maxima in the case of chromium potassium alum ν_1 = 17,700 cm^{-1}, ν_2 = 24,600 cm^{-1}, ν_3 = 38,750 cm^{-1}, and in the case of synthetic ruby (Al_2O_3-Cr_2O_3) ν_1 = 17,750 cm^{-1}, ν_2 = 24,700 cm^{-1} ν_3 = 39,500 cm^{-1}, (Figures 2 and 3).

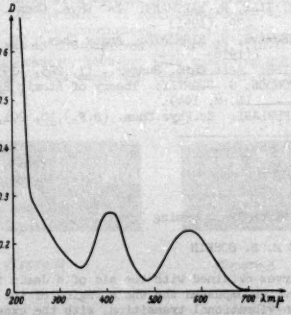

Figure 1. Absorption spectrum of a solution of chromium potassium alum in water.

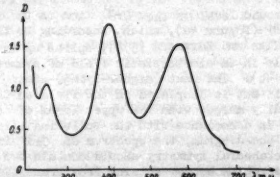

Figure 2. Absorption spectrum of chromium potassium alum crystal.

The existence of three absorption bands in the spectra of the crystals studied appears surprising from the point of view of crystal field theory which predicts the number of bands in the spectrum to be dependent upon the symmetry of the field in which the ion is located.

As is well-known, in crystals of chromium potassium alum the Cr^{3+} ion is surrounded by H_2O molecules, forming a regular octahedron [1]. Upon dissolving the crystal in water the chromium ion forms the complex $[Cr(H_2O)_6^{3+}]$, having an analogous structure.

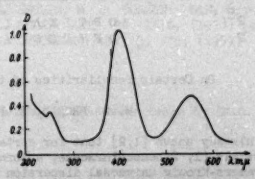

Figure 3. Absorption spectrum of synthetic ruby crystal.

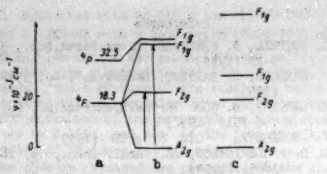

Figure 4. Level diagram of Cr^{3+} ion.
a- free ion; b- ion in field of symmetry O_h (without including interaction between the F_{1g} levels); c- ion in field of symmetry O_h (taking into account interaction between the F_{1g} levels).

In both cases the dipoles of the H_2O molecules create an electrostatic field having the symmetry O_h at the location of the Cr^{3+} ion. In ruby crystals the Cr3 ion. is surrounded by six oxygen ions, arranged in the form of a regular octahedron [2]. The field they create also has the symmetry O_h,but in addition there acts upon the ion under consideration a very weak field of trigonal symmetry generated by ions lying outside of the limits of the indicated octahedron.

The ground level of the Cr^{3+} ion in the free state is ^4F (Figure 4a), which, according to the theory of Ilse and Hartmann [3,4], splits up into three levels in an electrostatic field of symmetry O_h (Figure 4b). The next (higher-lying) state ^4P is not split but is displaced in the field so that it practically merges with the upper level of the ^4F state. In accordance with the splitting illustrated in the diagram, the spectrum of Cr^{3+} in a field of octahedral symmetry should contain two intense absorption bands, arising from transitions between the levels of the ^4F state [$A_{2g}(^4F) \rightarrow F_{2g}(^4F)$ and $A_{2g}(^4F) \rightarrow F_{1g}(^4F)$] and a series of intercombination bands corresponding to transitions from the $A_{2g}(^4F)$ level to levels of the ^2P, ^2D, and ^2F-states, whose intensity is less by an order of magnitude. Upon lowering the symmetry of the electrostatic field acting upon the Cr^{3+} ion to D_{4h} or D_{3d}, four intense absorption bands should be observed in the absorption spectrum, and upon fully removing the degeneracy of the 3d-level (field symmetry C_{2h}, D_{2h}, C_{2v} or C_2) six absorption bands should be observed in the spectrum [5]. Thus it is evident that crystal field theory in the form applied by Ilse and Hartmann to groups of transition metals does not explain the origin of three absorption bands in the spectra of the crystals colored with chromium ions which were investigated. According to this theory two bands should be observed in the absorption spectra of crystals and solutions of chromium potassium alum, and either two or four bands , in ruby, depending on how great is the influence of the additional weak trigonal field.

In order to explain the origin of three bands in the spectra investigated, it is evidently necessary to take into consideration configuration interaction between levels having the same symmetry F_{1g}, but belonging to states with a different value of the orbital quantum number $L - F_{1g}(^4F)$ and $F_{1g}(^4P)$. It can be shown that this effect leads to a mutual repulsion of the interacting levels (Figure 4c), so that they lose the character of pure ^4F and ^4P states, and the selection rule $\Delta L = 0, \pm 1$ vanishes [6]. The possibility arises of transitions $A_{2g}(^4F) \rightarrow F_{1g}(^4F, ^4P)$ and $A_{2g}(^4F) \rightarrow F_{1g}(^4P, ^4F)$. A detailed quantum-mechanical calculation for the analogous picture in the case of the Ni^{2+} complex has been carried out by Furlani [7].

It is evident that, since configuration interaction among the levels of the Cr^{3+} ion plays a large role in the crystals investigated, the ions or dipoles generating the electrostatic field are located near the absorbing ion. In solutions it does not appear to such an extent, since the H_2O molecules, evidently, are situated at greater distances from the Cr^{3+} ion and generate a field of smaller intensity. The displacement of the bands in the spectra of solutions toward longer wavelengths with respect to the spectra of crystals indicate this.

In conclusion I express deep thanks to Professor A. Kiss (Hungarian Peoples' Republic) for advice given during the accomplishment of this work.

February 18, 1959

References

1. H. LIPSON, C. BEEWERS: Proc.Roy.Soc., A148, 664, (1935)
2. N. V. BELOV: Structure of Ionic Crystals and Metallic Phases, Akad. Nauk, USSR, 1947
3. F. E. ILSE, H. HARTMANN: Zs. Phys. Chem., 197, 239, (1951)
4. A. NEUHAUS, W. RIEHARTZ: Angew.Chem., 70, 430, (1958)
5. A. KISS: Acta Chim. Hungar., 17, 225, (1958)
6. E. CONDON, G. SHORTLY: Theory of Atomic Spectra, IL, M, 1949
7. CL. FURLANI: Zs.Phys.Chem.,(N.F.),10, 291,(1957)

TOM VII, Vyp. 2 OPTIKA I SPEKTROSKOPIIA Avgust, 1959
VOL. VII, No. 2 OPTICS AND SPECTROSCOPY August, 1959

On Certain Peculiarities of the Dispersion of Strongly Absorbing Crystals

M. S. BRODIN, A. F. PRIKHOT'KO AND M. S. SOSKIN

We have already shown [1,2] that for certain molecular crystals (1, 2-benzanthracene, anthracene, etc.), the Kramers-Kronig universal dispersion relations are violated, and that the degree of violation increases with decreasing temperature. The dispersion curves obtained with the aid of a Jamin interferometer encompassed the whole region of the first electron-vibrational transition, with the exception of the zones of maximum absorption in the region of strong bands, — places corresponding to anomalous

behavior of the dispersion curves. In this connection, it seemed of interest to make a detailed study of the shape of the interference pattern within these bands as well, using the thinnest crystals possible. It should be remarked that the literature does not appear to contain any investigations of the dispersion of crystals in the region of electronic transitions by the interference method in which the interference bands extend throughout the entire region of strong absorption and still maintain satisfactory contrast.

We have succeeded in obtaining crystals of 1, 2-benzanthracene and anthracene which are sufficiently thin to permit the observation of interference patterns within the strongest absorption bands. In connection with this investigation, we observed an interesting systematic peculiarity.

Figure 1.

Figure 1 shows a photograph of the interference pattern obtained with the b-component of a crystal of 1,2-benzanthracene 0.25 μ thick at a temperature of 20° K (the exposure was made in polarized light with the monoclinic b-axis of the crystal oriented vertically). The arrow indicates the maximum of the first long wavelength absorption band. As is evident from the photograph, the interference bands within the indicated absorption band are as if split and overlapped, which is contrary to the usual rule for dispersion curves. Actually, the interference bands describing the change in the refractive index, upon passing through the absorption maximum, should remain continuous and have two characteristic extrema. But the character of the interference pattern near the indicated maximum is entirely different, and allows one to postulate that in the indicated region of the spectrum two identically polarized waves with unequal path differences propagate in the crystal. At room temperature, with these same 1, 2-benzanthracene crystals, this peculiarity was not observed (Figure 2). In the case of anthracene, however, this splitting and overlapping of the bands was observed even at room temperature.

Figure 2

Figure 3

The unusual character of the phenomenon described demands that the conditions of the experiment be cautiously and carefully analyzed from the point of view of possible errors, both of an intrumental character and those related to the properties of the specimen. The phase change caused by the complexity of the index of refraction and by the influence of interference effects due to multiple reflections in the thin crystal amounts here, as is shown by calculations according to the exact formula [3], to less than 4% of the total value of the phase change for the most unfavorable conditions. Crystallites with strictly plane-parallel surfaces were selected for the measurement. It remains to be determined whether the deformation of the crystal caused by its rigid mounting has any effect upon the interference pattern. A uniform deformation of the crystal, which we believe takes place in the case of 1,2-benzanthracene [4], cannot qualitatively change the shape of the fringes, but can only displace them somewhat. Incidentally, there is no thermal deformation in the anthracene crystal at room temperature. On the other hand, even nonuniform deformations cannot lead to the observed splitting of the bands, since a nonuniformly deformed crystal is equivalent to a pile of infinitely thin uniformly deformed layers. Therefore, in our opinion, the observed effect cannot be regarded as due to possible experimental errors.

The presence of two or more waves not caused by ordinary birefringence in the region of exciton absorption of crystals was predicted in recent theoretical papers [5,6]. It is possible that the peculiarities we observed are connected with this same effect. In that case this effect should not be observed in impure crystals. Judging by the photographs* of the interference pattern obtained in the absorption region of anthracene molecules contained in solid solution in a crystal of dihydroanthracene, the indicated peculiarities are actually not present in this case. (Figure 3).

Hence, attention is called to the fact that the abovementioned peculiarities are observed in those cases in which the Kramers-Kronig dispersion relations are violated.

February 21, 1959

References

1. M. S. BRODIN, M. S. SOSKIN: IAN, USSR, FS, 22, 1316, (1958) (See CTT Bulletin)
2. M. S. BRODIN, A. F. PRIKHOT'KO, M. S. SOSKIN: OiS, 6, p 12 (1959)
3. O. S. HEAVENS: Optical Properties of Thin Solid Films, London, 1955
4. M. S. BRODIN, M. S. SOSKIN: OiS, 6, p 392, (1959)
5. S. I. PEKAR: ZETF, 34, 1176, (1958) (See Sov. Phys. JETP)
6. A. F. LUBCHENKO: UFZ, 3, 575, (1959)

* These photographs were taken by IA.O. Doveg.

TOM VII, Vyp. 2 OPTIKA I SPEKTROSKOPIIA Avgust, 1959
VOL. VII, No. 2 OPTICS AND SPECTROSCOPY August, 1959

Infrared Spectra of Some Disubstituted Allenic Hydrocarbons

A. A. PETROV, T. V. IAKOVLEVA AND V. A. KORMER

Vibrational spectra of mono-substituted allenic hydrocarbons were studied in some instances [1-3]. It was established that in the infrared spectra allenic groups correspond to an intense band near 1960 cm-1. In the Raman spectra this frequency is expressed weakly. The allenic grouping is characterized in these spectra by frequencies in the 1050-1150 cm-1 region.

After a simple method of obtaining disubstituted allenes was worked out in our laboratory [4], the possibility appeared of studying the vibrational spectra of this group of allenic hydrocarbons.

We have taken the infrared spectra of the following 9 allenes: heptadiene-2,3; 6,6-dimethylheptadiene-2,3; octadiene-3,4; 7-methyloctadiene-2,3 and -3,4; 7,7-dimethyl-octadiene-3,4; nonadiene-2,3 and -3,4; and decadiene-3,4.

The most characteristic and intense bands in the spectra of these hydrocarbons were the bands of the allenic grouping at 1960-1965 cm-1 and the non-planar deformation vibrations of the grouping of C=C=CH- in the 870-875 cm-1 region. Planar deformation vibrations of this grouping were not notable either in position or in intensity.

In the stretching CH vibration region of the spectra of all the allenes from three to seven bands with frequencies below 3000 cm-1 are present. The high frequencies characteristic for the 1,3 dienes are not found here.

There are intense bands in the region of the CH deformational vibrations in the spectra near 1465, 1456 and 1370 cm-1. In compounds with a normal (straight) chain there are also intense bands near 1280 and 1320 cm-1, which are noticeably weakened with the appearance of branching in the chain.

Upon replacement of the methyl group in the allene grouping by ethyl the band in the 760-775 cm-1 region disappears, and a band at 780-790 cm-1 appears. This substitution also leads to disappearance of the band at 1410-1420 cm-1.

With the presence in the chain of the allene of more than one CH_2 group, a characteristic band appears in the 730-750 cm-1 region, which shifts in the direction of lower frequency with increase in the number of methylene groups.

Branching of the chain at the second carbon atom causes the appearance in the spectrum of a band in the 1380-1390 cm-1 region. Introduction into the allene molecule of the tertiary butyl radical is accompanied by the appearance or increase of intensity of bands in the regions 900, 1200, 1240, 1390, 1475 and 2750 cm-1.

Similar regularities are found also in other series of saturated and unsaturated hydrocarbons [1].

The allenic hydrocarbons were obtained by the addition of lithium alkyls to vinylalkylacetylenes [4]. Their constants were presented earlier.

Infrared spectra were taken on an IKS-14 spectrophotometer using a NaCl prism up to 1800 cm-1 and a LiF prism beyond. Slit width was approximately 0.03 mm. The data obtained are presented in the table and figure.

February 23, 1959

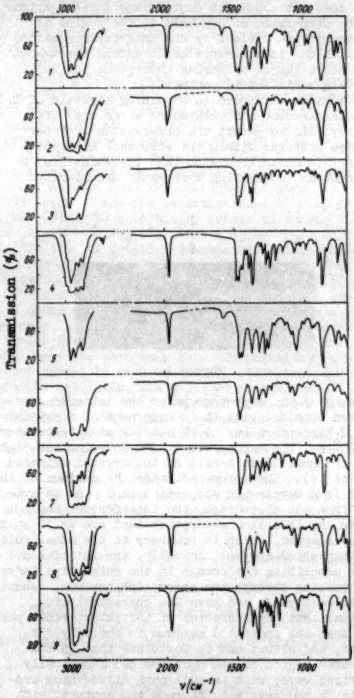

Infrared Transmission Spectra

1) heptadiene-2,3; 2) nonadiene-2,3; 3) 7-methyl-octadiene-2,3; 4) 6,6-dimethylheptadiene-2,3; 5) octadiene-3,4; 6) nonadiene-3,4; 7) 7-methyl-octadiene-3,4; 8) decadiene-3,4; 9) 7,7-dimethyl-octadiene-3,4.

References

1. L.J.BELLAMY: Infrared Spectra of Molecules (IL, Moscow,1957)
2. L. PIAUX, M. GAUDEMAR: C.R., 240, 2328, (1955)
3. L. PIAUX, M. GAUDEMAR, L. HENRY: Bull soc.chim., 794, (1956)
4. A. A. PETROV, V. A. KORMER: DAN USSR, 125, 1041, (1959)

Infrared Spectra of R-CH=C=CH-R' Hydrocarbons

Radical R								
CH_3				C_2H_5				
Radical R'								
C_3H_7	C_5H_{11}	C_5H_{11}-iso	$CH_2C_4H_9$-tert	C_3H_7	C_4H_9	C_4H_9-iso	C_5H_{11}	$CH_2C_4H_9$-tert
700 m.	700 m.	697 m.	695 s.	695 m.	698 m.	690 m.	695 m.	703 m.
747 m.	728 w.	—	—	746 m.	735 w.	—	730 m.	—
—	—	—	—	—	742* w.	—	—	—
773 m.	772 w.	762 w.	763 m.	—	—	—	—	757 w.
—	—	—	—	783 m.	788 v.w.	786 w.	786 w.	789 w.
838 m.	845* w.	—	839 w.	831* v.w.	—	826 v.w.	—	837* v.w.
871 v.s.	872 v.s.	890 v.s.	876 v.s.	878 v.s.	874 v.s.	875 v.s.	875 v.s.	873 v.s.
—	893* w.	—	—	—	—	—	—	887 s.
—	—	900 w.	900 m.	—	—	—	909 v.w.	906 w.
—	—	932 v.w.	932 v.w.	933 v.w.	916 v.w.	920 v.w.	940 v.w.	930 v.w.
958 w.	963 w.	952 v.w.	—	949 w.	964 v.w.	930 w.	967 v.w.	963 v.w.
977 w.	—	988 v.w.	992 w.	—	—	970 v.w.	—	—
—	1015 v.w.	—	—	1011 v.w.	—	—	1012 v.w.	1011 v.w.
—	1030 v.w.	1031 v.w.	1028 v.w.	—	1022 v.w.	1022 v.w.	1028 v.w.	1028 v.w.
1041 w.	—	—	1050 v.w.	1042* w.	—	—	—	—
1071 m.	1071 w.	1074 w.	1070 w.	1068 s.	1071 w.	1070 w.	1068 m.	1066 m.
1100 w.	1105 v.w.	1110 v.w.	—	1100 m.	1105 w.	1105 w.	1105 w.	—
1140 v.w.	1155 v.w.	1162 w.	1150 w.	1140 w.	1137 v.w.	1169 w.	1153 v.w.	1159 w.
1213 v.w.	1208 v.w.	1200 v.w.	1200 m.	1215 v.w.	1204 v.w.	1222 v.w.	1209 v.w.	1200 m.
—	1230 v.w.	1243 w.	1243 m.	—	1238 w.	—	—	1242 s.
1261 s.	—	—	1266 m.	1260 s.	—	1264 m.	—	1264 m.
1285 s.	1276 m.	1278 w.	1292 w.	1283 s.	1276 m.	1284 m.	1276 m.	1287 w.
1325 m.	1340 v.w.	1322 v.w.	1318 v.w.	1325 s.	1326 m.	1328 m.	1325 m.	1329 w.
1373 s.	1373 s.	1368 v.s.	1367 v.s.	1378 s.	1375 m.	1369 s.	1378 s.	1350 v.s.
—	—	1383 m.	1393 m.	—	—	1384 s.	—	1389 s.
1416 m.	1414 v.w.	1413 v.w.	1415 w.	—	1418* w.	—	—	—
1444 v.s.	1444 v.s.	1444 s.	1441 m.	1446* s.	1446* s.	—	—	—
1456 v.s.	1456 v.s.	1456 v.s.	1456 v.s.	1456 v.s.	1455 v.s.	1456 v.s.	1456 v.s.	1456 s.
1464 v.s.	1464 v.s.	1466 v.s.	1469 v.s.	1466 v.s.	1464 v.s.	1465 v.s.	1465 v.s.	1466 v.s.
—	—	—	1476 v.s.	—	—	—	—	1475 v.s.
1565 v.w.	1574 v.w.	—	—	1581 v.w.	—	—	—	—
1964 s.	1964 s.	1965 s.	1964 s.	1964 s.	1960 m.	1960 s.	1964 s.	1964 s.
2722 v.w.	2128 v.w.	2722 v.w.	2723 v.w.	—	2729 v.w.	2728 v.w.	—	2717 v.w.
—	—	—	2749 v.w.	—	—	—	—	2748 v.w.
—	2857 s.	—	—	—	2863 v.s.	2847 s.	2859 v.s.	2847 s.
2874 s.	2877 s.	2872 s.	2868 v.s.	2876 v.s.	2872 v.s.	2873 v.s.	2875 v.s.	2870 v.s.
2904 s.	—	—	2905 v.s.	—	—	2897 v.s.	—	2900 v.s.
2930 v.s.	2923 v.s.	2928 v.s.	—	2931 v.s.	2922 v.s.	2929 v.s.	2926 v.s.	2934 v.s.
2958 v.s.	2957 v.s.	2952 v.s.	2959 v.s.	2962 v.s.	2961 v.s.	2963 v.s.	2960 v.s.	2954 v.s.
—	—	—	2989 v.s.	—	—	—	—	—

ТОМ VII, Вып. 2 ОПТИКА И СПЕКТРОСКОПИЯ Avgust, 1959
VOL. VII, No. 2 OPTICS AND SPECTROSCOPY August, 1959

Normal Vibration Frequencies of Zirconium Halides

I. N. GODNEV, A. M. ALEKSANDROVSKAIA, I. V. RIGINA

In a previous article [1] we reported the calculation of normal vibration frequencies of TiI_4. In the present communication a solution of the analogous problem for the zirconium halides is proposed. These calculations are of interest, since some zirconium halides find wide application (see, for example, [2]) but data on frequencies and bond lengths do not exist in the literature, except for the inter-atomic spacing $r_{Zr\text{-}Cl} = 2.33$ Å [3] and one frequency $\nu_1 = 383$ cm^{-1} [4]* for $ZrCl_4$.

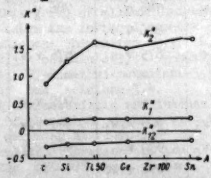

For the solution of the problem indicated above, we modified the method which we applied earlier (see [1, 5, 6]), having plotted the referred interaction coefficients not as a function of the inter-atomic spacing r, but as a function of the atomic weight of the central atom, where these curves were constructed separately for fluorides, chlorides, bromides, and iodides.

In calculation of the frequencies of ZrX_4 according to the referred interaction coefficients, it is necessary to know inter-atomic spacings. The latter were determined as in [1], by constructing plots of the inter-atomic spacings as a function of the atomic number Z of the peripheral atom (see the figure in reference [1],) where the plot for zirconium halides was drawn above the curve of SnX_4 through the point with r = 2.33 Å corresponding to $ZrCl_4$. Such a method of constructing a plot for ZrX_4 is justified by the presence of the electronic configuration d^2s^2 in Ti, Zr, Hf, which differs from the electronic configuration s^2p^2 in C, Si, Ge, and Sn [curve r = f(Z) for TiX_4 passes above the curve for GeX_4]. The inter-atomic spacings r found by such a method are presented in table 1, where they are compared with the sums of covalent radii taken from the more recent tables of Pauling [7]. The sums of covalent radii indicate, as expected, large inter-atomic spacings, the maximum divergence occurring for ZrF_4.

For the determination of the reduced interaction coefficients k^*_{ij}, as indicated above, we used the functions $k^*_{ij} = f(A_{center})$ for halides of the fourth group**. The application of such plots permits one, on the one hand, to avoid extrapolation***, and, on the other, to find k^*_{ij} without knowledge of the inter-atomic spacings. The curves of the dependence of the coefficients k^*_1, k^*_{11}, and k^*_{12} upon A_{centre} in the case of halides of the fourth group appear almost monotonic, which permits one to find these coefficients directly from the curve. In the curves for k^*_2 and k^*_{22} in particular, corresponding to titanium, there is a break (see the figure where the curves k^*_1, k^*_{12}, and k^*_2 for bromides are shown). Therefore the coefficients k^*_2 and k^*_{22} were determined from the smoothed curve drawn through the point Ti with exactly the same electronic configuration (d^2s^2) as Zr. The interaction coefficients for $ZrCl_4$, $ZrBr_4$, and ZrI_4 found by this method are presented in table 2, and in table 3 are presented the frequencies of normal vibrations of the indicated molecules found according to the coefficients of table 2, with the help of well-known equations (see [1]).

It should be observed that if in place of the curves $k^*_{ij} = f(A_{center})$ one uses the curves $k^*_{ij} = f(Z_{center})$, then one obtains interaction coefficients close to those cited in table 2. ****

Table 1

Inter-atomic spacings r(Zr-X) for ZrX_4

Molecule	r calculated (in Å)	Sum of covalent radii (in Å)
ZrF_4	1.85	2.09
$ZrCl_4$	2.33*	2.45
$ZrBr_4$	2.47	2.60
ZrI_4	2.67	2.79

* Experimental value (see [3]).

Table 2

Reduced interaction coefficients

$k^* \cdot 10^{-6}$ cm^2 for $ZrCl_4$, $ZrBr_4$, ZrI_4

Molecule	k^*_1	k^*_2	k^*_{11}	k^*_{12}	k^*_{22}
$ZrCl_4$	0.21	1.73	0.26	-0.09	1.78
$ZrBr_4$	0.27	1.87	0.31	-0.16	1.89
ZrI_4	0.37	2.21	0.42	-0.29	2.35

*In the spectrum of $ZrCl_4$ the band 117-123 cm^{-1} was observed [4] the reference to which is difficult.

**The necessary data for construction of the indicated curves were taken from the works [1, 5, 6]. The interaction coefficients of SiI_4, $SnCl_4$, $SnBr_4$, and SnI_4 are calculated by us on the basis of frequencies [8, 9, 10] and dimensions [3, 11].

***With the exception of ZrF_4.

****For the determination of the frequencies, as our calculations showed, it is possible to use also curves of the dependence of the force constants upon A_{center}. The calculated frequencies appear close to the values quoted in table 3.

Table 3

The normal vibration frequencies of ZrX_4 in cm^{-1}

Molecule	ν_1 (A_1)	ν_2 (E)	ν_3 (F_2)	ν_4 (F_2)
$ZrCl_4$	382	108	423	114
$ZrBr_4$	224	65	309	78
ZrI_4	152	44	211	55
ZrF_4	600-725	150-200	?	180-230

Table 4

The normal vibration frequencies of $SiCl_4$ in cm^{-1}

Frequency	Experimental	Calculated
ν_1 (A_1)	424	425
ν_2 (E)	150	154
ν_3 (F_2)	610	585
ν_4 (F_2)	221	228

For ZrF_4 the above mentioned method requires extrapolation of the interaction coefficients, and therefore, we were able to determine only the limits between which the frequencies ν_1, ν_2 and ν_4 lie (see table 3). The utilization of the triple extrapolation method [5] gives the same results for ZrF_4.

An estimate of the error in calculating the frequencies of $ZrCl_4$, $ZrBr_4$, and ZrI_4 carried out analogously [1], yields $\Delta\nu_1 = \pm 20$, $\Delta\nu_2 = \pm 10$, $\Delta\nu_3 = \pm 30$, and $\Delta\nu_4 = \pm 10$ cm^{-1}.

The method described above was verified by calculating the frequencies of $SiCl_4$, $SiBr_4$, and SiI_4, which came out close to the experimental values. In table 4, the data are presented for $SiCl_4$. In the case of zirconium halides the calculated frequency $\nu_1 = 362$ cm^{-1} likewise agrees well with the experimental (383 cm^{-1}).

February 23, 1959

References

1. N. I. USHANOVA, I. N. GODNEV, I. V. ORLOVA: OiS, 5, 567, (1958)
2. V. S. EMEL'ANOV, P. D. NYSTROV, A. I. EVSTIUKHIN: AE, (1), 43, (1956); (3), 122, (1956)
3. M. W. LISTER, L. E. SUTTON: Trans. Faraday Soc., 37, 393, (1941)
4. M. L. DELWAULLE, F. FRANCOIS: J. Phys. Rad., 7, 15, (1946)
5. I. N. GODNEV, A. S. SVERDLIN, N. I. USHANOVA: OiS, 2, 704, (1957)
6. A. S. SVERDLIN: ZFKh, 32, 659, (1958)
7. L. PAULING: JACS, 69, 592, (1947)
8. M. L. DELWAULLE: J. Phys. Chem. 56, 355, (1952)
9. H. L. WELSH, M. F. CRAWFORD, G. D. SCOTT: J.Chem. Phys., 16, 97, (1948)
10. H. STAMMREICH, R. FORNERIS, Y. TAVARES: J.Chem. Phys., 25, 1278 (1956)
11. H. A. SKINNER, L. E. SUTTON: Trans.Farad.Soc., 40, 164, (1944)

TOM VII, Vyp. 2 OPTIKA I SPEKTROSKOPIIA Avgust, 1959
VOL. VII, No. 2 OPTICS AND SPECTROSCOPY August, 1959

The Functional Description of Spectrum Line Profiles in the Cowan-Dieke and Bartels Theories

N. G. PREOBRAZHENSKII

In the years 1948 to 1950, Cowan and Dieke [1] in the U. S. A. and Bartels [2, 3] in Germany independently constructed theories making it possible to relate the spectroscopic characteristics of an optically dense inhomogeneous gas discharge plasma to the form of the spectral line profile emitted in such a plasma.

So far, however, there has been no attempt to make a systematic comparison of the two theories. In this report, we attempt to compare Cowan and Dieke's final expression $I_C(\nu)$, for the profile of the spectrum line with the corresponding expression $I_B(\nu)$ of Bartels. In making such a comparison, the latter must be taken as representing the case in which the profile of the unreabsorbed line does not vary across the discharge column [1, 2].

It is not difficult to convince oneself that casting these expressions into symmetrical form and using similar symbols does not reduce them to identical formulas for $I_C(\nu)$ and $I_B(\nu)$. Actually, if the dependence of the intensity of a line on frequency ν is introduced in both cases by means of its relation to the optical thickness of the layer

$$(1) \qquad \mu = \frac{\pi e^2}{2mc} f \cdot N_a \cdot P(\nu),$$

where f is the oscillator strength of the line, $P(\nu)$ is the function describing the unreabsorbed profile, and N_a is the total number of absorbent atoms of the line in question along the line of sight, then one may write

$$(2) \qquad I_C(\mu) = 2\mu e^{-\mu} \left\{ 1 + \sum_{k=1}^{\infty} \frac{\mu^{2k} \Gamma(n+1)}{\Gamma(n+2k+1)} \right\},$$

$$(3) \qquad I_B(\mu) = 2\mu e^{-\mu} \left\{ 1 + \sum_{k=1}^{\infty} \frac{\mu^{2k}}{(2k+1)!} P^{f(k,p)} \right\}.$$

In formula (2) the parameter n, which enters into the argument of the gamma function, characterizes the degree of inhomogeneity of the source and may vary between the limits $1 \leq n < \infty$. Its value determines all the terms of the series in expression (2). In formula (3) a similar role is played by the parameter p, where $0 \leq p \leq 1$. The function $f(k,p)$, introduced by us to facilitate comparison of (2) and (3), must be continuous in p and comply with the condition

$$1 \leq f(k = i,\ p) \leq i. \tag{4}$$

In this case, for a fixed p only the first term of the series in formula (3) is established uniquely. Consequently, in any concrete case represented by relation (1), the function of n in the Cowan-Dieke theory is to establish a unique line profile, but the purpose of p in the Bartels theory is to establish a manifold of profiles, whose differences are most marked on the flanks of the line (in the presence of self-reversal) but gradually disappear as one goes from the center of the line profile to its wings. The imposition of the condition

$$p = \frac{6}{(n+2)(n+1)} \tag{5}$$

which is obtained very simply by equating the first terms of series (2) and (3), and the assignment of a form to the function $f(k,p)$ make it possible to obtain the line profile corresponding to the Cowan-Dieke theory from the manifold of Bartels profiles as a particular case. For example, if it is assumed that

$$f(k,\ p) = k^{\alpha(k,p)}, \tag{6}$$

where, according to (4), $0 \leq \alpha(k,p) \leq 1$, then a simple calculation shows that the condition

$$\alpha(k,\ p) = \frac{\lg \lg L^{-1} - \lg \lg p^{-1}}{\lg k} \tag{7}$$

where

$$L = \frac{(2k+1)!}{\prod_{j=1}^{2k}(n+j)}$$

should, in addition to (5), correspond to the Cowan-Dieke profile.

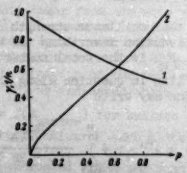

1) Relation between coefficient γ and p.
2) Relation between 1/n and p.

In the Bartels papers [2,3] considerable use is made of both the general formulation (3) and the one-parameter family of curves,

$$\tilde{I}_B(\mu) = \frac{1}{2}\,[I'_B(\mu) + I''_B(\mu)], \tag{8}$$

where $I'_B(\mu)$ in our notation is obtained when $f(k,\ p) = k$, and $I''_B(\mu)$ when $f(k,p) = 1$. Formula (3) readily gives the following expressions for $I'_B(\mu)$ and $I''_B(\mu)$

$$I'_B(\mu) = \frac{2}{\sqrt{p}}\ e^{-\mu} \sin\ \mu\sqrt{p}, \tag{9}$$

$$I''_B(\mu) = 2e^{-\mu}[\mu(1-p) + p\ \mathrm{sh}\ \mu].$$

Conversion to the Cowan-Dieke profile with the aid of (9) may be considered as a somewhat specialized averaging of the curves $I'_B(\mu)$ and $I''_B(\mu)$ according to the general formula:

$$I_C(\mu) = I''_B(\mu) - \gamma(\mu,p)[I''_B(\mu) - I'_B(\mu)]. \tag{10}$$

Formula (8) is a particular case of such averaging with $\gamma(\mu,p) = 1/2$. It is easy to satisfy oneself by calculation that for optical thicknesses μ not exceeding 8 to 10, the coefficient of averaging is $\gamma(\mu,p) \simeq \gamma(p)$. In the conditions of the arc discharge [4], a value of 8 to 10 for μ already corresponds to a very strongly self-reversed line, in which the distance between peaks is 2 to 2.5 times as great as the width of the line in the absence of re-absorption.

The illustration shows γ(p) calculated from a comparison of formulae (2) and (10). This makes it possible, with the help of (5), (9) and (10), to go from the Bartels family of profiles to the Cowan-Dieke contour for $0 \leq \mu \leq 8$ to 10. The maximum error which may result in this connection is only 2% of the calculated value. This requirement is fully satisfied by the experimental conditions for recording and constructing line profiles [5]. The second curve in the same figure shows the relation between the parameters 1/n and p in the Cowan-Dieke and Bartels theories on the basis of formula (5).

Thus, even in the special case where the line shape corresponding to an infinitely thin radiating layer does not depend on the spatial coordinates, the theory of Bartels is broader and more complete than the Cowan-Dieke theory. The reason for this is the different degrees of generality achieved in solving the variational problem, which consists of giving concrete form to the function characterizing the inhomeneity of the source.

February 24, 1959

References

1. R. COWAN, G. DIEKE: Rev.Mod.Phys., 20, 418, (1948)
2. H. BARTELS: Zeit.f.Phys., 125, 597, (1948); 126, 108, (1949); 127, 243, (1950) 136, 411, (1953)
3. H. BARTELS, R. BEUCHELT: f.Phys., 149, 594, (1957)
4. I.V.DVORNIKOVA, I.M. NAGIBINA: OiS, 4, 421, (1958)
5. N. G. PREOBRAZHENSKII: OiS, 6, p 74 (1959)

TOM VII, Vyp. 2 OPTIKA I SPEKTROSKOPIIA Avgust, 1959
VOL. VII, No. 2 OPTICS AND SPECTROSCOPY August, 1959

On the Question of the Effect of Light Gases on the Absorption of Vapors of Aromatic Compounds

S. O. MIRUMIANTS

In 1945 Neporent [1] detected a specific effect of light gases on the intensity of electron absorption of β-naphthylamine. The phenomenon consisted of a diminution of the intensity of absorption of the vapors of the substance being investigated as light gases were added. Under these conditions the absorption initially diminishes rapidly, and then very slowly up to a certain limiting value, corresponding to a high pressure of the foreign gas. It was established, that the phenomenon is due completely to the effect of molecules of the light gases on the unexcited complex molecules. Later works [2,3] have shown, that the specific effect of light gases on the intensity of the electron absorption is characteristic for the majority of aromatic compounds.

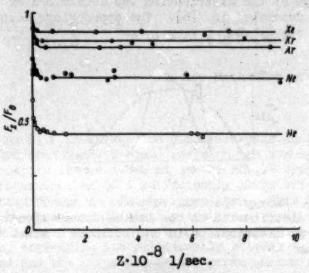

Figure 1

With the object of obtaining new information concerning the mechanism of the phenomenon being considered we investigated the effect of atoms of all the noble gases, and also of the molecules of the diatomic gases (H_2, D_2, and N_2) on the absorption of vapors of 3-dimethylamine-6-aminophthalimide. For the investigations we availed ourselves of, as was done in [1], the luminescence method, which is suitably different from the method of absorption as regards simplicity and precision.

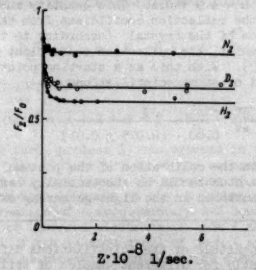

Figure 2

On figures 1 and 2 are presented the results of our measurements. On the ordinate axis are plotted the relative intensities of fluorescence of vapors of 3-dimethylamino-6-amino-phthalimide $\frac{F_z}{F_o}$, where F_o and F_z are the intensities of fluorescence in the absence and presence of the foreign gas; along the abscissa — Z — is the number of collisions (per second) of the molecules being investigated with the molecules of the foreign gas. The vapor tension of the vapors being investigated was $5.4 \cdot 10^{-3}$ mm Hg. The experiments were conducted at the temperature of the vapors $T = 528^{\circ}K$. The general character of the curves of figures 1 and 2 agree with the data, obtained earlier for other substances.

It is a noteworthy fact, that in the case of the inert gases, the magnitude of the limiting attenuation of the fluorescence (of the absorption) $1 - \frac{F_\infty}{F_o}$ is proportional to the average relative speed of the colliding molecules, which in its turn is proportional to the reciprocal of the square root of the reduced mass of the participants in the collision. This fact is illustrated by the data of figure 3, where plotted along the horizontal axis are the average relative velocities of the molecules. It should be noted, that the linear dependence of the magnitude of the limiting attenuation of the fluorescence (of the absorption) on the average relative velocity of the molecules is conserved only for the inert gases, whose atoms possess similar characteristic electron shells.

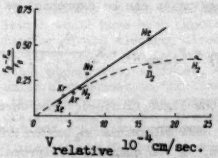

Figure 3

What has been stated is confirmed by the data presented on figure 3 for the diatomic molecules H_2, D_2, and N_2, the collisions with which, and their result depend not only on the average relative velocity of the partners in the collision, but, evidently, also on other properties of the molecules being considered.

I avail myself of the opportunity to express profound gratitude to B. S. Neporent for guidance in carrying out the present work.

March 3, 1959

References

1. B. S. NEPORENT: Dissertation, GOI (1945); DAN USSR, 72, 35-38 (1950)
2. B. S. NEPORENT, A. A. SOLODOVNIKOV: OiS, 1, 951-952 (1956)
3. B. S. NEPORENT, V.P.KLOCHKOV: OiS, 3, 529-535,(1957)

TOM VII, Vyp. 2
VOL. VII, No. 2

OPTIKA I SPEKTROSKOPIIA
OPTICS AND SPECTROSCOPY

Avgust, 1959
August, 1959

Luminescent Energy Yield for Gamma Scintillations in a Stilbene Crystal

Z. A. CHIZHIKOVA

The magnitude of the energy yield during gamma scintillations in a naphthalene crystal with anthracene was obtained in [1] as equal to 0.7%. The corresponding quantity, converted for the anthracene crystal by means of relative data was obtained as 1.7%. This value is lower than that obtained of 8-10% in [2], or 3.8% in [3] and 5% in [4]. Recently, results have appeared on the energy yield of gamma scintillations in plastic scintillators, in which a higher value, 3.8% [5], was also obtained. Consequently, it would be interesting to repeat the measurement of such a fundamental quantity as the energy yield of gamma scintillations for some kind of organic crystal by the same method as was used in [1]. A stilbene crystal was selected for the investigation and the method described in [1] was used except that a photometric sphere was not used but the light collection was estimated by computation. The yield was measured by an impulse method, i. e., by means of the light energy liberated in the individual scintillations. The scintillation energy was determined by using a calibrated spectrometric FEU photomultiplier. The impulses were amplified and their magnitude was determined by using a differential discriminator.

CALIBRATION OF THE PHOTOMULTIPLIER. In order to determine the energy response f_λ of the FEU, the photo-cathode was exposed to the light of a calibrated, photometric incandescent lamp (luminosity 122.2 candles and color temperature 2854°C) through SS-14 and SZS-9 filters. The energy distribution of this etalon source is shown in the sketch. Hence, the transition from light units to energy units can be expressed as follows:

$$F_{(\text{watts})} = F_{(\text{lumen})} \cdot k_o \frac{\int \Phi_\lambda \cdot \varepsilon_\lambda \cdot d\lambda}{\int V_\lambda \cdot \Phi_\lambda \cdot d\lambda},$$

where F is the light flux, Φ_λ the energy distribution in the lamp spectrum, ε_λ the transmissivity of the filters, k_o a quantity reciprocal to the mechanical equivalent of light ($k_o = 683$) $\frac{\text{lumens}}{\text{watt}}$, V_λ a factor of the relative visibility to the average eye.

The spectral response of the FEU was measured by comparison with a thermopile in the longwave region and by using a luminophore (light yellow lumogen) with a constant quantum yield in the shortwave region. The energy distribution (see sketch) in the luminescence spectrum of the stilbene crystal was determined during photo-excitation by $\lambda = 254$ mμ light. The correction for the difference between the etalon source and the stilbene spectra was about 2%.

AMPLIFIER AND DISCRIMINATOR CALIBRATION. The time constant of the amplifier input circuit was two orders of magnitude larger than the scintillation duration so that the amplitude of the output impulse was proportional to the scintillation energy. The amplifier and discriminator were calibrated by sending short light impulses which were obtained by using a rotating mirror (see [1]). The energy of these impulses was expressed in terms of the product of the FEU photocurrent under stationary exposure and impulse duration. Furthermore, the impulse amplitude distribution at the discriminator was found. The value of a discriminator division was defined by means of the maximum of this distribution.

YIELD CALCULATION. Using the calibrated photomultiplier and discriminator, curves of the distribution of impulses from Compton electrons in a stilbene* crystal under the influence of a collimated beam of Co^{60} gamma rays were measured. The energy corresponding to the edge of the Compton distribution is 6 MeV if the gamma ray energy is taken to be 1.25 MeV on the average. The position of the edge of the distribution was determined by the method described in [6]. The appropriate scintillation energy was 1.33×10^3 eV.

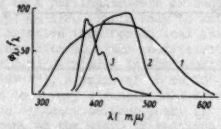

1- Energy spectral response of the FEU; 2- Energy distribution in the etalon source spectrum; 3- Energy distribution in the stilbene luminescence spectrum

In order to find the total scintillation energy, the light-gathering coefficient must be known. To do this, a polished crystal was mounted on the photocathode without immersion; reflectors were not used in this case. It should be noted here that the light gathering occurred in a solid angle defined by the angle of total reflection. An average refractive index of stilbene in the region of the luminescent spectrum was used to estimate the magnitude of this angle. According to [7], two of the principal refractive indices of stilbene for the middle wavelengths of the luminescence spectra are 2.0 and 1.8. The light gathering coefficient is 0.075 ± 0.010 for $n = 1.9 + 0.1$. This quantity must be revised by the reflection coefficient from the inner surface of the crystal (according to the Fresnel formulas, the reflection coefficient is 20% for $n = 1.9$). With this as a starting point, the energy yield of gamma scintillations is:

$$\frac{1.33 \cdot 10^3 \text{ eV}}{1.06 \cdot 10^6 \text{ eV}} \cdot \frac{1}{0.80 \cdot (0.075 \pm 0.01)} = 0.021 \pm 0.003.$$

The errors in the calibration of the photomultiplier and the apparatus should be substantially less than the error mentioned in the light-gathering estimate.

*The magnitude of the scintillations differed insignificantly for different samples of stilbene crystals.

The radio-luminescent yield of an anthracene crystal is apparently approximately twice the yield from stilbene [1, 8]. Therefore, from the results obtained, the yield of anthracene can be considered to equal about 4%.

Since the quantum yield of anthracene photo-luminescence is almost unity, the value obtained for the energy yield corresponds to the "excitation efficiency" of radio-luminescence (i.e., to the ratio between the radio-luminescence and the photo-luminescence quantum yields). It is in good agreement with the excitation efficiency obtained in [9] for solutions by the method of comparing luminescence with Vavilov-Cherenkov radiation.

The author is grateful to M. D. Galanin for supervising this research, to G. S. Belikov for preparing the stilbene samples and to M.I. Epshtein for suggestions on the photometric measurements.

March 5, 1959

References

1. M. D. GALANIN, A. P. GRISHIN: ZETF, 30, 33 (1956) (See Sov. Physics, JETP)
2. M. FURST, H. KALMANN: Phys. Rev., 91, 766, (1953)
3. J. B. BIRKS, M. E. SZENDREI: Phys. Rev., 91, 197 (1953)
4. G. T. WRIGHT: Proc. Phys. Soc., B68, 929 (1955)
5. E. A. ANDREESHCHEV, I. M. ROZMAN: OiS, 5, 39 (1958)
6. D. MAEDER, R. MUELLER, V. WINTERSTEIGER: Helv. Phys. Asta, 27, 3, (1954)
7. M. S. BRODIN: OiS, 1, 876 (1956)
8. J. W. IRVINE: Nucleonics, 10, 3, 37, (1952)
9. Z. A. CHIZHIKOVA: OiS, 7, 223 (1959) (See this Issue)

TOM VII, Vyp. 2 OPTIKA I SPEKTROSKOPIIA Avgust, 1959
VOL. VII, No. 2 OPTICS AND SPECTROSCOPY August, 1959

On the Mechanism of Formation of a Strong Hydrogen Bond

IA. I. RYSKIN

As is well known, the donor-acceptor concept of the hydrogen bond (H-bond) rests on the assumption of polarity of the A-H bond in the AH...B system and concentration of a sufficiently large effective positive charge on the hydrogen atom. This assumption has been insufficiently confirmed by direct experiments. At the same time, the aggregate of facts, expressing the relationship between a strong H-bond and the structure of the proton-donor AH molecules, argues in its favor. One can express the following statement (closely linked with the theories of the hydrogen bond, and of acid-base interaction): for a given proton-acceptor force of the B atom, the strength of the hydrogen bond depends on the conditions which determine the degree of "protonization" of the hydrogen. For a short H-bond to arise, it is necessary, that the electron cloud ε', which is liberated during the drawing off of a proton, should not be retained within the A-H bond, but be fixed outside it.

In systems known to us, the indicated fixation of the ε' charge is performed by one of the following methods: 1) by a filse in the multiplicity of the A-X bond:

$$R_nX - A - H + B \rightarrow R_nX \overset{\varepsilon'}{\cdots} A - H \ldots B;$$

2) by the creation of a new A-Y bond:

$$R_nX - A - H + B + Y \rightarrow R_nX \overset{Y}{\underset{\varepsilon'}{}} A - H \ldots B.$$

In turn, process 1) can proceed in two ways: 1a) via the redistribution of the valence electrons of atom X, possible in the presence of multiple (greater than 1) bonds at the X atom; 1 b) via the formation of a supplementary A-X bond, in which a pair of unshared electrons of Atom A and a vacant orbital of the valence shell of atom X are used.

Let us present examples, which clarify the course of processes 1-a and 2, after which we shall dwell in somewhat more detail on process 1-b, which has been studied slightly.

Among the compounds capable of forming aggregates with short H-bonds, the carboxylic acids are very widely represented. In the formation of hydrogen bridges between molecules of these acids, there occurs a lowering of the carbonyl frequency. Thus, for example, in formic acid in the transition from the monomeric to the dimeric form (in vapors), the carbonyl frequency is lowered from 1790 to 1735 cm^{-1}. This change is evoked by a lowering of the multiplicity of the C=O bond and of necessity is attended by a raising of the order of the C-OH bond. The latter would have been impossible without a partial transfer of the electron cloud ε' via the O atom in the direction of the C=O oxygen bond. The acid carbonates, phosphates, sulfates, and certain other acid salts also belong to the class of compounds with the given type of attachment of the ε' charge and characterized by short H-bonds.

A second method of extracting the ε' charge beyond the limits of the A-H bond is accomplished in crystal-hydrates, in which the molecules of water are simultaneously donors and acceptors of protons. It is well known, that the dipole moment of the O-H bond of an isolated molecule of water is insignificant and insufficient for the realization of the donor-acceptor mechanism of the H-bond. However, if one turns to specific structures, one can then see that the formation of short H-bonds, in which water plays the role of a proton donor, is accompanied (and is explained) by the formation of a third covalent bond of the oxygen atom of water with a proton of the acid anion or with another molecule of water. In the limiting cases, for example, in the crystal $HNO_3 \cdot H_2O$, $(H_3O)^+$ ions are formed with practically equivalent O-H bonds.

Compounds, in the molecules of which there are no conditions for sufficiently full protonization of the hydrogen of the AH group, do not form hydrogen bonds which have considerable force. Thus, for example, methyl alcohol, in which the four valences of the C atom are occupied by four simple bonds, in the associated complexes $CH_3OH \ldots O(C_2H_5)_2$ is

characterized by a very moderate H-bond ($\Delta\nu$ = 151 cm^{-1}), in spite of the considerable proton-acceptor nature of the ether. In $\underset{CH_3}{O-H}\ldots\underset{CH_3}{O-H}\ldots\underset{CH_3}{O-H}$ chains, the ε' charge is used for the creation of a bond with the proton of the preceding molecule, because of which the polarizability of the hydroxyl groups is enhanced and, together with it — the strength of the hydrogen bond.

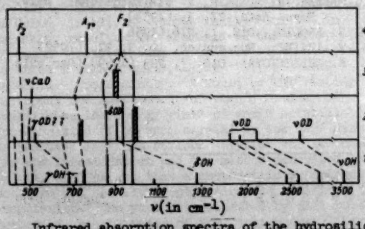

Infrared absorption spectra of the hydrosilicates of calcium $2CaO\cdot SiO_2\cdot H_2O$-α [1], $2CaO\cdot SiO_2\cdot D_2O$-α [2], of bicalcium orthosilicate β-Ca_2SiO_4 [3] and of the tetrahedral ion $[SiO_4]$ (spectrum 4 according to the data of [5]).

The H-bond in hydroxyl-containing compounds of silicon presents great interest. In the R_3SiOH molecules, just as in the R_3COH molecules, four valences of the central atom are distributed between four bonds. However, the presence of a vacant 3d orbital on the Si atom and of a pair of unshared electrons on the O atom renders possible the formation of $p_\pi - d_\pi$ bonds between Si and O [1,2] and, consequently, the lowering of the intensity, created by the ε' charge on the O atom (case 1-b). Thus, one can expect the formation of a strong Si-O-H...B hydrogen bond in compounds with sufficiently strong acceptors of the proton B. Actually, a short H-bond is realized between the O_3SiOH anions in afwillite [3].

We investigated the infrared absorption spectrum of the hydrosilicate $2CaO\cdot SiO_2\cdot H_2O$-α (α-hydrate), which, according to preliminary data from an incomplete X-ray-structural analysis, appears to be an orthosilicate and is characterized by short $O\ldots O(O_3SiOH\ldots OH^-)$ spacings [4]. A direct demonstration of the presence of the SiOH grouping in the compounds would have been the appearance of a band of the deformation vibration δOH in the 1000-1400 cm^{-1} range, since the frequency δOH depends on the covalent fraction of the hydroxyl bond with the central atom, while for the AlOH and POH groups, the frequency δOH lies within the limits 1000-1100 cm^{-1} and 1200-1400 cm^{-1}, respectively. Moreover, one would expect the appearance in the 700-800 cm^{-1} region of an intense $\nu_1(A_1)$ band of the SiO_3OH ion, inactive in absorption, in the absence of hydrogen [5].

The experimental data, schematically presented in the figure, correspond to the expected phenomena. The νOH bands of the hydroxyl groups with the short H-bonds (νOH = 2450, 2594, and 2847 cm^{-1}; νOD = 1790, 1910 and 2115 cm^{-1}; k = νOH/νOD = 1.36 ± ± 0.01) are identified by means of the isotopic shift revealed when the spectra of the α-hydrate and its deutero-analog $2CaO\cdot SiO_2\cdot D_2O$-α are compared. The δOH = 1282 cm^{-1} band (δOD = 910 cm^{-1}, k = 1.41) is also displayed *. Finally, one can assign the split band 747, 754 cm^{-1} in the spectrum of the α-hydrate, and 732, 745 cm^{-1} in the spectrum of its deutero analog to the vibration $\nu_1(A_1)$. In the spectrum of the orthosilicate β-Ca_2SiO_4, which is closest in composition, and which is presented for comparison, this band is absent. Thus, the assignment of a short H-bond in the α-hydrate to the atomic grouping $O_3SiOH\ldots O_1$ can be considered demonstrated.

At the present time it is difficult to say, whether the acceptor of the proton (O_1) is actually an OH^- ion, since the ionized oxygen atom of the neighboring anion O_3SiOH also represents a strong electron donor. This question will be considered in more detail subsequently.

An experiment remains to be indicated, which can be considered a direct confirmation of the formation of a $p_\pi - d_\pi$ bond between O and Si under the influence of an H-bond. In the investigation of the absorption spectra of silanols in pyridine, we detected that in dimers of triethylsilanol-pyridine the frequency of vibration ν(Si-O) is raised by 56 cm^{-1}, i.e., by 7% in relation to its value in isolated molecules (in dilute solutions of silanol in CS_2). So considerable a rise in the frequency can be considered as due chiefly to a rise in the multiplicity of the Si-O bond.

Thus, in all the structures considered with short H-bonds there is detected the action of one or another mechanism of fixation of the electron cloud ε' of the hydrogen atom (being displaced under the influence of a proton acceptor) beyond the limits of the A-H bond.

March 10, 1959

References

1. IA. I. RYSKIN: OiS, 4, (4), 532-534, (1958)
2. L. ALLRED, E. G. ROCHOW, F. G. A. STONE: J.Inorg. Nucl. Chem., 2, 416, (1956)
3. H. D. MEGAW : Acta Cryst., 5, 477-491, (1952)
4. L. HELLER: Acta Cryst., 5, 724-728, (1952)
5. H. SIEBERT: Zeitschrift f.anorg.Chem., 275, 225-240, (1954)

*Let us note, that the δOH and δOD bands are distinguished by a very small width, which, in combination with the limitingly high isotopic coefficient k indicates the high harmonicity of the δOH vibrations for a short H-bond.

TOM VII, Vyp. 2 OPTIKA I SPEKTROSKOPIIA Avgust, 1959
VOL. VII, No. 2 OPTICS AND SPECTROSCOPY August, 1959

CHRONICLE

Resolutions of the International Commission on Molecular Spectroscopy

After preliminary meetings during the Gordon Conference on Infrared Spectra (18-20 August, 1958, in Meriden, U. S. A.), the regular official meeting of the Commission on Molecular Spectroscopy of the International Union of Pure and Applied Chemistry took place on October 8, 1958, in Liege, Belgium. There, resolutions on the following matters were adopted.

1. UNITS AND TERMINOLOGY. The commission recommends adopting the angstrom as the basic unit of wavelength in the ultraviolet region of the spectrum. Use of the unit millimicron, though undesirable, is permissible in individual cases. The Commission did not support a proposal to introduce a new unit of frequency K, equal to $3 \cdot 10^{10}$ sec^{-1}, for the infrared region of the spectrum.

2. INFRARED WAVELENGTH STANDARDS. The Commission is preparing a proposal on "standards of high resolution" (line atomic spectra and gas absorption spectra) and their use for low resolution instruments. After necessary verification in several laboratories, the tables of standards will be included in the Manual proposed for publication.

3. DOCUMENTATION OF INFRARED SPECTRA. The existing collections of spectra and chart systems (Sadtler, DMS, NRC, API, GAMS, ASTM, etc.) are sources of sufficiently complete and adequate information and therefore the Commission does not see the necessity for working out any kind of new system; however, every possibility for establishing relations between the existing systems should be supported in every way possible.

4. DOCUMENTATION OF ULTRAVIOLET SPECTRA. The Commission considers it necessary to exhibit photocopies of the original traces of spectra. In doing so, as the minimum requirement there should be indicated a) the position of all absorption maxima in angstroms, b) the intensity of all absorption maxima, c) the state of aggregation or solvent, and d) the concentration, gas pressure, and temperature. If the errors in determination of the position of the maxima exceed ± 5Å wavelengths should be indicated in millimicrons. If necessary, the unit cm^{-1} may also be used. For solutions in clear solvent absorption intensity at a given wavelength λ is given by the extinction value

$$\epsilon_\lambda = \frac{1}{bc} \log_{10} \left(\frac{I_o}{I}\right)_\lambda,$$

where b is the thickness of the absorbing film in cm, c is the concentration (number of moles of substance per liter of solution), I_o is the intensity incident on the samples, and I is the intensity passing through the samples. If ϵ_λ fluctuates greatly, it is permissible to use the value $\log_{10} \epsilon_\lambda$. Use of other values (passage in %, coefficient k) is not recommended except when the molecular weight of the substance is unknown.

5. INFRARED INTENSITY MEASUREMENTS. For integrated intensity the Commission recommends the following three units:

a) An absolute unit given by the value

$$\frac{1}{bn} \int \ln \left(\frac{I_o}{I}\right)_\nu d(\ln \nu)$$

where b is the thickness of the absorbing film in cm, n is the concentration (number of molecules per cm^3), and ν is the frequency in sec^{-1}. The dimensionality of the absolute unit is $cm^2 sec^{-1} molecule^{-1}$.

b) A unit to be used in certain theoretical studies

$$\frac{1}{bn} \int \ln \left(\frac{I_o}{I}\right)_\nu d(\ln \nu)$$

with the dimensions $cm^2 molecule^{-1}$.

c) A practical unit for quantitative spectral analysis of the solutions

$$\int_{\nu_1}^{\nu_2} \epsilon_\nu d\nu,$$

where $\epsilon_\nu = \left(\frac{1}{bc}\right) \log_{10} \left(\frac{I_o}{I}\right)_\nu$, c is the concentration in moles/liter, b is in cm, and ν, ν_1 and ν_2 are in cm^{-1}. The dimensions of the unit are $mole^{-1} cm^{-2} liter$.

The Commission is continuing consideration of the question of selection of notations and symbols for these units and also study of the problems connected with apparatus functions and the evaluation of spectral slit width. The Commission is working on the selection of compounds whose absorption bands could be used as intensity standards in the infrared region.

The next meeting of the Commission will be August 27-28, 1959, in Munich.

Members of the Commission: Dr. H. W. Thompson - Chairman (England), Prof. B. L. Crawford - Secretary (U.S.A.), Prof. G. V. M. Duyckaerts (Belgium), Prof. J. A. Ketelaar (Netherlands), Prof. J. Lecomte (France), Prof. R. C. Lord (U.S.A.), Prof. A. Mangini (Italy), Prof. R. Mecke (West Germany), Prof. S. Mizushima (Japan), Acad. A. N. Terenin (USSR).

In the USSR work on standardization of intensity measurements in the infrared region is conducted by a Subcommittee of the Commission consisting of: A. N. Terenin - Chairman, P. A. Bazhulin (FIAN, Physical Institute of the Academy of Sciences), B. S. Neporent (GOI, State Optical Institute), V. M. Chulanovskii (LGU, Leningrad State University), A. V. Iogansen (Inst. NEFTI, Petroleum Institute), V. I. Malyshev (FIAN, Physical Institute of the Academy of Sciences), I. V. Peisakhson (GOI, State Optical Institute), G. G. Petrash (FIAN, Physical Institute of the Academy of Sciences), M. M. Sushchinskii (FIAN, Physical Institute of the Academy of Sciences), P. P. Shorygin (IOKh, AN, Institute of Organic Chemistry of the Academy of Sciences), V. A. Nikitin - Secretary (GOI, State Optical Institute), S. G. Rautian - Secretary (FIAN, Physical Institute of the Academy of Sciences).

The Thirteenth Rozhdestvenskii Lecture

At the thirteenth D. S. Rozhdestvenskii lecture, which took place on May 7, 1959, in the S.I.Vavilov State Optical Institute, two reports were read.

A. N. Zakhar'evskii's report dealt with interference biological microscopes, with which contrasting images of colorless and transparent microscopic objects can be obtained. Unlike phase microscopes, they make possible measurement of phase differences introduced by the objects and, on this basis, determination of the weight of the dry substance and its concentration in the object as well as of the index of refraction and the thickness of the object. Interference microscopes are used in biology chiefly for studying the changes taking place in normal and pathological cells in the process of their active life, and can serve for diagnosing illnesses.

The reporter described several designs of such microscopes, which have great magnification and apertures and are based on the interference of polarized rays. In them bifurcation and reunion of the interfering rays is brought about by using plane-parallel crystal plates cemented onto the frontal lenses of the objectives and condensorts.

V. N. Vertsner's report on work in electron microscopy described the basic stages in the development of electron microscopy research in the State Optical Institute (GOI). The characteristics of the EM-3 and EM-5 electron microscopes, of a simplified photoelectronic microscope, and of an auxiliary apparatus for them, were described.

The reporter also described the work on calculation and study of the electron optical systems of electron microscopes and related instruments, an electron microscope with a television arrangement, and an X-ray spectrograph to study the content of the elements from Mg to U with local analysis up to 1-2 μ. He also described the results of using shadow electron-optical methods in research on the potential in the micro-regions of the samples under study, particularly in the zone of the p — n function of germanium rectifers.

TOM VII, Vyp. 2
VOL. VII, No. 2

OPTIKA I SPEKTROSKOPIIA
OPTICS AND SPECTROSCOPY

Avgust, 1959
August, 1959

Jubilees and Dates

VLADIMIR MIKHAILOVICH CHULANOVSKII

(On His 70th Birthday)

Seventy years have passed since the birth of Professor Dr. of Physical and Mathematical Sciences, Vladimir Mikhailovich Chulanovskii, one of the greatest Soviet specialists on molecular spectroscopy and spectral analysis.

In 1918, Vladimir Mikhailovich began working in the State Optical Institute (GOI) where he became one of the leading co-workers. In 1923, V. M. Chulanovskii began teaching in Leningrad University. He organized a school laboratory of an advanced type (the third physical laboratory), which he directed for 15 years. Since 1944, he has held the theoretical and applied spectroscopy professorship which he created. V. M. Chulanovskii began his scientific career with the study of the electronic spectra of molecules in the far ultraviolet. In order to do this, he built a precision diffraction vacuum spectrograph, worked out a brilliant method for illuminating the slit, and substantially improved the technique of preparing Schumann plates and processing spectrograms. As a result he succeeded in obtaining results which were a record of accuracy, and in approximating the theoretical limit to the resolving power of the apparatus. V. M. Chulanovskii's studies of the electronic spectra of diatomic homopolar molecules (CO and NO in particular), when they became widely known, led to discovery of fundamental features of the structure of molecular electronic shells and the determination of bonding and anti-bonding orbit functions. This made it possible to explain the origin of the Rydberg series observed in molecular spectra, and to lay the foundation for spectroscopic study of free electron pairs. Ability manifest in these works to penetrate the physical essence of the phenomenon under study, without being enclosed within the limits of the spectral systematism, is characteristic of the entire scientific activity of V. M. Chulanovskii.

In subsequent years, V. M. Chulanovskii turned to the study of the vibrational spectra of molecules. The work which he and his co-workers carried out in the study of intermolecular interaction in liquids and solutions not only has great scientific significance but is the foundation of a series of methods of molecular spectral analysis. Through them have been discovered the enormous possibilities of spectroscopy for the study of properties of solutions, far surpassing in their selectivity the usual method of classical physical chemistry. The series of studies on hydrogen bonds led to establishment of a number of general rules of this type of intermolecular interaction.

A significant number of the works completed by V. M. Chulanovskii and under his direction, is devoted to the solution of actual industrial problems. The analytical method which he worked out, and the apparatus created for this purpose, are used in the chemical, petroleum and food industries, and in the production of non-ferrous and rare metals. V. M. Chulanovskii's book "Introduction to Molecular Spectral Analysis" is in its second edition; it is the only textbook on this subject in the Soviet Union.

V. M. Chulanovskii was one of the first to introduce molecular spectroscopy into the various branches of the national economy. He is a member of the Spectroscopy Commission of the Academy of Sciences of the USSR and takes part in the international program for documentation of infrared spectra. He has organized a great many spectroscopy laboratories in branch institutes and enterprises, and has trained their specialists.

The editors of "Optics and Spectroscopy", on behalf of all Soviet workers in optics and spectroscopy, congratulate Vladimir Mikhailovich on his seventieth birthday and wish him health and further success.

ABBREVIATIONS OFTEN ENCOUNTERED AND USED HEREIN

DAN USSR	Doklady Akademii Nauk	(Reports of the Academy of Sciences of the USSR)
DAN UkrSSR	Dopovidi Akademii Nauk UkrSSR	(Reports of the Academy of Sciences of the Ukraine SSR)
DAN ArmSSR	Doklady Akademii Nauk ArmSSR	(Reports of the Academy of Sciences of the Armenia SSR)
IAN USSR	Izvestiia Akademii Nauk USSR	(Bulletin of the Academy of Sciences of the USSR)
	SF Seriia fizika	(Physics series)
	SM Seriia matematika	(Mathematics series)
	OKhN Otdelenie khimicheskikh	(Section of Chemical sciences)
OiS	Optika i Spektroskopiia	(Optics and Spectroscopy)
PiTE	Pribory i Tekhnika Eksperimenta	(Instruments and Techniques of Experiment)
AE	Atomnaia Energiia	(Atomic Energy)
AZ	Astronomicheskii Zhurnal	(Astronomy Journal)
FMM	Fizika Metallov i Metallovedenie	(Physics of Metals and Metallography)
Radiotekh.	Radiotekhnika	(Radio Engineering)
RiE	Radiotekhnika i Elektronika	(Radio Engineering and Electronics)
UK	Uspekhi Khimii	(Progress in Chemistry)
UFN	Uspekhi Fizicheskikh Nauk	(Progress in Physical Sciences)
UFZ	Ukraninskii Fizichni Zhurnal	(Ukraine Physical Journal)
ZETF	Zhurnal Eksperimental'noi Teoreticheskoi Fiziki	(Journal of Experimental Theoretical Physics - JETP)
ZTF	Zhurnal Tekhnicheskoi Fiziki	(Journal of Technical Physics)
FTT	Fizika Tverkogo Tel	(Solid State Physics)
ZFKh	Zhurnal Fizicheskoi Khimii	(Journal of Physical Chemistry)
ZOKh	Zhurnal Obshchee Khimii	(Journal of General Chemistry)
ZNKh	Zhurnal Neorganicheskoi Khimii	(Journal of Inorganic Chemistry)
ZPKh	Zhurnal Prikladnoi Khimii	(Journal of Applied Chemistry)
Tr.	Trudy	(Transactions, as for instance, Tr. FIAN)
FIAN	Fizicheskii Institut Akademii Nauk USSR	(P.N.Lebedev Physical Institute of the Academy of Sciences USSR)
Sb.	Sbornik	(Collection, as for instance, Fizich. sb. L'vovskogo Universitet) Fizich. sb. Fizicheskaia sbornik (Physics Collection)
Uch. Zap.	Uchenye Zapiskii	(Scientific Records)
Vestn.	Vestnik	(Herald or Messenger)
FTIAN	Fiziko-Tekhnicheskii Institut A Akademii Nauk	(Physical-Technical Institute of the Academy of Sciences)
GOI	Gosudarstvennyi Opticheskii Institut	(State Optical Institute)
VEI	Vsesoiuznyi Elektrotechnicheskii Institut	(All-Union Electrotechnical Journal)
MFTI	Moskovskaia Fiziko-Tekhnicheskii Institut	(Moscow Institute of Physics and Technology)
NIIZMIR	Nauchno-Issledovatel'skii Institut Zemnogo Magnetizma, Ionosfery i Rasprostraneniia	(Research Institute of Terrestrial Magnetism and Ionospheric Propagation)
GIPTI	Gor'kovskii Issledovatel'skii Fiziko-Tekhnicheskii Institut	(Gor'kii Research Institute of Physics and Technology)
NIFI	Nauchno-Issledovatel'skii Fizicheskii Institut	(Scientific Research Institute of Physics, Leningrad Univ.)
NIRFI	Nauchno-Issledovatel'skii Radio-fizicheskii Institut	(Scientific Research Institute of Radiophysics, Gor'kii Univ.)
GITTL	Gostekhizdat-Gosudarstvennoe Izdatel'stvo Tekhniko-Teoreticheskoi Literatury	(State Publishers of Technical-Theoretical Literature)
GIFML	Fizmatgizdat-Gosudarstvennoe Izdatel'stvo Fiziko-Matematicheskoi Literatury	(State Publishers of Physical-Mathematical Literature) formerly Gostekhizdat)
IL or IIL	Izdatel'stvo Inostrannoi Literature	(Publishers of Foreign Literature)
Izd. AN USSR	Izdatel'stvo Akademiia Nauk USSR	(Academy of Sciences Press)
ZL	Zavodskaia Laboratoriia	(Factory Laboratory)
GOST	Gosudarstvennyi Obshchesoiuznyi Standart	(All-Union State Standard)
LIPAN USSR	Laboratoriia izmeritel'nykh priborov AN USSR	(Laboratory of Measuring Instruments)
IFAN UkrSSR	Institut Fiziki AN UkrSSR, Kiev	(Physics Institute AN UkrSSR)
SFTI	Sibirskii Fiziko-Tekhnicheskii Institut, Tomsk	(Siberia Physical-Technical Institute)
IFAAN ESSR	Institut Fiziki i Astronomii AN ESSR, Tartu	(Institute of Physics and Astronomy)
IFA AN USSR	Institut Fiziki atmosfery AN USSR	(Institute of the Physics of the Atmosphere)

SYMBOLS FOR SOURCES OF TRANSLATIONS

AIP
American Institute of Physics
335 East 45th Street
New York 17, New York

ATS
Associated Technical Services Inc.
P. O. Box 271
East Orange, New Jersey

CB
Consultants Bureau, Inc.
227 West 17th Street
New York 11, New York

CCT
Consultants Custom Translations, Inc.
227 West 17th Street
New York 11, New York

CTT
Columbia Technical Translations
5 Vermont Avenue
White Plains, New York

HB
Henry Brutcher
P. O. Box 157
Altadena, California

LC
Photoduplication Service
Publication Board Project
Library of Congress
Washington 25, D. C.

MDF
Morris D. Friedman, Inc.
P. O. Box 35
West Newton 65, Mass.

NRCC
National Research Council Library
Ottawa 2, Canada

OTS
Office of Technical Services
Department of Commerce
Washington 25, D. C.

PS
Primary Sources
11 Bleecker Street
New York 12, New York

RIS
Research Information Service
40 East 23rd Street
New York 10, New York

SLA
SLA Translation Center
The John Crerar Library
86 East Randolph Street
Chicago 1, Illinois

L. A. BOROVINSKII, L. M. FEDOROVA
Sopostavlenie energeticheskikh urovnei v trekhmernoi i odnomernoi metallicheskoi modeli molekuly benzola 253

A. O. SALI', S. V. STANEVICH
Ispol'zovanie izbiratel'nogo izlucheniia gaza v infrakrasnykh gazoanalizatorakh 256

V. M. PIVOVAROV, L. A. KIR'IONOVA, IA. S. BOBOVICH, G. N. TARKHOV
Fotoelektricheskaia registratsiia spektrov kombinatsionnogo rasseianiia vozbuzhdennykh liniei $\lambda = 5875$ Å gelievoi lampy 258

A. N. GORBAN', V. A. SOKOLOV
K voprosu o fiziko-khimicheskoi prirode kandoliuminestsentsii 259

V. A. KOLESOVA IA. I. RYSKIN
Infrakrasnyi spektr pogloshcheniia gidrargillita $Al(OH)_3$ 261

I. I. ANTINOVA-KARATAEVA
Issledovanie i interpretatsiia polos v spektrakh pogloshcheniia kristallov, okrashennykh ionami khroma 263

M. S. BRODIN, A. F. PRIKHOTK'KO, M. S. SOSKIN
O nekotorykh osobennostiakh dispersii sil'no pogloshchaiushchikh kristallov 266

A. A. PETROV, T. V. IAKOVLEVA, V. A. KORMER
Infrakrasnye spektry nekotorykh dvuzameshchennykh allenovykh uglevodorodov 267

I. N. GODNEV, A. M. ALEKSANDROVSKAIA, I.V.RIGINA
Chastoty normal'nykh kolebanii galogenidov tsirkoniia 271

N. G. PREOBRAZHENSKII
O funktsional'nom opisanii konturov spektral'nykh linii v teoriiakh Kouena-Dike i Bartel'sa 722

S. O. MIRUMIANTS
K voprosu o deistvii legkikh gazov na pogloshchenie parov aromaticheskikh soedinenii 275

Z. A. CHIZHIKOVA
Energeticheskii vykhod liuminestsentsii pri γ - stsintilliatsiiakh v kristalle stil'bena 276

IA. I. RYSKIN
O mekhanizme obrazovaniia sil'noi vodorodnoi sviazi 278

KHRONIKA

Reshenia Mezhdunarodnoi Komissii po molekuliarnoi spektroskopii 281

Trinadtsatye chteniia imeni akad. D. S. Rozhdestvenskogo 282

IUBILEI I DATY

V. M. CHULANOVSKII (k 70-letiiu so dnia rozhdeniia) 283

A Comparison of the Energy Levels of a Three-Dimensional and a One-Dimensional Metallic Model of the Benzene Molecule 160

The Use of Selective Radiation of Gas in Infrared Gas Analyzers 162

Photoelectric Recording of Raman Spectra Excited by the 5875 Å Line of a Helium Lamp 163

On the Question of Physico-Chemical Nature of Candoluminescence 164

Infrared Absorption Spectrum of Hydrargillite $Al(OH)_3$ 165

Investigation and Interpretation of Bands in the Absorption Spectra of Crystals Colored by Chromium Ions 167

On Certain Peculiarities of the Dispersion of Strongly Absorbing Crystals 168

Infrared Spectra of Some Disubstituted Allenic Hydrocarbons 170

Normal Vibration Frequencies of Zirconium Halides 172

The Functional Description of Spectrum Line Profiles in the Cowan-Dieke and Bartels Theories 173

On the Question of the Effect of Light Gases on the Absorption of Vapors of Aromatic Compounds 175

Luminescent Energy Yield for Gamma Scintillations in a Stilbene Crystal 176

On the Mechanism of Formation of a Strong Hydrogen Bond 177

CHRONICLE

Resolutions of the International Commission on Molecular Spectroscopy 179

The Thirteenth Rozhdestvenskii Lecture 180

JUBILEES AND DATES

VLADIMIR MIKHAILOVICH CHULANOVSKII (On His 70-th Birthday) 181

Abbreviation Often Encountered And Used Herein 182

Addresses of Translators 183

TOM VII, Vyp. 2 Avgust, 1959
VOL. VII, No. 2 August, 1959

[redacted]

L. A. KOROSYLEVA, [redacted]
Izotopicheskoe [redacted] ium Spectrum
urana 89

N. S. TSKHAI, S. L. MANDEL'SHTAM
O vliianiakh na intensivnost' spektral'nykh linii v spektre plameni 141
Influences on the Intensities of Spectral Lines in Flame Spectra 91

L. M. SVERDLOV
Teoriia intensivnostei infrakrasnykh spektrov molekul dvuokisi sery, ammiaka i fosfina, IV 152
Theory of Infra-Red Spectra Intensities of Sulfur Dioxide, Ammonia and Phosphine Molecules, IV 97

R. S. LEBEDEV, A. V. SEMKACHEV
K voprosu o silovykh postoiannykh molekuly tsiklopentana 164
On the Question of Force Constants of the Cyclopentane Molecule 104

L. S. MAIANTS, E. M. POPOV, M. I. KABACHNIK
Raschet kharakteristichnykh kolebanii soedinenii fosfora. II 170
Investigation of the Characteristic Vibrations of Phosphorus Compounds. II 108

V. T. ALEKSANIAN, KH. E. STERIN, M. IU. LUKINA, I. L. SAFANOVA, B. A. KAZANSKII
Spektroskopicheskoe issledovanie vliianiia vzaimnoi orientatsii tsiklopropanovykh i fenil'nykh kolets na ikh sopriazhenie 178
Spectroscopic Investigation of the Influence of the Mutual Orientation of Cyclopropane and Phenyl Rings Upon Their Conjugation 114

M. O. BULANIN, G. S. DENISOV, D. N. SHCHEPKIN
Ob izluchenii ravnovesii, obuslovlennykh obrazovaniem vodorodnoi sviazi v rastvorakh, po infrakrasnym spektram poglosheniia. Sluchii nerazdeliaiushchikhsia polos 187
On the Study of Hydrogen Bonding Equilibria in Solutions by Infrared Absorption Spectra. Case of Unseparated Bands 119

V. N. SMIRNOV, P. A. BAZHULIN
Issledovanie temperaturnoi zavisimosti intensivnosti infrakrasnykh polos poglosheniia v gazakh 193
Investigation of the Temperature Dependence of the Intensity of Infrared Absorption Bands of Gases 123

A. V. RAKOV
Vliianie mezhmolekuliarnogo vzaimodeistviia na shirinu linii spektrov kombinatsionnogo rasseianiia v zhidkostiakh 202
The Influence of Intermolecular Interaction on Line Width in the Raman Spectra of Liquids 128

V. M. ASLANIAN, M. V. VOL'KENSHTEIN
Opticheskaia aktivnost' i mezhmolekuliarnoe vzaimodeistvie 208
Optical Activity and Intermolecular Interaction 132

T. N. BOLOTNIKOVA
Spektroskopiia nekotorykh prostykh aromaticheskikh uglevodorodov v zamorozhennykh kristallicheskikh rastvorakh 217
Spectroscopy of Certain Simple Aromatic Hydrocarbons in Frozen Crystalline Solutions 138

Z. A. CHIZHIKOVA
Liuminestsentsiia i izluchenie Vavilova-Cherenkova v rastvorakh pod deistviem γ - luchei 223
Luminescence and Vavilov-Cherenkov Radiation in Solutions Bombarded by Gamma Rays 141

Z. L. MORGENSHTERN
Svechenie neaktivirovannykh monokristallov CsI 231
Luminescence of Unactivated CsI Monocrystals 146

V. L. LEVSHIN, V. N. REBANE
Sravnitel'noe izuchenie zapasaniia svetovykh summ i temperaturnogo tusheniia fosfora ZnS-Ag pri vozbuzhdeniia β-luchami i svetom 236
Comparative Study of the Storage of Light Sums and the Temperature Quenching of ZnS-Ag Phosphor Excited by β-rays and light 149

L. A. VINOKUROV, M. V. FOK
Ob odnovremennom deistvii foto- i elektrovozbuzhdeniia na elektroliuminofory 241
On the Simultaneous Effect of Photo- and Electroexcitation on Electroluminophors 152

V. K. MILOSLAVSKII
Infrakrasnoe poglosheniе tonkikh sloev dvuokisi olova 244
Infrared Absorption of Thin Films of Tin Dioxide 154

KRATKIE SOOBSHCHENIIA
SHORT COMMUNICATIONS

G. P. SKORNIAKOV, I. I. SASOVSKAIA
O roli ugla padeniia sveta pri nabliudenii ul'trafioletovogo minimuma otrazheniia serebra 249
On the Role of the Angle of Light Incidence in Observation of the Ultraviolet Minimum of Silver Reflectance 157

T. ABDUSADYKOV
Tsentry liuminestsentsii v shchelochno-galoidnykh fosforakh s bol'shimi kontsentratsiiami aktivatora i mikrodefektov osnovnoi reshetki 250
Centers of Luminescence in Alkali-Halide Phosphors with Large Concentrations of the Activator and Microdefects of the Host Lattice 158